Oxidative Medicine and Cellular Longevity

Oxidative Stress in Muscle Diseases: Current and Future Therapy 2019

Lead Guest Editor: Andrey J. Serra
Guest Editors: José R. Pinto, Marko D. Prokić, Gisela A. Cunha, and Andrea Vasconsuelo

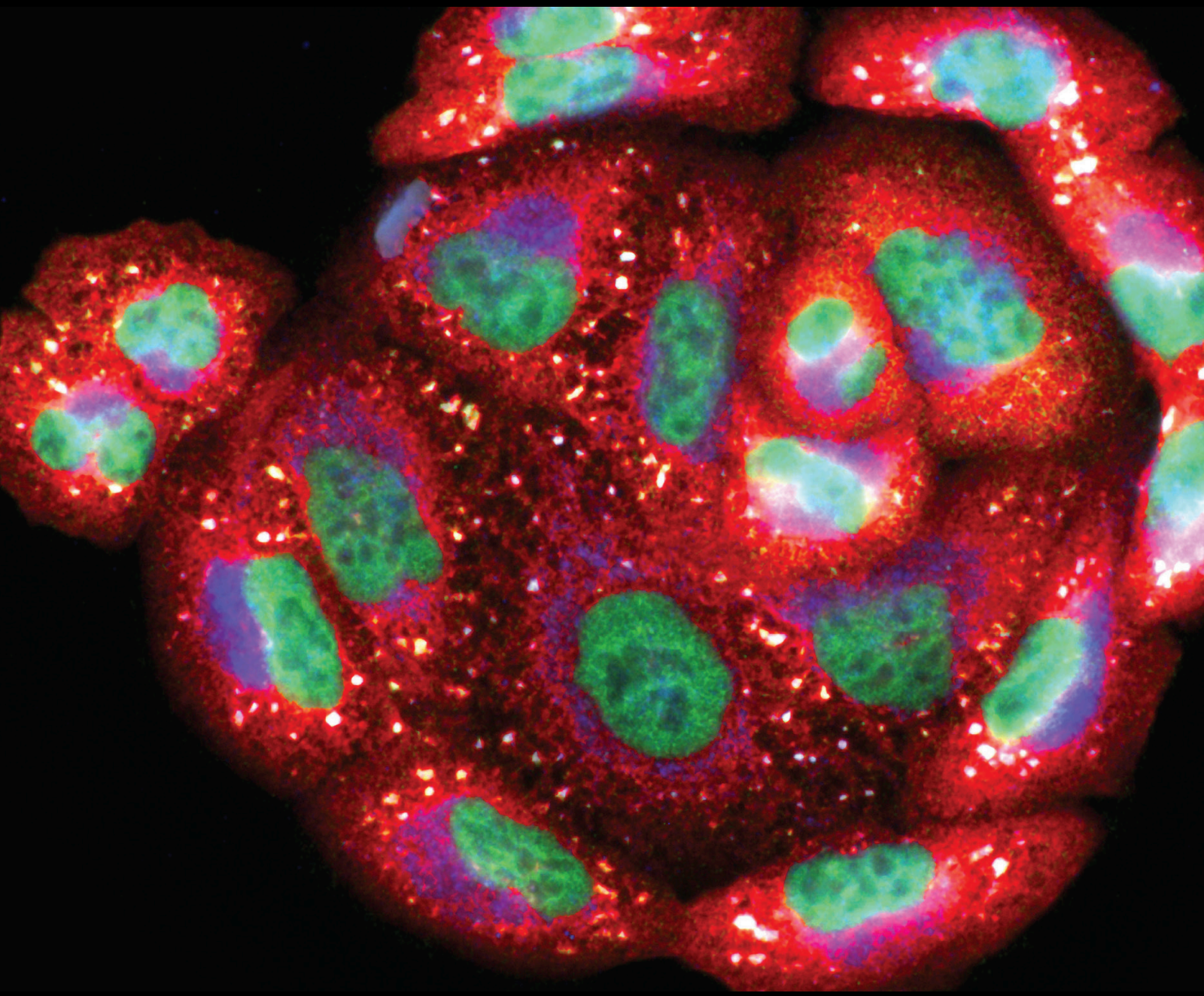

Oxidative Stress in Muscle Diseases: Current and Future Therapy 2019

Oxidative Medicine and Cellular Longevity

Oxidative Stress in Muscle Diseases: Current and Future Therapy 2019

Lead Guest Editor: Andrey J. Serra
Guest Editors: José R. Pinto, Marko D. Prokić, Gisela A. Cunha, and Andrea Vasconsuelo

Contents

Oxidative Stress in Muscle Diseases: Current and Future Therapy 2019
Andrey Jorge Serra, José Renato Pinto, Marko D. Prokić, Gisela Arsa, and Andrea Vasconsuelo
Editorial (4 pages), Article ID 6030417, Volume 2020 (2020)

Dynamic Resistance Training Improves Cardiac Autonomic Modulation and Oxidative Stress Parameters in Chronic Stroke Survivors: A Randomized Controlled Trial
Bruno Bavaresco Gambassi, Hélio José Coelho-Junior, Camila Paixão dos Santos, Ivan de Oliveira Gonçalves, Cristiano Teixeira Mostarda, Emanuele Marzetti, Samir Seguins Sotão, Marco Carlos Uchida, Kátia De Angelis, and Bruno Rodrigues
Clinical Study (12 pages), Article ID 5382843, Volume 2019 (2019)

Infrared Low-Level Laser Therapy (Photobiomodulation Therapy) before Intense Progressive Running Test of High-Level Soccer Players: Effects on Functional, Muscle Damage, Inflammatory, and Oxidative Stress Markers—A Randomized Controlled Trial
Shaiane Silva Tomazoni, Caroline dos Santos Monteiro Machado, Thiago De Marchi, Heliodora Leão Casalechi, Jan Magnus Bjordal, Paulo de Tarso Camillo de Carvalho, and Ernesto Cesar Pinto Leal-Junior
Clinical Study (12 pages), Article ID 6239058, Volume 2019 (2019)

Increased Circulating Levels of Interleukin-6 Affect the Redox Balance in Skeletal Muscle
Laura Forcina, Carmen Miano, Bianca M. Scicchitano, Emanuele Rizzuto, Maria Grazia Berardinelli, Fabrizio De Benedetti, Laura Pelosi, and Antonio Musarò
Research Article (13 pages), Article ID 3018584, Volume 2019 (2019)

Oxidative Stress in Cell Death and Cardiovascular Diseases
Tao Xu, Wei Ding, Xiaoyu Ji, Xiang Ao, Ying Liu, Wanpeng Yu, and Jianxun Wang
Review Article (11 pages), Article ID 9030563, Volume 2019 (2019)

Kynurenine, a Tryptophan Metabolite That Increases with Age, Induces Muscle Atrophy and Lipid Peroxidation
Helen Kaiser, Kanglun Yu, Chirayu Pandya, Bharati Mendhe, Carlos M. Isales, Meghan E. McGee-Lawrence, Maribeth Johnson, Sadanand Fulzele, and Mark W. Hamrick
Research Article (9 pages), Article ID 9894238, Volume 2019 (2019)

Ankrd2 in Mechanotransduction and Oxidative Stress Response in Skeletal Muscle: New Cues for the Pathogenesis of Muscular Laminopathies
Vittoria Cenni, Snezana Kojic, Cristina Capanni, Georgine Faulkner, and Giovanna Lattanzi
Review Article (15 pages), Article ID 7318796, Volume 2019 (2019)

Effect of Telmisartan in the Oxidative Stress Components Induced by Ischemia Reperfusion in Rats
Simón Quetzalcoatl Rodríguez-Lara, Walter Angel Trujillo-Rangel, Araceli Castillo-Romero, Sylvia Elena Totsuka-Sutto, Teresa Arcelia Garcia-Cobián, Ernesto German Cardona-Muñoz, Alejandra Guillermina Miranda-Díaz, Ernesto Javier Ramírez-Lizardo, and Leonel García-Benavides
Research Article (13 pages), Article ID 1302985, Volume 2019 (2019)

Chlorella vulgaris Improves the Regenerative Capacity of Young and Senescent Myoblasts and Promotes Muscle Regeneration
Nurhazirah Zainul Azlan, Yasmin Anum Mohd Yusof, Ekram Alias, and Suzana Makpol
Research Article (16 pages), Article ID 3520789, Volume 2019 (2019)

Vitamin D Deficiency Is Associated with Muscle Atrophy and Reduced Mitochondrial Function in Patients with Chronic Low Back Pain
Katarzyna Patrycja Dzik, Wojciech Skrobot, Katarzyna Barbara Kaczor, Damian Jozef Flis, Mateusz Jakub Karnia, Witold Libionka, Jedrzej Antosiewicz, Wojciech Kloc, and Jan Jacek Kaczor
Research Article (11 pages), Article ID 6835341, Volume 2019 (2019)

Age-Dependent Oxidative Stress Elevates Arginase 1 and Uncoupled Nitric Oxide Synthesis in Skeletal Muscle of Aged Mice
Chirayu D. Pandya, Byung Lee, Haroldo A. Toque, Bharati Mendhe, Robert T. Bragg, Bhaumik Pandya, Reem T. Atawia, Carlos Isales, Mark Hamrick, R. William Caldwell, and Sadanand Fulzele
Research Article (9 pages), Article ID 1704650, Volume 2019 (2019)

Hindawi
Oxidative Medicine and Cellular Longevity
Volume 2020, Article ID 6030417, 4 pages
https://doi.org/10.1155/2020/6030417

Editorial

Oxidative Stress in Muscle Diseases: Current and Future Therapy 2019

Andrey Jorge Serra,[1] **José Renato Pinto**,[2] **Marko D. Prokić**,[3] **Gisela Arsa**,[4] **and Andrea Vasconsuelo**[5]

[1]*Federal University of Sao Paulo, Sao Paulo, Brazil. Nove de Julho University, Sao Paulo, Brazil*
[2]*Florida State University, Tallahassee, USA*
[3]*University of Belgrade, Belgrade, Serbia*
[4]*Federal University of Mato Grosso, Cuiaba, Brazil*
[5]*Universidad Nacional del Sur, Bahia Blanca, Argentina*

Correspondence should be addressed to Andrey Jorge Serra; andreyserra@gmail.com

Received 14 March 2020; Accepted 14 March 2020; Published 21 April 2020

Increased oxidative stress has important molecular, structural, and functional muscle implications. In pathological conditions, reactive oxygen species (ROS) burst contributes to cellular dysfunction and the progression of muscle diseases. This special issue was designed to advance knowledge in the role of oxidative stress on muscle remodeling, in turn leading to innovative therapeutic approaches in a wide range of muscle diseases. Therefore, this special issue provides recent scientific advancements with researchers and practitioners who work in muscle scope. Articles included in this special issue address the molecular and cellular mechanisms involved in these processes as well as current therapies.

One of the studies published in the special issue examined the impact of 8-week dynamic resistance training with elastic bands on oxidative stress in stroke survivors. Functional fitness, hemodynamic, and cardiac autonomic modulation were also evaluated. The exercise protocol consisted of a sequence of three combinations of two consecutive exercises (i.e., seated row and squat on the chair, vertical chest press and squat on the chair, and knee extension and squat on the chair) in a dynamic manner, without intervals of absolute rest throughout the session. Exercise volume was increased over the 8-week protocol, in which three sets of 6-8 repetitions at moderate intensity (3 to 5 points on Borg scale) were performed in the first four weeks and three sets of 10-12 repetitions at moderate intensity were performed in subsequent weeks. The main findings were a plasma reduction in the levels of thiobarbituric acid reactive substances (TBARS) and carbonyls and an increased activity of superoxide dismutase (SOD). Exercised patients also showed improvements in functional fitness and sympathovagal balance. Therefore, the study has addressed the importance of resistance training using simple equipment such as elastic bands to reduce oxidative stress and improve cardiac autonomic control and functionality in chronic stroke survivors.

Excessive oxidative stress has been stimulated by exercise. The increase in ROS can be dependent on the type, duration, and load of the exercise [1]. ROS at low levels, a phenomenon similar to hormesis, plays an important role in exercise-induced physiological adaptation [2]. However, excessive oxidative stress can result in impaired physical performance and maladaptive skeletal muscle recovery [3]. Recently, experimental studies in rodents have indicated that photobiomodulation (PBM) could be a new alternative to modulate the excessive oxidative stress induced by exercise [4–10]. Several positive findings were highlighted, including (i) lower damage, inflammation, and lipoperoxidation of muscle; (ii) increased activity of antioxidant enzymes; and (iii) delayed muscle fatigue. On a translational perspective

of these findings, in this special issue has included a randomized, triple-blind, placebo-controlled crossover trial conducted by S. S. Tomazoni et al. The authors applied PBM (using infrared low-level laser therapy; a total of 850 J of energy) before a high-intensity progressive running test until exhaustion in soccer players. The PBM application brought about improvements in rates of oxygen uptake and time until exhaustion. Moreover, PBM showed to decrease muscle damage, interleukin 6 (IL-6), TBARS, and carbonylated protein levels. On the other hand, PBM led to increased activity of SOD and catalase (CAT) enzymes. Thus, PBM could be a promising approach to improve physical performance and to counter damage, inflammation, and oxidative stress associated with running high-intensity exercise. Further studies are needed to understand the influence of different irradiation dosages and whether the effects published by S. S. Tomazoni et al. can exist in distinct types of exercises.

Several studies support the existence of an interdependent relationship between inflammation and oxidative stress [11, 12]. Among factors playing a key role in skeletal muscle pathophysiology and potentially linking inflammation and oxidative stress, IL-6 is a possible candidate [13]. In this regard, L. Forcina et al. tried to investigate whether elevated circulating levels of the IL-6 could disturb the redox balance in skeletal muscle, independent of tissue damage and inflammatory response. Using NSE/IL-6 transgenic mice characterized by systemically elevated levels of IL-6, the authors show enhanced ROS production and accumulation in the diaphragm muscle. Alteration of the IL-6-linked homeostasis redox appears to require a complex network of interactions that involve the regulation of hydrogen peroxide, nicotinamide adenine dinucleotide phosphate-dependent superoxide scavengention, and mitochondrial antioxidant defense. This special issue also covers the role of ROS played in the development of cell death and cardiovascular diseases. The review article of T. Xu et al. also explored the potential application of the anti-ROS approach in the treatment of cardiovascular diseases. First, the authors documented the different ROS sources and the role of ROS accumulation in vascular dysfunction and cardiac remodeling. Second, the proposal was to address the repercussion of excessive ROS production in the induction of cell death. It has been registered as ROS is closely related to cardiomyocyte apoptosis, autophagy, ferroptosis, and necrosis. Third, the authors reviewed important aspects for several antioxidant agents, including tripeptide glutathione, SOD, CAT, thioredoxin, oxidative stress response transcription factors (e.g., AP-1, HSF1, Nrf2, and FOXO3a), N-acetylcysteine, vitamin E, and NAD^+. The last concerns were targeted to clinical trials that evaluated the impact of inhibiting oxidative stress in cardiovascular diseases, in which they have failed to mitigate cardiac remodeling and the evolution of heart failure.

Kynurenine (KYN) is a circulating tryptophan metabolite that increases with age and is implicated in several age-related disorders [14]. In this regard, H. Kaiser et al. hypothesized that an increase in KYN with age contributes to muscle atrophy and oxidative stress. *In vitro* experiments showed that KYN treatment of mouse and human myoblasts increased levels of ROS. Young mice had higher muscle lipid peroxidation and reduced muscle size and strength in response to KYN treatment. Aged mice treated with indoleamine 2,3-dioxygenase inhibitor, an enzyme involved in the generation of KYN, showed an increase in muscle fiber size and muscle strength. Protein expression assays revealed very long-chain acyl-CoA dehydrogenase as a factor activated by KYN that may increase ROS and lipid peroxidation. Collectively, these findings make it possible to consider KYN involvement in sarcopenia with age. It appears that the deleterious effects of chronic KYN exposure are mediated by increased oxidative stress. V. Cenni et al. presented an interesting review that describes the effects of the Ankrd2 modulation stimulate by mechanotransduction and cellular ROS. Moreover, they demonstrated a possible relation with the pathogenesis of muscular laminopathies. First, the authors documented the Ankrd2 in striated muscles focusing on expression in skeletal and cardiac muscles, as well as, mechanotransduction in skeletal muscle. They demonstrated how physical exercise could stimulate an Ankrd2 upregulation from oxidative and mechanical stresses. Second, they proposed pathogenic mechanisms in which Ankrd2 might be involved. Third, it showed the perspectives of the study of Lamin-AAnkrd2 interplay, specifically the mechanosignaling through Ankdr2 and therapeutic perspectives. It is important to highlight that the authors showed illustrations for the complex network that involve the relation between Ankrd2 and pathogenesis of muscular laminopathies.

Another interesting study was carried out by S. Q. Rodríguez-Lara et al. which showed a pharmacological approach to reduce ischemia-reperfusion (I/R) damage. This phenomenon can be induced by cellular ROS, resulting in deleterious effects on the lesion, and there is no pharmacological approach to avoid or decrease these dangerous effects. However, the authors presented Telmisartan as a possible pharmacological approach because it seems to affect the concentration and activity of enzymatic scavengers, which could decrease lesion development. For this, male Wistar rats were submitted to treatment with Telmisartan for seven days before I/R lesion and then were evaluated at 1 h, 24 h, 72 h, 7, and 14 days following reperfusion. Muscle samples were obtained to determine SOD-2 and CAT gene expression. The biochemical assay was used to determine the oxidative and antioxidative markers. Histological tissue evaluation from the right gastrocnemius muscle was performed. The main results were that the approach of Telmisartan (i) produced changes in the SOD-2 and CAT gene expression regarding reperfusion, (ii) reduced oxidative markers levels in the local tissue, and (iii) promoted injury attenuation between 24 h and 14 days. A novel pharmacological approach with Telmisartan demonstrated to be promissory to reduce damages during I/R damage. The elderly population has been increasing, and sarcopenia became a vital topic to be studied because it affects autonomy in daily life and compromises the quality of life [15]. In this issue, N. Z. Azlan et al. described several strategies to counter sarcopenia and among them presented the *Chlorella vulgaris*, a green alga that seems to promote muscle regeneration. The authors aimed to establish

the effects of the differentiation of myoblast cells during the formation of mature myotubes in culture. For this, human myoblast cells were obtained from young men and women and then were cultured on adequate conditions and stimulates until reaching senescence. Cells were treated with *Chlorella vulgaris* and incubated for up to seven days to induce differentiation. Different techniques were used to analyze the ability of *Chlorella vulgaris* to promote myoblast differentiation (e.g., cellular morphology, real-time monitoring, cell proliferation, senescence-associated B-galactosidase expression, myogenic differentiation, myogenic expression, and cell cycle profiling). *Chlorella vulgaris* improved the regenerative capacity of young and senescent myoblasts, stimulating differentiation, demonstrating to have a high potential to treat sarcopenia.

K. P. Dzik et al. show in this issue the relations among muscle atrophy and vitamin D deficiency. The authors describe the muscle function affected by vitamin D deficiency and the development of muscle atrophy. Lumbar back pain (LBP) patients showed paravertebral muscle atrophy. The authors investigated muscle atrophy markers, signaling proteins, and mitochondrial capacity in LBP patients according to sex and vitamin D levels. Men and women were distributed into three groups according to levels of vitamin D received for five weeks. Three dosages of vitamin D were established to reach deficiency, normal, and above normal levels. The key results were that the vitamin D deficiency-induced stress oxidative, which is involved in a cascade of enzymatic events that leads to muscle atrophy and mitochondrial dysfunction, is most present in women due to higher Atrogin-1 levels. Normal or higher levels of vitamin D increase the mitochondrial function and inhibit muscle atrophy.

C. D. Pandya et al. described the role of oxidative stress on aging and their mechanisms that results in sarcopenia and osteoporosis. They empathize the possible effects of regulation of arginase from oxidative stress on the survival and differentiation of myoblasts. The authors aimed to investigate the arginase activity and expression in the skeletal muscle in young and aged mice. First, arginase activity and arginase 1 expression were determined. Second, the expression of oxidative stress-related signaling molecules in muscles of aged mice was performed. Third, *in vitro* studies were conducted with myoblast cell line (C2C12) and arginase inhibitor (ABH). The main results were an elevated arginase activity in aged muscle and a reduced NO production that occurs by the competition for L-arginine and eNOS uncoupling. Also, the authors highlighted that it is possible to prevent or slow down the degenerative effect in muscle aging by limiting arginase activity.

We hope that this special issue has been successful in providing new insights into the impact of oxidative stress in muscle physiology and several muscle disorders. Editors considered the interdisciplinary nature of the papers included as necessary to expand on fundamental concepts, i.e., basic research as well as those important to applied sciences. Therefore, the readers of this special issue should find information of interest, relevant to their respective areas of scientific investigations.

Disclosure

The funding sources listed do not influence the selection of data presented in this editorial.

Conflicts of Interest

The authors declare that there is no conflict of interest regarding the publication of this special issue.

Authors' Contributions

Andrey Jorge Serra and Gisela Arsa wrote the editorial; José Renato Pinto, Marko D. Prokić, and Andrea Vasconsuelo revised the editorial.

Acknowledgments

The guest editorial team would like to thank all authors of the contributed papers and review articles submitted to this special issue. We are very grateful to the reviewers, who have donated their time, knowledge, and experience to assess the manuscripts. Andrey Jorge Serra is a research fellow from the Fundação de Amparo à Pesquisa do Estado de São Paulo (FAPESP) (no. 2018/06865-7) and Conselho Nacional de Desenvolvimento Científico e Tecnológico (CNPq) (nos. 305527/2017-7 and 404702/2016-3).

Andrey Jorge Serra
José Renato Pinto
Marko D. Prokić
Gisela Arsa
Andrea Vasconsuelo

References

[1] P. Steinbacher and P. Eckl, "Impact of oxidative stress on exercising skeletal muscle," *Biomolecules*, vol. 5, no. 2, pp. 356–377, 2015.

[2] M. Kozakowska, K. Pietraszek-Gremplewicz, A. Jozkowicz, and J. Dulak, "The role of oxidative stress in skeletal muscle injury and regeneration: focus on antioxidant enzymes," *Journal of Muscle Research and Cell Motility*, vol. 36, no. 6, pp. 377–393, 2015.

[3] S. M. Sunemi, F. A. Silva, E. L. Antonio, P. J. F. Tucci, and A. J. Serra, "Photobiomodulation: newly discovered actions in resistance exercise," *Reactive Oxygen Species*, vol. 7, no. 21, pp. 148–153, 2019.

[4] C. de Souza Oliveira, H. A. de Oliveira, I. L. A. Teixeira et al., "Low-level laser therapy prevents muscle apoptosis induced by a high-intensity resistance exercise in a dose-dependent manner," *Lasers in Medical Science*, 2020.

[5] H. A. de Oliveira, E. L. Antonio, F. A. Silva et al., "Protective effects of photobiomodulation against resistance exercise-induced muscle damage and inflammation in rats," *Journal of Sports Sciences*, vol. 36, no. 20, pp. 2349–2357, 2018.

[6] C. Ferraresi, N. A. Parizotto, M. V. Pires de Sousa et al., "Light-emitting diode therapy in exercise-trained mice increases muscle performance, cytochrome c oxidase activity, ATP and cell proliferation," *Journal of Biophotonics*, vol. 8, no. 9, pp. 740–754, 2015.

[7] A. A. de Oliveira Silva, E. C. P. Leal-Junior, K. de Angelis Lobo D'Avila et al., "Pre-exercise low-level laser therapy improves performance and levels of oxidative stress markers in mdx mice subjected to muscle fatigue by high-intensity exercise," *Lasers in Medical Science*, vol. 30, no. 6, pp. 1719–1727, 2015.

[8] M. Frigero, S. A. dos Santos, A. J. Serra et al., "Effect of photobiomodulation therapy on oxidative stress markers of gastrocnemius muscle of diabetic rats subjected to high-intensity exercise," *Lasers in Medical Science*, vol. 33, no. 8, pp. 1781–1790, 2018.

[9] H. A. de Oliveira, E. L. Antonio, G. Arsa et al., "Photobiomodulation leads to reduced oxidative stress in rats submitted to high-intensity resistive exercise," *Oxidative Medicine and Cellular Longevity*, vol. 2018, Article ID 5763256, 9 pages, 2018.

[10] A. J. Serra, M. D. Prokić, A. Vasconsuelo, and J. R. Pinto, "Oxidative stress in muscle diseases: current and future therapy," *Oxidative Medicine and Cellular Longevity*, vol. 2018, Article ID 6439138, 4 pages, 2018.

[11] S. K. Powers, L. L. Ji, A. N. Kavazis, and M. J. Jackson, "Reactive oxygen species: impact on skeletal muscle," *Comprehensive Physiology*, vol. 1, no. 2, pp. 941–969, 2011.

[12] S. J. Forrester, D. S. Kikuchi, M. S. Hernandes, Q. Xu, and K. K. Griendling, "Reactive oxygen species in metabolic and inflammatory signaling," *Circulation Research*, vol. 122, no. 6, pp. 877–902, 2018.

[13] P. Munoz-Canoves, C. Scheele, B. K. Pedersen, and A. L. Serrano, "Interleukin-6 myokine signaling in skeletal muscle: a double-edged sword?," *FEBS Journal*, vol. 280, no. 17, pp. 4131–4148, 2013.

[14] J. de Bie, J. Guest, G. J. Guillemin, and R. Grant, "Central kynurenine pathway shift with age in women," *Journal of Neurochemistry*, vol. 136, no. 5, pp. 995–1003, 2016.

[15] B. Manrique-Espinoza, A. Salinas-Rodríguez, O. Rosas-Carrasco, L. M. Gutiérrez-Robledo, and J. A. Avila-Funes, "Sarcopenia is associated with physical and mental components of health-related quality of life in older adults," *Journal of the American Medical Directors Association*, vol. 18, no. 7, pp. 636.e1–636.e5, 2017.

Hindawi
Oxidative Medicine and Cellular Longevity
Volume 2019, Article ID 5382843, 12 pages
https://doi.org/10.1155/2019/5382843

Clinical Study

Dynamic Resistance Training Improves Cardiac Autonomic Modulation and Oxidative Stress Parameters in Chronic Stroke Survivors: A Randomized Controlled Trial

Bruno Bavaresco Gambassi,[1,2] **Hélio José Coelho-Junior**,[1,3] **Camila Paixão dos Santos**,[4] **Ivan de Oliveira Gonçalves**,[5] **Cristiano Teixeira Mostarda**,[6] **Emanuele Marzetti**,[3] **Samir Seguins Sotão**,[2] **Marco Carlos Uchida**,[1] **Kátia De Angelis**,[4] **and Bruno Rodrigues**[1]

[1]*School of Physical Education, University of Campinas (UNICAMP), Campinas, SP, Brazil*
[2]*Ceuma University, São Luis, MA, Brazil*
[3]*Department of Geriatrics, Neurosciences and Orthopedics, Teaching Hospital "Agostino Gemelli", Catholic University of the Sacred Heart, Rome, Italy*
[4]*Department of Physiology, Federal University of São Paulo (UNIFESP), São Paulo, SP, Brazil*
[5]*Center of Health Sciences, University of Mogi das Cruzes (UMC), Mogi das Cruzes, SP, Brazil*
[6]*Physical Education Department, Federal University of Maranhão (UFMA), São Luis, MA, Brazil*

Correspondence should be addressed to Bruno Rodrigues; prof.brodrigues@gmail.com

Received 29 May 2019; Revised 12 September 2019; Accepted 8 October 2019; Published 20 November 2019

Academic Editor: Eric E. Kelley

Stroke survivors are at substantial risk of recurrent cerebrovascular event or cardiovascular disease. Exercise training offers nonpharmacological treatment for these subjects; however, the execution of the traditional exercise protocols and adherence is constantly pointed out as obstacles. Based on these premises, the present study investigated the impact of an 8-week dynamic resistance training protocol with elastic bands on functional, hemodynamic, and cardiac autonomic modulation, oxidative stress markers, and plasma nitrite concentration in stroke survivors. Twenty-two patients with stroke were randomized into control group (CG, $n = 11$) or training group (TG, $n = 11$). Cardiac autonomic modulation, oxidative stress markers, plasma nitrite concentration, physical function and hemodynamic parameters were evaluated before and after 8 weeks. Results indicated that functional parameters (standing up from the sitting position ($P = 0.011$) and timed up and go ($P = 0.042$)) were significantly improved in TG. Although not statistically different, both systolic blood pressure ($\Delta = -10.41$ mmHg) and diastolic blood pressure ($\Delta = -8.16$ mmHg) were reduced in TG when compared to CG. Additionally, cardiac autonomic modulation (sympathovagal balance–LF/HF ratio) and superoxide dismutase were improved, while thiobarbituric acid reactive substances and carbonyl levels were reduced in TG when compared to the CG subjects. In conclusion, our findings support the hypothesis that dynamic resistance training with elastic bands may improve physical function, hemodynamic parameters, autonomic modulation, and oxidative stress markers in stroke survivors. These positive changes would be associated with a reduced risk of a recurrent stroke or cardiac event in these subjects.

1. Introduction

Stroke, a neurological disease commonly caused in response to abnormal blood perfusion of the brain tissue, is the leading cause of permanent disability worldwide [1]. Neuromuscular impairments, such as muscle loss, dynapenia, and reduced muscle power are commonly observed in patients with stroke and represent a crucial risk factor for the development of limited physical function, disability, and poor prognosis [2–4].

In addition to the neuromuscular alterations, marked oxidative stress, impairment in blood pressure control mechanisms (e.g., baroreflex sensitivity), and severe autonomic

dysfunction, characterized by an elevated sympathetic activity, combined with a reduced or unchanged parasympathetic activity [5–7] might also been observed in stroke survivors and collaborated to genesis of cardiovascular complications (e.g., hypertension and myocardial infarction) in this population [8].

On the other hand, the practice of physical exercise has been considered an effective nonpharmacological strategy for poststroke individuals, since it mitigates physical, neurological, and cardiovascular sequelae. Indeed, prior studies have found improved cardiovascular health and physical function in stroke survivors after exercise training protocols [9, 10].

Nevertheless, researchers have argued that resistance training (RT), a type of physical exercise in which muscle contractions occur against a predetermined load [11], should receive priority attention in rehabilitation protocols for stroke survivors to maximize gains in mobility and independence [12]. A recent review of our group [12] indicated that the benefits of RT in stroke survivors go beyond the neuromuscular system and may include improvements in anxiety levels and quality of life.

However, most studies investigated RT protocols and stroke were based on exercise and isokinetic machines, limiting their external validity [12, 13]. Besides that, evidence for the effects of RT on cardiac autonomic modulation and oxidative stress markers in stroke survivors are still scarce.

Based on these premises, the present study investigated the impact of an 8-week dynamic RT protocol with elastic bands on the physical function, hemodynamic parameters, cardiac autonomic modulation, oxidative stress markers, and plasma nitrite concentration in stroke survivors. We hypothesized that all these parameters may be improved in response to our protocol of dynamic RT.

2. Materials and Methods

2.1. Experimental Design. This is an interventional, controlled, randomized study conducted upon approval by the São Judas Tadeu University Ethical Committee (São Paulo, SP, Brazil) (CAAE: 64859916.0.0000.0089). The study was conducted according to the Declaration of Helsinki and registered in the Brazilian database of clinical trials (Register ID: U1111-1202-8242; 26/09/2017).

2.2. Participants. Participants were recruited by convenience from the rehabilitation center of the Albert Sabin Municipal Physiotherapy Center located in Poá, Brazil. Prior to recruitment, volunteers of the present study were participating of a physical activity program, which aimed to restore social life and increase individual's levels of physical movement. The program was offered to those patients who have finished the neurological poststroke rehabilitation program but stayed at home for a long time and were not able to reestablish the same performance of activities of daily living (ADL) and social life that they had prior stroke. Motivational and religious dialogues were proposed at the beginning and end of each session. Physical movements aimed to stimulate body movement were performed with the individual's sitting in a chair for 25-30 minutes without external load. Movements included put arms and legs up, down, forward, and backward, rotate the trunk to the right and left sides, and move the trunk forward and backward. Individuals who did not want or could not perform the exercises were not discouraged from attending the sessions and were common to observe that some of them went to the sessions to talk to other people. Most individuals were from low-income families and were taken to the rehabilitation center by a minibus offered by the city hall. Sessions occurred twice a week for 40-50 minutes under the supervision of a physical educator. A washout period of 4 weeks separated was concluded prior to baseline evaluations.

Subjects were eligible to take part of the present study if they: (a) aged 45-75 years; (b) were able to walk with or without a walking aid; (c) were independent to perform basic activities of daily living, according to Barthel index [14]; (d) had a clinical diagnosis of stroke confirmed by computed tomography or magnetic resonance imaging at least 6 months prior to enrollment; (e) lived in the community; and (f) completed a standard neurological poststroke rehabilitation program. Candidate participants were excluded if they were not able to sign the informed consent form, had history of smoking or alcohol abuse in the last 6 months, had history of uncontrolled hypertension and/or diabetes mellitus according to medical records, used beta blockers, showed disabling pain during exercise, were incapable to perform exercise sessions and/or any of the evaluations (self-reported), and not attended at least 90% of training sessions. Participants had not been engaged in regular exercise training programs during the previous 6 months, according to the Baecke Habitual Physical Activity Questionnaire [15], and no changes in dose and drug classes were registered during the protocol.

Twenty-seven stroke patients were enrolled in this study and five subjects were excluded. Twenty-two consenting patients were randomized 1 : 1 into the control group (CG, $n = 11$) and trained group (TG, $n = 11$) (Figure 1).

2.3. Resistance Training (RT) Intervention. The dynamic RT protocol was performed two times per week over an 8-week period with a 48 h rest interval provided between each exercise session. Resistance exercises were performed using elastic bands [16] (Thera Band®, Ohio, USA) and ankle wrist weights. The physical exercises were performed in the following order: (1^{st}) seated row, (2^{nd}) squat on the chair, (3^{rd}) vertical chest press, and (4^{th}) knee extension (Figure 2). Physical exercises were adapted due to the limitations caused by the paretic limb in the range of motion (ROM). To seated row, the paretic hand was anchored in the wrist of the nonparetic hand, while the elastic band was positioned between the palm of the paretic hand, the palm of the nonparetic hand, and the wrist. To chest press, the elastic band was anchored in the paretic side, and the abduction of the shoulder was performed according to ROM limitations. No specific changes were performed in squat on the chair exercise. The nonparetic limb executed the exercises across the full ROM.

The dynamic resistance training protocol consisted of a sequence of 3 combinations of 2 consecutive exercises

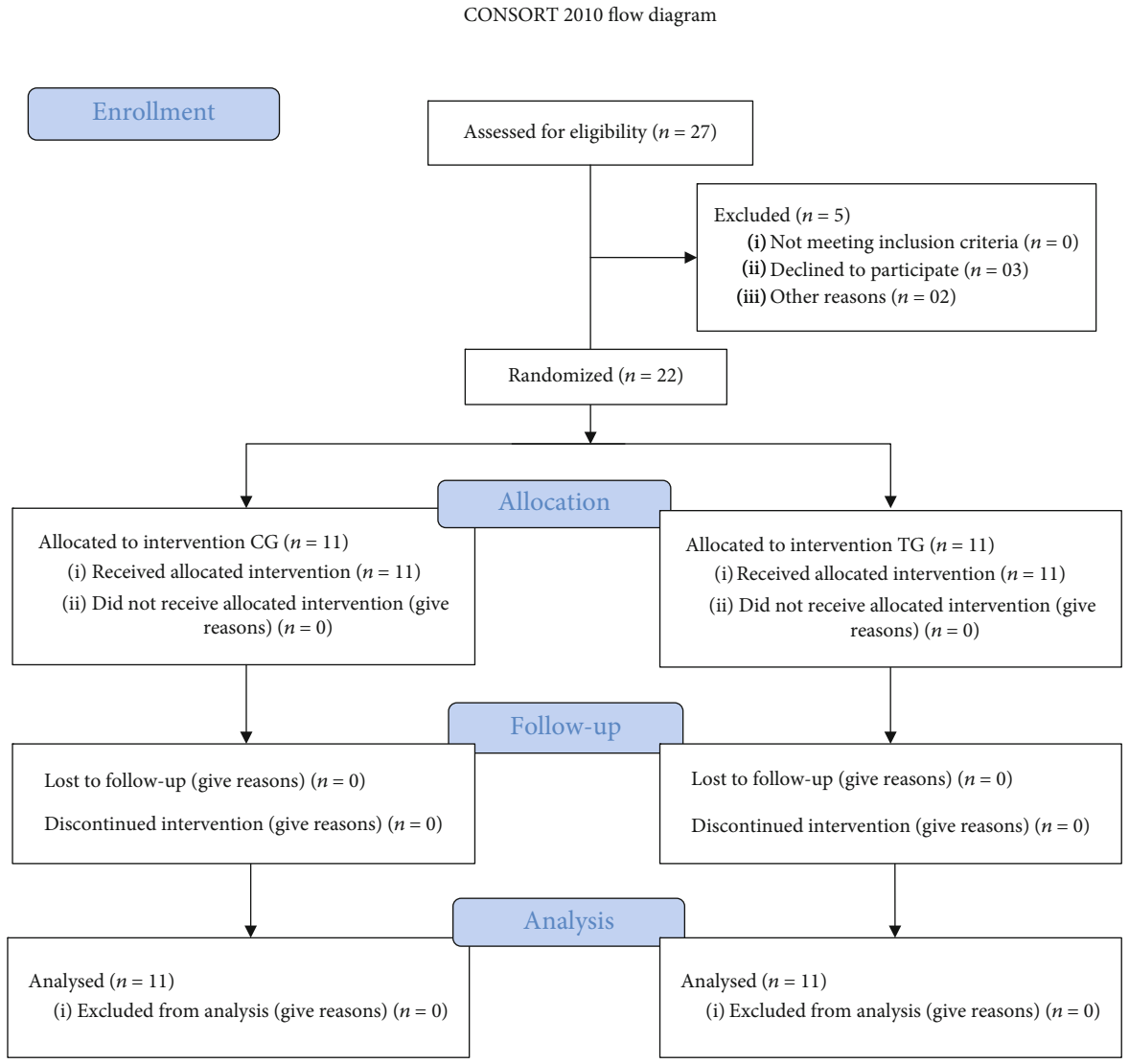

Figure 1: CONSORT flow diagram.

(i.e., seated row and squat on the chair, vertical chest press and squat on the chair, knee extension and squat on the chair) in a dynamic manner, without intervals of absolute rest throughout the session. The concentric contractions were performed as fast as possible, while the eccentric contractions were performed within 3 s. The exercise volume was increased over the 8-week protocol, so that 3 sets of 6-8 repetitions at moderate intensity (3 to 5 points on adapted Borg Scale of 1-10 [17]) were performed in the first 4 weeks and 3 sets of 10-12 repetitions at moderate intensity were performed in subsequent weeks.

The exercise intensity was controlled according to the tension of elastic bands based on the rate of perceived exertion (RPE) method [17]. According to a study by Colado and Triplett [18], the combination of target repetitions with a subjective effort scale may be considered a valid strategy to control the intensity when RT is performed with elastic bands. The RPE was reported after the end of each set of exercise and, if the participant reported an RPE below the expectations (low intensity), the tension of the elastic band was increased (moderate intensity).

All patients were performed neurological physical therapy treatment two times per week in addition to the 8-week RT program.

2.4. Control Group (CG). Patients in the CG remained performed two sessions per week over 8 weeks of a neurological physical therapy program, which consisted of physical movements that mimic basic and instrumental ADL, postural changes, and gait exercises on parallel bars.

2.5. Evaluations

2.5.1. Functional Parameters. A researcher detailed the operational procedures, demonstrated the test, and evaluated the motor pattern of participants during each physical performance test. All participants performed a familiarization trial to ensure that they had understood the test. All tests were

Figure 2: Representation of resistance training protocol execution.

performed in triplicate, and the mean result was used in the final analysis. A 1 min rest was allowed between consecutive trials. Four physical tests were administered in the following order: (a) isometric handgrip of paretic and nonparetic limbs (IHGPL and IHGNPL), (b) 10 m walking test (10MWT), (c) five-repetition sit-to-stand (5XSTS), and (d) timed "up and go" (TUG).

2.5.2. Isometric Handgrip of Paretic and Nonparetic Limbs. Isometric handgrip strength was measured using a Jamar® handheld hydraulic dynamometer (Sammons Preston, Bolingbrook, IL, USA). The measure was obtained with the participant seated in a chair with the shoulders abducted, elbows near the trunk and flexed at 90°, and wrists in a neutral position (thumbs up). The contralateral arm remained relaxed under the thigh. To determine handgrip strength, participants performed a maximal contraction during 3-5 s with the paretic (IHGPL) and nonparetic (IHGNPL) limbs [19]. The maximum grip strength (kgf) was taken from the digital display. The test reliability in the present study was ≥0.8 ($\kappa = 0.99$).

2.5.3. 10 m Walking Speed (10MWT). Walking speed was measured over 10 m. Participants were required to walk 12 m at their fastest possible pace without running. Before the evaluation, both feet of each participant remained on the starting line. The time measurement started when a foot reached the 1 m line and was stopped when a foot reached the 11 m line. The 1 m intervals at the beginning and the end of the course were used to avoid early acceleration and/or deceleration [20]. The following formula was used to calculate walking speed:

$$10\text{MWT} = \frac{10}{\text{time to complete the test}}. \quad (1)$$

The test reliability in the present study was ≥0.8 ($\kappa = 0.98$).

2.5.4. 5-Repetition Sit-To-Stand (5XSTS). Participants were requested to rise from a standard armless chair five times as quick as possible with arms folded across the chest. The stopwatch was started when participants raised their buttocks off the chair and was stopped when participants seated back at the end of the fifth stand [21]. The test reliability in the present study was ≥0.8 ($\kappa = 0.95$).

2.5.5. Timed "Up and Go." The TUG involved getting up from a chair (total height: 87 cm; seat height: 45 cm; width: 33 cm), walking three meters around a cone placed on the floor, coming back to the same position, and sitting back on the chair. The volunteer wore regular footwear, with the back against the chair, arms resting on the chair's arms, and the feet in contact with the ground. A researcher instructed the volunteer to, on the word "go," get up, walk as fast as possible without compromising safety through the demarcation of three meters on the ground, turn, return to the chair, and sit down again. The timing was started when participants got up from the chair and was stopped when the participants back touched the backrest of the chair [22, 23]. The test reliability in the present study was ≥0.8 ($\kappa = 0.95$).

2.5.6. Hemodynamic Parameters

(1) Blood Pressure Measurement. Blood pressure (BP) was measured between 08 : 00 and 10 : 00 am according to the procedures detailed in the 7th Brazilian Arterial Hypertension Guidelines [24]. Participants were instructed to refrain from exercising during the previous 48 h and from drinking caffeinated beverages and/or alcohol 24 h before the evaluation. After remained seated on a comfortable recliner chair for 15 min in a quiet room, an appropriate cuff was placed at approximately the midpoint of the participant's upper left arm. An automatic, noninvasive, calibrated, and

Table 1: Baseline clinical characteristics of participants.

	CG ($n = 11$)	TG ($n = 11$)	P value
Age (years)	60.5 ± 13.2	66.4 ± 10.1	0.334
Body mass index (kg/cm^2)	26.0 ± 3.2	25.4 ± 2.9	0.089
Women (%)	63.6	54.5	0.120
Poststroke duration (years)	4.9 ± 4.2	6.6 ± 5.0	0.120
Paretic side (left) (%)	90.9	54.5	0.987
Basic functional independence (Barthel Index)	90.0 ± 6.3	87.3 ± 11.9	0.350
Baecke Habitual Physical Activity Questionnaire	3.8 ± 0.6	3.2 ± 0.4	0.884
Associated comorbidities (%)			
Hypertension	90.9	90.9	1.000
T2DM	54.5	56.4	0.916
Medications (%)			
ACE inhibitors	70.3	74.5	0.842
HMG-CoA reductase inhibitor	88.2	85.3	0.859
Diuretics	77.8	75.9	0.898
Acetylsalicylic acid	45.3	47.8	0.973
Antidiabetics	55.7	58.2	0.948

Data are shown as mean ± SD. CG: control group; TG: training group; T2DM: diabetes mellitus type II; ACE: angiotensin-converting enzyme; HMG-CoA: 3-hydroxy-3-methylglutaryl coenzyme A reductase.

validated arterial BP monitor (Microlife-BP 3BT0A, Microlife, Widnau, Switzerland) [24] was used to measure systolic BP (SBP), diastolic BP (DBP), and heart rate (beats per min, bpm). The double product (DP) was calculated as follows:

$$\text{DP} = \text{SBP} \times \text{heart rate}. \quad (2)$$

(2) Assessment of Heart Rate Variability (Cardiac Autonomic Modulation). A Polar V800 heart rate monitor (Polar Electro Oy, Kempele, Finland) was used to continuously record beat-to-beat intervals (R-R interval) with the patients in the supine position [25]. The spectrum resulting from the fast Fourier transforms modeling was derived from the highest value in one of the for 5-minute window recorded; it includes the entire signal variance, regardless of whether its frequency components appear as specific spectral peaks or as nonpeak broadband powers. The R-R interval variability was evaluated in the time and frequency domains. Spectral power for low (LF: 0.03–0.15 Hz) and high (HF: 0.15–0.4 Hz) frequency bands was calculated using power spectrum density integration within each frequency bandwidth, using a customized routine (MATLAB 6.0, Natick, MA, USA). The LF/HF ratio was calculated based on normalized LF and HF. The time domain measurements included standard deviation of the of normal sinus beats (SDNN, ms) and root mean square of successive R-R interval differences (RMSSD, ms).

The nonlinear geometric measures have been derived from the 5-minute Poincaré plot representing a diagram in which each R-R interval of tachogram is plotted against the previous R-R interval. The length of the longitudinal line is defined as the SD2 of the plot data. The length of the transverse line is defined as the SD1 of the plot data in a perpendicular direction.

2.5.7. Oxidative Stress Markers. Blood samples were collected by venipuncture in heparinized vacutainers after 12 h fasting and immediately centrifuged at 4000 rpm for 5 min to separate plasma. Participants were advised to avoid foods rich in nitrates (e.g., beet, cabbage, spinach, lettuce) the day before blood collection. Protein concentration was determined according to the method described by Lowry et al. [26], using bovine albumin solution at a concentration of 1 mg/mL as the standard and 10 μL samples.

Thiobarbituric acid reactive substances (TBARS), carbonyls, NADPH oxidase, hydrogen peroxide (H_2O_2), superoxide dismutase (SOD), and plasma nitrite analyses were conducted in accordance with Jacomini et al. [27].

2.6. Statistical Analysis. Data distribution and equality of variance were tested by the Shapiro-Wilk and Levene tests, respectively. Repeated measures ANOVA (followed by the Sidak post hoc test) was used to detect differences between different times of evaluations and treatments. 10MWT (s), SBP (mmHg), and HF band (ms^2) showed irregular distribution and within- and between-group differences were analyzed using the Wilcoxon and Mann–Whitney tests, respectively. Chi-square (χ^2) statistics were used to compare categorical variables. Cohen's ES d was calculated to assess the magnitude of the results. Delta (Δ) values were calculated as follows:

$$\Delta = \text{Mean post} - \text{Mean baseline}. \quad (3)$$

Table 2: Physical function at baseline and after 10 weeks.

Variables	CG ($n = 11$)		Δ (ES)	TG ($n = 11$)		Δ (ES)
	Baseline	Post		Baseline	Post	
IHGPL (kgf)	10.4 ± 8.9	7.9 ± 7.7 ∗	-2.5 (0.3)	13.8 ± 10.7	13.9 ± 10.0	0.1 (-0.0)
IHGNPL (kgf)	28.5 ± 13.9	23.7 ± 10.8 ∗	-4.8 (0.4)	28.5 ± 7.3	28.1 ± 8.0	-0.4 (0.1)
10MWT (s)	14.5 (10.4–31.5)	13.5 (10.0–32.0)	0.7 (-0.1)	13.8 (10.0–42.4)	10.2 (7.9–22.2)∗†	-6.4 (0.8)
Sit-to-stand (s)	15.1 ± 2.9	14.4 ± 2.4	-0.7 (0.3)	15.7 ± 3.0	11.3 ± 1.7∗†	-4.4 (1.9)
TUG (s)	22.2 ± 9.3	22.0 ± 7.1	-0.2 (0.0)	19.2 ± 8.3	14.1 ± 5.6∗†	-5.1 (0.7)

SD: standard deviation of the mean; ES: effect size; CG: control group; TG: training group; IHGPL: isometric handgrip of the paretic limb; IHGNPL: isometric handgrip of the nonparetic limb; 10MWT: 10-meter walking speed; TUG: timed up and go. Data are shown as mean ± SD or median; $^{*}P < 0.05$ vs. baseline; $^{\dagger}P < 0.05$ vs. CG.

Table 3: Hemodynamic and autonomic parameters at baseline and after 10 weeks.

Variables	CG ($n = 11$)		Δ (ES)	TG ($n = 11$)		Δ (ES)
	Baseline	Post		Baseline	Post	
Hemodynamics						
SBP (mmHg)	133 (94-139)	129 (99-140)	0.3 (-0.0)	130 (94–139)	121 (95–137)	-5.6 (0.4)
DBP (mmHg)	79.2 ± 11.9	79.8 ± 10.9	0.6 (-0.1)	72.5 ± 14.4	71.6 ± 12.4	-0.9 (0.1)
HR (bpm)	74.8 ± 14.4	76.5 ± 11.2	1.7 (-0.1)	71.5 ± 11.9	65.1 ± 9.5†	-6.4 (0.6)
DP (mmHg × bpm)	9938.1 ± 2226.8	9949.5 ± 1852.6	10.9 (0)	8890.6 ± 1607.1	7722.0 ± 1375.2†	-1168.0 (0.8)
Autonomics						
Time domain indexes						
SDNN (ms)	20.4 ± 8.2	19.4 ± 6.8	-1.0 (0.1)	23.9 ± 7.5	33.3 ± 10.8∗†	9.4 (-1.0)
rMSSD (ms)	17.2 ± 9.9	12.7 ± 5.2	-4.5 (0.6)	16.6 ± 8.3	23.7 ± 11.6∗†	7.1 (-0.7)
Nonlinear indexes						
SD1 (ms)	12.2 ± 7.0	9.0 ± 3.7	-3.2 (0.6)	11.7 ± 5.8	16.8 ± 8.2∗†	5.1 (-0.7)
SD2 (ms)	25.7 ± 10.5	25.7 ± 9.6	0 (0)	31.3 ± 10.5	43.1 ± 15.9∗†	11.8 (-0.9)

SD: standard deviation of the mean; ES: effect size; CG: control group; TG: training group; SBP: systolic blood pressure; DBP: diastolic blood pressure; DP: double product; SDNN: selected standard deviation of normal R-R intervals; rMSSD: square root of the mean squared differences between adjacent normal R-R intervals, expressed in ms; SD1: short variation of R-R interval; SD2: represents HRV in long-term records. Data are shown as mean ± SD or median; $^{*}P < 0.05$ vs. baseline; $^{\dagger}P < 0.05$ vs. CG.

The level of significance was set at alpha = 5% ($P < 0.05$), and all analyses were performed using the GraphPad Prism 7.00 (San Diego, CA).

3. Results

Twenty-seven volunteers were recruited and accepted to be evaluated for eligibility. Three candidates declined to participate, while two decided to engage in another exercise program, leaving a total of 22 stroke survivors who were randomized into two groups (i.e., CG [$N = 11$] or TG [$N = 11$]). There were no withdrawals from either group (Figure 1).

The baseline characteristics of the study participants are shown in Table 1. The mean time since stroke was 5 years. The mean age of the whole sample was 62.2 ± 10.8 years and the mean body mass index (BMI) value was 24.8 ± 3.0 (kg/m^2). The most common pharmacological therapy was diuretics, followed by statins, angiotensin-converting enzyme inhibitor (ACEi), and antidiabetic agents, which can be explained by the high prevalence of hypertension and type 2 diabetes mellitus observed in our sample. No significant differences were observed among the groups.

3.1. Physical Function. Physical function is shown in Table 2. No significant differences were observed among the groups at baseline. After 8 weeks, TG improved 10MWT ($P = 0.0001$, $\Delta = -38.3\%$, $d = -0.8$), sit-to-stand ($P = 0.0001$, $\Delta = -30.6\%$, $d = -1.9$), and TUG tests ($P = 0.0001$, $\Delta = -23.0\%$, $d = -0.7$). In contrast, a significant reduction in IHGPL ($P = 0.017$, $\Delta = -24.0\%$, $d = -0.3$) and IHGNPL ($P = 0.016$, $\Delta = -16.8\%$, $d = -0.4$) was observed in the CG. Between-group comparisons indicated better TUG ($P = 0.042$, $\Delta = -28.2\%$; $d = -1.2$) and sit-to-stand ($P = 0.011$, $\Delta = -29.1\%$, $d = -1.5$) performances in TG when compared to CG. A larger ES classification was attributed to changes on 10MWT in TG in comparison to CG ($d = -0.9$).

3.2. Hemodynamic Parameters. Hemodynamic parameters are shown in Table 3. No significant differences were

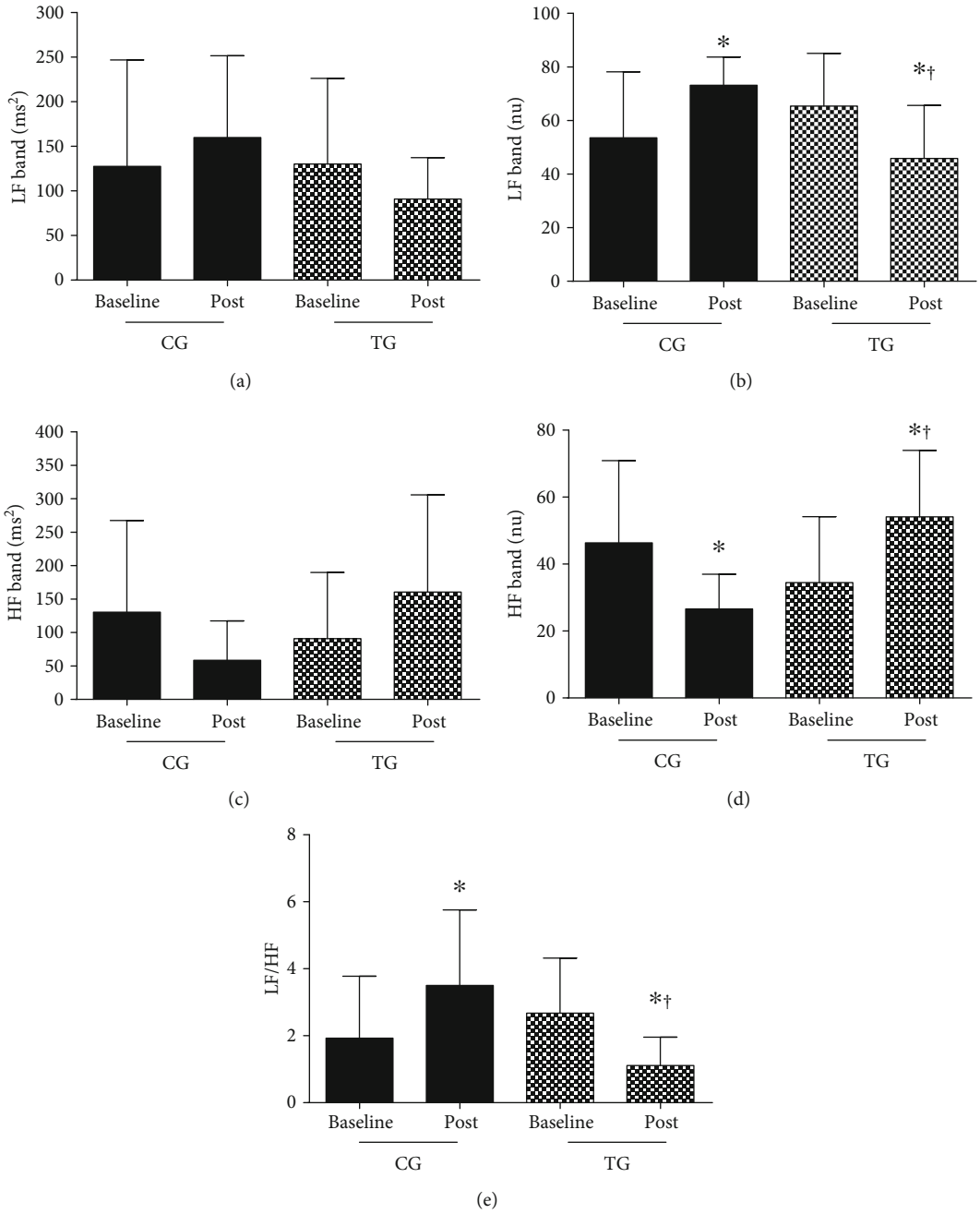

Figure 3: Cardiac autonomic modulation. (a) Low-frequency band (LF, ms^2). (b) Low-frequency band (LF, nu). (c) High-frequency band (HF, ms^2). (d) High-frequency band (HF, nu). (e) Autonomic balance (LF/HF). Data are shown as mean ± SD or median. CG: control group; TG: training group; LF: low-frequency band; HF: high-frequency band; $^*P < 0.05$ in comparison to baseline; $^\dagger P < 0.05$ in comparison to CG at the same moment.

observed among the groups at baseline. SBP and DBP remained unchanged in both TG and CG over the experimental period. In contrast, heart rate ($P = 0.047$, $\Delta = -11.5$, $d = -0.6$) and DP ($P = 0.011$, $\Delta = -13.1\%$, $d = -1.4$) were significantly reduced in TG in comparison with CG after 8 weeks ($P = 0.047$, $\Delta = -11.5$, $d = -0.6$).

3.3. Cardiac Autonomic Modulation. Cardiac autonomic modulation parameters are shown in Table 3 and Figure 3. No significant differences were observed among the groups at baseline. SDNN ($P = 0.0001$, $\Delta = 39.3\%$, $d = 1.0$), rMSSD ($P = 0.014$, $\Delta = 30\%$, $d = 0.70$), SD1 ($P = 0.014$, $\Delta = 30.4\%$, $d = 0.71$), SD2 ($P = 0.002$, $\Delta = 27.3\%$, $d = 0.87$), LF band in ms^2 (Figure 3(a), no difference was observed), LF band in nu (Figure 3(b)) ($P = 0.004$, $\Delta = -29.9\%$, $d = -1.5$), HF band in ms^2 (Figure 3(c), no difference was observed), HF in nu (Figure 3(d)) ($P = 0.003$, $\Delta = 57.0\%$, $d = 1.5$), and LF/HF ratio (Figure 3(e)) ($P = 0.004$, $\Delta = -1.56\%$, $d = -1.5$) were improved in response to exercise when compared to baseline values and CG. On the other hand, elevated LF

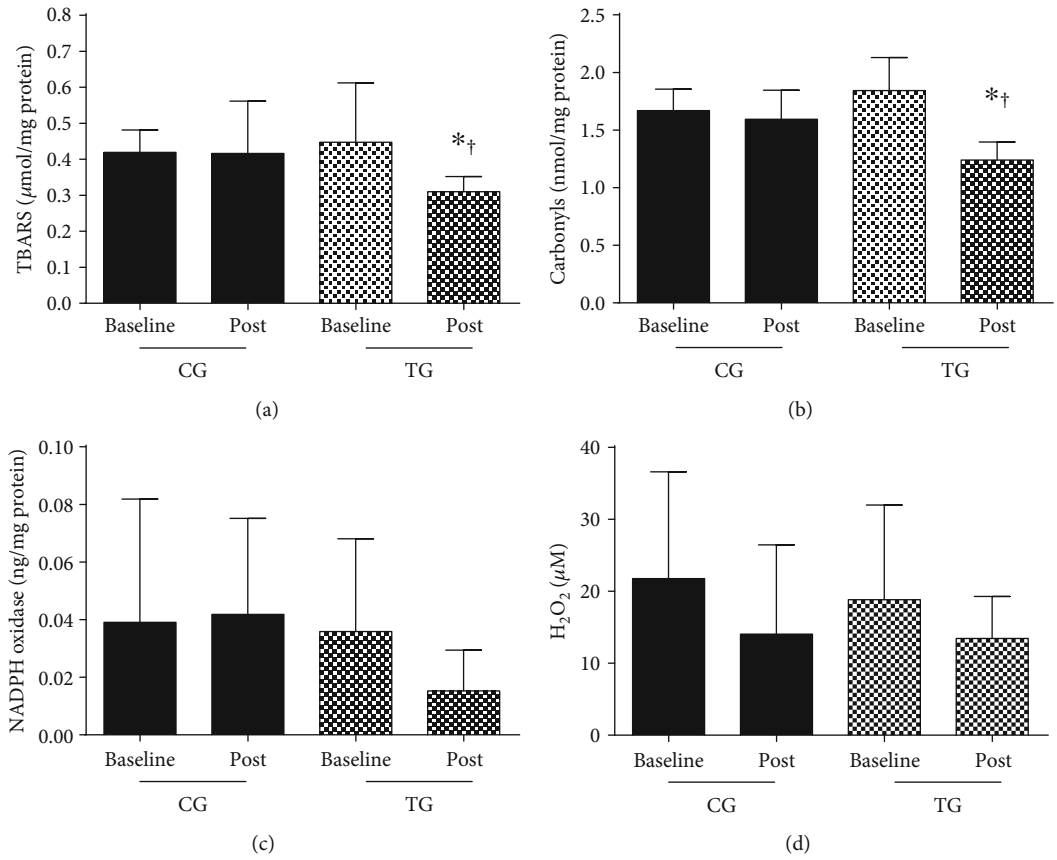

Figure 4: Oxidant markers. (a) Thiobarbituric acid reactive substances. (b) Carbonyls. (c) NADPH oxidase. (d) Nitrite peroxide (H_2O_2). Data are shown as mean ± SD. CG: control group; TG: training group. $^*P < 0.05$ in comparison to baseline; $^\dagger P < 0.05$ in comparison to CG at the same moment.

(nu) ($P = 0.006$, $\Delta = 36.7\%$, $d = 1.5$) and reduced HF (nu) ($P = 0.006$, $\Delta = -42.6\%$, $d = -1.5$) were observed in CG in comparison to baseline.

3.4. Oxidative Stress Markers. Oxidative stress markers are shown in Figures 4 and 5. No significant differences were observed among the groups at baseline. TG improved TBARS (Figure 4(a); $P = 0.0428$), carbonyls (Figure 4(b); $P < 0.0001$), and SOD (Figure 5(a); $P = 0.0001$) levels in comparison to baseline and CG. CAT (Figure 5(b); $P = 0.3219$) and nitrite (Figure 5(c); $P = 0.5662$) levels were unchanged over the experimental period.

4. Discussion

The main findings of the present study indicate that 8-week dynamic resistance training protocol with elastic bands improved physical function, hemodynamic parameters, autonomic modulation, and oxidative markers in stroke patients. In contrast, a significant reduction in upper-limb muscle strength (i.e., IHGPL and IHGNPL) was observed in CG.

Although many studies [28–30] have investigated the effects of RT on the physical of stroke survivors, results are still not conclusive. Supporting our findings, Hill et al. [30] observed significative improvements in the gait ability and TUG performance of stroke patients after a lower-limb high-intensity RT protocol. On the other hand, no RT effects in gait velocity were reported in other protocols [28, 29, 31].

A possible explanation for the differences among the studies may that concentric contractions in the present study were performed as fast as possible, given that many aspects of the physical function seem to be more closely associated with muscle power than muscle strength [32] and greater gains in physical performance have been observed after power training in comparison to traditional RT [32–34].

These findings have important clinical and public health implications since better physical performance in patients with stroke is associated with a higher likelihood of social integration, independence to perform ADL, and better quality of life [35–37]. Besides that, stroke survivors with poor physical function are more likely to experience a recurrent stroke and die in a short-term interval after the first event in comparison with those with proper physical function [38, 39].

Another significant finding of the present study is regarding the importance of upper-limb resistance exercises to stroke survivors since IHGPL and IHGNPL were significantly reduced in CG, while it remained unchanged in TG. IHG has been used as an essential measurement of muscle strength, and it is well-accepted as part of the assessment of sarcopenia [40, 41]. Nevertheless, IHG is

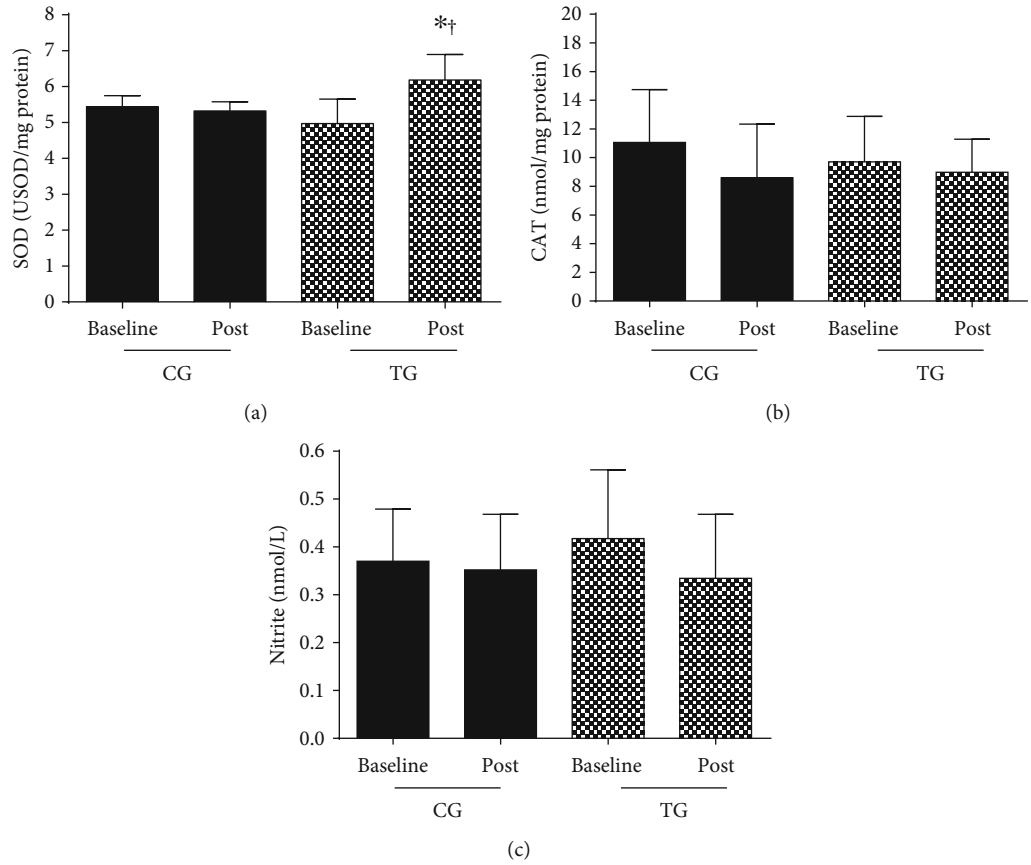

Figure 5: Antioxidant markers and plasma nitrite concentration. (a) Superoxide dismutase (SOD). (b) Catalase (CAT). (c) Nitrite. Data are shown as mean ± SD. CG: control group; TG: training group. $^{*}P < 0.05$ in comparison to baseline; $^{\dagger}P < 0.05$ in comparison to CG at the same moment.

strongly associated with upper-limb muscle strength in stroke, and it has a critical role in the physical performance of this population [3, 38].

No significant differences in SBP ($\Delta = -10.41$ mmHg) and DBP ($\Delta = -8.16$ mmHg) were observed between TG and CG after 8 weeks. These findings are supported by prior studies that observed reduced blood pressures in hypertensive people after exercise training [42–44] and indicate that our exercise protocol may be associated with a significant reduction in cardiovascular and restroke risk [42, 45].

A recent meta-analysis of 12 studies evaluated the effects of aerobic exercises on blood pressure values of stroke survivors and found reductions of 4.3 mmHg and 2.5 mmHg in SBP and DBP, respectively, after the intervention [43]. Similarly, most randomized clinical trials investigating pharmacological therapy showed blood reductions of approximately 5 mmHg for SBP and 4 mmHg for DBP [39, 45]. Therefore, RT effects on blood pressure of stroke survivors are favorably similar or even more substantial than the impact of aerobic exercise and pharmacological therapy, suggesting that RT may be an essential tool in the management of blood pressure and cardiovascular risk in patients with stroke [42–44].

Cardiac autonomic modulation and oxidative stress markers were investigated as two possible mechanisms associated with blood pressure lowering in response to RT. Our findings suggest that RT improved vagal modulation (i.e., rMSSD, SD1, SD2, HF) and sympathovagal balance (i.e., LF/HF ratio).

Notably, changes in cardiac autonomic modulation are not commonly observed in response to RT protocol [44, 46, 47], while substantial evidence have reported this phenomenon after aerobic training [47, 48]. A hypothesis that may account for our findings lies in the dynamic characteristic of our RT protocol, in which absolute rest intervals between sets and exercises were not provided, so that the cardiovascular and neuromuscular systems were stimulated simultaneously throughout each session [49]. In this context, our RT protocol had an aerobic component able to improve cardiac autonomic modulation, as usually occurs with the practice of aerobic training [47, 48].

Although exercise may acutely increase reactive oxygen species, a compensatory mechanism seems to occur after chronic exercise training, in which exercise training upregulatesthe amount and efficiency of antioxidant enzymes [48]. Findings of the present study support this hypothesis by observing increased SOD levels and reduced TBARS and carbonyls levels after RT.

There are some limitations in the present study which should be addressed by future investigations to confirm and expand our findings, as the short period of intervention and the absence of muscle strength assessments of all trained

muscle groups. Our sample size is also a limitation of our study since a post hoc sample size calculation estimated that about 14 participants in each group would be needed to detect improvements in physical function, hemodynamic parameters, and oxidative markers considering within- and between-group comparisons, with 80% power at the 5% significance level. Finally, unexpected changes on upper-limb muscle strength (i.e., IHGPL and IHGNPL) and autonomic modulation (i.e., RMSSD and SD1) were observed in CG. Although pain (Terwee et al., 2006), white matter lesions (Zerna et al., 2018), or even the presence of other comorbidities may explain the substantial declines in IHGPL and IHGNPL, as well as psychosocial stress may impact cardiac modulation (Lucini et al., 2005), future studies are still needed to confirm our findings.

5. Conclusions

Our findings indicate that an 8-week dynamic resistance training protocol with elastic bands improved physical function, hemodynamic parameters, autonomic modulation, and oxidative stress markers in chronic ischemic stroke survivors.

Data Availability

The data used in this study is available from the corresponding author upon request.

Conflicts of Interest

The authors declare that they have no conflict of interest.

Authors' Contributions

Bruno Bavaresco Gambassi and Hélio José Coelho-Junior contributed equally to this work.

Acknowledgments

Bruno Bavaresco Gambassi and Hélio José Coelho-Junior are grateful to the Conselho Nacional de Desenvolvimento Científico e Tecnológico (CNPq) and Coordenação de Aperfeiçoamento de Pessoal de Nível Superior (CAPES) for their scholarships. Bruno Rodrigues received financial support from Fundação de Amparo à Pesquisa do Estado de São Paulo (FAPESP; processo n. #2017/21320-4). Kátia De Angelis and Bruno Rodrigues received financial support from CNPq-BPQ.

References

[1] E. J. Benjamin, S. S. Virani, C. W. Callaway et al., "Heart disease and stroke statistics—2018 update: a report from the American Heart Association," *Circulation*, vol. 137, no. 12, pp. e67–492, 2018.

[2] C. English, H. McLennan, K. Thoirs, A. Coates, and J. Bernhardt, "Loss of skeletal muscle mass after stroke: a systematic review," *International Journal of Stroke*, vol. 5, no. 5, pp. 395–402, 2010.

[3] H. J. Coelho Junior, B. B. Gambassi, T. A. Diniz et al., "Inflammatory mechanisms associated with skeletal muscle sequelae after stroke: role of physical exercise," *Mediators of Inflammation*, vol. 2016, Article ID 3957958, 19 pages, 2016.

[4] M. T. Farzadfard, M. S. Sheikh Andalibi, A. G. Thrift et al., "Long-term disability after stroke in Iran: evidence from the Mashhad Stroke Incidence Study," *International Journal of Stroke*, vol. 14, no. 1, pp. 44–47, 2019.

[5] S. E. Khoshnam, W. Winlow, M. Farzaneh, Y. Farbood, and H. F. Moghaddam, "Pathogenic mechanisms following ischemic stroke," *Neurological Sciences*, vol. 38, no. 7, pp. 1167–1186, 2017.

[6] T. Lees, F. Shad-Kaneez, A. M. Simpson, N. T. Nassif, Y. Lin, and S. Lal, "Heart rate variability as a biomarker for predicting stroke, post-stroke complications and functionality," *Biomarker Insights*, vol. 13, article 117727191878693, 2018.

[7] J. V. F. Grilletti, K. B. Scapini, N. Bernardes et al., "Impaired baroreflex sensitivity and increased systolic blood pressure variability in chronic post-ischemic stroke," *Clinics*, vol. 73, article e253, 2018.

[8] J. F. Scheitz, C. H. Nolte, W. Doehner, V. Hachinski, and M. Endres, "Stroke-heart syndrome: clinical presentation and underlying mechanisms," *The Lancet Neurology*, vol. 17, no. 12, pp. 1109–1120, 2018.

[9] M. Y. Pang, J. J. Eng, A. S. Dawson, and S. Gylfadóttir, "The use of aerobic exercise training in improving aerobic capacity in individuals with stroke: a meta-analysis," *Clinical Rehabilitation*, vol. 20, no. 2, pp. 97–111, 2006.

[10] S. Mehta, S. Pereira, R. Viana et al., "Resistance training for gait speed and total distance walked during the chronic stage of stroke: a meta-analysis," *Topics in Stroke Rehabilitation*, vol. 19, no. 6, pp. 471–478, 2012.

[11] W. Kraemer, *Sports NR-M and science in, 2004 undefined. Fundamentals of resistance training: progression and exercise prescription*August 2018, http://www.exercicescorriges.com/i_348104.pdf.

[12] B. B. Gambassi, H. J. Coelho-Junior, P. A. Schwingel et al., "Resistance training and stroke: a critical analysis of different training programs," *Stroke Research and Treatment*, vol. 2017, Article ID 4830265, 11 pages, 2017.

[13] G. Hendrey, A. E. Holland, B. F. Mentiplay, R. A. Clark, and G. Williams, "Do trials of resistance training to improve mobility after stroke adhere to the American College of Sports Medicine guidelines? A systematic review," *Archives of Physical Medicine and Rehabilitation*, vol. 99, no. 3, pp. 584–597, 2018.

[14] S. Shah, F. Vanclay, and B. Cooper, "Improving the sensitivity of the Barthel Index for stroke rehabilitation," *Journal of Clinical Epidemiology*, vol. 42, no. 8, pp. 703–709, 1989.

[15] J. A. Baecke, J. Burema, and J. E. Frijters, "A short questionnaire for the measurement of habitual physical activity in epidemiological studies," *The American Journal of Clinical Nutrition*, vol. 36, no. 5, pp. 936–942, 1982.

[16] B. Bavaresco Gambassi, M. D. Lopes dos Santos, and F. J. Furtado Almeida, "Basic guide for the application of the main variables of resistance training in elderly," *Aging Clinical and Experimental Research*, vol. 31, no. 7, pp. 1019-1020, 2019.

[17] C. Foster, J. A. Florhaug, J. Franklin et al., "A new approach to monitoring exercise training," *Journal of Strength and Conditioning Research*, vol. 15, no. 1, pp. 109–115, 2001.

[18] Colado J and NT-TJ of S&, 2008 U, *Effects of a short-term resistance program using elastic bands versus weight machines for sedentary middle-aged women*August 2018, https://journals.lww.com/nsca-jscr/Fulltext/2008/09000/Effects_of_a_Short_Term_Resistance_Program_Using.9.aspx.

[19] H. Coelho Junior, M. Uchida, I. O. Goncalves et al., "Age- and gender-related changes in physical function in community-dwelling Brazilian adults aged 50-102 years," *Journal of Geriatric Physical Therapy*, 2019, No prelo.

[20] H. J. Coelho Junior, B. Rodrigues, S. S. Aguiar et al., "Hypertension and functional capacities in community-dwelling older women: a cross-sectional study," *Blood Pressure*, vol. 26, no. 3, pp. 156–165, 2017.

[21] J. M. Guralnik, E. M. Simonsick, L. Ferrucci et al., "A short physical performance battery assessing lower extremity function: association with self-reported disability and prediction of mortality and nursing home admission," *Journal of Gerontology*, vol. 49, no. 2, pp. M85–M94, 1994.

[22] D. Podsiadlo and S. Richardson, "The Timed "Up & Go": A Test of Basic Functional Mobility for Frail Elderly Persons," *Journal of the American Geriatrics Society*, vol. 39, no. 2, pp. 142–148, 1991.

[23] H. J. Coelho-Junior, B. Rodrigues, I. D. O. Gonçalves, R. Y. Asano, M. C. Uchida, and E. Marzetti, "The physical capabilities underlying timed "Up and Go" test are time-dependent in community-dwelling older women," *Experimental Gerontology*, vol. 104, pp. 138–146, 2018.

[24] A. C. Cuckson, A. Reinders, H. Shabeeh, and A. H. Shennan, "Validation of the Microlife BP 3BTO-A oscillometric blood pressure monitoring device according to a modified British Hypertension Society protocol," *Blood Pressure Monitoring*, vol. 7, no. 6, pp. 319–324, 2002.

[25] D. J. Feriani, H. J. Coelho-Júnior, K. B. Scapini et al., "Effects of inspiratory muscle exercise in the pulmonary function, autonomic modulation, and hemodynamic variables in older women with metabolic syndrome," *Journal of Exercise Rehabilitation*, vol. 13, no. 2, pp. 218–226, 2017.

[26] O. H. Lowry, N. J. Rosebrough, A. L. Farr, and R. J. Randall, "Protein measurement with the Folin phenol reagent," *The Journal of Biological Chemistry*, vol. 193, no. 1, pp. 265–275, 1951.

[27] A. M. Jacomini, D. da Silva Dias, J. de Oliveira Brito et al., "Influence of estimated training status on anti and pro-oxidant activity, nitrite concentration, and blood pressure in middle-aged and older women," *Frontiers in Physiology*, vol. 8, p. 122, 2017.

[28] M. M. Ouellette, N. K. LeBrasseur, J. F. Bean et al., "High-intensity resistance training improves muscle strength, self-reported function, and disability in long-term stroke survivors," *Stroke*, vol. 35, no. 6, pp. 1404–1409, 2004.

[29] M.-J. Lee, S. L. Kilbreath, M. F. Singh et al., "Comparison of Effect of Aerobic Cycle Training and Progressive Resistance Training on Walking Ability After Stroke: A Randomized Sham Exercise–Controlled Study," *Journal of the American Geriatrics Society*, vol. 56, no. 6, pp. 976–985, 2008.

[30] T. R. Hill, T. I. Gjellesvik, P. M. R. Moen et al., "Maximal strength training enhances strength and functional performance in chronic stroke survivors," *American Journal of Physical Medicine & Rehabilitation*, vol. 91, no. 5, pp. 393–400, 2012.

[31] T. A. Miszko, M. E. Cress, J. M. Slade, C. J. Covey, S. K. Agrawal, and C. E. Doerr, "Effect of strength and power training on physical function in community-dwelling older adults," *The Journals of Gerontology Series A: Biological Sciences and Medical Sciences*, vol. 58, no. 2, pp. M171–M175, 2003.

[32] K. F. Reid and R. A. Fielding, "Skeletal muscle power: a critical determinant of physical functioning in older adults," *Exercise and Sport Sciences Reviews*, vol. 40, no. 1, pp. 4–12, 2012.

[33] R. Ramírez-Campillo, A. Castillo, C. I. de la Fuente et al., "High-speed resistance training is more effective than low-speed resistance training to increase functional capacity and muscle performance in older women," *Experimental Gerontology*, vol. 58, pp. 51–57, 2014.

[34] M. Almkvist Muren, M. Hütler, and J. Hooper, "Functional capacity and health-related quality of life in individuals post stroke," *Topics in Stroke Rehabilitation*, vol. 15, no. 1, pp. 51–58, 2008.

[35] S. Baseman, K. Fisher, L. Ward, and A. Bhattacharya, "The relationship of physical function to social integration after stroke," *Journal of Neuroscience Nursing*, vol. 42, no. 5, pp. 237–244, 2010.

[36] I. J. Hubbard, K. Vo, P. M. Forder, and J. E. Byles, "Stroke, physical function, and death over a 15-year period in older Australian women," *Stroke*, vol. 47, no. 4, pp. 1060–1067, 2016.

[37] A. J. Cruz-Jentoft, G. Bahat, J. Bauer et al., "Sarcopenia: revised European consensus on definition and diagnosis," *Age and Ageing*, vol. 48, no. 1, pp. 16–31, 2019.

[38] E. Ekstrand, J. Lexell, and C. Brogårdh, "Grip strength is a representative measure of muscle weakness in the upper extremity after stroke," *Topics in Stroke Rehabilitation*, vol. 23, no. 6, pp. 400–405, 2016.

[39] P. Rashid, J. Leonardi-Bee, and P. Bath, "Blood pressure reduction and secondary prevention of stroke and other vascular events," *Stroke*, vol. 34, no. 11, pp. 2741–2748, 2003.

[40] A. J. Cruz-Jentoft, J. P. Baeyens, J. M. Bauer et al., "Sarcopenia: European consensus on definition and diagnosis: report of the European Working Group on Sarcopenia in Older People," *Age and Ageing*, vol. 39, no. 4, pp. 412–423, 2010.

[41] H. J. Coelho-Junior, E. R. Villani, R. Calvani et al., "Sarcopenia-related parameters in adults with Down syndrome: a cross-sectional exploratory study," *Experimental Gerontology*, vol. 119, pp. 93–99, 2019.

[42] H. J. Coelho-Júnior, I. O. Gonçalves, N. O. S. Câmara et al., "Non-periodized and daily undulating periodized resistance training on blood pressure of older women," *Frontiers in Physiology*, vol. 9, p. 1525, 2018.

[43] C. Wang, J. Redgrave, M. Shafizadeh, A. Majid, K. Kilner, and A. N. Ali, "Aerobic exercise interventions reduce blood pressure in patients after stroke or transient ischaemic attack: a systematic review and meta-analysis," *British Journal of Sports Medicine*, no. article 098903, 2018.

[44] B. Gambassi, P. Schwingel, F. Mesquita et al., "Influence of resistance training practice on autonomic cardiac control of hypertensive elderly women," September 2019, https://www.researchgate.net/profile/Candida_Alves3/publication/330740598_Influence_of_resistance_training_practice_on_autonomic_cardiac_control_of_hypertensive_elderly_women/links/5c51de5e299bf12be3ee905b/Influence-of-resistance-training-practice-on-autonomic-cardiac-control-of-hypertensive-elderly-women.pdf.

[45] A. H. Katsanos, A. Filippatou, E. Manios et al., "Blood pressure reduction and secondary stroke prevention: a systematic

review and metaregression analysis of randomized clinical trials," *Hypertension*, vol. 69, no. 1, pp. 171–179, 2017.

[46] T. ACM, R. C. Melo, R. J. Quitério, E. Silva, and A. M. Catai, "The effect of eccentric strength training on heart rate and on its variability during isometric exercise in healthy older men," *European Journal of Applied Physiology*, vol. 105, no. 2, pp. 315–323, 2009.

[47] E. L. Melanson and P. S. Freedson, "The effect of endurance training on resting heart rate variability in sedentary adult males," *European Journal of Applied Physiology*, vol. 85, no. 5, pp. 442–449, 2001.

[48] C. M. Friedenreich, V. Pialoux, Q. Wang et al., "Effects of exercise on markers of oxidative stress: an ancillary analysis of the Alberta Physical Activity and Breast Cancer Prevention Trial," *BMJ Open Sport & Exercise Medicine*, vol. 2, no. 1, article e000171, 2016.

[49] M. R. Moraes, R. F. P. Bacurau, J. D. S. Ramalho et al., "Increase in kinins on post-exercise hypotension in normotensive and hypertensive volunteers," *Biological Chemistry*, vol. 388, no. 5, pp. 533–540, 2007.

Hindawi
Oxidative Medicine and Cellular Longevity
Volume 2019, Article ID 6239058, 12 pages
https://doi.org/10.1155/2019/6239058

Clinical Study

Infrared Low-Level Laser Therapy (Photobiomodulation Therapy) before Intense Progressive Running Test of High-Level Soccer Players: Effects on Functional, Muscle Damage, Inflammatory, and Oxidative Stress Markers—A Randomized Controlled Trial

Shaiane Silva Tomazoni,[1] Caroline dos Santos Monteiro Machado,[2,3] Thiago De Marchi,[4] Heliodora Leão Casalechi,[2] Jan Magnus Bjordal,[1] Paulo de Tarso Camillo de Carvalho,[3] and Ernesto Cesar Pinto Leal-Junior[2,3]

[1]*Physiotherapy Research Group, Department of Global Public Health and Primary Care, University of Bergen, Bergen, Norway*
[2]*Laboratory of Phototherapy and Innovative Technologies in Health (LaPIT), Nove de Julho University, São Paulo, SP, Brazil*
[3]*Postgraduate Program in Rehabilitation Sciences, Nove de Julho University, São Paulo, SP, Brazil*
[4]*Faculty Cenecista of Bento Gonçalves (CNEC), Bento Gonçalves, RS, Brazil*

Correspondence should be addressed to Ernesto Cesar Pinto Leal-Junior; ernesto.leal.junior@gmail.com

Received 20 February 2019; Accepted 9 October 2019; Published 16 November 2019

Guest Editor: José R. Pinto

The effects of preexercise photobiomodulation therapy (PBMT) to enhance performance, accelerate recovery, and attenuate exercise-induced oxidative stress were still not fully investigated, especially in high-level athletes. The aim of this study was to evaluate the effects of PBMT (using infrared low-level laser therapy) applied before a progressive running test on functional aspects, muscle damage, and inflammatory and oxidative stress markers in high-level soccer players. A randomized, triple-blind, placebo-controlled crossover trial was performed. Twenty-two high-level male soccer players from the same team were recruited and treated with active PBMT and placebo. The order of interventions was randomized. Immediately after the application of active PBMT or placebo, the volunteers performed a standardized high-intensity progressive running test (ergospirometry test) until exhaustion. We analyzed rates of oxygen uptake ($VO_{2\ max}$), time until exhaustion, and aerobic and anaerobic threshold during the intense progressive running test. Creatine kinase (CK) and lactate dehydrogenase (LDH) activities, levels of interleukin-1β (IL-1-β), interleukin-6 (IL-6), and tumor necrosis factor alpha (TNF-α), levels of thiobarbituric acid (TBARS) and carbonylated proteins, and catalase (CAT) and superoxide dismutase (SOD) activities were measured before and five minutes after the end of the test. PBMT increased the $VO_{2\ max}$ (both relative and absolute values—$p < 0.0467$ and $p < 0.0013$, respectively), time until exhaustion ($p < 0.0043$), time ($p < 0.0007$) and volume ($p < 0.0355$) in which anaerobic threshold happened, and volume in which aerobic threshold happened ($p < 0.0068$). Moreover, PBMT decreased CK ($p < 0.0001$) and LDH ($p < 0.0001$) activities. Regarding the cytokines, PBMT decreased only IL-6 ($p < 0.0001$). Finally, PBMT decreased TBARS ($p < 0.0001$) and carbonylated protein levels ($p < 0.01$) and increased SOD ($p < 0.0001$)and CAT ($p < 0.0001$) activities. The findings of this study demonstrate that preexercise PBMT acts on different functional aspects and biochemical markers. Moreover, preexercise PBMT seems to play an important antioxidant effect, decreasing exercise-induced oxidative stress and consequently enhancing athletic performance and improving postexercise recovery. This trial is registered with Clinicaltrials.gov NCT03803956.

1. Introduction

In soccer, as well as in other high-level sport activities, players experience acute muscle fatigue in the hours or even days following a single match [1, 2]. Since the number of competitive matches per season is very high (up to 65 to 76 matches per season) and the time to recovery between two successive matches may be insufficient (around 72 to 96 hours), players may experience also chronic fatigue [1–3]. The development of muscle fatigue is a complex and multifaceted process that may be associated with muscular oxidative stress [4] caused by increased reactive oxygen species (ROS) production after strenuous exercise [5, 6]. The process of fatigue leads to a decline in physical performance and injury in some cases [1–3]; therefore, it is indispensable that athlete recovery be as fast and effective as possible [7].

A recovery strategy involves the implementation of a single technique or a combination of techniques in order to enhance and accelerate recovery after matches and to best prepare the athlete for the next match, besides potentially reducing the risk of injuries [7, 8]. Among them, the most widely used are nutritional strategies [9–12], active recovery [13, 14], cold water immersion [15, 16], compression garments [17], and massage [18]. However, the evidence about the effectiveness of some of these strategies to recovery is still conflicting [17–19].

Some ergogenic agents associated with recovery strategies may be used for enhanced performance in high-level sports activities [20]. Supplements such as creatine are widely used for this purpose [21]. Currently, increasing evidence has demonstrated the potential of photobiomodulation therapy (PBMT) as an ergogenic agent, since it is able to enhance athletic performance, as well as improve postexercise recovery [22–29].

PBMT is a nonthermal therapy that uses nonionizing light sources, such as lasers, light-emitting diodes (LEDs), and broadband light from the visible to the infrared spectrum, to interact with chromophores and trigger photochemical and photophysical reactions in different tissues [30]. Studies have demonstrated the positive effects of PBMT in improving biomarkers related to muscle damage [31], modulating inflammation [32, 33], and decreasing oxidative stress [33, 34]. Moreover, it has been shown that PBMT is able to increase the number of repetitions, time until exhaustion, and peak torque (strength) if applied before an exercise session [31]. Despite the existence of data reporting neutral effects of PBMT on athletic performance, this absence of benefit is often related to the lack of adherence to the optimal or optimized parameters and/or to the clinical and scientific recommendations to apply the therapy [30, 31]. Moreover, the current evidence points to beneficial effects of this therapy (for more details, read the clinical and scientific recommendations authored by Leal-Junior et al. [30] and the systematic review with meta-analysis authored by Vanin et al. [31]).

In recent years, there was an exponential increase of evidence about the use of PBMT for enhancing performance and also accelerating postexercise recovery. However, some aspects have not been fully and/or well established so far. There are still few studies that have been performed in order to investigate the effects of PBMT as an ergogenic agent in high-level athletes [7, 32, 33, 35–37], and studies on the effects of PBMT on aspects related to aerobic endurance, for instance, are even more scarce [36]. In addition, although some studies have investigated the effects of preexercise PBMT on oxidative stress [33–35], the evidence remains conflicting, and the role of the therapy as redox intervention to enhance performance and postexercise recovery is still not well understood.

To the best of our knowledge, there are no studies evaluating the acute effects of PBMT on aerobic capacity, as well as on markers of muscle damage, inflammation, and oxidative stress of high-level soccer players. Moreover, differently to another previous study investigating the effects of infrared low-level laser therapy PBMT in a progressive running test in healthy untrained individuals [34], our study used an optimized dose [32] and optimized power output [33] previously tested in high-level soccer athletes.

Then, we hypothesized that preexercise PBMT, with optimized parameters, can increase aerobic capacity and decrease muscle damage and inflammation through decreased oxidative stress and increased antioxidant activity.

Therefore, we performed this study aiming to evaluate the effects of PBMT (using infrared low-level laser therapy) applied before a progressive running test on functional aspects, muscle damage, and inflammatory and oxidative stress markers in high-level soccer players.

2. Methods

2.1. Study Design and Ethics Statements. A randomized, triple-blind (evaluators, therapist, and volunteers), placebo-controlled crossover trial was performed at the Laboratory of Phototherapy and Innovative Technologies in Health (LaPIT), Nove de Julho University, São Paulo, Brazil. This trial received approval from the institutional Research Ethics Committee (Protocol No. 397774/2011), and the protocol has been prospectively registered on Clinicaltrials.gov (NCT03803956). There were no deviations from the registered protocol.

2.2. Characterization of Sample. Twenty-two high-level male soccer players from the same team were recruited. The sample size was calculated based on a previous trial conducted by our research group [34], in which the primary outcome (oxygen uptake relative to body mass—$VO_{2\ max}$ relative), the PBMT device, and the standardized progressive running exercise protocol were the same employed in our study. The sample size was calculated considering a β of 20% and an α of 5%. The decision to recruit volunteers from the same team was made to enhance the homogeneity of the sample.

2.3. Inclusion Criteria

(i) High-level soccer players

(ii) Age between 18 and 35 years

(iii) Male gender

(iv) Minimum of 80% participation in team practice sessions in the last two months

(v) Agreement to participate through signed statement of informed consent

2.4. Exclusion Criteria

(i) History of musculoskeletal injury to hips, knees, or ankles in the previous 2 months

(ii) Use of pharmacological agents for chronic injuries/diseases

(iii) Smokers and alcoholics

(iv) Occurrence of musculoskeletal injury during the study

(v) Any change in practice routine in relation to the rest of the team during the study

(vi) Any change in nutritional routine (including supplements intake) during the study

2.5. Randomization and Blinded Procedures. The order of intervention was randomized. We generated codes through a website (random.org) to ensure that 50% of the volunteers received the active intervention and 50% of the volunteers received the placebo intervention at the first stage, in order to counterbalance participants between the two interventions tested (active PBMT and placebo PBMT) during execution of the two stages. During the second stage, volunteers received the opposite treatment compared to their first stage. Randomization was performed by a participating researcher not involved with the recruitment or evaluation of volunteers. This same researcher was responsible for programming the PBMT device according to the result of the randomization and he/she was instructed not to disclose the programmed intervention to the therapist, the assessors, or any of the volunteers and other researchers involved in the study until its completion. The PBMT device used in the present study emitted the same sounds, regardless of the programmed mode (active or placebo PBMT), and the infrared light was not visible. Concealed allocation was achieved through the use of sequentially numbered, sealed, and opaque envelopes.

2.6. Interventions. The active PBMT and placebo PBMT were performed using the same device and the irradiated sites were the same in both therapies.

2.6.1. Photobiomodulation Therapy. A five-diode cluster laser device was used. The optical power was verified before irradiation in each volunteer using a Thorlabs thermal power meter (Model S322C; Thorlabs, Newton, NJ, USA). PBMT was applied using a dose of 10 J per diode (50 J per site) as previously optimized by Aver Vanin et al. [32], and with a power output of 100 mW also previously optimized by De Oliveira et al. [33]. The full description of PBMT parameters is provided in Table 1. PBMT was performed in direct contact with the skin at nine different sites of the knee extensor muscles (three medial, three lateral, and three central sites), six different sites of the knee flexor muscles (three medial and three lateral sites), and two different sites of the ankle plantar flexor muscles (one medial and one lateral site) of both lower limbs, and these sites were the same used in previous studies [7, 38, 39] (Figure 1). As the cluster had 5 diodes and 17 different sites were irradiated, a total of 85 points were irradiated in each lower limb, with a total of 850 J of energy delivered per lower limb (50 J per site). The use of a cluster probe was fundamental, considering the extensive irradiation area covered in the present study.

Table 1: PBMT parameters and specifications.

Wavelength	810 nm (infrared)
Number of diodes	5
Frequency	Continuous output
Optical output (per diode)	100 mW or 0 mW (placebo)
Spot size (per diode)	0.0364 cm^2
Power density (per diode)	2.75 W/cm^2 or 0.00 W/cm^2 (placebo)
Energy (per diode)	10 J
Energy density (per diode)	275 J/cm^2 or 0 J/cm^2 (placebo)
Exposure time	100 s
Number of irradiated sites per lower limb	9 sites on knee extensor muscles (3 medial, 3 lateral, and 3 central) 6 sites on knee flexor muscles (3 medial and 3 lateral) 2 sites on plantar flexor muscles (1 medial and 1 lateral)
Total number of points per lower limb	85
Total energy delivered per lower limb	850 J (450 J on knee extensor muscles, 300 J on knee flexor muscles, and 100 J on plantar flexor muscles)
Cluster area	9.6 cm^2
Administration technique	Cluster in stationary position with slight pressure and direct contact with skin

2.6.2. Placebo Therapy. Placebo PBMT was delivered using the same device as the active PBMT but without any emission of therapeutic dose or power. Volunteers received a total dose of 0 J in the placebo mode. Placebo PBMT was applied in the same sites and with the same time of irradiation as the active PBMT. To ensure blinding, the device emitted the same sound regardless of the programmed mode (active or placebo PBMT).

2.7. Procedures. The study was performed in two stages, since it was a crossover study, with a washout period of 14 days between stages. The Consolidated Standards of Reporting Trials flowchart that summarizes the experimental procedures and volunteers is shown in Figure 2.

2.7.1. Blood Samples and Biochemical Analysis. Blood samples (10 ml) were taken by a qualified nurse (blinded to group allocation) from the antecubital vein of the volunteers before

Figure 1: PBMT irradiation sites in the anterior and posterior regions of lower limbs.

the stretching and intervention (active or placebo PBMT) and then, exactly 5 minutes after the intense progressive running test (ergospirometry test), blood samples were collected again. Up to one hour after collection, each sample was centrifuged at 3000 rpm for 20 min. Pipettes were used to transfer the serum to Eppendorf tubes, which were stored at -80°C until analysis. Blood analysis involved the determination of specific skeletal muscle creatine kinase (CK) isoform and lactate dehydrogenase (LDH) activities through spectrophotometry and specific reagent kits (Labtest, Brazil) following the manufacturer's instructions. The analyses of interleukin-1β (IL-1β), interleukin-6 (IL-6), and tumor necrosis factor alpha (TNF-α) levels were performed employing enzyme-linked immunosorbent assays (ELISA) and specific reagents (BD Biosciences, USA). The analyses of thiobarbituric acid (TBARS), carbonylated proteins, catalase (CAT), and superoxidedismutase (SOD) activities were performed using spectrophotometry and specific reactions previously described in literature [40–43].

2.7.2. Stretching. Immediately after the collection of blood samples, the volunteers performed one 60 sec set of active stretching exercise of the knee extensors and flexors; hip extensors, flexors, abductors, and adductors; and ankle plantar and dorsal flexor muscles of both lower limbs.

2.7.3. Application of Therapy. Immediately after performing stretching, the volunteers received an application of active PBMT or placebo PBMT according to prior randomization.

2.7.4. Intense Progressive Running Test (Ergospirometry Test). Immediately after the application of intervention (active or placebo PBMT), skin asepsis of the volunteers and electrode placement (for cardiac monitoring) were performed. Then the nozzle coupled to the gas analyzer was placed in volunteers, as well as the nasal clip. The ergospirometry test started exactly 5 minutes after the application of the interventions (active or placebo PBMT). We used a progressive treadmill exercise protocol, previously used in studies conducted by our research group [34, 38, 39]. Volunteers performed a standardized progressive running protocol on a motor-driven treadmill with a fixed inclination of 1%. The initial velocity was 3 km/h during the first 3 minutes (warm-up phase). After the warm-up phase, the velocity was increased 1 km/h at each minute until it reached 16 km/h. Volunteers performed the exercise protocol until exhaustion, and they were instructed to use hand signals to request termination of the test at any time. After the exercise protocol, the volunteers performed a recovery phase with a velocity of 6 km/h. The entire test was monitored by electrocardiogram and blood pressure measurements. The test was stopped if any abnormal changes were observed in heart rate or blood pressure by the assessor in charge of the test, or if the test was terminated prematurely on request by the volunteer.

2.8. Outcomes. The primary outcome was oxygen uptake relative to body mass ($VO_{2\ max}$ relative) measured by the software of the ergospirometry system, during the intense progressive running test. The secondary outcomes were rates of $VO_{2\ max}$ in absolute values, time until exhaustion, and aerobic and anaerobic threshold, measured through the ergospirometer during the intense progressive running test. Moreover, muscle damage (CK and LDH), inflammation (IL-1β, IL-6, and TNF-α), and oxidative stress (TBARS, carbonylated proteins, CAT, and SOD) were measured through blood samples collected before and 5 minutes after the end of the intense progressive running test. All assessments were performed by a blinded researcher.

2.9. Statistical Analysis. The statistical analysis was conducted following the principles of intention-to-treat analysis [44]. The Shapiro-Wilk test was used to determine the distribution of the data, which were then expressed as mean and standard deviation. Data regarding the ergospirometry test (rates of oxygen uptake ($VO_{2\ max}$), time until exhaustion, and aerobic and anaerobic thresholds) were analyzed using the paired, two-tailed Student t-test. Data regarding biochemical analysis were analyzed using a two-way ANOVA test, followed by the Bonferroni post hoc test. The significance level was set at $p < 0.05$. Data in graphs are expressed as mean and standard error of the mean (SEM).

3. Results

Twenty-two male high-level soccer players from the same team were recruited and finished all the procedures of this study. Therefore, there were no dropouts and the intention-to-treat analysis was not necessary. The mean age of volunteers was 18.85 (±0.61), height was 175.84 cm (±4.01), and body mass was 68.22 kg (±8.26). No adverse effects were reported during the study.

In order to assess possible residual effects of PBMT and placebo from the first test to the second test, we performed an analysis of variables regarding the progressive

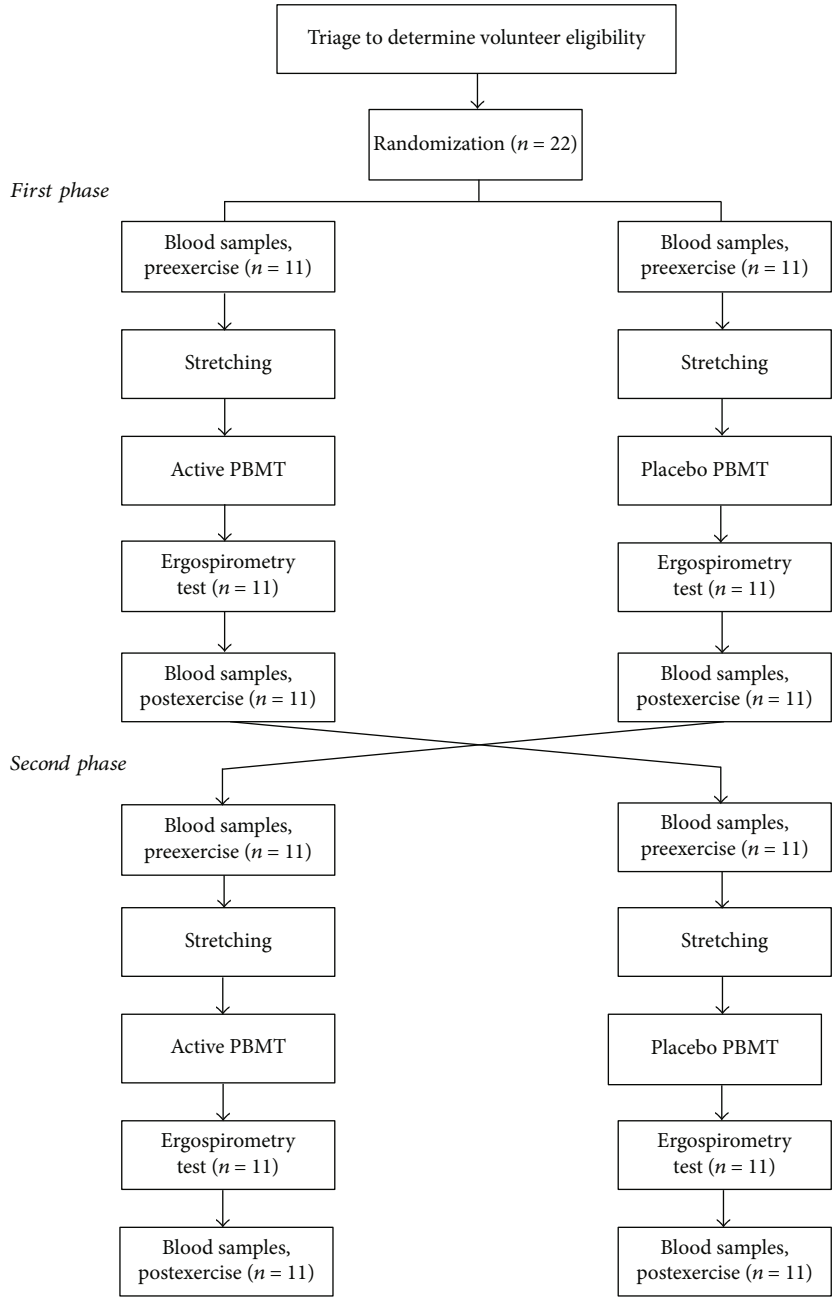

Figure 2: Flowchart of the study.

running test, and also baseline values of all biochemical markers. This analysis was performed only considering the values obtained in test 1 and test 2, regardless the treatment given before the tests. As can be observed in Table 2, there were no residual effects.

The application of active PBMT before the intense progressive running test significantly increased the oxygen uptake ($VO_{2\ max}$), both in relative ($p < 0.0467$) and absolute values ($p < 0.0013$), as well as the total time until exhaustion ($p < 0.0043$) compared to the application of preexercise placebo PBMT (Figure 3). Moreover, active PBMT significantly increased the anaerobic threshold, both in time ($p < 0.0007$) and volume ($p < 0.0355$), while it only significantly increased aerobic threshold in volume ($p < 0.0068$), compared to placebo PBMT.

Regarding assessment of muscle damage, the results demonstrated that active PBMT applied before the exercise protocol significantly decreased the activity of both postexercise CK and LDH ($p < 0.0001$) compared to placebo PBMT (Figure 4).

The evaluation of inflammatory markers demonstrated that there was no significant difference between active PBMT and placebo PBMT, applied before the exercise protocol, on postexercise levels of IL-1β and TNF-α. However, active PBMT decreased significantly the postexercise levels of IL-6 ($p < 0.0001$) when compared to placebo PBMT (Figure 5).

Table 2: Outcomes in test 1 vs. test 2 regardless of the treatment given (values are expressed as mean and standard deviation).

		Baseline	Postexercise	p value
$VO_{2\ max}$ relative (l/kg·min)	Test 1 Test 2	—	58.50 (±5.22) 57.67 (±5.68)	0.62
$VO_{2\ max}$ absolute (l/min)	Test 1 Test 2	—	3.75 (±0.59) 3.81 (±0.54)	0.73
Time until exhaustion (s)	Test 1 Test 2	—	535.91 (±161.82) 532.88 (±159.59)	0.95
Anaerobic threshold (s)	Test 1 Test 2	—	415.60 (±62.16) 409.15 (±65.12)	0.74
Anaerobic threshold (l/min)	Test 1 Test 2	—	3.15 (±0.47) 3.09 (±0.51)	0.69
Aerobic threshold (s)	Test 1 Test 2	—	179.42 (±48.21) 181.78 (±46.28)	0.87
Aerobic threshold (l/min)	Test 1 Test 2	—	2.08 (±0.34) 2.14 (±0.41)	0.60
CK ($U{\cdot}l^{-1}$)	Test 1 Test 2	217.96 (±36.12) 228.66 (±38.17)	—	0.34
LDH ($U{\cdot}l^{-1}$)	Test 1 Test 2	289.81 (±45.87) 294.09 (±43.80)	—	0.75
IL-1β (pg/ml)	Test 1 Test 2	3.18 (±0.49) 3.11 (±0.54)	—	0.65
IL-6 (pg/ml)	Test 1 Test 2	33.65 (±5.99) 34.78 (±5.74)	—	0.53
TNF-α (pg/ml)	Test 1 Test 2	57.37 (±8.98) 59.39 (±8.79)	—	0.46
TBARS (nmol/ml)	Test 1 Test 2	3.90 (±0.80) 3.67 (±0.85)	—	0.36
Carbonylated proteins (nmol of DNPH/g/dl of protein)	Test 1 Test 2	2.14 (±0.59) 2.07 (±0.68)	—	0.72
SOD (U SOD/g of protein)	Test 1 Test 2	2.85 (±0.69) 2.97 (±0.72)	—	0.58
CAT (U CAT/g of protein)	Test 1 Test 2	2.82 (±0.74) 2.76 (±0.78)	—	0.79

For oxidative stress markers, active PBMT applied before the exercise protocol significantly decreased postexercise TBARS ($p < 0.0001$) and carbonylated protein levels ($p < 0.01$) when compared to placebo PBMT. Moreover, active PBMT significantly increased SOD ($p < 0.0001$) and CAT ($p < 0.0001$) postexercise activity compared to placebo PBMT (Figure 6). All the outcomes (mean and standard deviation) about the functional aspects, muscle damage, and inflammatory and oxidative stress markers are fully described in Table 3.

4. Discussion

This study evaluated for the very first time the effects of PBMT (using infrared low-level laser therapy with optimized parameters) applied before a progressive running test on aerobic endurance, muscle damage, inflammatory process, and oxidative stress of high-level soccer athletes. In general, our results demonstrated that PBMT applied before an aerobic exercise protocol is effective in improving functional and biochemical aspects, enhancing athletic performance and postexercise recovery. Differently to another previous study investigating the effects of infrared low-level laser therapy PBMT in a progressive running test in healthy untrained individuals [34], our study used an optimized dose [32] and optimized power output [33] previously tested in high-level soccer athletes.

Evidence has shown that PBMT applied before exercise is able to increase aerobic endurance in healthy, nonathletic subjects [34, 38] as well as in competitive cyclists [36]. To the best of our knowledge, our study is the first to investigate the effects of preexercise PBMT on aerobic endurance in high-level soccer athletes, and we observed that the therapy was able to increase oxygen uptake ($VO_{2\ max}$) and athletes' anaerobic and aerobic thresholds during exercise. In addition, we observed that preexercise PBMT was effective in increasing time to reach exhaustion during the intense progressive running test, corroborating with a recent systematic review, as well as with the recent clinical and scientific recommendations made by experts in this field [31]. The effect of PBMT on muscle cells, in particular increasing cytochrome c-oxidase activity [45, 46], may increase cell metabolism and ATP production. Thus, our results suggest that this mechanism of PBMT contributed to modulate aerobic

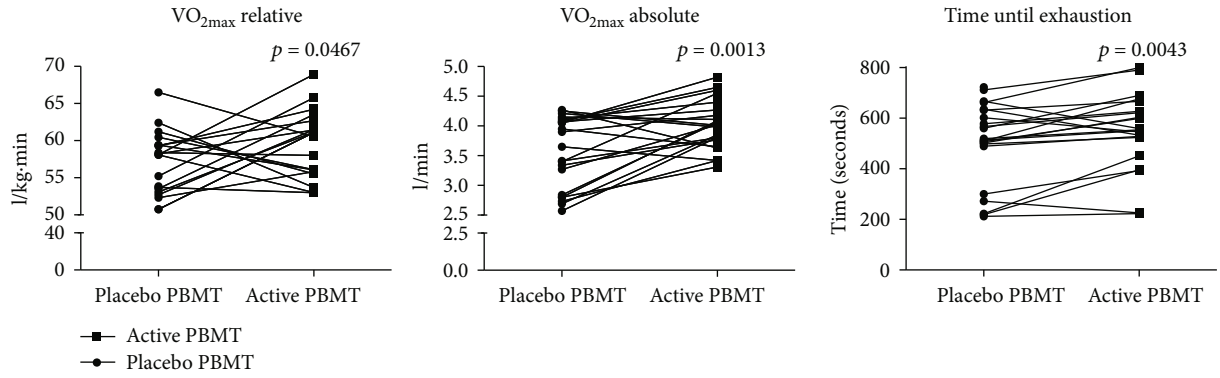

Figure 3: Oxygen uptake—$VO_{2\ max}$ (relative and absolute)—and time until exhaustion.

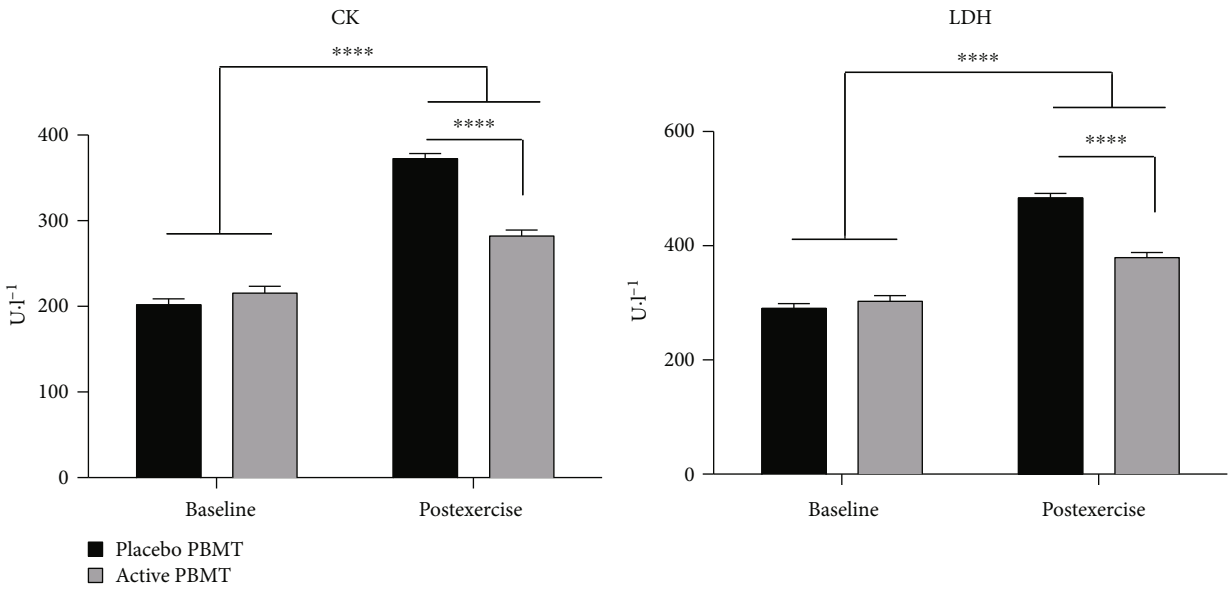

Figure 4: Activity of CK and LDH. Data are expressed as mean and SEM. $^{****}p < 0.0001$.

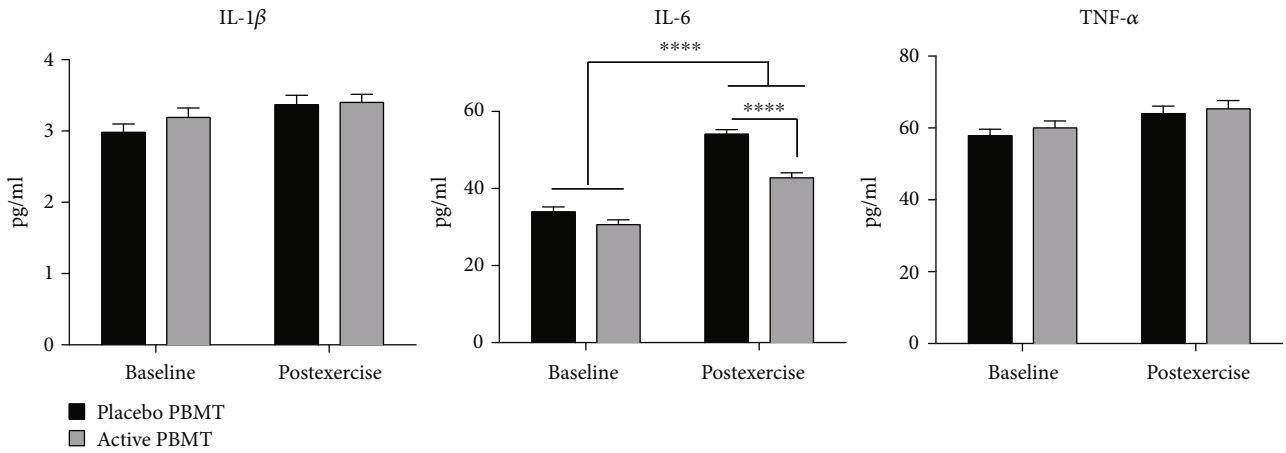

Figure 5: Levels of IL-1β, IL-6, and TNF-α. Data are expressed as mean and SEM. $^{****}p < 0.0001$.

endurance, and therefore, to enhance the performance of high-level soccer players, increasing both oxygen uptake and time to reach exhaustion.

Muscle damage can disturb the time course of recovery and performance of soccer athletes after matches, and currently some biomarkers, such as CK and LDH, are monitored

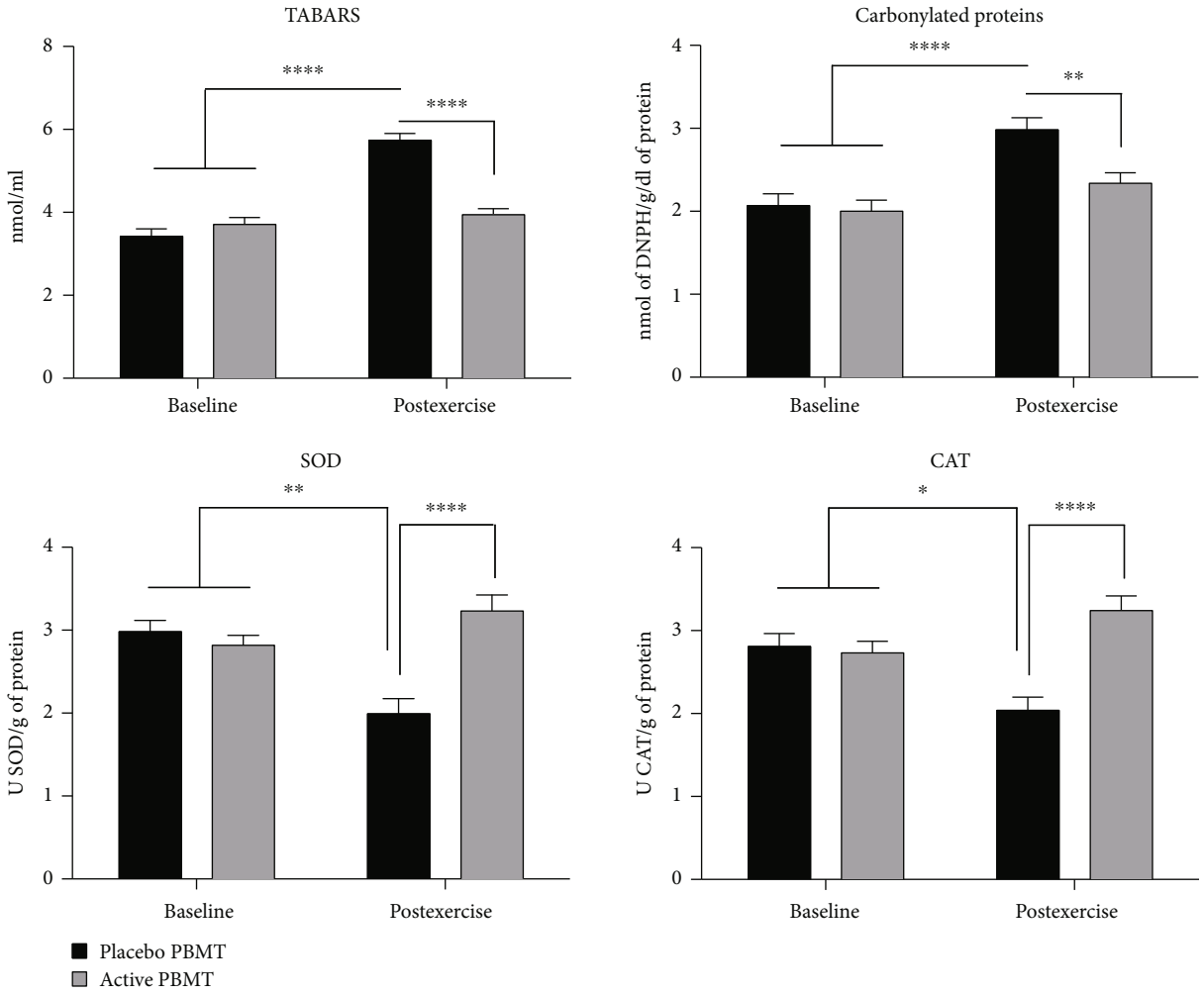

Figure 6: Levels of TBARS and carbonylated proteins and activity of SOD and CAT. Data are expressed as mean and SEM. $^{*}p < 0.05$, $^{**}p < 0.01$, and $^{****}p < 0.0001$.

daily to assess the muscle status of soccer athletes [3]. Several studies have demonstrated that preexercise PBMT is able to decrease both CK and LDH postexercise activities [25, 32–35] and consequently contribute to performance enhancement and postexercise recovery. Our results corroborate with studies performed with nonathletes [25, 34] and high-level athletes [24, 32, 33, 35], in which the irradiation of PBMT before the exercise was able to decrease the expected increase in these enzyme activities. On the other hand, one study also performed with soccer players showed that preexercise PBMT was not effective in decreasing CK activity [47]. However, it is important to highlight that several PBMT parameters used by Dos Reis et al. [47] were very different from those used in our study, such as dose per point, dose per site, total dose, power output, energy density, power density, and length of irradiation. This demonstrates very clearly that previous optimization of PBMT parameters is paramount for the effectiveness of the therapy as previously demonstrated by De Marchi et al. [48].

The systemic increase of muscle damage markers due to a soccer match may be responsible for triggering an inflammatory response in athletes, increasing cytokine levels, such as TNF-α and IL-6 [49–51]. Our results demonstrated that the preexercise PBMT was effective in decreasing IL-6 levels, as demonstrated in previous studies [32, 33]. We believe that the modulation of this cytokine has been an important aspect in the performance enhancement and postexercise recovery of athletes, since it is one of the most potent mediators of the acute phase of inflammatory response in skeletal muscles. On the other hand, our results demonstrated that IL-1β and TNF-α levels remained unchanged. Our results corroborate with the previous study carried out by De Oliveira et al. [33], in which preexercise PBMT did not change the levels of these cytokines immediately after an eccentric exercise protocol. However, this same study [33] demonstrated that the peak release of IL-1β and TNF-α occurred between 24 and 48 hours after the exercise protocol. Despite the differences between a progressive running test and an eccentric exercise protocol, this aspect could partially explain our results, since, possibly immediately after the progressive running test there still was no increase in these cytokines levels. Therefore, further research must assess these markers between 24 and 48 hours.

Table 3: Outcomes (values are expressed as mean and standard deviation).

		Baseline	Postexercise
$VO_{2\ max}$ relative (l/kg·min)	Placebo PBMT	—	55.69 (±5.55)
	Active PBMT		59.40 (±5.08)[a]
$VO_{2\ max}$ absolute (l/min)	Placebo PBMT	—	3.57 (±0.60)
	Active PBMT		4.02 (±0.41)[a]
Time until exhaustion (s)	Placebo PBMT	—	504.59 (±160.44)
	Active PBMT		563.27 (±159.46)[a]
Anaerobic threshold (s)	Placebo PBMT	—	384.86 (±63.53)
	Active PBMT		440.73 (±58.58)[a]
Anaerobic threshold (l/min)	Placebo PBMT	—	2.93 (±0.46)
	Active PBMT		3.26 (±0.40)[b]
Aerobic threshold (s)	Placebo PBMT	—	169.73 (±45.40)
	Active PBMT		184.36 (±44.84)
Aerobic threshold (l/min)	Placebo PBMT	—	2.20 (±0.43)
	Active PBMT		2.53 (±0.29)[a]
CK ($U{\cdot}l^{-1}$)	Placebo PBMT	201.76 (±32.98)	372.43 (±29.11)
	Active PBMT	215.61 (±37.22)	282.03 (±33.26)[c]
LDH ($U{\cdot}l^{-1}$)	Placebo PBMT	290.02 (±41.82)	483.55 (±38.09)
	Active PBMT	302.13 (±46.73)	378.97 (±41.52)[c]
IL-1β (pg/ml)	Placebo PBMT	2.98 (±0.56)	3.37 (±0.61)
	Active PBMT	3.19 (±0.62)	3.40 (±0.54)
IL-6 (pg/ml)	Placebo PBMT	33.92 (±6.09)	54.08 (±5.56)
	Active PBMT	30.6 (±5.89)	42.77 (±6.01)[c]
TNF-α (pg/ml)	Placebo PBMT	57.81 (±8.75)	63.99 (±9.87)
	Active PBMT	60.04 (±9.03)	65.34 (10.71)
TBARS (nmol/ml)	Placebo PBMT	3.42 (±0.85)	5.74 (±0.78)
	Active PBMT	3.71 (±0.79)	3.94 (±0.71)[c]
Carbonylated proteins (nmol of DNPH/g/dl of protein)	Placebo PBMT	2.07 (±0.67)	2.98 (±0.70)
	Active PBMT	2.00 (±0.63)	2.34 (±0.59)[a]
SOD (U SOD/g of protein)	Placebo PBMT	2.98 (±0.65)	1.99 (±0.86)
	Active PBMT	2.82 (±0.55)	3.23 (±0.91)[c]
CAT (U CAT/g of protein)	Placebo PBMT	2.81 (±0.73)	2.04 (±0.75)
	Active PBMT	2.73 (±0.66)	3.24 (±0.83)[c]

[a]Difference of placebo PBMT ($p < 0.01$). [b]Difference of placebo PBMT ($p < 0.05$). [c]Difference of placebo PBMT ($p < 0.0001$).

Besides muscle damage, physical exercise that generates high-intensity muscle contractions leads to increased ROS production, and consequently oxidative stress [6]. Our results demonstrated that preexercise PBMT was able to decrease lipid peroxidation and carbonylated protein production, related to oxidative damage to lipids and proteins caused by exercise protocol, as previously demonstrated [33, 35]. On the other hand, our results diverged from the findings of De Marchi et al. [34], in which preexercise PBMT was not able to modulate CAT activity, reinforcing the importance of optimizing PBMT parameters to achieve positive results in all outcomes related to oxidative stress and antioxidant activity. Moreover, it is important to highlight that our study was performed with high-level athletes while the study by De Marchi et al. [34] was performed with non-athletes, which could also partially explain the difference of results between studies. Furthermore, also in disagreement with our results, there was evidence that preexercise PBMT was not able to modulate SOD and CAT activity [33]. To date, the evidence regarding the effects of PBMT on exercise-induced muscular oxidative damage is sparse and divergent. Finally, our outcomes regarding oxidative stress markers and antioxidant activity might diverge from some studies [52]. However, it is important to highlight that this is a controversial aspect with conflicting findings in the literature, and therefore, further studies are needed. Further research must also investigate how long preexercise PBMT can upregulate antioxidant activity.

Our results also demonstrated that preexercise PBMT was able to modulate redox activity, increasing the activity of SOD and CAT, enzymes responsible for preventing oxidative damage. Our findings were promising to demonstrate that the therapy has a potential antioxidant effect, playing an important role in the enhancement of athletic performance and postexercise recovery. Thus, we suggest that one of the possible mechanisms of action by which PBMT is

able to promote this enhancement in both performance and postexercise recovery is precisely through the upregulation of antioxidant activity and consequently decreasing exercise-induced oxidative stress. Further studies evaluating the effects of preexercise PBMT on different oxidative stress markers are needed to confirm our results and also to establish this therapy as an antioxidant agent. In addition, it is important to further investigate the possible redox mechanism promoted by PBMT.

4.1. Strengths and Limitations. The strengths of this study are the high methodological quality, since it is a triple-blinded, randomized, placebo-controlled and prospectively registered clinical trial. The sample size was calculated to provide the appropriate statistical power to detect a precise difference in the primary outcome. Moreover, the statistical analysis was designed following the principles of intention-to-treat analysis. Finally, the parameters of PBMT used were previously optimized in order to investigate the effects of PBMT application before an exercise protocol performed by high-level athletes, without extrapolation between populations. The limitation of the study was not having measured the effects of PBMT on local oxygen concentration (oxyhemoglobin, deoxyhemoglobin, and total hemoglobin), as well as only assessing immediate effects.

5. Conclusion

In summary, our results demonstrated that preexercise PBMT as a stand-alone therapy was able to improve different functional aspects related to athletic performance and biochemical markers related to muscle damage and inflammatory process in high-level athletes. In addition, it is important to highlight that preexercise PBMT had an interesting antioxidant effect, being able to decrease exercise-induced oxidative stress, which suggests that this might be one of the possible mechanisms of action through which PBMT promotes ergogenic effects and protective effects to skeletal muscles. It is very likely that the sum of the different mechanisms of action was determinant for the therapy to improve aerobic endurance and postexercise recovery.

Data Availability

The data sets generated and analyzed during the current study are available from the corresponding author on reasonable request.

Conflicts of Interest

Professor Ernesto Cesar Pinto Leal-Junior receives research support from Multi Radiance Medical (Solon, OH, USA), a laser device manufacturer. The remaining authors declare that they have no conflict of interests.

Acknowledgments

This study was supported by research grant #2010/52404-0 from the São Paulo Research Foundation (FAPESP) and research grant #310281/2017-2 from the National Council for Scientific and Technological Development (CNPq) (Professor Ernesto Cesar Pinto Leal-Junior), as well as research grant #2017/06422-5 from the São Paulo Research Foundation (FAPESP) for the masters degree scholarship of Caroline dos Santos Monteiro Machado.

References

[1] H. Andersson, T. Raastad, J. Nilsson, G. Paulsen, I. Garthe, and F. Kadi, "Neuromuscular fatigue and recovery in elite female soccer: effects of active recovery," *Medicine and Science in Sports and Exercise*, vol. 40, no. 2, pp. 372–380, 2008.

[2] I. Ispirlidis, I. G. Fatouros, A. Z. Jamurtas et al., "Time-course of changes in inflammatory and performance responses following a soccer game," *Clinical Journal of Sport Medicine*, vol. 18, no. 5, pp. 423–431, 2008.

[3] M. Nédélec, A. McCall, C. Carling, F. Legall, S. Berthoin, and G. Dupont, "Recovery in soccer: part I—post-match fatigue and time course of recovery," *Sports Medicine*, vol. 42, no. 12, pp. 997–1015, 2012.

[4] M. B. Reid, K. E. Haack, K. M. Franchek, P. A. Valberg, L. Kobzik, and M. S. West, "Reactive oxygen in skeletal muscle. I. Intracellular oxidant kinetics and fatigue in vitro," *Journal of Applied Physiology*, vol. 73, no. 5, pp. 1797–1804, 1992.

[5] N. B. Vollaard, J. P. Shearman, and C. E. Cooper, "Exercise-induced oxidative stress: myths, realities and physiological relevance," *Sports Medicine*, vol. 35, no. 12, pp. 1045–1062, 2005.

[6] M. B. Reid, "Redox interventions to increase exercise performance," *The Journal of Physiology*, vol. 594, no. 18, pp. 5125–5133, 2016.

[7] H. D. Pinto, A. A. Vanin, E. F. Miranda et al., "Photobiomodulation therapy improves performance and accelerates recovery of high-level rugby players in field test: a randomized, crossover, double-blind, placebo-controlled clinical study," *Journal of Strength and Conditioning Research*, vol. 30, no. 12, pp. 3329–3338, 2016.

[8] G. Dupont, M. Nedelec, A. McCall, D. McCormack, S. Berthoin, and U. Wisløff, "Effect of 2 soccer matches in a week on physical performance and injury rate," *The American Journal of Sports Medicine*, vol. 38, no. 9, pp. 1752–1758, 2010.

[9] S. M. Shirreffs, A. J. Taylor, J. B. Leiper, and R. J. Maughan, "Post-exercise rehydration in man: effects of volume consumed and drink sodium content," *Medicine and Science in Sports and Exercise*, vol. 28, no. 10, pp. 1260–1271, 1996.

[10] R. Jentjens and A. Jeukendrup, "Determinants of post-exercise glycogen synthesis during short-term recovery," *Sports Medicine*, vol. 33, no. 2, pp. 117–144, 2003.

[11] J. L. Ivy, "Regulation of muscle glycogen repletion, muscle protein synthesis and repair following exercise," *Journal of Sports Science and Medicine*, vol. 3, no. 3, pp. 131–138, 2004.

[12] C. M. Kerksick, C. D. Wilborn, M. D. Roberts et al., "ISSN exercise & sports nutrition review update: research & recommendations," *Journal of the International Society of Sports Nutrition*, vol. 15, no. 1, p. 38, 2018.

[13] K. Sairyo, K. Iwanaga, N. Yoshida et al., "Effects of active recovery under a decreasing work load following intense muscular exercise on intramuscular energy metabolism," *International Journal of Sports Medicine*, vol. 24, no. 3, pp. 179–182, 2003.

[14] K. Koizumi, Y. Fujita, S. Muramatsu, M. Manabe, M. Ito, and J. Nomura, "Active recovery effects on local oxygenation level

during intensive cycling bouts," *Journal of Sports Sciences*, vol. 29, no. 9, pp. 919–926, 2011.

[15] G. J. Rowsell, A. J. Coutts, P. Reaburn, and S. Hill-Haas, "Effect of post-match cold-water immersion on subsequent match running performance in junior soccer players during tournament play," *Journal of Sports Sciences*, vol. 29, no. 1, pp. 1–6, 2011.

[16] J. Ingram, B. Dawson, C. Goodman, K. Wallman, and J. Beilby, "Effect of water immersion methods on post-exercise recovery from simulated team sport exercise," *Journal of Science and Medicine in Sport*, vol. 12, no. 3, pp. 417–421, 2009.

[17] F. Brown, C. Gissane, G. Howatson, K. van Someren, C. Pedlar, and J. Hill, "Compression garments and recovery from exercise: a meta-analysis," *Sports Medicine*, vol. 47, no. 11, pp. 2245–2267, 2017.

[18] M. Nédélec, A. McCall, C. Carling, F. Legall, S. Berthoin, and G. Dupont, "Recovery in soccer: part II—recovery strategies," *Sports Medicine*, vol. 43, no. 1, pp. 9–22, 2013.

[19] W. Poppendieck, M. Wegmann, A. Ferrauti, M. Kellmann, M. Pfeiffer, and T. Meyer, "Massage and performance recovery: a meta-analytical review," *Sports Medicine*, vol. 46, no. 2, pp. 183–204, 2016.

[20] L. A. Thein, J. M. Thein, and G. L. Landry, "Ergogenic aids," *Physical Therapy*, vol. 75, no. 5, pp. 426–439, 1995.

[21] D. G. Liddle and D. J. Connor, "Nutritional supplements and ergogenic AIDS," *Primary Care*, vol. 40, no. 2, pp. 487–505, 2013.

[22] E. C. Leal Junior, R. A. Lopes-Martins, B. M. Baroni et al., "Effect of 830 nm low-level laser therapy applied before high-intensity exercises on skeletal muscle recovery in athletes," *Lasers in Medical Science*, vol. 24, no. 6, pp. 857–863, 2009.

[23] E. C. Leal Junior, R. A. Lopes-Martins, B. M. Baroni et al., "Comparison between single-diode low-level laser therapy (LLLT) and LED multi-diode (cluster) therapy (LEDT) applications before high-intensity exercise," *Photomedicine and Laser Surgery*, vol. 27, no. 4, pp. 617–623, 2009.

[24] E. C. Leal Junior, R. A. Lopes-Martins, R. P. Rossi et al., "Effect of cluster multi-diode light emitting diode therapy (LEDT) on exercise-induced skeletal muscle fatigue and skeletal muscle recovery in humans," *Lasers in Surgery and Medicine*, vol. 41, no. 8, pp. 572–577, 2009.

[25] E. C. Leal Junior, R. A. Lopes-Martins, L. Frigo et al., "Effects of low-level laser therapy (LLLT) in the development of exercise-induced skeletal muscle fatigue and changes in biochemical markers related to postexercise recovery," *The Journal of Orthopaedic and Sports Physical Therapy*, vol. 40, no. 8, pp. 524–532, 2010.

[26] E. C. Leal Junior, V. de Godoi, J. L. Mancalossi et al., "Comparison between cold water immersion therapy (CWIT) and light emitting diode therapy (LEDT) in short-term skeletal muscle recovery after high-intensity exercise in athletes—preliminary results," *Lasers in Medical Science*, vol. 26, no. 4, pp. 493–501, 2011.

[27] B. M. Baroni, E. C. Leal Junior, T. De Marchi, A. L. Lopes, M. Salvador, and M. A. Vaz, "Low level laser therapy before eccentric exercise reduces muscle damage markers in humans," *European Journal of Applied Physiology*, vol. 110, no. 4, pp. 789–796, 2010.

[28] B. M. Baroni, E. C. Leal Junior, J. M. Geremia, F. Diefenthaeler, and M. A. Vaz, "Effect of light-emitting diodes therapy (LEDT) on knee extensor muscle fatigue," *Photomedicine and Laser Surgery*, vol. 28, no. 5, pp. 653–658, 2010.

[29] R. L. Toma, H. T. Tucci, H. K. Antunes et al., "Effect of 808 nm low-level laser therapy in exercise-induced skeletal muscle fatigue in elderly women," *Lasers in Medical Science*, vol. 28, no. 5, pp. 1375–1382, 2013.

[30] E. C. P. Leal-Junior, R. Á. B. Lopes-Martins, and J. M. Bjordal, "Clinical and scientific recommendations for the use of photobiomodulation therapy in exercise performance enhancement and post-exercise recovery: current evidence and future directions," *Brazilian Journal of Physical Therapy*, vol. 23, no. 1, pp. 71–75, 2019.

[31] A. A. Vanin, E. Verhagen, S. D. Barboza, L. O. P. Costa, and E. C. P. Leal-Junior, "Photobiomodulation therapy for the improvement of muscular performance and reduction of muscular fatigue associated with exercise in healthy people: a systematic review and meta-analysis," *Lasers in Medical Science*, vol. 33, no. 1, pp. 181–214, 2018.

[32] A. Aver Vanin, T. de Marchi, S. Silva Tomazoni et al., "Pre-exercise infrared low-level laser therapy (810 nm) in skeletal muscle performance and postexercise recovery in humans, what is the optimal dose? A randomized, double-blind, placebo-controlled clinical trial," *Photomedicine and Laser Surgery*, vol. 34, no. 10, pp. 473–482, 2016.

[33] A. R. De Oliveira, A. A. Vanin, S. S. Tomazoni et al., "Pre-exercise infrared photobiomodulation therapy (810 nm) in skeletal muscle performance and postexercise recovery in humans: what is the optimal power output?," *Photomedicine and Laser Surgery*, vol. 35, no. 11, pp. 595–603, 2017.

[34] T. De Marchi, E. C. Leal Junior, C. Bortoli, S. S. Tomazoni, R. A. Lopes-Martins, and M. Salvador, "Low-level laser therapy (LLLT) in human progressive-intensity running: effects on exercise performance, skeletal muscle status, and oxidative stress," *Lasers in Medical Science*, vol. 27, no. 1, pp. 231–236, 2012.

[35] T. De Marchi, E. C. P. Leal-Junior, K. C. Lando et al., "Photobiomodulation therapy before futsal matches improves the staying time of athletes in the court and accelerates post-exercise recovery," *Lasers in Medical Science*, vol. 34, no. 1, pp. 139–148, 2019.

[36] F. J. Lanferdini, R. L. Krüger, B. M. Baroni et al., "Low-level laser therapy improves the VO_2 kinetics in competitive cyclists," *Lasers in Medical Science*, vol. 33, no. 3, pp. 453–460, 2018.

[37] F. J. Lanferdini, R. R. Bini, B. M. Baroni, K. D. Klein, F. P. Carpes, and M. A. Vaz, "Improvement of performance and reduction of fatigue with low-level laser therapy in competitive cyclists," *International Journal of Sports Physiology and Performance*, vol. 13, no. 1, pp. 14–22, 2018.

[38] E. F. Miranda, A. A. Vanin, S. S. Tomazoni et al., "Using pre-exercise photobiomodulation therapy combining super-pulsed lasers and light-emitting diodes to improve performance in progressive cardiopulmonary exercise tests," *Journal of Athletic Training*, vol. 51, no. 2, pp. 129–135, 2016.

[39] E. F. Miranda, S. S. Tomazoni, P. R. V. de Paiva, H. D. Pinto, D. Smith, and L. A. Santos, "When is the best moment to apply photobiomodulation therapy (PBMT) when associated to a treadmill endurance-training program? A randomized, triple-blinded, placebo-controlled clinical trial," *Lasers in Medical Science*, vol. 33, no. 4, pp. 719–727, 2018.

[40] E. D. Wills, "Mechanisms of lipid peroxide formation in animal tissues," *Biochemical Journal*, vol. 99, no. 3, pp. 667–676, 1996.

[41] R. L. Levine, D. Garland, C. N. Oliver et al., "Determination of carbonyl content in oxidatively modified proteins," *Methods in Enzymology*, vol. 186, pp. 464–478, 1990.

[42] H. Aebi, "[13] Catalase _in vitro_," *Methods in Enzymology*, vol. 105, pp. 121–126, 1984.

[43] J. V. Bannister and L. Calabrese, "Assays for superoxide dismutase," *Methods of Biochemical Analysis*, vol. 32, pp. 279–312, 1987.

[44] M. R. Elkins and A. M. Moseley, "Intention-to-treat analysis," *Journal of Physiotherapy*, vol. 61, no. 3, pp. 165–167, 2015.

[45] G. M. Albuquerque-Pontes, R. P. Vieira, S. S. Tomazoni et al., "Effect of pre-irradiation with different doses, wavelengths, and application intervals of low-level laser therapy on cytochrome c oxidase activity in intact skeletal muscle of rats," *Lasers in Medical Science*, vol. 30, no. 1, pp. 59–66, 2015.

[46] C. R. Hayworth, J. C. Rojas, E. Padilla, G. M. Holmes, E. C. Sheridan, and F. Gonzalez-Lima, "In Vivo Low-level Light Therapy Increases Cytochrome Oxidase in Skeletal Muscle," *Photochemistry and Photobiology*, vol. 86, no. 3, pp. 673–680, 2010.

[47] F. A. Dos Reis, B. A. da Silva, E. M. Laraia et al., "Effects of pre- or post-exercise low-level laser therapy (830 nm) on skeletal muscle fatigue and biochemical markers of recovery in humans: double-blind placebo-controlled trial," *Photomedicine and Laser Surgery*, vol. 32, no. 2, pp. 106–112, 2014.

[48] T. De Marchi, V. M. Schmitt, C. D. da Silva Fabro et al., "Phototherapy for improvement of performance and exercise recovery: comparison of 3 commercially available devices," *Journal of Athletic Training*, vol. 52, no. 5, pp. 429–438, 2017.

[49] C. Kasapis and P. D. Thompson, "The effects of physical activity on serum C-reactive protein and inflammatory markers: a systematic review," *Journal of the American College of Cardiology*, vol. 45, no. 10, pp. 1563–1569, 2005.

[50] K. Ostrowski, T. Rohde, S. Asp, P. Schjerling, and B. K. Pedersen, "Pro-and anti-inflammatory cytokine balance in strenuous exercise in humans," *The Journal of Physiology*, vol. 515, no. 1, pp. 287–291, 1999.

[51] A. M. Petersen and B. K. Pedersen, "The anti-inflammatory effect of exercise," *Journal of Applied Physiology*, vol. 98, no. 4, pp. 1154–1162, 2005.

[52] P. Brancaccio, G. Lippi, and N. Maffulli, "Biochemical markers of muscular damage," *Clinical Chemistry and Laboratory Medicine*, vol. 48, no. 6, pp. 757–767, 2010.

Hindawi
Oxidative Medicine and Cellular Longevity
Volume 2019, Article ID 3018584, 13 pages
https://doi.org/10.1155/2019/3018584

Research Article

Increased Circulating Levels of Interleukin-6 Affect the Redox Balance in Skeletal Muscle

Laura Forcina,[1] **Carmen Miano**,[1] **Bianca M. Scicchitano**,[2] **Emanuele Rizzuto**,[3] **Maria Grazia Berardinelli**,[1] **Fabrizio De Benedetti**,[4] **Laura Pelosi**,[1] **and Antonio Musarò**[1]

[1]*DAHFMO-Unit of Histology and Medical Embryology, Sapienza University of Rome, Laboratory Affiliated to Istituto Pasteur Italia-Fondazione Cenci Bolognetti, Via A. Scarpa 14, 00161 Rome, Italy*
[2]*Istituto di Istologia ed Embriologia, Università Cattolica del Sacro Cuore, Fondazione Policlinico Universitario "Agostino Gemelli", IRCCS, 00168 Roma, Italy*
[3]*Department of Mechanical and Aerospace Engineering, Sapienza University of Rome, 00184 Rome, Italy*
[4]*Division of Rheumatology and Immuno-Rheumatology Research Laboratories, Bambino Gesù Children's Hospital, 00146 Rome, Italy*

Correspondence should be addressed to Antonio Musarò; antonio.musaro@uniroma1.it

Received 24 May 2019; Revised 1 August 2019; Accepted 26 September 2019; Published 16 November 2019

Guest Editor: Marko D. Prokić

The extent of oxidative stress and chronic inflammation are closely related events which coexist in a muscle environment under pathologic conditions. It has been generally accepted that the inflammatory cells, as well as myofibers, are sources of reactive species which are, in turn, able to amplify the activation of proinflammatory pathways. However, the precise mechanism underlining the physiopathologic interplay between ROS generation and inflammatory response has to be fully clarified. Thus, the identification of key molecular players in the interconnected pathogenic network between the two processes might help to design more specific therapeutic approaches for degenerative diseases. Here, we investigated whether elevated circulating levels of the proinflammatory cytokine Interleukin-6 (IL-6) are sufficient to perturb the physiologic redox balance in skeletal muscle, independently of tissue damage and inflammatory response. We observed that the overexpression of circulating IL-6 enhances the generation and accumulation of free radicals in the diaphragm muscle of adult NSE/IL-6 mice, by deregulating redox-associated molecular circuits and impinging the nuclear factor erythroid 2-related factor 2- (Nrf2-) mediated antioxidant response. Our findings are coherent with a model in which uncontrolled levels of IL-6 in the bloodstream can influence the local redox homeostasis, inducing the establishment of prooxidative conditions in skeletal muscle tissue.

1. Introduction

Basal levels of reactive oxygen and nitrogen species (ROS and RNS) in skeletal muscle operate as molecular signals and regulatory mediators of homeostatic processes, whereas the sustained production of free radicals is responsible for the oxidative damage of cellular components such as membrane lipids, proteins, and nucleic acids [1–4]. Thus, the impact of reactive molecules needs a tight modulation, guaranteed by the activation of a sophisticated system of antioxidant agents [5, 6]. A proper balance between prooxidant stimuli and antioxidant defence is necessary to allow the activation of redox-related physiologic pathways and to prevent the occurrence of oxidative alterations of muscle tissue [7–12]. One of the main sources of ROS production in skeletal muscle is the NADPH oxidase 2 (NOX2), an enzymatic complex responsible for the conversion of oxygen into superoxide, using NADPH as electron donor substrate [13–15]. As a compensatory mechanism, ROS can induce the nuclear translocation of Nrf2, which is considered the master regulator of the endogenous antioxidant defence [16, 17]. Indeed, Nrf2 protein regulates the expression of genes codifying for the main redox-regulating enzymes, such as glutamate-cysteine ligase (GCL), implicated in glutathione synthesis, NAD(P)H quinone dehydrogenase 1 (NQO1) and the heme-oxygenase 1 (HO-1), involved in superoxide detoxification, superoxide

dismutase (SOD) engaged in ROS neutralization, and catalase (CAT), which can convert hydrogen peroxide (H_2O_2) into oxygen and water [18–24].

An efficient antioxidant chain can actively reduce the biodisponibility of superoxide, avoiding its combination with nitric oxide (NO) to generate RNS and thus favouring the physiologic signalling mediated by NO in skeletal muscle. Conversely, the uncontrolled production of ROS can induce an impairment of the Nrf2-dependent pathway, shunting muscle balance toward prooxidative conditions and leading to oxidative stress and tissue damage [25–28].

Indeed, the loss of the homeostatic redox balance represents a critical pathogenic mechanism contributing to muscle diseases [7–9, 11, 29]. In recent years, mounting evidence indicated that the excessive production of ROS plays a crucial role in a wide range of degenerative and inflammatory-related diseases, such as Duchenne muscular dystrophy (DMD), aging, diabetes, and cancer, leading to protein carbonylation and nitration, DNA damage, and RNA oxidation [1–4, 30, 31]. In particular, the perturbation of pivotal redox signalling pathways in dystrophic muscles has been related with the progression of DMD pathology and our studies supported the central role of ROS in promoting degenerative events in dystrophin-deficient muscles [27, 28, 31, 32]. However, the production of ROS has been generally considered as a secondary mechanism associated to chronic inflammation, which represents a major contributor to the pathogenesis of many musculoskeletal diseases [2, 33].

Although ROS production has been generally associated to the extent of chronic inflammation in DMD, we revealed an alteration of muscle redox status in presymptomatic DMD patients and in dystrophic animal models early before the onset of the pathology, characterized by myofiber necrosis and inflammatory infiltrate [27, 28]. Several studies support the existence of an interdependent relationship between inflammation and oxidative stress, and the interplay between these pathogenic mechanisms represents a critical issue to define the precise pathogenic events associated with neuromuscular diseases and to design more specific therapeutic approaches.

Among factors playing a critical role in skeletal muscle physiopathology and potentially linking inflammation and oxidative stress, Interleukin-6 (IL-6) is an elective candidate. IL-6 is a cytokine with pleiotropic functions in muscle environment, exerting positive and negative roles in tissue homeostasis. It has been extensively described that the dual nature of its action can be associated to the activation of different signalling pathways [34–36]. In particular, the activation of the classical signalling, mediated by the membrane IL-6 receptor alpha (mIL6R) and the ubiquitous receptor gp130, is physiologically restricted to responsive cells and has been involved in anti-inflammatory and proregenerative pathways in skeletal muscle [37–40]. The spectrum of action of IL-6 is known to be extended by the interaction of the cytokine with a soluble form of IL6R (sIL6R). This alternative receptor system activates the so-called trans-signalling with proinflammatory and profibrotic implications [41–44]. Of note, circulating levels of IL-6, which are normally undetectable, are increased in several disease conditions and IL-6 has been recognized as a proinflammatory, profibrotic, and prooxidant factor in different pathologic contexts [34, 35].

We recently provided evidence that IL-6 is causally linked to the pathogenesis of muscular dystrophy using two different experimental approaches: (i) increasing the circulating levels of IL-6 in mdx mice and analysing its effects in a stage normally spared by the absence of dystrophin and (ii) blocking IL-6 signalling in mdx mice at the prenecrotic stage and analysing its effects at the acute onset of the pathology. We demonstrated that the overexpression of IL-6 in dystrophic mdx mice (mdx/IL-6 murine model) induced the exacerbation of the dystrophic phenotype at 24 weeks of age, the stage in which the classical mdx model shows a stabilization of the disease [45], whereas the inhibition of IL-6 signalling in dystrophin-deficient mice reduces ROS accumulation, myonecrosis, and inflammation in the diaphragm muscle, which represents the most compromised muscular district in DMD [28, 36, 37, 46]. Noticeably, we recently highlighted a role for deregulated amounts of IL-6 in contributing to the alteration of local and systemic redox signalling markers in DMD patients and dystrophic mice [27, 28].

Nevertheless, it remained to be defined whether the alteration in redox balance was strictly related to the absence of dystrophin expression, and therefore to the disease, or whether increased levels of IL-6 are able alone to trigger a perturbation of redox balance in muscle milieu.

Thus, based on previous works performed on dystrophic murine models and human samples of DMD patients, we investigated the oxidative status of NSE/IL-6 muscle, in which the impact of increased levels of IL-6 cannot be biased against degenerating tissue and other related pathogenic mechanisms typical of dystrophic muscles, to better clarify the role of nonphysiologic levels of IL-6 in promoting the alteration of muscle oxidative balance. Indeed, although NSE/IL-6 mice have shown a decreased growth rate, no evidence of degeneration, fibrosis, or infiltrated inflammatory cells has been observed in the muscles of NSE/IL-6 mice.

We revealed that increased circulating levels of IL-6 act as a central player in deregulating the redox balance in diaphragm muscle. Of note, high plasma levels of IL-6 induce muscle atrophy and alteration in the functional performance of different muscle types, suggesting that, enhancing ROS production and impairing the antioxidant response, IL-6 fosters the molecular circuits generally associated to the extent of chronic tissue damage.

2. Materials and Methods

2.1. Mice. Wild-type C57Bl/6J mice and NSE/IL-6 transgenic mice [47] of 24 weeks of age were used in the current study. In particular, NSE/IL-6 mice, in which the rat neurospecific enolase (NSE) promoter drives the expression of human IL-6 cDNA, were derived from the original line 26 [46] and are characterized by elevated levels of circulating IL-6 since early after birth.

Animals were maintained as per the institutional guidelines of the animal facility of the unit of Histology and Medical Embryology. All the experiments on animal models were approved by the ethics committee of the Sapienza

University of Rome-Unit of Histology and Medical Embryology and were performed in accordance with the current version of the Italian Law on the Protection of Animals.

2.2. RNA Extraction and Real-Time PCR Analysis. Liquid nitrogen-frozen diaphragm muscles of wild-type and NSE/IL-6 mice were powdered and homogenized in TRI Reagent (Sigma-Aldrich) by Tissue Lyser (Qiagen). Total RNA was extracted, and one microgram of each RNA sample was retrotranscribed using QuantiTect Reverse Transcription Kit (Qiagen), to obtain double-stranded cDNA. To synthesize single-stranded cDNA, ten nanograms of total RNA was reverse transcribed using the TaqMan MicroRNA Reverse Transcription Kit (Applied Biosystems). The analysis of mRNA and miRNA expression was performed on ABI PRISM 7500 SDS (Applied Biosystems). Specific TaqMan assays for SOD1, SOD2, NQO1, CAT1, Nrf2, GCL, SIRT1, Txnrd2, Atrogin1, MURF-1, CTSL, LC3, and miR-1 (Applied Biosystems) were used, and relative quantification was performed using Hprt and U6 snRNA as endogenous controls for mRNA and miRNA, respectively. Data were analysed using the 2-DDCt method and reported as mean fold change in gene expression relative to wild type.

2.3. Protein Extraction, Western Blot Analysis, and ELISA. Diaphragm muscles were isolated from 24-week-old wild-type and NSE/IL-6 mice, and liquid nitrogen powdered samples were homogenized in protein lysis buffer (Tris-HCl, pH 7.5/20 mM, EDTA/2 mM, EGTA/2 mM, Sucrose/250 mM, DTT/5 mM, Triton-X/0.1%, PMSF/1 mM, NaF/10 mM, SOV4/0.2 mM, Cocktail Protease Inhibitors/1x (Sigma-Aldrich)). For western blotting analysis, 70 μg of protein extract was used, and filters were blotted with primary antibodies against gp91phox (BD Transduction), G6PD (Santa Cruz), Nitrotyrosine (Millipore), and GAPDH (Santa Cruz) and appropriate HRP-conjugated secondary antibodies (Bethyl Laboratories). Nitrotyrosine quantification was performed using the Stain-Free blot method for normalization (Criterion TGX Stain-Free Precast Gels; Bio-Rad).

Signals were captured by Chemi Doc™ XRS 2015 (Bio-Rad Laboratories), and densitometric analysis was performed using Image Lab software (version 5.2.1; Bio-Rad Laboratories©).

For the evaluation of circulating human IL-6, an ELISA was performed on serum samples using Quantikine® Colorimetric Sandwich ELISAs (R&D Systems), according to the manufacturer's protocol.

2.4. Histological Analysis and Dihydroethidium Staining. Diaphragm and EDL muscles from 24-week-old wild-type and NSE/IL-6 mice were embedded in tissue freezing medium and snap frozen in nitrogen-cooled isopentane. For general morphology, cryostat transversal sections were stained with Haematoxylin and Eosin according to standard protocols. Bright-field images were obtained using Axio Imager A2 microscope (Carl Zeiss Microimaging, Inc.) and analysed using ImageJ software (v.1.51j8; National Institutes of Health) to quantify the cross-sectional area of single myofibers. For dihydroethidium (DHE) staining, 10 μm thick muscle cryosections were incubated with 5 μM DHE (Molecular Probes #D23107) in PBS at 37°C for 30 minutes, photomicrographed using Axio Imager A2 microscope (Carl Zeiss Microimaging, Inc.), and processed by ZEN2 software (Blue edition). DHE-derived fluorescence was analysed by ImageJ software. The evaluation of the DHE-derived fluorescence was performed on at least five transversal sections of each muscle, and a minimum of eight fields arbitrarily chosen from each section was analysed.

2.5. Functional Analysis. Ex vivo functional analysis was performed on EDL muscles isolated from 24-week-old NSE/IL-6 and wild-type mice, as previously described [48]. Briefly, the muscle to be tested was mounted in a temperature-controlled chamber containing a Krebs-Ringer bicarbonate buffer continuously gassed with a mixture of 95% O_2 and 5% CO_2. Maximum force (Fmax) was evoked stimulating the muscle with 300 mA train of pulses delivered at 180 Hz. Specific force was computed as Fmax/CSA [48].

2.6. Data Analysis and Statistics. Statistical analysis was performed with GraphPad Prism Software (San Diego, CA, USA). All data were expressed as mean ± SEM. Differences among wild-type and NSE/IL-6 groups were assessed with Mann-Whitney test or Student's t-test assuming two-tailed distributions. $p < 0.05$ was considered statistically significant. The sample size was predetermined based on the variability observed in preliminary and similar experiments. All experiments requiring animal models were subjected to randomization based on litter.

3. Results

3.1. The Enhanced Expression of Circulating Interleukin-6 Promotes the Production and Accumulation of ROS in the Diaphragm Muscle. In this study, we extended previous works [27, 28] with the aim to define, in NSE/IL-6 transgenic mice, the contribution of circulating increased levels of IL-6 on redox balance perturbation. NSE/IL-6 mice express human IL-6 (hIL-6) cDNA under the rat neurospecific enolase (NSE) promoter, resulting in increased amounts of circulating IL-6 early after birth [47]. To verify whether hIL-6 levels were maintained elevated in the bloodstream during adulthood, serum levels of transgenic IL-6 were measured, by ELISA, in 24-week-old NSE/IL-6 mice. The protein content of hIL-6 was of 13.8 ± 2.8 ng/ml, compared to the undetectable levels of the wild-type mice (data not shown). Noticeably, the circulating levels of IL-6 observed in the serum of NSE/IL-6 mice were comparable with the levels reported for the serum of mdx/IL-6 mice at the same age [45].

We thus analysed the generation, accumulation, and impact of oxidizing products in the diaphragm muscle of both 24-week-old NSE/IL-6 and wild-type (WT) mice (Figure 1). The rationale of considering the diaphragm muscle of 24-week-old NSE/IL-6 mice lies with the evidence that this specific muscle showed a significant redox alteration in age-matched dystrophic mice expressing comparable IL-6 levels of NSE/IL-6 transgenic mice [45].

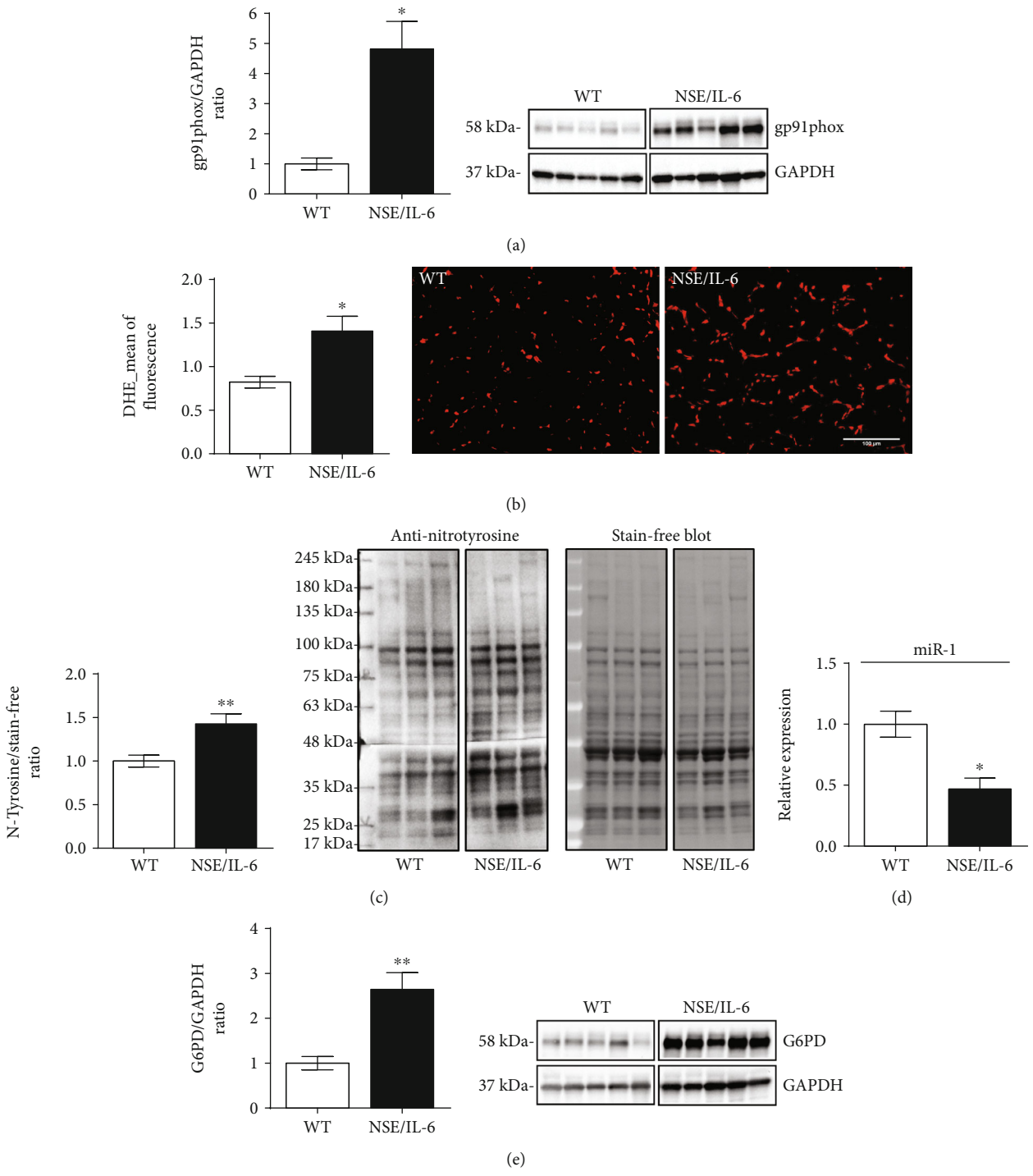

Figure 1: IL-6 induced the enhanced ROS production and accumulation in the diaphragm muscle. Western blot analysis (right panels show representative images) for the expression of gp91phox (a) and G6PD (e) proteins in 24-week-old NSE/IL-6 and wild-type (WT) mice. Values represent mean ± SEM; $n = 5$ to 6 mice per group. $^{*}p < 0.05$, $^{**}p < 0.005$ by Student's two-tailed unpaired t-test. Lanes were run on the same gel but were not contiguous. Original images are shown in Figure S1 and Figure S3. (b) Quantitative analysis (left panel) of the mean intensity of fluorescence derived from DHE staining on diaphragm muscle sections from 24-week-old NSE/IL-6 and WT mice. Right panels show representative images of DHE staining on muscle sections of indicated genotypes (scale bar 100 μm). Values represent mean ± SEM; $n = 3$ to 5 mice per group. $^{*}p < 0.05$ by unpaired t-test. (c) Western blot analysis for the detection of nitrated proteins (right panels show representative images) in the diaphragm muscle of NSE/IL-6 and WT mice. Values represent mean ± SEM; $n = 6$ mice per group. $^{**}p < 0.005$ by unpaired t-test. Lanes were run on the same gel but were not contiguous. Original images are shown in Figure S2. (d) Real-time PCR analysis of the expression of miR-1 performed on diaphragm muscle samples from NSE/IL-6 and WT mice at 24 weeks of age. Values represent mean ± SEM; $n = 3$ to 5 mice per genotype. $^{*}p < 0.05$ by unpaired t-test. DHE: dihydroethidium; G6PD: glucose 6-phosphate dehydrogenase.

We evaluated the expression of gp91phox protein, the catalytic subunit of the enzymatic complex NADPH oxidase 2 (NOX2), responsible for the conversion of molecular oxygen to superoxide (O_2^-) [13, 15]. A significant increase of gp91phox protein expression was observed in NSE/IL-6 muscle compared to that in wild-type mice (Figure 1(a)), suggesting an enhanced generation of superoxide in muscles exposed to nonphysiologic levels of circulating IL-6.

Since superoxide can be efficiently neutralized by the endogenous antioxidant defence, we verified whether the enhanced expression of gp91phox, observed in NSE/IL-6 mice, could effectively result in increased production and persistence of reactive radicals in muscle tissue. The accumulation of ROS in skeletal muscle has been evaluated by DHE, a fluorescent redox-sensitive probe able to mainly detect not only superoxide anion but also peroxynitrite ($ONOO^-$) and hydroxyl ($^{\cdot}OH$) radicals [49–54]. Quantitative analysis performed by fluorescence microscopy revealed that the diaphragm muscles of NSE/IL-6 mice presented a significant increase of DHE-derived fluorescence compared to wild-type muscles (Figure 1(b)), indicating that IL-6 overexpression induces the accumulation of ROS within muscle tissue.

It is well known that overproduced ROS can interact with nitric oxide (NO), a molecular mediator of critical cellular functions, giving rise to peroxynitrite ($ONOO^-$) [55]; peroxynitrite can, in turn, interact with proteins leading to the nitration of tyrosine residues [56].

To investigate whether the abundance of ROS detected in NSE/IL-6 diaphragm muscle can induce the oxidative modification of proteins, we evaluated the presence of nitrotyrosine in NSE/IL-6 and wild-type muscles as a marker of nitrooxidative stress (Figure 1(c)). We revealed that the content of nitrated proteins was higher in NSE/IL-6 diaphragm compared to wild-type muscle, indicating that NOX2-derived ROS can be combined with NO, with consequent induction of nitrooxidative damage. Notably, protein nitration not only represents a posttranslational modification able to alter protein structure and function but can also disturb the physiologic NO signalling [56–59].

The NOX2-dependent production of O_2^- is strictly dependent on the availability of nicotinamide adenine dinucleotide phosphate (NADPH), although this substrate is also necessary for the activity of antioxidant systems contributing to the neutralization of ROS. The cytosolic enzyme designated to the maintenance of cellular levels of NADPH is the glucose-6-phosphate dehydrogenase (G6PD), which appears as a common player in both pro- and antioxidant systems [60]. The altered expression of G6PD and of its negative regulator miR-1 has been described in dystrophic muscles, as a direct consequence of the impaired NO signalling [57]. Thus, we investigated whether the enhancement of prooxidant stimuli in muscle milieu induced by IL-6 can be responsible for the alteration of redox-connected molecular circuits, such as the miR-1/G6PD axis (Figures 1(d) and 1(e)) [57, 61]. We observed a significant downregulation of miR-1 (Figure 1(d)) and a significant increase of G6PD protein (Figure 1(e)) in the diaphragm muscles of 24-week-old NSE/IL-6 mice compared to wild-type mice. These data indicated that the overexpression of IL-6 can induce, through the deregulation of redox-related circuits, a sustained production of NADPH which can in turn foster the NOX2-dependent ROS production.

3.2. The Nrf2-Mediated Antioxidant Response Is Impaired in NSE/IL-6 Diaphragm Muscle. The oxidative impact of ROS in skeletal muscle is physiologically counterbalanced by the activation of the endogenous antioxidant response [2, 62]. A central mediator in this protective mechanism is the redox-sensitive transcription factor Nrf2 [19, 63]. Under prooxidant conditions, Nrf2 is known to act as a master regulator of the antioxidant program, by inducing the expression of genes involved in the neutralization of reactive species such as superoxide dismutase (SOD1/2), thioredoxin reductase (Txnrd2), catalase (CAT-1), and NAD(P)H quinone dehydrogenase (NQO1). In addition, Nrf2 can influence the efficiency of the glutathione system modulating the expression of genes involved in the glutathione synthesis, namely, glutathione cysteine ligase (GCL) [64, 65].

We previously reported that the imbalanced redox status of dystrophic muscles involved both the enhanced production of ROS and the impinged antioxidant response. In fact, it has been proposed that elevated levels of ROS within muscle tissue might overcome the endogenous antioxidant system [28]. To define whether sustained levels of circulating IL-6 might be sufficient, independently from a genetic degenerative disease, to determine an alteration of the local antioxidant profile of skeletal muscle, we analysed important mediators of the antioxidant response in diaphragm muscles of both adult mice overexpressing IL-6 and wild-type control mice (Figure 2). We found that the expression of Nrf2 (Figure 2(a)) and SIRT1 (Figure 2(b)), pivotal players of the redox-signalling cascade [66], was downmodulated in 24-week-old NSE/IL-6 diaphragm compared to wild-type muscle. Nevertheless, gene expression analysis revealed a differential modulation of the Nrf2 target genes (Figures 2(c)–2(h)). Indeed, we observed a significant downregulation of CAT-1 (Figure 2(f)), NQO1 (Figure 2(g)), and GCL (Figure 2(h)) in NSE/IL-6 diaphragm compared to wild type, whereas SOD1 (Figure 2(c)) was expressed at similar levels in both NSE/IL-6 and wild-type muscles. Notably, the reduced expression of GCL and NQO1 can impair the availability of reduced glutathione (GSH), contributing to the undeterred accumulation of ROS.

Since mitochondria are known to be active producers of ROS, as well as sensor of the cellular redox status [67], we further analysed the expression of important antioxidant genes involved in the mitochondrial redox regulation, namely, SOD2 and Txnrd2 (Figures 2(d) and 2(e)). Although SOD2 expression was not modulated (Figure 2(d)), we found a significant reduction of Txnrd2 expression in NSE/IL-6 diaphragm muscles compared to wild type (Figure 2(e)). Of note, Txnrd2 is a thioredoxin reductase enzyme participating in the maintenance of a proper mitochondrial redox balance and the impairment of Txnrd2 gene expression has been found in aged muscles and has been associated to the loss of mitochondrial integrity in cardiomyocytes [68, 69]. These data suggest that the deregulation of Nrf2-dependent genes

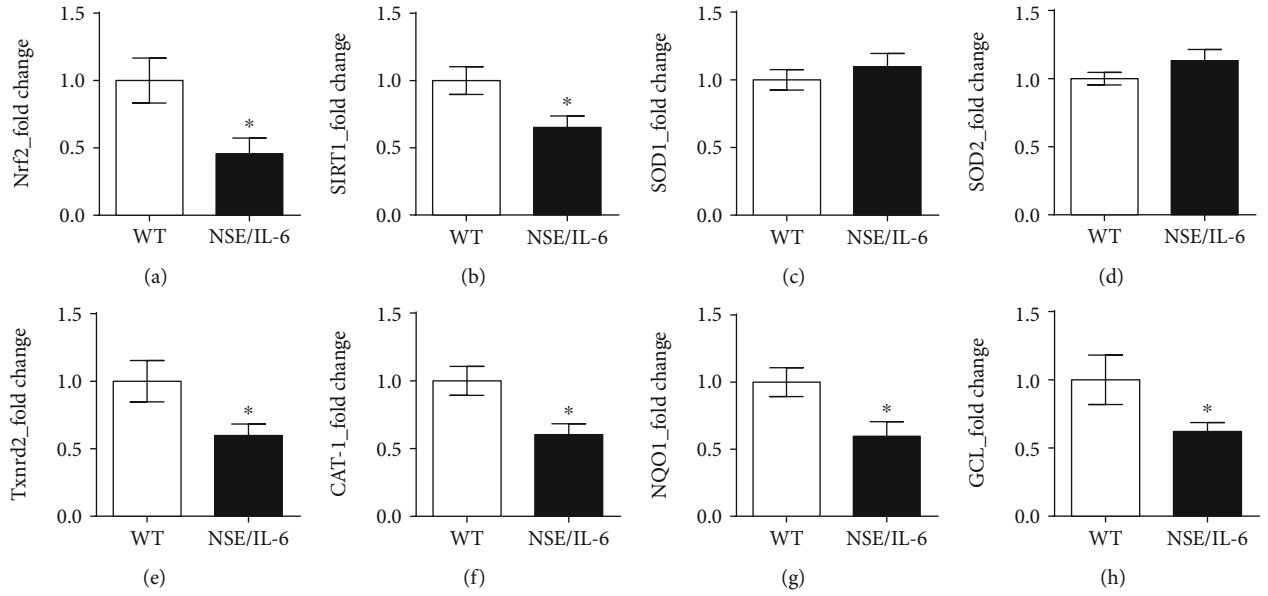

Figure 2: Nrf2-dependent antioxidant genes are differentially modulated in NSE/IL-6 diaphragm muscles. Real-time PCR analysis of the expression of Nrf2 (a), SIRT1 (b), and Nrf2-dependent genes: SOD1 (c), SOD2 (d), Txnrd2 (e), CAT-1 (f), NQO1 (g), and GCL (h). Gene expression analysis was performed on diaphragm muscle samples deriving from wild-type (WT) and NSE/IL-6 mice at 24 weeks of age. Values represent mean ± SEM; n = at least 4 mice per genotype. $^*p < 0.05$ by unpaired t-test. Nrf2: nuclear factor erythroid 2-related factor 2; SIRT1: sirtuin 1; SOD: superoxide dismutase; Txnrd2: thioredoxin reductase 2; CAT-1: catalase-1; NQO1: NAD(P)H quinone dehydrogenase 1; GCL: glutamate-cysteine ligase.

can influence the mitochondrial scavenging of ROS in muscles deriving from IL-6-overexpressing mice.

3.3. Increased Systemic Levels of IL-6 Impinge Morphofunctional Properties of Skeletal Muscle. The uncontrolled generation and accumulation of reactive molecules and the impairment of antioxidant systems are, as a whole, a critical stressor contributing to the disturbance of muscle function [70]. Indeed, oxidative stress has been recognized as a pivotal mechanism contributing to skeletal muscle alteration, inducing the oxidative modification of cellular components and participating to the imbalance between protein synthesis and degradation [71].

To evaluate the effective impact of elevated levels of ROS on skeletal muscle tissue, we performed histological analysis of the diaphragm muscle of 24-week-old NSE/IL-6 and wild-type mice. Noticeably, the evaluation of the general morphology of the NSE/IL-6 diaphragm muscle did not reveal evident signs of infiltrating mononuclear cells, degenerating fibers, or the presence of regenerating centrally nucleated myofibers (Figure 3(a)). However, morphometric analysis, performed on the diaphragm muscle of NSE/IL-6 and wild-type mice, revealed a significant reduction in the cross-sectional area (CSA) of single myofibers in NSE/IL-6 mice compared to wild-type mice (Figure 3(b)). The reduced calibre of fibers observed in transgenic muscles suggested that elevated levels of IL-6, along with the increased amount of intracellular ROS, might induce muscle atrophy in NSE/IL-6 mice.

Indeed, it is well known that IL-6 is a catabolic factor able to induce muscle atrophy when its levels are deregulated [72] and a role for ROS in promoting proteolysis in skeletal muscle has been proposed [71, 73]. We thus analysed pivotal mediators of the main protein degradation pathways involved in muscle atrophy [74]. In particular, we evaluated the expression markers of the ubiquitin-proteasome pathway, the muscle-specific E3 ubiquitin ligases MAFbx/Atrogin1 and Muscle RING Finger-1 (MURF-1) (Figures 3(c) and 3(d)). Real-time PCR analysis revealed a significant upregulation of both Atrogin1 (Figure 3(c)) and MURF-1 (Figure 3(d)) expression in the diaphragm muscle of 24-week-old NSE/IL-6 mice compared to age-matched wild type. In contrast, the analysis of important players of the autophagy-lysosome system, cathepsin L (CTSL) and the microtubule-associated protein 1 light chain 3 (LC3), did not reveal significant variation in gene expression between NSE/IL-6 and wild-type muscles (Figures 3(e) and 3(f)).

In order to evaluate the impact of nonphysiologic amounts of circulating IL-6 levels on a fast-twitch muscle, morphofunctional analysis was performed on extensor digitorum longus (EDL) muscle of both NSE/IL-6 and wild-type mice at 24 weeks of age (Figures 3(g)–3(j)). As reported for the diaphragm muscle (Figure 3(b)), also the EDL muscle showed a reduced cross-sectional area of single myofibers when compared to the EDL of age-matched wild-type mice (Figure 3(h)). In addition, functional analysis showed a significant reduction (-22%) in the capability of NSE/IL-6 EDL to generate maximum force (Figure 3(i)). No significant differences were measured in the specific force (Figure 3(j)).

Overall, these data support the role of deregulated levels of circulating IL-6 in affecting muscle mass with a significant impact on muscle function.

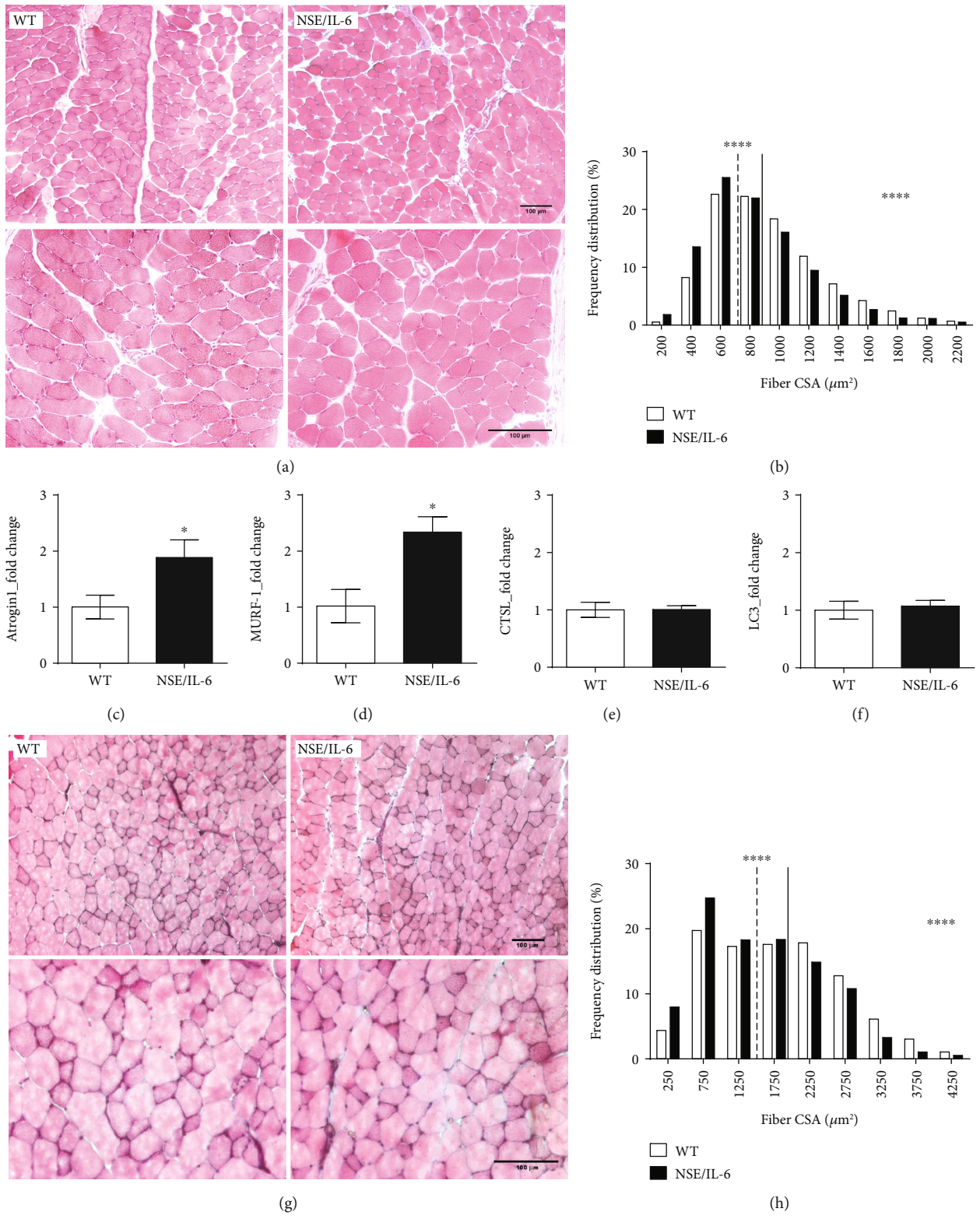

Figure 3: Continued.

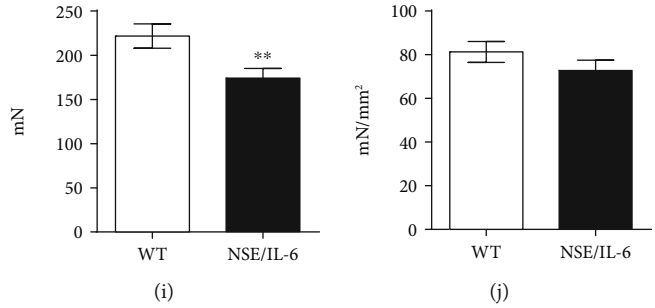

Figure 3: Morphofunctional analysis of NSE/IL-6 and wild-type muscles at 24 weeks of age. (a) Representative image of Haematoxylin and Eosin staining of transverse sections of diaphragm from 24-week-old wild-type (WT) and NSE/IL-6 mice. Scale bar, 100 μm. (b) Frequency distribution of myofiber cross-sectional area (CSA) in transgenic (NSE/IL-6) and wild-type (WT) diaphragm muscle. Data are represented as medians; $n = 4$; $^{****}p < 0.0001$. Real-time PCR analysis for the expression of Atrogin1 (c), MURF-1 (d), CTSL (e), and LC3 (f). Values represent mean ± SEM; $n \geq 5$ mice per genotype. $^{*}p < 0.05$ by unpaired t-test. (g) Haematoxylin and Eosin staining of transverse section of extensor digitorum longus (EDL) muscles from indicated genotypes. Scale bar, 100 μm. (h) Frequency distribution of myofiber cross-sectional area (CSA) in transgenic (NSE/IL-6) and wild-type (WT) EDL muscle. Data are represented as medians; $n \geq 3$; $^{****}p < 0.0001$. Physiological properties of EDL muscles from 24-week-old wild-type (WT) and NSE/IL-6 mice: (i) Maximum force (mN) and (j) specific force (mN/mm^2). Data are represented as mean ± SD of EDL muscle maximum force (i) and specific force (j); $n > 31$; $^{**}p < 0.01$. Atrogin1: MAFbx/Atrogin1; MURF-1: Muscle RING Finger-1; CTSL: cathepsin L; LC3: microtubule-associated protein 1 light chain 3.

4. Discussion

Reactive oxygen species are physiologically produced, especially in metabolic active tissues like skeletal muscle, and are considered important secondary mediators involved in homeostatic processes. However, the excessive production and accumulation of reactive oxygen and nitrogen species are known to induce cell damage by the peroxidation of membrane lipids, protein carbonylation/nitration, and genome insults [1–4]. The extent of ROS production and oxidative damage has been related to the pathogenesis of chronic inflammatory conditions and degenerative diseases such as Duchenne muscular dystrophy [8, 31, 32]. Although inflammation and ROS production have been described as interrelated processes, the precise mechanism linking inflammation and oxidative stress has still to be defined. We recently reported that the overexpression of the proinflammatory cytokine IL-6 in dystrophin-deficient mice (mdx/IL-6 model) is able to exacerbate the dystrophic muscle phenotype, fostering pathologic changes in skeletal muscle and closely approximating the disease progression of DMD patients [27, 28, 31]. Since the increased expression of circulating IL-6 in dystrophic mice has been related to the perturbation of muscle redox signalling even before the occurrence of early signs of the pathology, namely, necrosis and inflammation, we hypothesized that elevated levels of IL-6 can play a pivotal role in the alteration of the muscle redox balance, triggering pathogenic mechanisms associated with muscle degeneration.

Here, we investigated the direct impact of IL-6 on the homeostatic muscle redox balance in a noninjured context, verifying whether high levels of IL-6 are sufficient to induce the establishment of a prooxidant environment in skeletal muscle. To address this issue, we analysed the diaphragm muscle of adult NSE/IL-6 mice characterized by systemically elevated levels of IL-6 [47].

A central mediator of ROS production in skeletal muscle tissue is gp91phox protein, the catalytic subunit of NOX2 complex, which is known to be overexpressed in muscles of DMD patients and dystrophic mice [13, 15, 27, 28, 75]. Thus, we evaluated the extent of prooxidative stimuli in muscles exposed to elevated levels of circulating IL-6 to verify whether nonphysiologic levels of IL-6 can induce the overproduction and accumulation of ROS in a nondystrophic background. We observed not only a strong upregulation of gp91phox protein in the diaphragm muscle of adult NSE/IL-6 mice, compared to age-matched wild type, but also an increased accumulation of ROS in NSE/IL-6 muscles, highlighted by the extent of DHE-derived fluorescence. These data indicate that the overexpression of IL-6, independently from the absence of a functional dystrophin protein, is able to induce the establishment of prooxidant conditions in skeletal muscle tissue that can result in the occurrence of oxidative stress.

The detrimental impact of ROS on cellular and molecular processes was supported by the increased content of nitrated proteins, which are considered markers of nitrooxidative damage and have been related to the alteration of the physiologic NO signalling [3].

It is well known that NADPH content represents a critical factor supporting the activity of both NOX2 and glutathione system, one of the main cellular antioxidant systems. Indeed, NADPH is the electron carrier necessary for the conversion of molecular oxygen into superoxide, by NOX2, and for the reconstitution of reduced/active glutathione. The enzyme responsible for the production of NADPH is G6PD, a member of the NO/HDAC2/miR-1 molecular circuit, which is known to be altered in DMD muscles and reported as directly deregulated by the absence of dystrophin protein [57]. In particular, it has been described that in dystrophin-deficient muscles, the reduced availability of nitric oxide resulted in the decreased S-nitrosylation of proteins, including epigenetic regulators as HDAC2. Nonnitrosylated HDAC2 actively reduces the expression of the muscle-specific microRNA, miR-1, leading to the enhanced expression of G6PD, with a consequent increase of NADPH

content in dystrophic muscles. This deregulated pathway provides substrate mainly for the activity of NOX2, since the glutathione system is known to be impaired in DMD muscles. Thus, to investigate potential mechanisms associated to a redox disequilibrium and responsible for the enhanced production of ROS in skeletal muscle exposed to elevated levels of serum IL-6, we evaluated central mediators of the HDAC2/miR-1/G6PD axis in NSE/IL-6 diaphragm muscles. We revealed a significant downmodulation of miR-1 and a concomitant upregulation of G6PD expression in NSE/IL-6 diaphragm compared to wild-type muscle. These data indicate that increasing levels of IL-6 not only induced the enhanced expression of NOX2 protein but are also involved in the perturbation of critical redox-related molecular circuits which are able to potentiate the NOX2-dependent ROS production in skeletal muscle.

Another critical mechanism participating in the maintenance of a proper cellular redox balance is the activation of the endogenous antioxidant response. It has been described that Nrf2, a redox-sensible transcription factor, can induce the activation of the endogenous antioxidant defence and the expression of important players involved in the cellular stress response, such as IL-6 [19–23]. Indeed, it has been reported that not only Nrf2 can induce IL-6 expression by interacting with a responsive element in the IL-6 promoter but also that IL-6 can in turn enhance the Nrf2-mediated antioxidant response [76]. However, under pathologic conditions such as sepsis, characterized by a massive cytokine release, including IL-6, the antioxidant defence is impaired suggesting an hormetic stress response to IL-6 cytokine [77]. We recently reported that elevated levels of IL-6 in dystrophic muscles are related to the impairment of the Nrf2-mediated antioxidant response, promoting the extent of local and systemic oxidative damage and contributing to the progression of the pathology [27, 28]. Thus, to clarify the impact of abnormal levels of IL-6 on the physiologic response to oxidative conditions, we evaluated the Nrf2-dependent antioxidant response in NSE/IL-6 and wild-type muscles. The reduced expression of Nrf2 and the deregulation of Nrf2-dependent antioxidant genes, observed in NSE/IL-6 mice, clearly indicate that IL-6 can impair the detoxification of ROS in muscle tissue. Indeed, although the expression of SOD1 gene in NSE/IL-6 muscles was similar to wild-type levels, we revealed an impaired expression of CAT-1, NQO1, and GCL genes in mice overexpressing IL-6. In particular, CAT-1 is responsible for the neutralization of H_2O_2, NQO1 is a NADPH-dependent superoxide scavenger, and GCL represents the rate-limiting enzyme for the de novo synthesis of glutathione (GSH) [78, 79]. Thus, our data indicate that in NSE/IL-6 muscles the superoxide produced by NOX2 can be dismutated into H_2O_2, whereas the detoxification of hydrogen peroxide can be impaired. In addition, the reduced expression of NQO1 and GCL in NSE/IL-6 diaphragm suggests that the G6PD-derived NADPH can be preferentially used as a substrate for ROS production instead of ROS neutralization. The alteration of the muscle redox status in IL-6-overexpressing mice is further supported by the reduced expression of SIRT1, a multifunctional regulator of the cellular antioxidant defence, which has been also correlated to the modulation of inflammatory factors and to the biogenesis of mitochondria [80].

Mitochondria are pivotal cell source of ROS deriving from unpaired electrons produced during the oxidative phosphorylation process [81]. Based on their active production of oxidant species, these organelles retain the ability to efficiently counteract the oxidative impact of free radicals, maintaining their structural and functional integrity, through the action of antioxidant effectors such as catalase, MnSOD, and the glutathione and the thioredoxin systems. Of note, SOD2 and Txnrd2 genes have been recognized as potential target of Nrf2 [82–84]. Thus, we investigated whether the impaired expression of Nrf2 in NSE/IL-6 muscle could affect the expression of important regulators of the mitochondrial redox status. We found a significant downmodulation of Txnrd2, but not SOD2 gene expression, in adult NSE/IL-6 muscles compared to control mice. These results suggest that the alteration of the muscle redox status induced by high levels of IL-6 might negatively influence the efficacy of the mitochondrial antioxidant defence, with possible implication on mitochondrial integrity.

The dysfunction of cellular organelles, along with the altered structure of membranes and proteins, is a feature of a deregulated redox condition, namely, oxidative stress, which can profoundly affect the morphofunctional properties of skeletal muscle [70]. Since oxidative stress is known to result from the imbalance between ROS generation and neutralization, we investigated whether the altered muscle redox balance, observed in our model, might effectively afflict muscle phenotype.

Although the histological evaluation of the NSE/IL-6 diaphragm muscle did not reveal evident signs of necrosis, fibrosis, and mononuclear infiltrating cells, morphometric analysis showed a significant reduction of myofiber calibre in NSE/IL-6 diaphragm compared to wild-type muscle. We thus reasoned that the reduced size of single myofibers in muscles exposed to aberrant levels of systemic IL-6 might be related to the activation of atrophic pathways, considering the acknowledged catabolic action of both IL-6 and ROS in skeletal muscle. Molecular analysis was performed to evaluate markers of the main atrophy-related molecular networks, and we revealed a significant upregulation of mediators of the ubiquitin-proteasome pathway in the diaphragm muscle of 24-week-old NSE/IL-6 mice compared to age-matched control mice, whereas the expression markers of the autophagic system were not modulated. These data supported the hypothesis of a direct involvement of IL-6 in the induction of a ROS-mediated alteration of skeletal muscle tissue.

In addition, morphofunctional analysis performed on EDL muscles of both NSE/IL-6 and wild-type mice revealed that also the EDL muscle, which has been recognized as a fast-twitch muscle, showed a reduced cross-sectional area of single myofibers when compared to age-matched wild-type mice. Since skeletal muscle atrophy is known to be characterized by the loss of both muscle mass and contractile properties [70], we evaluated the ability of EDL muscles to generate force upon electrical stimulation. The EDL muscle derived from 24-week-old NSE/IL-6 mice revealed a significant

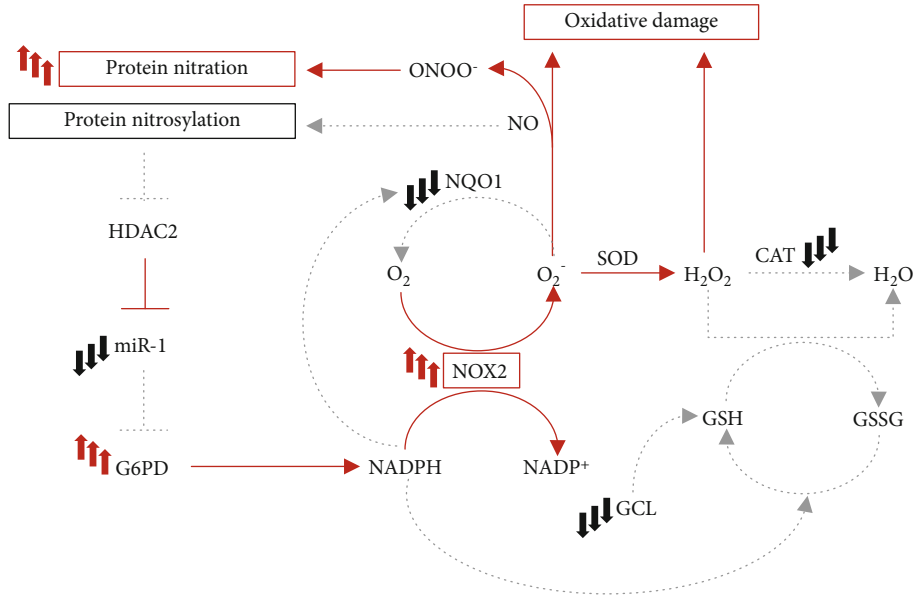

Figure 4: A proposed model of the impact of elevated levels of circulating IL-6 on skeletal muscle redox balance. The reported scheme represents molecular circuits involved in the generation and neutralization of reactive species in skeletal muscle. Red lines indicate mechanisms that are potentially enhanced by elevated levels of circulating IL-6. Grey dot lines represent processes which might be impaired in NSE/IL-6 muscle. In the presence of nonphysiologic amounts of serum IL-6, NOX2 expression is enhanced in diaphragm muscle, inducing a sustained generation of superoxide (O_2^-). The downmodulation of NQO1 in muscle tissue exposed to increased levels of serum IL-6 indicates that the NOX2-derived superoxide might be not efficiently neutralized. On the other hand, O_2^- is converted by SOD into hydrogen peroxide (H_2O_2), whilst its further detoxification can be impaired by the reduced expression of CAT. H_2O_2 can also be neutralized through the oxidation of glutathione. The reduced expression of the rate-limiting enzyme to produce glutathione (GSH), GCL, might reflect an impaired activity of the glutathione system. The excess of O_2^- can also interact with nitric oxide (NO) inducing protein modifications. Moreover, the altered regulation of the NO signalling pathway might induce a deregulated expression of glucose 6-phosphate dehydrogenase (G6PD), the enzyme responsible for the production of NADPH, further enhancing the activity of the NOX2 complex in a feed-forward circuit. NOX2: NADPH oxidase 2; NQO1: NAD(P)H quinone dehydrogenase 1; SOD: superoxide dismutase; CAT: catalase; GCL: glutamate-cysteine ligase; $ONOO^-$: peroxynitrite; HDAC2: histone deacetylase 2; GSSG: oxidized glutathione.

reduction of the tetanic force compared to age-matched wild type, thereby confirming the induction of an atrophic phenotype.

The observed decline of important morphofunctional parameters in NSE/IL-6 muscle suggested that elevated levels of systemic IL-6 might exert a local action, through the enhanced generation and accumulation of ROS, negatively influencing skeletal muscle tissue and function.

5. Conclusions

IL-6 has been recognized as a myokine exerting important functions in skeletal muscle physiopathology. Based on the opposite roles of IL-6 in body and muscle homeostasis, the spectrum of action of IL-6 is tightly regulated and its production is physiologically maintained at very low levels in serum. Elevated circulating levels of IL-6 are instead associated to different pathologic conditions in human and murine models. Herein, we take the advantage of the NSE/IL-6 mouse model to evaluate the impact of altered serum levels of IL-6 on skeletal muscle physiology. We highlighted that circulating IL-6, when deregulated, profoundly affects muscle homeostasis inducing the establishment of prooxidant conditions, which influence the local redox balance that can in turn amplify tissue degeneration under pathologic conditions (Figure 4).

Data Availability

The datasets used to support the findings of this study are included in the present article and are available from the corresponding author upon request.

Disclosure

Laura Forcina and Carmen Miano are co-first authors. Laura Pelosi and Antonio Musarò are co-senior authors.

Conflicts of Interest

The authors declare that there is no conflict of interest regarding the publication of this paper.

Acknowledgments

This work was supported by Ricerca Finalizzata (WFR RF-2013-02358910), ASI, Fondazione Roma, Progetti di Ateneo-Sapienza Università di Roma and Progetto di ricerca d'interesse di Ateneo-Linea D.3.2-Anno 2015-Università Cattolica del Sacro Cuore. The authors thank Carmine Nicoletti, Livia Donzelli, and Marika Berardini for the technical support.

Supplementary Materials

Figure S1 the original image of western blot of gp91phox and GAPDH proteins. Figure S2: original images of western blot for nitrotyrosinated proteins and of stain-free blot. Figure S3: the original image of western blot of G6PD and GAPDH proteins. We refer to these figures in Section 3.1. *(Supplementary Materials)*

References

[1] A. Musarò, S. Fulle, and G. Fanò, "Oxidative stress and muscle homeostasis," *Current Opinion in Clinical Nutrition and Metabolic Care*, vol. 13, no. 3, pp. 236–242, 2010.

[2] S. K. Powers, L. L. Ji, A. N. Kavazis, and M. J. Jackson, "Reactive oxygen species: impact on skeletal muscle," *Comprehensive Physiology*, vol. 1, no. 2, pp. 941–969, 2011.

[3] S. Di Meo, T. T. Reed, P. Venditti, and V. M. Victor, "Role of ROS and RNS sources in physiological and pathological conditions," *Oxidative Medicine and Cellular Longevity*, vol. 2016, 44 pages, 2016.

[4] E. Le Moal, V. Pialoux, G. Juban et al., "Redox control of skeletal muscle regeneration," *Antioxidants and Redox Signaling*, vol. 27, no. 5, pp. 276–310, 2017.

[5] E. Barbieri and P. Sestili, "Reactive oxygen species in skeletal muscle signaling," *Journal of Signal Transduction*, vol. 2012, 17 pages, 2012.

[6] M. Kozakowska, K. Pietraszek-Gremplewicz, A. Jozkowicz, and J. Dulak, "The role of oxidative stress in skeletal muscle injury and regeneration: focus on antioxidant enzymes," *Journal of Muscle Research and Cell Motility*, vol. 36, no. 6, pp. 377–393, 2015.

[7] L. Zuo and B. K. Pannell, "Redox characterization of functioning skeletal muscle," *Frontiers in Physiology*, vol. 6, p. 338, 2015.

[8] M. H. Choi, J. R. Ow, N.-D. Yang, and R. Taneja, "Oxidative stress-mediated skeletal muscle degeneration: molecules, mechanisms, and therapies," *Oxidative Medicine and Cellular Longevity*, vol. 2016, Article ID 6842568, 13 pages, 2016.

[9] G. Dobrowolny, M. Martini, B. M. Scicchitano et al., "Muscle expression of $SOD1^{G93A}$ triggers the dismantlement of neuromuscular junction via PKC-theta," *Antioxidants and Redox Signaling*, vol. 28, no. 12, pp. 1105–1119, 2018.

[10] G. Dobrowolny, E. Lepore, M. Martini et al., "Metabolic changes associated with muscle expression of $SOD1^{G93A}$," *Frontiers in Physiology*, vol. 9, p. 831, 2018.

[11] B. M. Scicchitano, L. Pelosi, G. Sica, and A. Musarò, "The physiopathologic role of oxidative stress in skeletal muscle," *Mechanisms of Ageing and Development*, vol. 170, pp. 37–44, 2018.

[12] B. M. Scicchitano, G. Dobrowolny, G. Sica, and A. Musarò, "Molecular insights into muscle homeostasis, atrophy and wasting," *Current Genomics*, vol. 19, no. 5, pp. 356–369, 2018.

[13] N. P. Whitehead, E. W. Yeung, S. C. Froehner, and D. G. Allen, "Skeletal muscle NADPH oxidase is increased and triggers stretch-induced damage in the mdx mouse," *PLoS One*, vol. 5, no. 12, p. e15354, 2010.

[14] M. Mittal, M. R. Siddiqui, K. Tran, S. P. Reddy, and A. B. Malik, "Reactive oxygen species in inflammation and tissue injury," *Antioxidants and Redox Signaling*, vol. 20, no. 7, pp. 1126–1167, 2014.

[15] L. F. Ferreira and O. Laitano, "Regulation of NADPH oxidases in skeletal muscle," *Free Radical Biology and Medicine*, vol. 98, pp. 18–28, 2016.

[16] W. Li and A.-N. Kong, "Molecular mechanisms of Nrf2-mediated antioxidant response," *Molecular Carcinogenesis*, vol. 48, no. 2, pp. 91–104, 2009.

[17] Y. Guo, S. Yu, C. Zhang, and A.-N. T. Kong, "Epigenetic regulation of Keap1-Nrf2 signaling," *Free Radical Biology and Medicine*, vol. 88, Part B, pp. 337–349, 2015.

[18] K. Itoh, T. Chiba, S. Takahashi et al., "An Nrf2/small Maf heterodimer mediates the induction of phase II detoxifying enzyme genes through antioxidant response elements," *Biochemical and Biophysical Research Communications*, vol. 236, no. 2, pp. 313–322, 1997.

[19] A. Kobayashi, T. Ohta, and M. Yamamoto, "Unique function of the Nrf2-Keap1 pathway in the inducible expression of antioxidant and detoxifying enzymes," *Methods in Enzymology*, vol. 378, pp. 273–286, 2004.

[20] H. Motohashi and M. Yamamoto, "Nrf2-Keap1 defines a physiologically important stress response mechanism," *Trends in Molecular Medicine*, vol. 10, no. 11, pp. 549–557, 2004.

[21] C. J. Wruck, K. Streetz, G. Pavic et al., "Nrf2 induces interleukin-6 (IL-6) expression via an antioxidant response element within the IL-6 promoter," *Journal of Biological Chemistry*, vol. 286, no. 6, pp. 4493–4499, 2011.

[22] J. W. Kaspar, S. K. Niture, and A. K. Jaiswal, "Nrf2:INrf2 (Keap1) signaling in oxidative stress," *Free Radical Biology and Medicine*, vol. 47, no. 9, pp. 1304–1309, 2009.

[23] A. Loboda, M. Damulewicz, E. Pyza, A. Jozkowicz, and J. Dulak, "Role of Nrf2/HO-1 system in development, oxidative stress response and diseases: an evolutionarily conserved mechanism," *Cellular and Molecular Life Science*, vol. 73, no. 17, pp. 3221–3247, 2016.

[24] S. Vomund, A. Schäfer, M. J. Parnham, B. Brüne, and A. von Knethen, "Nrf2, the master regulator of anti-oxidative responses," *International Journal of Molecular Sciences*, vol. 18, no. 12, p. 2772, 2017.

[25] E. Birben, U. M. Sahiner, C. Sackesen, S. Erzurum, and O. Kalayci, "Oxidative stress and antioxidant defense," *World Allergy Organization Journal*, vol. 5, no. 1, pp. 9–19, 2012.

[26] Q. Ma, "Role of nrf2 in oxidative stress and toxicity," *Annual Review of Pharmacology and Toxicology*, vol. 53, pp. 401–426, 2013.

[27] S. Petrillo, L. Pelosi, F. Piemonte et al., "Oxidative stress in Duchenne muscular dystrophy: focus on the NRF2 redox pathway," *Human Molecular Genetics*, vol. 26, no. 14, pp. 2781–2790, 2017.

[28] L. Pelosi, L. Forcina, C. Nicoletti, B. M. Scicchitano, and A. Musarò, "Increased circulating levels of interleukin-6 induce perturbation in redox-regulated signaling cascades in muscle of dystrophic mice," *Oxidative Medicine and Cellular Longevity*, vol. 2017, Article ID 1987218, 10 pages, 2017.

[29] M. Moulin and A. Ferreiro, "Muscle redox disturbances and oxidative stress as pathomechanisms and therapeutic targets in early-onset myopathies," *Seminars in Cell and Developmental Biology*, vol. 64, pp. 213–223, 2017.

[30] J. Lugrin, N. Rosenblatt-Velin, R. Parapanov, and L. Liaudet, "The role of oxidative stress during inflammatory processes," *Biological Chemistry*, vol. 395, no. 2, pp. 203–230, 2014.

[31] L. Forcina, L. Pelosi, C. Miano, and A. Musarò, "Insights into the pathogenic secondary symptoms caused by the primary loss of dystrophin," *Journal of Functional Morphology and Kinesiology*, vol. 2, no. 4, p. 44, 2017.

[32] J. R. Terrill, H. G. Radley-Crabb, T. Iwasaki, F. A. Lemckert, P. G. Arthur, and M. D. Grounds, "Oxidative stress and pathology in muscular dystrophies: focus on protein thiol oxidation and dysferlinopathies," *The FEBS Journal*, vol. 280, no. 17, pp. 4149–4164, 2013.

[33] S. J. Forrester, D. S. Kikuchi, M. S. Hernandes, Q. Xu, and K. K. Griendling, "Reactive oxygen species in metabolic and inflammatory signaling," *Circulation Research*, vol. 122, no. 6, pp. 877–902, 2018.

[34] P. Munoz-Canoves, C. Scheele, B. K. Pedersen, and A. L. Serrano, "Interleukin-6 myokine signaling in skeletal muscle: a double-edged sword?," *The FEBS Journal*, vol. 280, no. 17, pp. 4131–4148, 2013.

[35] L. Forcina, C. Miano, and A. Musarò, "The physiopathologic interplay between stem cells and tissue niche in muscle regeneration and the role of IL-6 on muscle homeostasis and diseases," *Cytokine and Growth Factor Reviews*, vol. 41, pp. 1–9, 2018.

[36] L. Forcina, C. Miano, B. Scicchitano, and A. Musarò, "Signals from the niche: insights into the role of IGF-1 and IL-6 in modulating skeletal muscle fibrosis," *Cells*, vol. 8, no. 3, p. 232, 2019.

[37] P. C. Heinrich, I. Behrmann, G. Müller-Newen, F. Schaper, and L. Graeve, "Interleukin-6-type cytokine signalling through the gp130/Jak/STAT pathway," *Biochemical Journal*, vol. 334, Part 2, pp. 297–314, 1998.

[38] P. C. Heinrich, I. Behrmann, S. Haan, H. M. Hermanns, G. Müller-Newen, and F. Schaper, "Principles of interleukin (IL)-6-type cytokine signalling and its regulation," *Biochemical Journal*, vol. 374, Part 1, pp. 1–20, 2003.

[39] A. L. Serrano, B. Baeza-Raja, E. Perdiguero, M. Jardí, and P. Muñoz-Cánoves, "Interleukin-6 is an essential regulator of satellite cell-mediated skeletal muscle hypertrophy," *Cell Metabolism*, vol. 7, no. 1, pp. 33–44, 2008.

[40] J. A. Carson and K. A. Baltgalvis, "Interleukin-6 as a key regulator of muscle mass during cachexia," *Exercise and Sport Sciences Reviews*, vol. 38, no. 4, pp. 168–176, 2010.

[41] M. R. Douglas, K. E. Morrison, M. Salmon, and C. D. Buckley, "Why does inflammation persist: a dominant role for the stromal microenvironment?," *Expert Reviews in Molecular Medicine*, vol. 4, no. 25, pp. 1–18, 2002.

[42] S. Rose-John, "IL-6 trans-signaling via the soluble IL-6 receptor: importance for the pro-inflammatory activities of IL-6," *International Journal of Biological Sciences*, vol. 8, no. 9, pp. 1237–1247, 2012.

[43] S. O'Reilly, M. Ciechomska, R. Cant, and J. M. van Laar, "Interleukin-6 (IL-6) trans signaling drives a STAT3-dependent pathway that leads to hyperactive transforming growth factor-β (TGF-β) signaling promoting SMAD3 activation and fibrosis via gremlin protein," *The Journal of Biological Chemistry*, vol. 289, no. 14, pp. 9952–9960, 2014.

[44] C. Garbers, S. Heink, T. Korn, and S. Rose-John, "Interleukin-6: designing specific therapeutics for a complex cytokine," *Nature Reviews Drug Discovery*, vol. 17, no. 6, pp. 395–412, 2018.

[45] L. Pelosi, M. G. Berardinelli, L. Forcina et al., "Increased levels of interleukin-6 exacerbate the dystrophic phenotype in mdx mice," *Human Molecular Genetics*, vol. 24, no. 21, pp. 6041–6053, 2015.

[46] L. Pelosi, M. G. Berardinelli, L. De Pasquale et al., "Functional and morphological improvement of dystrophic muscle by interleukin 6 receptor blockade," *eBioMedicine*, vol. 2, no. 4, pp. 285–293, 2015.

[47] F. De Benedetti, T. Alonzi, A. Moretta et al., "Interleukin 6 causes growth impairment in transgenic mice through a decrease in insulin-like growth factor-I. a model for stunted growth in children with chronic inflammation," *Journal of Clinical Investigation*, vol. 99, no. 4, pp. 643–650, 1997.

[48] Z. Del Prete, A. Musarò, and E. Rizzuto, "Measuring mechanical properties, including isotonic fatigue, of fast and slow MLC/mIgf-1 transgenic skeletal muscle," *Annals of Biomedical Engineering*, vol. 36, no. 7, pp. 1281–1290, 2008.

[49] A. Gomes, E. Fernandes, and J. L. F. C. Lima, "Fluorescence probes used for detection of reactive oxygen species," *Journal of Biochemical and Biophysical Methods*, vol. 65, no. 2–3, pp. 45–80, 2005.

[50] N. Patsoukis, I. Papapostolou, and C. D. Georgiou, "Interference of non-specific peroxidases in the fluorescence detection of superoxide radical by hydroethidine oxidation: a new assay for H_2O_2," *Analytical and Bioanalytical Chemistry*, vol. 381, no. 5, pp. 1065–1072, 2005.

[51] P. Wardman, "Fluorescent and luminescent probes for measurement of oxidative and nitrosative species in cells and tissues: progress, pitfalls, and prospects," *Free Radical Biology and Medicine*, vol. 43, no. 7, pp. 995–1022, 2007.

[52] J. Zielonka, M. Hardy, and B. Kalyanaraman, "HPLC study of oxidation products of hydroethidine in chemical and biological systems: ramifications in superoxide measurements," *Free Radical Biology and Medicine*, vol. 46, no. 3, pp. 329–338, 2009.

[53] B. Kalyanaraman, V. Darley-Usmar, K. J. A. Davies et al., "Measuring reactive oxygen and nitrogen species with fluorescent probes: challenges and limitations," *Radical Biology and Medicine*, vol. 52, no. 1, pp. 1–6, 2012.

[54] A. Wojtala, M. Bonora, D. Malinska, P. Pinton, J. Duszynski, and M. R. Wieckowski, "Methods to monitor ROS production by fluorescence microscopy and fluorometry," *Methods in Enzymology*, vol. 542, pp. 243–262, 2014.

[55] P. Pacher, J. S. Beckman, and L. Liaudet, "Nitric oxide and peroxynitrite in health and disease," *Physiological Reviews*, vol. 87, no. 1, pp. 315–424, 2007.

[56] R. Radi, "Protein tyrosine nitration: biochemical mechanisms and structural basis of functional effects," *Accounts of Chemical Research*, vol. 46, no. 2, pp. 550–559, 2013.

[57] D. Cacchiarelli, J. Martone, E. Girardi et al., "MicroRNAs involved in molecular circuitries relevant for the Duchenne muscular dystrophy pathogenesis are controlled by the dystrophin/nNOS pathway," *Cell Metabolism*, vol. 12, no. 4, pp. 341–351, 2010.

[58] J. C. Begara-Morales, B. Sánchez-Calvo, M. Chaki et al., "Antioxidant systems are regulated by nitric oxide-mediated post-translational modifications (NO-PTMs)," *Frontiers in Plant Science*, vol. 7, p. 152, 2016.

[59] M. J. Lee and M. B. Yaffe, "Protein regulation in signal transduction," *Cold Spring Harbor Perspectives in Biology*, vol. 8, no. 6, p. a005918, 2016.

[60] R. C. Stanton, "Glucose-6-phosphate dehydrogenase, NADPH, and cell survival," *IUBMB Life*, vol. 64, no. 5, pp. 362–369, 2012.

[61] L. Pelosi, A. Coggi, L. Forcina, and A. Musarò, "MicroRNAs modulated by local mIGF-1 expression in mdx dystrophic mice," *Frontiers in Aging Neuroscience*, vol. 7, p. 69, 2015.

[62] P. D. Ray, B.-W. Huanga, and Y. Tsuji, "Reactive oxygen species (ROS) homeostasis and redox regulation in cellular signaling," *Cellular Signalling*, vol. 24, no. 5, pp. 981–990, 2012.

[63] L. E. Tebay, H. Robertson, S. T. Durant et al., "Mechanisms of activation of the transcription factor Nrf2 by redox stressors, nutrient cues, and energy status and the pathways through which it attenuates degenerative disease," *Free Radical Biology and Medicine*, vol. 88, Part B, pp. 108–146, 2015.

[64] S. C. Lu, "Regulation of glutathione synthesis," *Molecular Aspects of Medicine*, vol. 30, no. 1–2, pp. 42–59, 2009.

[65] C. Tonelli, I. I. C. Chio, and D. A. Tuveson, "Transcriptional regulation by Nrf2," *Antioxidants and Redox Signaling*, vol. 29, no. 17, pp. 1727–1745, 2018.

[66] P. S. Pardo and A. M. Boriek, "The physiological roles of Sirt1 in skeletal muscle," *Aging*, vol. 3, no. 4, pp. 430–437, 2011.

[67] D. E. Handy and J. Loscalzo, "Redox regulation of mitochondrial function," *Antioxidants and Redox Signaling*, vol. 16, no. 11, pp. 1323–1367, 2012.

[68] S. Rohrbach, S. Gruenler, M. Teschner, and J. Holtz, "The thioredoxin system in aging muscle: key role of mitochondrial thioredoxin reductase in the protective effects of caloric restriction?," *American Journal of Physiology-Regulatory, Integrative and Comparative Physiology*, vol. 291, no. 4, pp. R927–R935, 2006.

[69] J. Horstkotte, T. Perisic, M. Schneider et al., "Mitochondrial thioredoxin reductase is essential for early postischemic myocardial protection," *Circulation*, vol. 124, no. 25, pp. 2892–2902, 2011.

[70] J. Ábrigo, A. A. Elorza, C. A. Riedel et al., "Role of oxidative stress as key regulator of muscle wasting during cachexia," *Oxidative Medicine and Cellular Longevity*, vol. 2018, Article ID 2063179, 17 pages, 2018.

[71] S. K. Powers, A. J. Smuder, and D. S. Criswell, "Mechanistic links between oxidative stress and disuse muscle atrophy," *Antioxidants and Redox Signaling*, vol. 15, no. 9, pp. 2519–2528, 2011.

[72] F. Haddad, F. Zaldivar, D. M. Cooper, and G. R. Adams, "IL-6-induced skeletal muscle atrophy," *Journal of Applied Physiology*, vol. 98, no. 3, pp. 911–917, 2005.

[73] S. K. Powers, A. J. Smuder, and A. R. Judge, "Oxidative stress and disuse muscle atrophy: cause or consequence?," *Current Opinion in Clinical Nutrition and Metabolic Care*, vol. 15, no. 3, pp. 240–245, 2012.

[74] M. Sandri, "Protein breakdown in muscle wasting: role of autophagy-lysosome and ubiquitin- proteasome," *The Internatioal Journal of Biochemistry and Cell Biology*, vol. 45, no. 10, pp. 2121–2129, 2013.

[75] J.-H. Kim, H.-B. Kwak, L. V. Thompson, and J. M. Lawler, "Contribution of oxidative stress to pathology in diaphragm and limb muscles with Duchenne muscular dystrophy," *Journal of Muscle Research and Cell Motility*, vol. 34, no. 1, pp. 1–13, 2013.

[76] M. R. Marasco, A. M. Conteh, C. A. Reissaus et al., "Interleukin-6 reduces β-cell oxidative stress by linking autophagy with the antioxidant response," *Diabetes*, vol. 67, no. 8, pp. 1576–1588, 2018.

[77] D. A. Lowes, N. R. Webster, M. P. Murphy, and H. F. Galley, "Antioxidants that protect mitochondria reduce interleukin-6 and oxidative stress, improve mitochondrial function, and reduce biochemical markers of organ dysfunction in a rat model of acute sepsis," *British Journal of Anaesthesia*, vol. 110, no. 3, pp. 472–480, 2013.

[78] D. Siegel, D. L. Gustafson, D. L. Dehn et al., "NAD(P)H: quinone oxidoreductase 1: role as a superoxide scavenger," *Molecular Pharmacology*, vol. 65, no. 5, pp. 1238–1247, 2004.

[79] O. M. Ighodaro and O. A. Akinloye, "First line defence antioxidants-superoxide dismutase (SOD), catalase (CAT) and glutathione peroxidase (GPX): their fundamental role in the entire antioxidant defence grid," *Alexandria Journal of Medicine*, vol. 54, no. 4, pp. 287–293, 2018.

[80] A. Salminen, K. Kaarniranta, and A. Kauppinen, "Crosstalk between oxidative stress and SIRT1: impact on the aging process," *International Journal of Molecular Sciences*, vol. 14, no. 2, pp. 3834–3859, 2013.

[81] J. Kang and S. Pervaiz, "Mitochondria: redox metabolism and dysfunction," *Biochemistry Research International*, vol. 2012, Article ID 896751, 14 pages, 2012.

[82] R. C. Taylor, G. Acquaah-Mensah, M. Singhal, D. Malhotra, and S. Biswal, "Network inference algorithms elucidate Nrf2 regulation of mouse lung oxidative stress," *PLoS Computational Biology*, vol. 4, no. 8, p. e1000166, 2008.

[83] T. M. Teixeira, D. C. Da Costa, A. C. Resende, C. O. Soulage, F. F. Bezerra, and J. B. Daleprane, "Activation of Nrf2-antioxidant signaling by 1,25-dihydroxycholecalciferol prevents leptin-induced oxidative stress and inflammation in human endothelial cells," *The Journal of Nutritional Biochemistry*, vol. 147, no. 4, pp. 506–513, 2017.

[84] Y. Kitaoka, Y. Tamura, K. Takahashi, K. Takeda, T. Takemasa, and H. Hatta, "Effects of Nrf2 deficiency on mitochondrial oxidative stress in aged skeletal muscle," *Physiological Reports*, vol. 7, no. 3, p. e13998, 2019.

Hindawi
Oxidative Medicine and Cellular Longevity
Volume 2019, Article ID 9030563, 11 pages
https://doi.org/10.1155/2019/9030563

Review Article

Oxidative Stress in Cell Death and Cardiovascular Diseases

Tao Xu,[1,2] **Wei Ding**,[3] **Xiaoyu Ji**,[1] **Xiang Ao**,[2] **Ying Liu**,[2] **Wanpeng Yu**,[1] **and Jianxun Wang**[1,2]

[1]*School of Basic Medical Sciences, Qingdao University, Qingdao, China*
[2]*Center for Regenerative Medicine, Institute for Translational Medicine, College of Medicine, Qingdao University, Qingdao, China*
[3]*Department of Comprehensive Internal Medicine, Affiliated Hospital, Qingdao University, Qingdao, China*

Correspondence should be addressed to Jianxun Wang; wangjx@qdu.edu.cn

Tao Xu and Wei Ding contributed equally to this work.

Received 23 May 2019; Accepted 11 September 2019; Published 4 November 2019

Guest Editor: Andrey J. Serra

ROS functions as a second messenger and modulates multiple signaling pathways under the physiological conditions. However, excessive intracellular ROS causes damage to the molecular components of the cell, which promotes the pathogenesis of various human diseases. Cardiovascular diseases are serious threats to human health with extremely high rates of morbidity and mortality. Dysregulation of cell death promotes the pathogenesis of cardiovascular diseases and is the clinical target during the disease treatment. Numerous studies show that ROS production is closely linked to the cell death process and promotes the occurrence and development of the cardiovascular diseases. In this review, we summarize the regulation of intracellular ROS, the roles of ROS played in the development of cardiovascular diseases, and the programmed cell death induced by intracellular ROS. We also focus on anti-ROS system and the potential application of anti-ROS strategy in the treatment of cardiovascular diseases.

1. Introduction

ROS refers to a group of small reactive molecules and is produced under both the normal life process and the various pathological conditions. ROS can function as a signaling molecule or a risk factor for the occurrence of diseases [1]. The levels of intracellular ROS are precisely regulated to limit it to a certain level. However, intracellular ROS can be damaged to the cell if ROS level is out of the normal range under the pathological conditions. The intracellular ROS is closely correlated with the pathogenesis of cardiovascular diseases, including the atherosclerosis, myocardial ischemia/reperfusion injury, myocardial hypertrophy, and heart failure [2]. However, the current therapeutic strategies to target the intracellular ROS are unsuccessful in the clinical trial of cardiovascular disease treatment. The reason of the failure is ascribed to the inability to clarify the specific roles of ROS and target the accurate ROS resources under different pathological conditions, and the nonspecific antioxidant approach cannot scavenge ROS properly and effectively [3]. Understanding the precise mechanism of ROS production, ROS-related signaling pathways, and the different roles ROS played under different pathological conditions is essential for increasing the chance of success during cardiovascular disease treatment. Moreover, cell death induced by ROS is closely related with the pathogenesis of cardiovascular diseases. Exploration of the mechanisms of cell death and the development of anticell death strategy will also provide opportunity for the cardiovascular disease treatment.

2. ROS Resources in the Cardiovascular Diseases

2.1. Excessive ROS in Vascular Dysfunction. Even though small amounts of intracellular ROS are continuously produced in cells, excessive generation of ROS, caused by pathological stimuli or the failure of ROS clearance system, is the major cause of various vascular dysfunctions. Accumulating evidences suggest that excessive ROS contributes to the

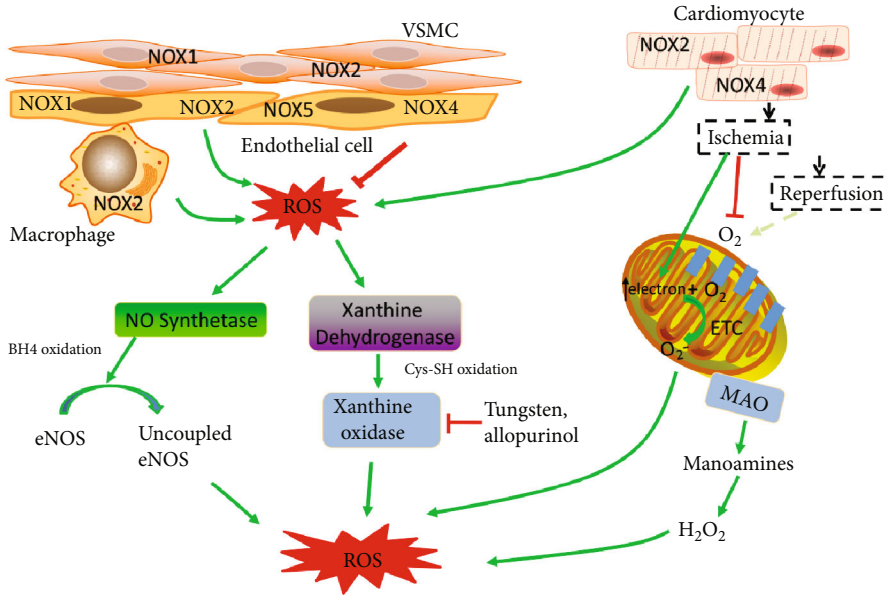

Figure 1: ROS resources during cardiovascular diseases. The NOX-derived ROS are the primary ROS resources. NOX1, NOX2, NOX4, and NOX5 are expressed in the endothelial cell. NOX1 and NOX2 are expressed in the VSMC. NOX2 and NOX4 are abundant in cardiomyocyte. The activity of NOX2 in the immune cells also contributes to the ROS production under pathological condition. NOX-derived ROS can uncouple the NO synthase and promote O_2^- generation. The xanthine dehydrogenase is transformed into xanthine oxidase by oxidation which uses oxygen as an electron acceptor and produces ROS. Ischemia disrupts the oxygen supply and promotes the electron accumulation of electron transport chain. Reperfusion recovers the oxygen and promotes O_2^- production. Monoamine oxidase (MAO) anchored on the mitochondrial outer membrane degrades the monoamines and produces H_2O_2.

altered vascular functions including endothelial dysfunction, vascular smooth muscle cell (VSMC) overgrowth, and structural remodeling. Moreover, oxidative stress could induce vascular inflammation and injury through activation of the transcription factors, upregulation of adhesion molecules, stimulation of chemokine production, and recruitment of inflammatory cells [4, 5]. Considering these important roles of ROS in the pathogenesis of vascular dysfucntion, a clear classification of the ROS resources and the roles it plays under different pathological conditions is urgently needed.

2.1.1. ROS from the NADPH Oxidase Activity. Although the intracellular ROS comes from multiple sources, the activities of NADPH oxidases (NOXs) are the only primary ROS resources (Figure 1) [6, 7]. NOXs could generate a large burst of O_2^- with NADPH serving as electron donor in the VSMC, endothelial cells, and fibroblasts [8]. Moreover, NOX-derived ROS can uncouple the NO synthase and promote O_2^- generation through oxidative degradation of NO synthase cofactor, H4B. There are 5 different NOX isoforms identified until now [8, 9]. NOXs are expressed in a cell- and tissue-specific fashion and are differently regulated under various pathological conditions (Figure 1).

The NOX1, NOX2, NOX4, and NOX5 are all expressed in endothelial cells [10]. Other cell types in the vascular wall, including VSMCs and the immune cells, also express NOXs, which also contribute to ROS production under certain conditions (Figure 1) [11–13]. NOX2 is likely to be the most important ROS resource under pathological conditions while NOX4 plays a protective role in contrast through promoting NO bioavailability and suppressing cell death [14]. The remnant lipoprotein particles (RLPs) or oxLDL, which are the coronary risk factors and predictors of cardiovascular events, will increase NOX2 expression and the subsequent ROS production but have no effect on the expression of NOX4 in endothelial cells [15]. It is shown that NOX2 knockout mice protect endothelial cells from ROS damage in the aorta in the atherosclerosis model, suggesting that NOX2-deprvied ROS is the major cause of atherosclerosis [16]. Angiotensin II is a potent inducer of vascular ROS production and promotes the vessel dysfunction. Evidences showed that Ang II could increase the expression of NOX2 and promote the acute assembly of this oxidase complex in the endothelial cells. In contrast, NOX4 could antagonize Ang II-induced endothelial dysfunction. NOX4 knockout mice accelerate the aortic medial hypertrophy and cytokine production in the mouse model [17].

2.1.2. Xanthine Oxidase. The activity of xanthine oxidase (XO) is another major source of intracellular ROS. There are two forms of XOs with different substrates. The dehydrogenase form uses both NAD+ and oxygen as an electron acceptor, with a preference to NAD+. The oxidase form of XO using the molecular oxygen as electron acceptor produces ROS without reducing NAD+. Evidences show that Ang II could increase the protein levels of XO. XO knockout dramatically decreases the ROS production during Ang II-induced vascular dysfunction, suggesting that XO activity is a major ROS resource under this condition [18]. NOX inhibition can prevent the Ang II-induced superoxide from XO,

suggesting that the activation of XO by Ang II needs the activity of NOX [19]. Cytokines can also stimulate the expression of XO, and XO is involved in ROS production induced by vascular inflammation [20, 21]. The activity of endothelial XO is also observed to be increased in the coronary disease patients. All these evidences support the application of targeting XOs during the cardiovascular disease treatment.

The protective roles of XO inhibitors have been tested in the animal models of cardiovascular diseases. Tungsten, an inhibitor of XO, can prevent the development of atherosclerosis in $ApoE^{-/-}$ mice [22]. Allopurinol, another inhibitor of XO, can attenuate endothelial dysfunction in HF patients [23]. In addition, the product of XO is a biomarker during the diagnosis of cardiovascular diseases [24]. These evidences suggest the important roles of XO in the vascular dysfunction, and targeting XO may represent an important way for disease treatment.

2.2. ROS in Cardiac Remodeling and Heart Failure. The cardiac pathological conditions including cardiomyocyte hypertrophy, dysregulation of cell death, and remodeling of the extracellular matrix contribute to the final heart failure. Accumulating evidences demonstrate that intracellular ROS and its related signaling pathways are actively involved in these cardiac functional abnormalities.

2.2.1. ROS from Enzymatic Activity. NOXs are also involved in the myocardial ROS production process (Figure 1). Both in the experimental models of the left ventricular hypertrophy (LVH) and in the end-stage failing human myocardium, the increased NOX activity is found to be closely correlated with these pathogenic processes [25, 26]. NOX2 and NOX4 are abundantly expressed in the cardiomyocytes. In the mouse model of LVH induced by angiotensin II or atrial natriuretic factor, ROS production is inhibited and cardiac function is improved by NOX2 knockout, indicating that NOX2-derived ROS plays a critical role in Ang II-induced hypertrophy [27, 28]. However, cardiac pressure overload-induced hypertrophy cannot be inhibited by NOX2 knockout, suggesting that NOX2 is not important in this process. In contrast, NOX4 promotes the LVH induced by pressure overload [29, 30]. Adverse remodeling of the left ventricle caused by myocardial infarction will develop into the final chronic heart failure (CHF) in patients. ROS generated from the NOXs activates the matrix metalloproteinase, which drives matrix turnover and promotes the left ventricle dilatation [31]. The NOX-derived ROS activity also plays an important role in myocardial infarction both in the mouse model and in the patients [25, 32]. The activity of xanthine oxidase (XO) also contributes to the cardiac adverse left ventricle remodeling after myocardial infarction in the mouse model. Inhibitor of XO improves the cardiac function in the mouse model of myocardial infarction (MI) [33]. Monoamine oxidase (MAO) is another ROS resource anchored in the outer membrane of mitochondria [34]. The activity of MAO increases the levels of H_2O_2 both in the mitochondria and the cytosol (Figure 1), which impairs the autophagy process, leading to the accumulation of damaged organelles and the final myocardial necrosis [35]. MAO is also involved in the pathogenesis of heart failure and myocardial ischemia/reperfusion injury [36, 37].

2.2.2. ROS from Mitochondria. The activity of mitochondria electron transport chain (ETC) produces ATP for the cellular energy demand with the oxygen as the electron acceptor (Figure 1), which is another ROS resource [38]. Moreover, mitochondrial dysfunction during the pathological process can lead to the ROS burst which activates multiple cell death signaling pathways. Evidences show that mitochondrial ROS is produced in both the ischemia stage and the reperfusion stage during myocardial ischemia/reperfusion injury. Ischemia disrupts the oxygen supply and induces the collapse of electron transport chain (ETC), with the accumulation of electron. The O_2 and ATP depletion during ischemia also sets the condition for the ROS production during reperfusion stage [39, 40]. Reestablishment of oxygen at the reperfusion stage acutely increases the generation of ROS, which leads to subsequent myocardial cell death [41]. Moreover, mitochondrial ROS will lead to the inactivation of iron-sulfur (Fe-S) centers, releasing free iron and leading to subsequent lipid oxidation through Fenton reaction [42].

3. ROS and Programed Cell Death

A direct outcome of excessive ROS production is the induction of cell death, which is the major cause of various cardiovascular diseases under different pathological conditions [43]. Programmed cell death is the important therapeutic target during disease treatment as it is regulated by the gene products [44]. Apoptosis is the first established programmed cell death and has been studied intensively in the past 2 decades. In addition to the apoptotic cell death, other modes of programed cell death have recently been identified and are demonstrated to contribute to the pathogenesis of cardiovascular diseases (Figure 2) [45]. Understanding the roles of different cell death processes in cardiovascular diseases and the underlying signaling pathways will improve the therapeutic strategy.

3.1. Apoptosis. Apoptosis is the firstly coined and mostly studied programmed cell death process. Numerous studies show that apoptosis contributes to both the acute loss of cardiomyocytes in myocardial ischemia/reperfusion injury and the chronic loss of cardiomyocytes in the chronic heart failure [46]. ROS is closely related with cardiomyocyte apoptosis. Both the extrinsic death receptor pathways and the intrinsic mitochondrial pathways are involved in the myocardial apoptosis induced by ROS. The binding of ligands with death receptor induces lipid raft formation and NOX assembly and activation, which leads to the ROS generation. ROS will promote the formation of lipid raft-derived signaling platforms, activating the death receptor-mediated apoptosis [47].

During the activation of the intrinsic mitochondrial apoptosis pathways, excessive ROS promotes the permeabilization of the mitochondrial outer membrane through activation of the proapoptotic Bcl-2 superfamily proteins [48]. Increased mitochondrial permeability will lead to the

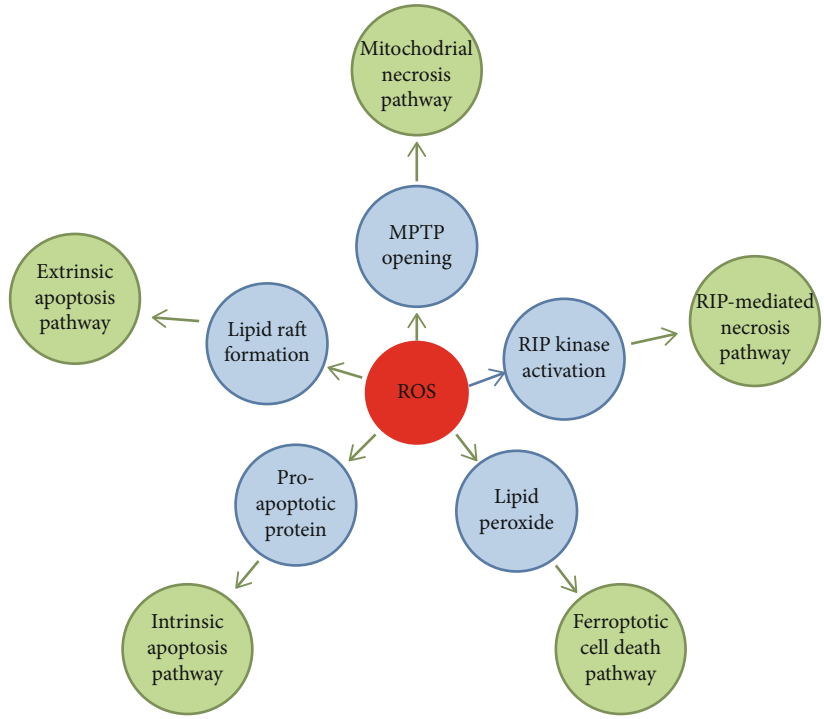

Figure 2: Schematic diagram of programmed cell death during ROS-induced myocardial injury.

release of apoptosis activators, triggering the activation of apoptosis [49]. What is more, ROS can induce apoptosis through the activation of apoptosis initiation signaling pathways or inhibition of the protective mechanisms of the cell [50, 51].

Although the myocardial apoptosis signaling pathways have been intensively studied and therapeutic targeting of apoptotic pathways shows potential in the treatment of heart failure, it is still not convincing to say that the inhibition of apoptosis can efficiently prevent heart failure in the patients. One reason may be that inhibition of apoptosis may activate the necrotic cell death, which is a major cell death process during the heart failure. Another important thing may be that it is important to initiate treatment at the most suitable time. For example, cell death may occur in a certain stage, such as the beginning of reperfusion stage.

3.2. Myocardial Necrosis. It is considered that myocardial necrosis has a stronger effect on the loss of cardiomyocyte than apoptosis [52]. Recent evidences demonstrate that some necrosis can also be regulated by multiple signaling pathways rather than a passive cell death process [53]. There are two major signaling pathways regulating the myocardial necrosis, the RIP-mediated necrosis pathway and the mitochondrial necrosis pathway [54]. The burst of intracellular ROS during the myocardial I/R injury through XO activity or mitochondria ROS formation leads to myocardial necrosis and promotes myocardial damage [55]. The role of ROS in the induction of myocardial necrosis can also be demonstrated from several recent works. Wang et al. showed that ROS will elevate the protein levels of RIP1 and RIP3, promoting the H_2O_2-induced necrosis in H9c2 cells. These results are also confirmed in the mouse model of ischemia/reperfusion injury [56]. Another study by Zhang et al. demonstrates that RIP3 can promote the activity of CAMK II under the doxorubicin or H/R-induced oxidative stress through phosphorylation and oxidation of CAMK II. CAMK II activation increases the mitochondrial calcium, which induces myocardial necrosis [57]. Evidences show that MPTP (mitochondrial permeability transition pore) opening at the beginning of the reperfusion stage contributes to almost 50% of the infarct size while ROS is the potent inducer of MPTP. Cypd is the most important component of MPTP. Cypd-deficient mice subject to ischemia/reperfusion injury lead to the smaller infarcted size than the wild-type mice. The inhibitor of Cypd, cyclosporin A (CsA), can also decrease infarcted size in the in vivo mouse model [58]. Another study shows that apoptosis repressor with card domain (ARC) can inhibit MPTP opening by interacting with Cypd and blocking the MPTP complex assembly. Under the oxidative condition, p53 is upregulated and represses the expression of ARC at transcriptional level, which releases the Cypd from binding with ARC and promotes the opening of MPTP [59].

Nec-1 is a specific RIP1 inhibitor and could markedly reduce infarct size in the cardiac ischemia/reperfusion injury. Nec-1 can also prevent the cardiac adverse remodeling after ischemia/reperfusion in the mouse model [60]. However, Nec-1 has been reported to cause cell death in some cases during the clinical trial. Fortunately, the Nec-1 analogue, Nec-1s, had been developed and the promotion of cell death is not observed [61]. There are also some other inhibitors of RIP-1 that have recently been developed. GSK963 is a new RIP1 inhibitor and is more effective than Nec-1 in inhibiting RIP1-dependent cell death. The clinical application of CsA is

validated only in a small number of patients, and these results are doubted by several studies and a larger clinical trial is required for the further confirmation [62, 63]. A present work reports that a modified mtCsA (mitochondria-targeted CsA) with a much-improved Cypd binding affinity yields better cardioprotective role than CsA in a mouse model of I/R [64]. Although these necrosis inhibitors show great potential in the treatment of heart diseases, its clinical significance is still under debate and needs to be further verified [65].

3.3. Autophagic Cell Death. A basal level of autophagy is essential for removal and renewal of dysfunctional organelles and damaged proteins. The cardiomyocytes also depend on autophagy to maintain intracellular homeostasis. Autophagy has also been linked to cardiovascular diseases under the oxidative stress [66]. Intense investigation of the role of autophagy under pathological conditions has currently been carried out. However, evidences show that autophagy seems to play dual roles in cardiovascular diseases caused by excessive ROS. On one side, there are numerous evidences showing that autophagy could protect the cardiomyocytes from injury in the cardiac dysfunction. During the ischemia/reperfusion injury, researchers find that autophagy flux is markedly reduced in cardiomyocytes with downregulation of LAMP2 and BECN1 [67, 68]. Upregulation of autophagy through rapamycin treatment can attenuate myocardial ischemia/reperfusion injury [69, 70]. In the models of doxorubicin cardiotoxicity, doxorubicin blocks cardiomyocyte autophagic flux accompanied by robust accumulation of undegraded autolysosomes. This impaired autophagy process is harmful to the cardiomyocytes, and clearance of these undegraded autolysosomes will relieve the doxorubicin cardiotoxicity [71]. On another side, there are also evidences supporting the negative roles of autophagy in the survival of cardiomyocytes under oxidative stress from several studies. In the high-glucose-induced ROS generation and cardiomyocyte dysfunction, autophagy flux is also inhibited. However, researchers show that this autophagy inhibition is only an adaptive response. Conversely, rapamycin treatment or BECN1 or ATG7 overexpression could increase autophagy and promote cardiomyocyte death induced by high glucose [72]. In another study, Liu et al. found that autophagy promotes the H_2O_2 and myocardial ischemia/reperfusion-induced cardiomyocyte injury which is attenuated by inhibition of autophagy through a LncRNA, a cardiac autophagy inhibitory factor (CAIF) [73]. These evidences support the roles of autophagy in promoting myocardial cell death. In summary, the role of autophagy in cardiomyocyte death depends on the specific situation. Moderate autophagy may promote survival by removing damaged organelles caused by ROS and recycling macromolecules to maintain energy levels. However, prolonged ischemia and subsequent reperfusion result in excessive autophagy which contributes to the self-digestion and ROS production.

3.4. Ferroptosis. Ferroptosis is a newly corned programmed cell death process. The distinct feature of ferroptosis is the iron-dependent lipid peroxide accumulation [74]. Ferroptosis also participates in the pathogenesis of cardiovascular diseases. In an ex vivo heart model of ischemia/reperfusion injury, inhibition of ferroptosis by treatment with glutaminolysis inhibitor compound 968 or iron chelator DFO could improve the heart function and reduce the infarct sizes [75]. Doxorubicin is a traditional antitumor drug whose clinical application is limited by its cardiotoxicity. Doxorubicin's cardiotoxicity is usually attributed to its role in myocardial apoptosis initiation [76]. However, the recent work by Fang et al. shows that ferroptosis occurs in the doxorubicin-induced cardiomyopathy. In this study, researchers find that doxorubicin can elevate the mitochondria iron level and cause mitochondrial lipid peroxide accumulation, which promotes an oxidative stress and the subsequent ferroptotic cell death [77]. Although the roles of ferroptosis have been partially delineated in the cardiomyocytes, the regulatory mechanism of ferroptosis remains largely unknown. Myocardial ferroptosis may occur in some other human pathological conditions. For example, high levels of heme iron in the diet will increase the iron levels in the circulation, which can be taken up by the cardiomyocyte. A fraction of the circulating iron is redox-active, and the excessive uptake of iron may contribute to oxidant-mediated ferroptotic cell death [78]. Until now, the cardioprotective role of ferroptosis is only tested in a mouse model. The application of ferroptosis inhibitors in the treatment of cardiovascular diseases needs to be further explored.

4. Anti-ROS Systems and Clinical Application

4.1. Endogenous Antioxidant System

4.1.1. GSH-Linked Enzymatic Defense Systems. To protect against the damaging effects of ROS, cells have developed multiple antioxidant systems to guarantee the timely removal of ROS. One of the most important is the tripeptide glutathione, GSH, and the GSH-linked enzymatic defense systems. GSH functions as a cofactor for the GSH-peroxidase families. GPX4 is one of the GSH-peroxidases and can interact with lipid hydroperoxides efficiently and catalyze the degradation of peroxides. The mitochondrial GPX4 is the first defense system to avoid ROS damage. The deletion of mitochondria GSH is closely correlated with the ROS toxicity-related cell death process (Figure 3). Although GSH also exists in the cytosol, it seems that cytosolic GSH is less important than that in the mitochondria [79]. Overexpression of mitochondrial GPX4 attenuates myocardial ischemia/reperfusion injury [79]. Recent experiments have also shown that GPX4 is an inhibitor of ferroptosis through the clearance of lipid peroxides (Figure 3). As ferroptosis also promotes the pathogenesis of cardiovascular diseases, the inhibition of ferroptosis by GPX4 will improve the cardiac function under certain pathological conditions [80]. GPX4 can also maintain the vascular homeostasis through its ROS clearance activity. Evidences show that overexpression of GPX4 could suppress the atherosclerosis in $ApoE^{-/-}$ mice [81].

4.1.2. Superoxide Dismutase (SOD) and Catalase. SODs are another antioxidant systems and protect against superoxide-

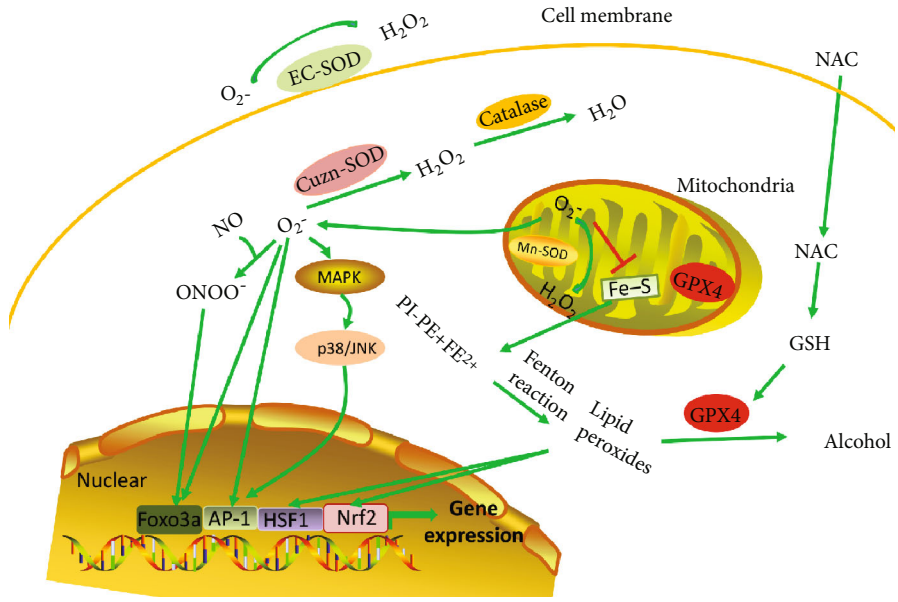

Figure 3: The anti-ROS system. SOD could transform the O_2^- into H_2O_2 and then could be reduced to water by catalase. There are three forms of SODs: EC-SOD (extracellular matrix), CuZn-SOD (cytoplasm), and Mn-SOD (mitochondria). Mitochondrial O_2^- inactivates iron-sulfur (Fe-S) centers and releases free iron, leading to subsequent lipid oxidation through Fenton reaction. GPX4 could catalase the lipid peroxides into alcohol. Antioxidant NAC could promote the synthesis of GSH which is a cofactor of GPX4. ROS will also activate a series of transcription factors (AP-1, Foxo3a, HSF-1, and Nrf2) whose target genes defend against the oxidative stress-related damage.

mediated cytotoxicity. There are three forms of SODs that have different intracellular localization. O_2^- is the main form of superoxide and is generated by complex I and complex III. SOD could transform the O_2^- into H_2O_2, which is a relatively stable and diffusible compared with many other ROS, and then could be reduced to water by catalase (Figure 3). Another role of SODs is to maintain the NO level in the endothelial cell which plays a major role in maintaining the basal vasodilator tone of the vessel. Superoxide could react with NO efficiently and make NO unavailable. Moreover, reaction of NO with superoxide will produce peroxynitrite, a potent oxidant with potential cytotoxicity (Figure 3) [82]. Thus, timely clearance of superoxide by SODs determines the bioactivity of NO. Overexpression of SODs in the mouse model of I/R exposed to ischemia/reperfusion injury can decrease levels of superoxide and infarcted size and improve cardiac function. Similarly, specific overexpression of catalase in cardiomyocyte is also found to reduce the adverse remodeling and prevent heart failure in a mouse model of dilated cardiomyopathy. Overexpression of SODs or catalase can also retard the atherosclerosis in the ApoE$^{-/-}$ mice [83]. All these results demonstrated the protective role of SODs against the ROS-induced cardiovascular diseases.

4.1.3. The Thioredoxin (Trx) System. The thioredoxin (Trx) system defends against oxidative stress through its disulfide reductase activity. The removal of ROS though the Trx system also plays important roles in defensing the oxidative stress under pathological conditions. Overexpression of thioredoxin 2 attenuates Ang II-induced vascular dysfunction [84]. Loss of mitochondrial Trx reductase causes the inflammation and endothelial dysfunction [85]. Thioredoxin is also actively involved in the protection of cardiac function. Evidences show that the thioredoxin activity, which is regulated by thioredoxin-interacting protein, controls cardiac hypertrophy [86]. Inactivation of nitrative thioredoxin promotes cardiomyocyte injury induced by high glucose and cardiac ischemia/reperfusion [87]. Thioredoxin activity can also be inhibited by methylglyoxal, aggravating cardiomyocyte ischemia/reperfusion injury [88]. All these evidences show the close correlation of the thioredoxin with the cardiovascular homeostasis.

4.1.4. Transcription Factors Activated in Defensing the Oxidative Stress. Cells could also activate a series of transcription factors whose target genes strongly defends against the oxidative stress through different ways. These transcriptional factors include the AP-1, HSF1, Nrf2, and the FOXO3a (Figure 3). These transcriptional factors are very sensitive to the intracellular oxidative stress and can drive the expression of target genes rapidly which will protect the cells from damage or kill the cells to avoid further damage. Ap-1 is a leucine zipper transcription factor and is activated by the H_2O_2 or JNK [89, 90]. AP-1 can bind to the promoter region of SOD in response to the oxidative stress and promote the expression of SOD to defend against the oxidative stress damage [91, 92]. However, the role of AP-1 during the pathogenesis of cardiovascular diseases is still under debate. Heat shock transcription factor 1 (HSF1) could translocate into the nuclear and assemble into a homotrimer, which can bind to the DNA and drive the expression of heat shock proteins (HSPs), in response to the oxidative stress [93]. The HSPs are considered to protect the cardiomyocytes from oxidative damage in the ischemic cardiac diseases [94, 95]. FOXO3a is another transcriptional factor exerting a strong protective role in the ROS-related cardiovascular diseases. FOXO3a

can increase the expression of p27 and inhibit smooth muscle cell proliferation which promotes the vascular dysfunction under oxidative stress [96]. FOXO3a is the most abundant isoform expressed in the heart among the Foxo transcription factors. FOXO3a knockout will exacerbate the myocardial ischemia/reperfusion injury with decreased expression of catalase or SOD [97]. FOXO3a also participates in myocardial autophagy regulation. Evidences showed that overexpression of FOXO3a will increase the autophagy level and prevent the cardiac hypertrophy [98]. Nrf2 has recently been found to prevent the ferroptotic cell death. One of the important targets of Nrf2 is the GSH-linked enzyme, GPX4, which is an active ROS antagonist as mentioned above [99]. Nrf2 can also regulate the iron metabolism genes and attenuate ferroptosis through preventing free iron availability.

4.2. Exogenous Antioxidant Strategy. N-acetylcysteine (NAC) is a potent antioxidant which promotes the synthesis of GSH, attenuates oxidative stress, and prevents cell death. Evidences from the animal models show that NAC can attenuate cardiac injury, prevent cardiac fibrosis and remodeling, and improve the cardiac function during the heart failure [100]. Moreover, NAC can also inhibit maladaptive autophagy, which promotes the pathogenesis, in pressure overload-induced cardiac remodeling in rats [101]. The role of NAC has also been validated in the myocardial infarction patients, although these results need to be further explored in a larger population [102]. Vitamin E is another antioxidant with the clinical potential to the treatment of cardiovascular diseases. Evidences from several experimental animal models show that vitamin E treatment is demonstrated to improve cardiac function [103]. However, vitamin E fails to prevent the atherosclerotic disease in the clinical trial. What is more, vitamin E is also proved to have no effect on both the acute myocardial injury and chronic heart failure patients [104, 105]. Recently, researchers found that high levels of NAD+ could improve cardiac function in a mouse model of heart failure. The role of NAD+ in defensing oxidative stress is also validated in several other works, showing the potential application in the anti-ROS strategy [106].

However, the inappropriate application of antioxidant strategy is also harmful to our body. ROS may function as a second messenger and participate in cell signaling transduction and redox regulation. These signalings mediated by mild ROS may even benefit cellular repair processes and improve protective systems [107]. However, the antioxidants cannot distinguish among the ROS with a beneficial physiological role and those that cause oxidative damage to the cell. The antioxidant may clear the most harmful ROS while on another side leave not enough ROS for their useful purposes. The direct outcome of anomaly low ROS may interfere with the immune system and essential defensive mechanisms for removal of damaged components of the cell, including those that are precancerous [108]. Thus, the overtaking of antioxidant may be harmful to our body.

4.3. Anti-ROS Strategy in Clinical Trial. In the clinical trials, researchers get disappointing results in cardiovascular disease treatment through oxidative stress inhibition strategy. The reason for these failure remains largely unknown. One reason may be that the inadequate understanding of the ROS production stage and the myocardial injury during different pathological conditions. In the myocardial ischemia/reperfusion injury, the ROS is largely produced at the beginning of reperfusion stage and mass myocardial cell death accrued at this stage. However, the current antioxidant therapies are not able to combat these ROS and cell death. Another reason may be that the ROS resources during the pathogenesis of heart failure are more complex than we now know. There are more complex ROS producers functioning in different pathological conditions. For example, oxypurinol, inhibitor of xanthine oxidase, has been shown to improve heart failure in a specific subset of patients with elevated uric acid. Thus, in these patients, targeting the xanthine oxidase may represent a better therapeutic strategy [109].

5. Conclusion

Excessive ROS production is the major cause of oxidative stress and cardiovascular diseases. Understanding the ROS production processes and the mechanism of anti-ROS systems in the cell will benefit the clinical practice in the treatment of cardiovascular diseases. Although the current antioxidants seem unsuccessful in the treatment of cardiovascular diseases, anti-ROS strategy still represents the most important ways for cardiovascular disease treatment. Efforts are still needed to illustrate the mechanisms of ROS production and how ROS promotes the pathogenesis of cardiovascular diseases under different conditions. Intracellular ROS is closely correlated with the myocardial cell death process, which takes an active role in the pathogenesis of cardiovascular diseases. Until now, there are several programmed cell death processes that are identified. However, whether all these cell death processes contribute to the pathogenesis of cardiovascular diseases and the major cell mode under different conditions in cardiovascular diseases are still needed to be illustrated. The revelation of the roles of different modes of cell death plays in the cardiovascular diseases will provide the precise drug target during disease treatment. Moreover, the exploration of ROS-related cell death signaling pathways will also help to develop the therapeutic strategy and protect cell death from oxidative stress.

Conflicts of Interest

The authors confirm that there are no conflicts of interest.

Authors' Contributions

TX, JW, and WD provided direction and guidance throughout the preparation of this manuscript. TX and WD collected and prepared the related literature. TX, JW, WD, XA, and XJ drafted the manuscript. XJ, YL, WY, and JW reviewed and made significant revisions to the manuscript. All authors have read and approved the final manuscript. Tao Xu and Wei Ding contributed equally to this work.

Acknowledgments

The authors thank all laboratory members for ongoing discussions. This work was funded by the National Natural Science Foundation of China (81622005 and 81770232), the Natural Science Foundation of Shandong Province (JQ201815), and the China Postdoctoral Science Foundation (2016M602095). The authors acknowledge all financial supports for this work.

References

[1] M. Valko, D. Leibfritz, J. Moncol, M. T. Cronin, M. Mazur, and J. Telser, "Free radicals and antioxidants in normal physiological functions and human disease," *The International Journal of Biochemistry & Cell Biology*, vol. 39, no. 1, pp. 44–84, 2007.

[2] M. M. Elahi, Y. X. Kong, and B. M. Matata, "Oxidative stress as a mediator of cardiovascular disease," *Oxidative Medicine and Cellular Longevity*, vol. 2, no. 5, pp. 259–269, 2009.

[3] I. Afanas'ev, "ROS and RNS signaling in heart disorders: could antioxidant treatment be successful?," *Oxidative Medicine and Cellular Longevity*, vol. 2011, Article ID 293769, 13 pages, 2011.

[4] S. R. Thomas, P. K. Witting, and G. R. Drummond, "Redox control of endothelial function and dysfunction: molecular mechanisms and therapeutic opportunities," *Antioxidants & Redox Signaling*, vol. 10, no. 10, pp. 1713–1765, 2008.

[5] U. Förstermann, "Oxidative stress in vascular disease: causes, defense mechanisms and potential therapies," *Nature Clinical Practice Cardiovascular Medicine*, vol. 5, no. 6, pp. 338–349, 2008.

[6] G. R. Drummond, S. Selemidis, K. K. Griendling, and C. G. Sobey, "Combating oxidative stress in vascular disease: NADPH oxidases as therapeutic targets," *Nature Reviews Drug Discovery*, vol. 10, no. 6, pp. 453–471, 2011.

[7] B. Lassegue, A. San Martin, and K. K. Griendling, "Biochemistry, physiology, and pathophysiology of NADPH oxidases in the cardiovascular system," *Circulation Research*, vol. 110, no. 10, pp. 1364–1390, 2012.

[8] K. K. Griendling, D. Sorescu, and M. Ushio-Fukai, "NAD(P)H oxidase: role in cardiovascular biology and disease," *Circulation Research*, vol. 86, no. 5, pp. 494–501, 2000.

[9] H. Sumimoto, K. Miyano, and R. Takeya, "Molecular composition and regulation of the Nox family NAD(P)H oxidases," *Biochemical and Biophysical Research Communications*, vol. 338, no. 1, pp. 677–686, 2005.

[10] A. C. Montezano and R. M. Touyz, "Reactive oxygen species and endothelial function – role of nitric oxide synthase uncoupling and Nox family nicotinamide adenine dinucleotide phosphate oxidases," *Basic & Clinical Pharmacology & Toxicology*, vol. 110, no. 1, pp. 87–94, 2012.

[11] M. A. Arruda and C. Barja-Fidalgo, "NADPH oxidase activity: in the crossroad of neutrophil life and death," *Frontiers in Bioscience*, vol. 14, pp. 4546–4556, 2009.

[12] B. Lassegue and R. E. Clempus, "Vascular NAD(P)H oxidases: specific features, expression, and regulation," *American Journal of Physiology-Regulatory, Integrative and Comparative Physiology*, vol. 285, no. 2, pp. R277–R297, 2003.

[13] J. Dharmarajah, J. F. Arthur, C. G. Sobey, and G. R. Drummond, "The anti-platelet effects of apocynin in mice are not mediated by inhibition of NADPH oxidase activity," *Naunyn-Schmiedeberg's Archives of Pharmacology*, vol. 382, no. 4, pp. 377–384, 2010.

[14] J. Rivera, C. G. Sobey, A. K. Walduck, and G. R. Drummond, "Nox isoforms in vascular pathophysiology: insights from transgenic and knockout mouse models," *Redox Report*, vol. 15, no. 2, pp. 50–63, 2010.

[15] M. Rouhanizadeh, J. Hwang, R. E. Clempus et al., "Oxidized-1-palmitoyl-2-arachidonoyl-sn-glycero-3-phosphorylcholine induces vascular endothelial superoxide production: implication of NADPH oxidase," *Free Radical Biology & Medicine*, vol. 39, no. 11, pp. 1512–1522, 2005.

[16] C. P. Judkins, H. Diep, B. R. Broughton et al., "Direct evidence of a role for Nox2 in superoxide production, reduced nitric oxide bioavailability, and early atherosclerotic plaque formation in ApoE$^{-/-}$ mice," *American Journal of Physiology Heart and Circulatory Physiology*, vol. 298, no. 1, pp. H24–H32, 2010.

[17] K. Schröder, M. Zhang, S. Benkhoff et al., "Nox4 is a protective reactive oxygen species generating vascular NADPH oxidase," *Circulation Research*, vol. 110, no. 9, pp. 1217–1225, 2012.

[18] U. Landmesser, S. Spiekermann, C. Preuss et al., "Angiotensin II induces endothelial xanthine oxidase activation: role for endothelial dysfunction in patients with coronary disease," *Arteriosclerosis, Thrombosis, and Vascular Biology*, vol. 27, no. 4, pp. 943–948, 2007.

[19] M. Isabelle, A. Vergeade, F. Moritz et al., "NADPH oxidase inhibition prevents cocaine-induced up-regulation of xanthine oxidoreductase and cardiac dysfunction," *Journal of Molecular and Cellular Cardiology*, vol. 42, no. 2, pp. 326–332, 2007.

[20] C. Zhang, "The role of inflammatory cytokines in endothelial dysfunction," *Basic Research in Cardiology*, vol. 103, no. 5, pp. 398–406, 2008.

[21] S. Page, D. Powell, M. Benboubetra et al., "Xanthine oxidoreductase in human mammary epithelial cells: activation in response to inflammatory cytokines," *Biochimica et Biophysica Acta (BBA) - General Subjects*, vol. 1381, no. 2, pp. 191–202, 1998.

[22] K. Schröder, C. Vecchione, O. Jung et al., "Xanthine oxidase inhibitor tungsten prevents the development of atherosclerosis in ApoE knockout mice fed a Western-type diet," *Free Radical Biology & Medicine*, vol. 41, no. 9, pp. 1353–1360, 2006.

[23] W. Doehner, N. Schoene, M. Rauchhaus et al., "Effects of xanthine oxidase inhibition with allopurinol on endothelial function and peripheral blood flow in hyperuricemic patients with chronic heart failure," *Circulation*, vol. 105, no. 22, pp. 2619–2624, 2002.

[24] D. Grassi, L. Ferri, G. Desideri et al., "Chronic hyperuricemia, uric acid deposit and cardiovascular risk," *Current Pharmaceutical Design*, vol. 19, no. 13, pp. 2432–2438, 2013.

[25] C. Heymes, J. K. Bendall, P. Ratajczak et al., "Increased myocardial NADPH oxidase activity in human heart failure," *Journal of the American College of Cardiology*, vol. 41, no. 12, pp. 2164–2171, 2003.

[26] J. A. Byrne, D. J. Grieve, J. K. Bendall et al., "Contrasting roles of NADPH oxidase isoforms in pressure-overload versus

angiotensin II–induced cardiac hypertrophy," *Circulation Research*, vol. 93, no. 9, pp. 802–805, 2003.

[27] A. J. Valente, R. A. Clark, J. M. Siddesha, U. Siebenlist, and B. Chandrasekar, "CIKS (Act1 or TRAF3IP2) mediates angiotensin-II-induced interleukin-18 expression, and Nox2-dependent cardiomyocyte hypertrophy," *Journal of Molecular and Cellular Cardiology*, vol. 53, no. 1, pp. 113–124, 2012.

[28] Y. H. Looi, D. J. Grieve, A. Siva et al., "Involvement of Nox2 NADPH oxidase in adverse cardiac remodeling after myocardial infarction," *Hypertension*, vol. 51, no. 2, pp. 319–325, 2008.

[29] B. C. Henderson, U. Sen, C. Reynolds et al., "Reversal of systemic hypertension-associated cardiac remodeling in chronic pressure overload myocardium by ciglitazone," *International Journal of Biological Sciences*, vol. 3, no. 6, pp. 385–392, 2007.

[30] G. Frazziano, I. Al Ghouleh, J. Baust, S. Shiva, H. C. Champion, and P. J. Pagano, "Nox-derived ROS are acutely activated in pressure overload pulmonary hypertension: indications for a seminal role for mitochondrial Nox4," *American Journal of Physiology Heart and Circulatory Physiology*, vol. 306, no. 2, pp. H197–H205, 2014.

[31] D. Kelly, S. Q. Khan, M. Thompson et al., "Plasma tissue inhibitor of metalloproteinase-1 and matrix metalloproteinase-9: novel indicators of left ventricular remodelling and prognosis after acute myocardial infarction," *European Heart Journal*, vol. 29, no. 17, pp. 2116–2124, 2008.

[32] F. Qin, M. Simeone, and R. Patel, "Inhibition of NADPH oxidase reduces myocardial oxidative stress and apoptosis and improves cardiac function in heart failure after myocardial infarction," *Free Radical Biology & Medicine*, vol. 43, no. 2, pp. 271–281, 2007.

[33] M. A. Sagor, N. Tabassum, M. A. Potol, and M. A. Alam, "Xanthine oxidase inhibitor, allopurinol, prevented oxidative stress, fibrosis, and myocardial damage in isoproterenol induced aged rats," *Oxidative Medicine and Cellular Longevity*, vol. 2015, Article ID 478039, 9 pages, 2015.

[34] N. Kaludercic, J. Mialet-Perez, N. Paolocci, A. Parini, and F. Di Lisa, "Monoamine oxidases as sources of oxidants in the heart," *Journal of Molecular and Cellular Cardiology*, vol. 73, pp. 34–42, 2014.

[35] Y. Santin, P. Sicard, F. Vigneron et al., "Oxidative stress by monoamine oxidase-A impairs transcription factor EB activation and autophagosome clearance, leading to cardiomyocyte necrosis and heart failure," *Antioxidants & Redox Signaling*, vol. 25, no. 1, pp. 10–27, 2016.

[36] N. Kaludercic, A. Carpi, T. Nagayama et al., "Monoamine oxidase B prompts mitochondrial and cardiac dysfunction in pressure overloaded hearts," *Antioxidants & Redox Signaling*, vol. 20, no. 2, pp. 267–280, 2014.

[37] V. Costiniti, I. Spera, R. Menabo et al., "Monoamine oxidase-dependent histamine catabolism accounts for post-ischemic cardiac redox imbalance and injury," *Biochimica et Biophysica Acta (BBA) - Molecular Basis of Disease*, vol. 1864, no. 9, pp. 3050–3059, 2018.

[38] M. P. Murphy, "How mitochondria produce reactive oxygen species," *The Biochemical Journal*, vol. 417, no. 1, pp. 1–13, 2009.

[39] Q. Chen, S. Moghaddas, C. L. Hoppel, and E. J. Lesnefsky, "Ischemic defects in the electron transport chain increase the production of reactive oxygen species from isolated rat heart mitochondria," *American journal of physiology Cell physiology*, vol. 294, no. 2, pp. C460–C466, 2008.

[40] K. Raedschelders, D. M. Ansley, and D. D. Y. Chen, "The cellular and molecular origin of reactive oxygen species generation during myocardial ischemia and reperfusion," *Pharmacology & Therapeutics*, vol. 133, no. 2, pp. 230–255, 2012.

[41] D. N. Granger and P. R. Kvietys, "Reperfusion injury and reactive oxygen species: the evolution of a concept," *Redox Biology*, vol. 6, pp. 524–551, 2015.

[42] A. Dhanasekaran, S. Kotamraju, C. Karunakaran et al., "Mitochondria superoxide dismutase mimetic inhibits peroxide-induced oxidative damage and apoptosis: role of mitochondrial superoxide," *Free Radical Biology & Medicine*, vol. 39, no. 5, pp. 567–583, 2005.

[43] S. Tan, D. Schubert, and P. Maher, "Oxytosis: a novel form of programmed cell death," *Current Topics in Medicinal Chemistry*, vol. 1, no. 6, pp. 497–506, 2001.

[44] Y. Zheng, S. E. Gardner, and M. C. H. Clarke, "Cell death, damage-associated molecular patterns, and sterile inflammation in cardiovascular disease," *Arteriosclerosis, Thrombosis, and Vascular Biology*, vol. 31, no. 12, pp. 2781–2786, 2011.

[45] T. Xu, W. Ding, M. A. Tariq et al., "Molecular mechanism and therapy application of necrosis during myocardial injury," *Journal of Cellular and Molecular Medicine*, vol. 22, no. 5, pp. 2547–2557, 2018.

[46] B. Freude, T. N. Masters, S. Kostin, F. Robicsek, and J. Schaper, "Cardiomyocyte apoptosis in acute and chronic conditions," *Basic Research in Cardiology*, vol. 93, no. 2, pp. 85–89, 1998.

[47] A. Y. Zhang, F. Yi, G. Zhang, E. Gulbins, and P. L. Li, "Lipid raft clustering and redox signaling platform formation in coronary arterial endothelial cells," *Hypertension*, vol. 47, no. 1, pp. 74–80, 2006.

[48] L. J. Martin, "Neuronal death in amyotrophic lateral sclerosis is apoptosis: possible contribution of a programmed cell death mechanism," *Journal of Neuropathology and Experimental Neurology*, vol. 58, no. 5, pp. 459–471, 1999.

[49] S. W. Tait and D. R. Green, "Mitochondria and cell death: outer membrane permeabilization and beyond," *Nature Reviews Molecular Cell Biology*, vol. 11, no. 9, pp. 621–632, 2010.

[50] M. Li, W. Ding, M. A. Tariq et al., "A circular transcript of ncx1 gene mediates ischemic myocardial injury by targeting miR-133a-3p," *Theranostics*, vol. 8, no. 21, pp. 5855–5869, 2018.

[51] H. Y. Li, J. Zhang, L. L. Sun et al., "Celastrol induces apoptosis and autophagy via the ROS/JNK signaling pathway in human osteosarcoma cells: an in vitro and in vivo study," *Cell Death & Disease*, vol. 6, p. e1604, 2015.

[52] A. Adameova, E. Goncalvesova, A. Szobi, and N. S. Dhalla, "Necroptotic cell death in failing heart: relevance and proposed mechanisms," *Heart Failure Reviews*, vol. 21, no. 2, pp. 213–221, 2016.

[53] S. He, L. Wang, L. Miao et al., "Receptor interacting protein kinase-3 determines cellular necrotic response to TNF-α," *Cell*, vol. 137, no. 6, pp. 1100–1111, 2009.

[54] A. Linkermann, J. H. Brasen, M. Darding et al., "Two independent pathways of regulated necrosis mediate ischemia-reperfusion injury," *Proceedings of the National Academy of Sciences of the United States of America*, vol. 110, no. 29, pp. 12024–12029, 2013.

[55] P. Pacher, A. Nivorozhkin, and C. Szabó, "Therapeutic effects of xanthine oxidase inhibitors: renaissance half a century after the discovery of allopurinol," *Pharmacological Reviews*, vol. 58, no. 1, pp. 87–114, 2006.

[56] J.-X. Wang, X.-J. Zhang, Q. Li et al., "MicroRNA-103/107 regulate programmed necrosis and myocardial ischemia/reperfusion injury through targeting FADD," *Circulation Research*, vol. 117, no. 4, pp. 352–363, 2015.

[57] T. Zhang, Y. Zhang, M. Cui et al.et al.et al, "CaMKII is a RIP3 substrate mediating ischemia- and oxidative stress-induced myocardial necroptosis," *Nature Medicine*, vol. 22, no. 2, pp. 175–182, 2016.

[58] T. Nakagawa, S. Shimizu, T. Watanabe et al., "Cyclophilin D-dependent mitochondrial permeability transition regulates some necrotic but not apoptotic cell death," *Nature*, vol. 434, no. 7033, pp. 652–658, 2005.

[59] T. Xu, W. Ding, X. Ao et al., "ARC regulates programmed necrosis and myocardial ischemia/reperfusion injury through the inhibition of mPTP opening," *Redox Biology*, vol. 20, pp. 414–426, 2019.

[60] M. I. F. J. Oerlemans, J. Liu, F. Arslan et al., "Inhibition of RIP1-dependent necrosis prevents adverse cardiac remodeling after myocardial ischemia–reperfusion in vivo," *Basic Research in Cardiology*, vol. 107, no. 4, p. 270, 2012.

[61] A. Szobi, T. Rajtik, and A. Adameova, "Effects of necrostatin-1, an inhibitor of necroptosis, and its inactive analogue Nec-1i on basal cardiovascular function," *Physiological Research*, vol. 65, no. 5, pp. 861–865, 2016.

[62] L. O. Karlsson, A. X. Zhou, E. Larsson et al., "Cyclosporine does not reduce myocardial infarct size in a porcine ischemia-reperfusion model," *Journal of Cardiovascular Pharmacology and Therapeutics*, vol. 15, no. 2, pp. 182–189, 2010.

[63] D. De Paulis, P. Chiari, G. Teixeira et al., "Cyclosporine A at reperfusion fails to reduce infarct size in the in vivo rat heart," *Basic Research in Cardiology*, vol. 108, no. 5, p. 379, 2013.

[64] H. Dube, D. Selwood, S. Malouitre, M. Capano, M. I. Simone, and M. Crompton, "A mitochondrial-targeted cyclosporin A with high binding affinity for cyclophilin D yields improved cytoprotection of cardiomyocytes," *The Biochemical Journal*, vol. 441, no. 3, pp. 901–907, 2012.

[65] S. B. Berger, P. Harris, R. Nagilla et al., "Characterization of GSK′963: a structurally distinct, potent and selective inhibitor of RIP1 kinase," *Cell Death Discovery*, vol. 1, p. 15009, 2015.

[66] X. Zhang, X. Cheng, L. Yu et al., "MCOLN1 is a ROS sensor in lysosomes that regulates autophagy," *Nature Communications*, vol. 7, no. 1, p. 12109, 2016.

[67] X. Ma, H. Liu, S. R. Foyil, R. J. Godar, C. J. Weinheimer, and A. Diwan, "Autophagy is impaired in cardiac ischemia-reperfusion injury," *Autophagy*, vol. 8, no. 9, pp. 1394–1396, 2012.

[68] X. Wang, D. Sun, Y. Hu et al., "The roles of oxidative stress and Beclin-1 in the autophagosome clearance impairment triggered by cardiac arrest," *Free Radical Biology & Medicine*, vol. 136, pp. 87–95, 2019.

[69] D. Dutta, J. Xu, J. S. Kim, W. A. Dunn Jr., and C. Leeuwenburgh, "Upregulated autophagy protects cardiomyocytes from oxidative stress-induced toxicity," *Autophagy*, vol. 9, no. 3, pp. 328–344, 2013.

[70] A. Shirakabe, P. Zhai, Y. Ikeda et al., "Drp1-dependent mitochondrial autophagy plays a protective role against pressure overload–induced mitochondrial dysfunction and heart failure," *Circulation*, vol. 133, no. 13, pp. 1249–1263, 2016.

[71] D. L. Li, Z. V. Wang, G. Ding et al., "Doxorubicin blocks cardiomyocyte autophagic flux by inhibiting lysosome acidification," *Circulation*, vol. 133, no. 17, pp. 1668–1687, 2016.

[72] S. Kobayashi, X. Xu, K. Chen, and Q. Liang, "Suppression of autophagy is protective in high glucose-induced cardiomyocyte injury," *Autophagy*, vol. 8, no. 4, pp. 577–592, 2012.

[73] C.-Y. Liu, Y.-H. Zhang, R.-B. Li et al., "LncRNA CAIF inhibits autophagy and attenuates myocardial infarction by blocking p53-mediated myocardin transcription," *Nature Communications*, vol. 9, no. 1, p. 29, 2018.

[74] S. J. Dixon, K. M. Lemberg, M. R. Lamprecht et al., "Ferroptosis: an iron-dependent form of nonapoptotic cell death," *Cell*, vol. 149, no. 5, pp. 1060–1072, 2012.

[75] M. Gao, P. Monian, N. Quadri, R. Ramasamy, and X. Jiang, "Glutaminolysis and transferrin regulate ferroptosis," *Molecular Cell*, vol. 59, no. 2, pp. 298–308, 2015.

[76] Q. Wan, T. Xu, W. Ding et al., "miR-499-5p attenuates mitochondrial fission and cell apoptosis via p21 in doxorubicin cardiotoxicity," *Frontiers in Genetics*, vol. 9, p. 734, 2018.

[77] X. Fang, H. Wang, D. Han et al., "Ferroptosis as a target for protection against cardiomyopathy," *Proceedings of the National Academy of Sciences of the United States of America*, vol. 116, no. 7, pp. 2672–2680, 2019.

[78] R. E. Fleming and P. Ponka, "Iron overload in human disease," *The New England Journal of Medicine*, vol. 366, no. 4, pp. 348–359, 2012.

[79] E. R. Dabkowski, C. L. Williamson, and J. M. Hollander, "Mitochondria-specific transgenic overexpression of phospholipid hydroperoxide glutathione peroxidase (GPx4) attenuates ischemia/reperfusion-associated cardiac dysfunction," *Free Radical Biology and Medicine*, vol. 45, no. 6, pp. 855–865, 2008.

[80] W. S. Yang, R. SriRamaratnam, M. E. Welsch et al., "Regulation of ferroptotic cancer cell death by GPX4," *Cell*, vol. 156, no. 1-2, pp. 317–331, 2014.

[81] Z. Guo, Q. Ran, L. J. Roberts 2nd et al., "Suppression of atherogenesis by overexpression of glutathione peroxidase-4 in apolipoprotein E-deficient mice," *Free Radical Biology and Medicine*, vol. 44, no. 3, pp. 343–352, 2008.

[82] J. S. Beckman and W. H. Koppenol, "Nitric oxide, superoxide, and peroxynitrite: the good, the bad, and ugly," *American Journal of Physiology-Cell Physiology*, vol. 271, no. 5, pp. C1424–C1437, 1996.

[83] H. Yang, L. J. Roberts, M. J. Shi et al., "Retardation of atherosclerosis by overexpression of catalase or both Cu/Zn-superoxide dismutase and catalase in mice lacking apolipoprotein E," *Circulation Research*, vol. 95, no. 11, pp. 1075–1081, 2004.

[84] J. D. Widder, D. Fraccarollo, P. Galuppo et al., "Attenuation of angiotensin II–induced vascular dysfunction and hypertension by overexpression of thioredoxin 2," *Hypertension*, vol. 54, no. 2, pp. 338–344, 2009.

[85] J. Kirsch, H. Schneider, J.-I. Pagel et al., "Endothelial dysfunction, and a prothrombotic, proinflammatory phenotype is caused by loss of mitochondrial thioredoxin reductase in endothelium," *Arteriosclerosis, Thrombosis, and Vascular Biology*, vol. 36, no. 9, pp. 1891–1899, 2016.

[86] J. Yoshioka, P. C. Schulze, M. Cupesi et al., "Thioredoxin-interacting protein controls cardiac hypertrophy through

regulation of thioredoxin activity," *Circulation*, vol. 109, no. 21, pp. 2581–2586, 2004.

[87] R. Luan, S. Liu, T. Yin et al., "High glucose sensitizes adult cardiomyocytes to ischaemia/reperfusion injury through nitrative thioredoxin inactivation," *Cardiovascular Research*, vol. 83, no. 2, pp. 294–302, 2009.

[88] X. L. Wang, W. B. Lau, Y. X. Yuan et al., "Methylglyoxal increases cardiomyocyte ischemia-reperfusion injury via glycative inhibition of thioredoxin activity," *American Journal of Physiology Endocrinology and Metabolism*, vol. 299, no. 2, pp. E207–E214, 2010.

[89] H. Keller, C. Dreyer, J. Medin, A. Mahfoudi, K. Ozato, and W. Wahli, "Fatty acids and retinoids control lipid metabolism through activation of peroxisome proliferator-activated receptor-retinoid X receptor heterodimers," *Proceedings of the National Academy of Sciences of the United States of America*, vol. 90, no. 6, pp. 2160–2164, 1993.

[90] N. Marx, T. Bourcier, G. K. Sukhova, P. Libby, and J. Plutzky, "PPARγ activation in human endothelial cells increases plasminogen activator inhibitor type-1 expression," *Arteriosclerosis, Thrombosis, and Vascular Biology*, vol. 19, no. 3, pp. 546–551, 1999.

[91] Y. S. Ho, A. J. Howard, and J. D. Crapo, "Molecular structure of a functional rat gene for manganese-containing superoxide dismutase," *American Journal of Respiratory Cell and Molecular Biology*, vol. 4, no. 3, pp. 278–286, 1991.

[92] B. B. Warner, L. Stuart, S. Gebb, and J. R. Wispe, "Redox regulation of manganese superoxide dismutase," *The American Journal of Physiology*, vol. 271, no. 1, pp. L150–L158, 1996.

[93] S. G. Ahn and D. J. Thiele, "Redox regulation of mammalian heat shock factor 1 is essential for Hsp gene activation and protection from stress," *Genes & Development*, vol. 17, no. 4, pp. 516–528, 2003.

[94] B. Kalmar and L. Greensmith, "Induction of heat shock proteins for protection against oxidative stress," *Advanced Drug Delivery Reviews*, vol. 61, no. 4, pp. 310–318, 2009.

[95] M. S. Marber, D. S. Latchman, J. M. Walker, and D. M. Yellon, "Cardiac stress protein elevation 24 hours after brief ischemia or heat stress is associated with resistance to myocardial infarction," *Circulation*, vol. 88, no. 3, pp. 1264–1272, 1993.

[96] M. R. Abid, K. Yano, S. Guo et al., "Forkhead transcription factors inhibit vascular smooth muscle cell proliferation and neointimal hyperplasia," *The Journal of Biological Chemistry*, vol. 280, no. 33, pp. 29864–29873, 2005.

[97] A. Sengupta, J. D. Molkentin, J. H. Paik, R. A. DePinho, and K. E. Yutzey, "FoxO transcription factors promote cardiomyocyte survival upon induction of oxidative stress," *The Journal of Biological Chemistry*, vol. 286, no. 9, pp. 7468–7478, 2011.

[98] A. Sengupta, J. D. Molkentin, and K. E. Yutzey, "FoxO transcription factors promote autophagy in cardiomyocytes," *The Journal of Biological Chemistry*, vol. 284, no. 41, pp. 28319–28331, 2009.

[99] A. Singh, T. Rangasamy, R. K. Thimmulappa et al., "Glutathione peroxidase 2, the major cigarette smoke–inducible isoform of GPX in lungs, is regulated by Nrf2," *American Journal of Respiratory Cell and Molecular Biology*, vol. 35, no. 6, pp. 639–650, 2006.

[100] B. Giam, P. Y. Chu, S. Kuruppu et al., "*N*-acetylcysteine attenuates the development of cardiac fibrosis and remodeling in a mouse model of heart failure," *Physiological Reports*, vol. 4, no. 7, 2016.

[101] B. Li, Y. Sun, J. P. Wang et al., "Antioxidant N-acetylcysteine inhibits maladaptive myocyte autophagy in pressure overload induced cardiac remodeling in rats," *European Journal of Pharmacology*, vol. 839, pp. 47–56, 2018.

[102] A. H. Talasaz, H. Khalili, F. Fahimi et al., "Effects of N-acetylcysteine on the cardiac remodeling biomarkers and major adverse events following acute myocardial infarction: a randomized clinical trial," *American Journal of Cardiovascular Drugs*, vol. 14, no. 1, pp. 51–61, 2014.

[103] R. Sethi, N. Takeda, M. Nagano, and N. S. Dhalla, "Beneficial effects of vitamin E treatment in acute myocardial infarction," *Journal of Cardiovascular Pharmacology and Therapeutics*, vol. 5, no. 1, pp. 51–58, 2000.

[104] I. Jialal and S. Devaraj, "Vitamin E supplementation and cardiovascular events in high-risk patients," *The New England Journal of Medicine*, vol. 342, no. 25, pp. 1917-1918, 2000.

[105] G. Riccioni, A. Frigiola, S. Pasquale, D. G. Massimo, and N. D'Orazio, "Vitamin C and E consumption and coronary heart disease in men," *Frontiers in Bioscience (Elite Edition)*, vol. E4, pp. 373–380, 2012.

[106] K. A. Hershberger, A. S. Martin, and M. D. Hirschey, "Role of NAD^+ and mitochondrial sirtuins in cardiac and renal diseases," *Nature Reviews Nephrology*, vol. 13, no. 4, pp. 213–225, 2017.

[107] F. Jiang, Y. Zhang, and G. J. Dusting, "NADPH oxidase-mediated redox signaling: roles in cellular stress response, stress tolerance, and tissue repair," *Pharmacological Reviews*, vol. 63, no. 1, pp. 218–242, 2011.

[108] R. I. Salganik, "The benefits and hazards of antioxidants: controlling apoptosis and other protective mechanisms in cancer patients and the human population," *Journal of the American College of Nutrition*, vol. 20, 5 Suppl, pp. 464S–472S, 2001.

[109] S. R. Steinhubl, "Why have antioxidants failed in clinical trials?," *The American Journal of Cardiology*, vol. 101, no. 10, pp. 14D–19D, 2008.

Hindawi
Oxidative Medicine and Cellular Longevity
Volume 2019, Article ID 9894238, 9 pages
https://doi.org/10.1155/2019/9894238

Research Article

Kynurenine, a Tryptophan Metabolite That Increases with Age, Induces Muscle Atrophy and Lipid Peroxidation

Helen Kaiser, Kanglun Yu, Chirayu Pandya, Bharati Mendhe, Carlos M. Isales, Meghan E. McGee-Lawrence, Maribeth Johnson, Sadanand Fulzele, and Mark W. Hamrick

Medical College of Georgia, Augusta University, Augusta, GA 30912, USA

Correspondence should be addressed to Mark W. Hamrick; mhamrick@augusta.edu

Received 12 February 2019; Revised 26 June 2019; Accepted 16 August 2019; Published 13 October 2019

Guest Editor: Gisela A. Cunha

The cellular and molecular mechanisms underlying loss of muscle mass with age (sarcopenia) are not well-understood; however, heterochronic parabiosis experiments show that circulating factors are likely to play a role. Kynurenine (KYN) is a circulating tryptophan metabolite that is known to increase with age and is a ligand of the aryl hydrocarbon receptor (Ahr). Here, we tested the hypothesis that KYN activation of Ahr plays a role in muscle loss with aging. Results indicate that KYN treatment of mouse and human myoblasts increased levels of reactive oxygen species (ROS) 2-fold and KYN treatment *in vivo* reduced muscle size and strength and increased muscle lipid peroxidation in young mice. PCR array data indicate that muscle fiber size reduction with KYN treatment reduces protein synthesis markers whereas ubiquitin ligase gene expression is not significantly increased. KYN is generated by the enzyme indoleamine 2,3-dioxygenase (IDO), and aged mice treated with the IDO inhibitor 1-methyl-D-tryptophan showed an increase in muscle fiber size and muscle strength. Small-molecule inhibition of Ahr *in vitro*, and Ahr knockout *in vivo*, did not prevent KYN-induced increases in ROS, suggesting that KYN can directly increase ROS independent of Ahr activation. Protein analysis identified very long-chain acyl-CoA dehydrogenase as a factor activated by KYN that may increase ROS and lipid peroxidation. Our data suggest that IDO inhibition may represent a novel therapeutic approach for the prevention of sarcopenia and possibly other age-associated conditions associated with KYN accumulation such as bone loss and neurodegeneration.

1. Introduction

The population of people 60 years of age or older is expected to increase from 8% of the world's population in 2013 to an estimated 21% of the world's population by 2050. This increase means that in the next 40 years, there will be more than 2 billion people over 60 years of age [1]. Extending the health span of the world population so that aged people can remain disease-free and independent is an important step toward easing the burden of medical costs and increasing the quality of life. Several factors contribute to age-related decline in independence with sarcopenia, the loss of muscle mass and power, being one of the most important. Sarcopenia occurs in over one-third of people over 70 years of age [2]. Sarcopenia is a multifactorial disease with unknown causes. Sarcopenia can be characterized by several broad symptoms: generalized muscle atrophy, increases in systemic cellular reactive oxygen species (ROS), mitochondrial dysfunction, replacement of muscle fibers with fibrotic factors and fat, and degradation of neuromuscular junctions [3]. Currently, there are no FDA-approved medications for sarcopenia [4].

Heterochronic parabiosis experiments have shown that circulating factors from young blood can help regenerate aged and injured muscle [5]. This suggests that some circulating factors in old blood may be harmful, or conversely that factors in young blood may be helpful, to aging muscle. Kynurenine (KYN) is a circulating tryptophan metabolite that increases with age and is implicated in several age-related disorders including neurodegeneration, osteoporosis, and inflammation [6, 7]. KYN is metabolized from tryptophan by two major enzymes: tryptophan 2,3-dioxygenase (TDO) in the liver and indoleamine 2,3-dioxygenase (IDO)

extrahepatically [8]. IDO is induced by several inflammatory cytokines including IL-6, IL-1β, and interferon-gamma (IFNγ) [9]. An increase in IDO activity has been linked to an increased mortality rate in humans [10], and frailty is associated with a marked increase in the KYN/TRP ratio [11].

We hypothesized that an increase in KYN with age contributes to muscle atrophy and oxidative stress. We also tested the hypothesis that inhibition of IDO to decrease the production of KYN in aged mice might attenuate muscle atrophy and oxidative stress. We used 1-methyl-D-tryptophan (1-MT), a specific antagonist of IDO that has been shown to deplete murine KYN levels [12]. We further sought to understand the mechanism behind KYN-induced ROS. Several previous studies have shown that KYN is a ligand for the aryl hydrocarbon receptor (Ahr), a xenobiotic drug response transcription factor [13, 14] that is associated with age-related changes in vascular tissues [15] and skin [16]. We also tested the hypothesis that KYN activation of Ahr with aging could contribute to sarcopenia by increasing oxidative stress and reducing muscle mass and strength. We used a known inhibitor of KYN-induced Ahr activation, CH-223191, to test the effect of KYN's activation of Ahr in skeletal muscle [17, 18].

2. Materials and Methods

2.1. Animal Experimental Design. All aspects of the animal research were conducted in accordance with the guidelines set by the Augusta University Institutional Animal Care and Use Committee (AU-IACUC) under an AU-IACUC-approved animal use protocol. For KYN and 1-MT treatment studies, 6-8-month-old (young adult) and 22-24-month-old (aged) female C57BL/6 mice were obtained from the aged rodent colony at the National Institute of Aging (NIA, Bethesda, MD, USA). Female mice were chosen due to higher rates of sarcopenia observed in women [19]. For Ahr studies, young adult male and female Ahr-knockout mice were obtained from Taconic (#9166). For KYN treatment and Ahr-KO studies, mice received daily intraperitoneal (I.P.) injections of vehicle (VEH; phosphate-buffered saline, PBS) or L-kynurenine (Sigma; #K8625) at 10 mg/kg body weight for 4 weeks ($n = 10$ per group). For 1-MT studies, 22-24-month-old (aged) C57BL/6 mice were used. Mice were split into 3 groups ($n = 20$ per group): aged VEH (sterile H_2O, 0.20 mL injection), aged low 1-MT (10 mg/kg 1-MT, 0.20 mL injection), and aged high 1-MT (100 mg/kg 1-MT, 0.20 injection). No acute adverse effects were detected with injected KYN or 1-MT. KYN doses were chosen based on previous work in bone [20]. 1-MT doses were chosen based on toxicology work on 1-MT in rats and dogs [21]. Mice were euthanized using CO_2 overdose followed by thoracotomy according to AU-IACUC-approved animal protocols. The right quadriceps was fixed in 10% formalin and stored in 70% ethanol for paraffin embedding and histology. The left quadriceps was frozen in liquid nitrogen for protein and gene expression analysis, and the right tibialis anterior was used for an Amplex™ Red assay immediately.

2.2. Cell Culture. C2C12 cells were obtained from ATCC (ATCC® CRL-1772™), and primary human myoblasts were obtained from Gibco. Both cell lines were cultured in Dulbecco's modified Eagle's medium (DMEM) (Gibco, USA) containing 10% fetal bovine serum (Gibco, USA) and 1% penicillin-streptomycin (Gibco, USA). Cells were seeded in the media and maintained at 37°C in a 5% CO_2 cell incubator (Thermo, USA) until 70%-80% confluence. KYN concentrations of 1 μM and 10 μM were chosen based on serum concentrations found in healthy vs. pathological humans [10].

2.3. Histological Staining. Quadriceps femoris muscles were fixed in 10% buffered formalin, paraffin embedded, and sectioned at 6-8 μm. Sections were deparaffinized and rehydrated, and nonspecific binding was blocked by 0.3% H_2O_2 in TBS. Sections were then incubated overnight at room temperature with rabbit polyclonal anti-laminin (dilution 1 : 1000, Sigma-Aldrich, USA) and rabbit anti-4HNE (Alpha Diagnostic HNE11-S, dilution 1 : 50) and ChromPure Bovine IgG antibodies (Jackson, 001-000-003, dilution 1 : 50). The laminin sections were washed with phosphate-buffered saline (PBS, pH 7.4) and incubated for 1 h at room temperature with a goat anti-rabbit Alexa Fluor 488-conjugated secondary antibody (Invitrogen, A11008). 4HNE and IgG sections were incubated with a polyvalent secondary antibody, followed by *streptavidin* solution (Abcam ab93697). 4HNE and IgG were visualized using DAB Liquid Chromogen Solution (Sigma D3939) and counterstained with hematoxylin (Fisher 245-677). Muscle fiber size was determined by creating a grid on ImageJ and measuring one muscle fiber in each voxel. One section was selected at random from each mouse ($N = 10$ per group in WT mice, $N = 9$ per group in Ahr-KO mice), and 10 muscle fibers per section were measured; then, an average fiber diameter per mouse was calculated. Percentage of 4HNE-positive staining was measured using Photoshop. All measurements were performed by an investigator blinded to group assignment.

2.4. Proteomics and Western Blot. In order to select protein candidates, proteomics were run on three quadriceps muscle samples from the following groups: young KYN, young VEH, old 1-MT (high dose), and old VEH. Quadriceps muscles were homogenized and protein was run at the Augusta University proteomics core using an Orbitrap Fusion™ Tribrid™ mass spectrometer. All proteins with a two-fold or greater difference were chosen from each group, and the protein candidate that was differentially expressed in the separate treatment groups was identified. For western blots, human myoblasts were lysed in radioimmunoprecipitation assay (RIPA) buffer (Tecnova) containing 1% protease inhibitor cocktail (Sigma). Protein concentrations were obtained using a BCA Protein Assay Kit (Sigma). Protein was run in SDS-polyacrylamide gels and transferred using electrophoresis onto a nitrocellulose membrane (Bio-Rad). Blots were incubated with a rabbit polyclonal anti-mitochondrial very-long chain acyl-CoA dehydrogenase (VLCADm) antibody (ab155138) overnight at 4°C. After washing with 1× PBS and blocking with 5% milk in 1× PBS, blots were incubated with an HRP-conjugated anti-rabbit secondary antibody (Santa Cruz Biotechnology) for 1 hr, followed by developing with the ECL Plus Western Blotting Detection System

(GE Healthcare). Chemiluminescence signals were captured on autoradiographic blue films (BioExpress). Films were scanned, and the densitometric values for the proteins of interest were corrected using β-actin with ImageJ Software (NIH).

2.5. MTT Assay. Myoblast viability after KYN treatment was determined using the MTS assay (Promega CellTiter 96® AQueous One MTS Cell Proliferation Assay). C2C12 myoblasts were plated in a 96-well plate at an initial seeding density of 2500 cells/cm^2 or 5000 cells/cm^2. After 24 hours, myoblasts ($N = 8$ per group) were treated with 1× PBS, 5 μM KYN, 10 μM KYN, or 40 μM KYN for 24 hours and 48 hours. After treatment, myoblasts were washed with PBS 2× and 20 μL of MTS assay buffer (MTS, CellTiter 96® AQueous One Solution Reagent, Promega) was added in 100 μL of media. The myoblasts were kept at 37°C in a humidified 5% CO2 incubator for 2 hours; then, optical density was read at 490 nm.

2.6. Amplex Red Assay. A fluorometric method was used to measure H_2O_2 in myoblasts treated with KYN using an Amplex Red assay kit. C2C12 myoblasts were plated in a 96-well plate at an initial seeding density of 5000 cells/cm^2. After 24 hours, myoblasts ($N = 6$ per group) were treated with 1× PBS, 1 μM KYN, or 10 μM KYN for 24 hours. After treatment, media were removed and cells were suspended in sodium phosphate buffer (0.05 M, pH 7.4, 100 mL) and plated in triplicate in a flat-bottom 96-well plate. The reaction was started by adding an Amplex™ Red reagent, horseradish peroxidase, and p-tyramine. After 30 min incubation in the dark, the production of H_2O_2 was quantified at 37°C in a multidetection microplate fluorescence reader (Synergy H1, BioTek Instruments) based on the fluorescence generated at an emission wavelength of 590 nm upon excitation at 545 nm. The specific final fluorescence emission was calculated against a standard curve of H_2O_2 incubated simultaneously.

2.7. PCR Array Plates. Quadriceps muscles from three young VEH mice and three young KYN-treated mice were sonicated, and RNA was isolated using the TRIzol reagent (Invitrogen) according to the manufacturer's instructions. Total RNA was purified using an RNeasy Mini Kit (Qiagen). 1 μg of total RNA was then reverse transcribed using the First-Strand Synthesis Kit (Qiagen) and subsequently loaded into Skeletal Muscle Myogenesis and Myopathy RT^2 Profiler PCR Arrays (Qiagen). PCR was run at the following conditions: 10 min at 95°C, 45 cycles of 15 s at 95°C, and 1 min at 60°C. Fold change was calculated by determining the ratio of mRNA levels to control values using the ΔCt method ($2^{-\Delta\Delta Ct}$). All data were normalized to an average of six housekeeping genes: Actb, B2m, Gapdh, Gusb, Hsp90ab1, and MGDC. PCR conditions used are as follows: hold for 10 min at 95°C, followed by 45 cycles of 15 s at 95°C and 60 s at 60°C.

2.8. Muscle Function Testing. Muscle peak twitch was measured using a whole mouse testing apparatus (1300A, Aurora Scientific Inc., Aurora, ON, Canada) and a force transducer (Aurora Scientific Inc., Canada). This apparatus provides torque measurements in milliNm of tetanic contraction while the animal is alive and with normal vasculature, innervation, and muscle orientation. Animals were maintained under anesthesia through a CO_2 and oxygen breathing cone. Animals were placed on a 37°C platform, and the right hind foot was stabilized to a foot lever with cloth tape at 20° of plantar flexion. Needle electrodes were placed under the skin below the knee to stimulate the peroneal nerve. Muscle peak twitch was then recorded. Tetanic contractions (350 ms train) at 10 to 250 Hz were elicited to obtain a force-frequency curve, with a 2-minute rest between each contraction. Results of single stimulations were collected in torque (milliNm). From torque measurements, the specific muscle force is obtained by normalizing the absolute force values (milliNm) to the animal's body weight. Peak muscle twitch values were selected from each animal.

2.9. Statistical Analysis. For all experiments with more than 2 groups, an ANOVA and a post hoc LSD test for differences between means were used. Results from the Ahr-KO studies were compared to WT experiments using a two-factor ANOVA (SPSS). Results for all experiments with 2 groups were determined using a 2-sample independent t-test to compare differences between means of groups. A minimum significance level of 5% ($P < 0.05$) was used. The datasets generated during and/or analyzed during the current study are available from the corresponding author on reasonable request.

3. Results

3.1. KYN Treatment Increases ROS Levels in Mouse and Human Myoblasts. In order to determine the effect of KYN on ROS production in muscle cells, we measured H_2O_2 levels from C2C12 myoblasts and primary human myoblasts that were treated with KYN for 24 hours. H_2O_2 levels were measured using an Amplex™ Red assay. In C2C12 myoblasts, H_2O_2 was increased two-fold with KYN treatment at only 1 μM (Figure 1(a)). The higher dose (10 μM) produced no further increase beyond the lower 1 μM dose. H_2O_2 was significantly increased in primary human myoblasts treated with 10 μM KYN (Figure 1(b)). KYN did not alter C2C12 myoblast viability at 5 μM, 10 μM, or 40 μM after 24 or 48 hours of treatment (Supplemental Figure 1).

3.2. KYN Treatment Decreases Muscle Fiber Size, Expression of Muscle Structural Muscle Protein Genes, and Peak Strength in Young Female Mice. Young (6-8 mo.) and aged (22-24 mo.) female C57/BL6 mice were given intraperitoneal injections with KYN (10 μg/kg Sigma k3750) or VEH (1× PBS) daily for 4 weeks to test the effect of increased KYN on skeletal muscle *in vivo*. Quadriceps weight relative to body weight was not significantly reduced in KYN-treated muscle compared to vehicle controls (Figure 1(c)), and muscle fiber size was significantly lower in young mice treated with KYN compared to VEH (Figures 1(d) and 1(e)). Positive 4HNE staining, indicative of lipid peroxidation from oxidative stress, was significantly increased in young mice treated

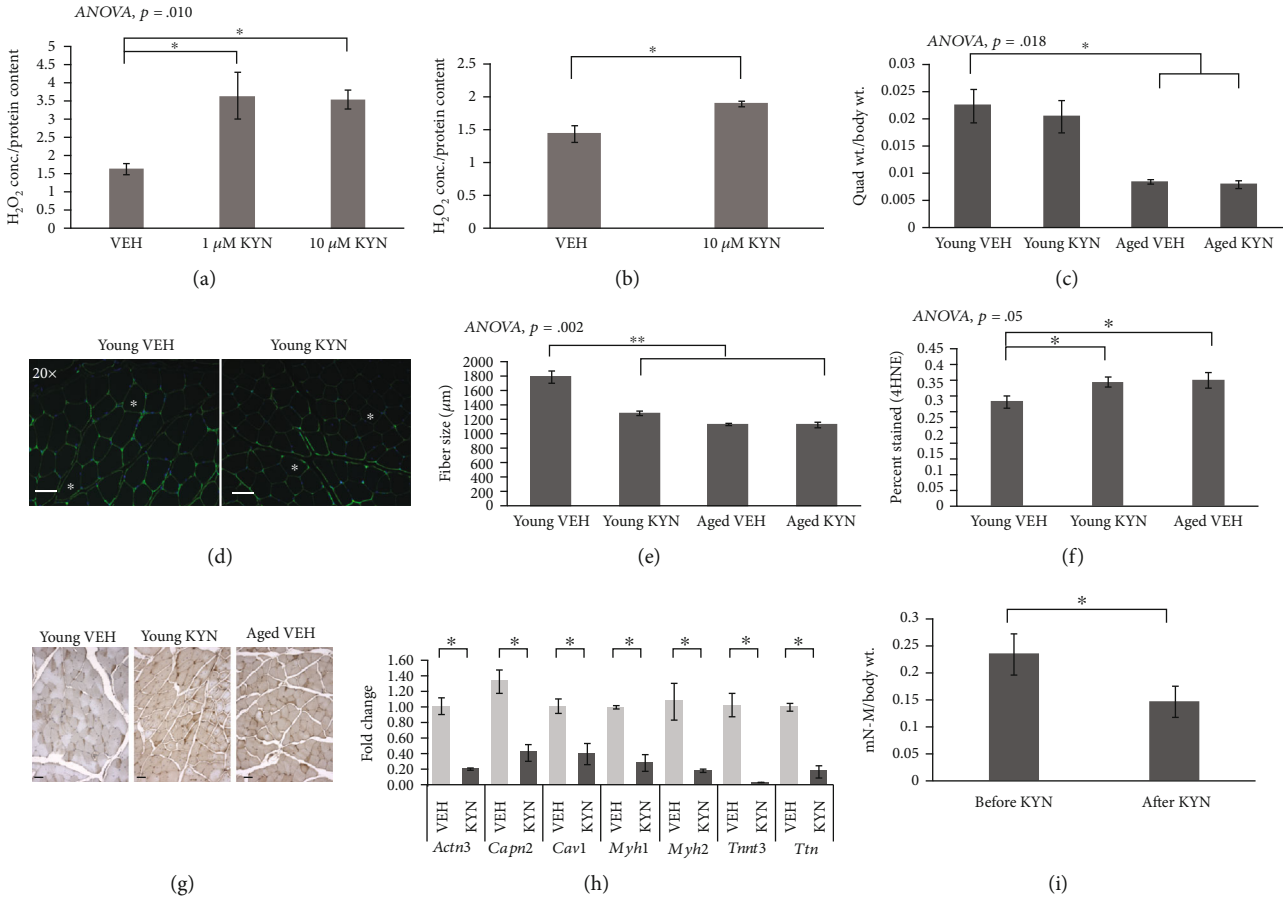

Figure 1: Increased measures of oxidative stress, reduction in muscle fiber size, and reduced muscle strength after KYN treatment *in vitro* and *in vivo*. (a) H_2O_2 levels were significantly increased in mouse C2C12 myoblasts after 24 hours of 1 μM and 10 μM KYN treatment compared to VEH treatment. $N = 6$/group. (b) H_2O_2 levels in human primary myoblasts were increased significantly after 24 hours of 10 μM KYN treatment compared to VEH treatment. $N = 5$/group. (c) After 4 weeks of treatment with KYN or VEH, young female mice did not have a reduction in quadriceps mass compared to body mass. (d, e) Quadriceps fiber size was significantly reduced with KYN treatment in young female mice, visualized with laminin staining (scale bar 100 μm). (f, g) Young female mice treated with KYN had a significant increase in lipid peroxidation, measured by 4HNE staining, when compared to young VEH mice or old VEH mice. (h) Changes in the expression of muscle structural protein genes in quadriceps muscles from young female mice treated with KYN compared to young VEH. (i) Young female mice lost significant peak muscle strength after 4 weeks of KYN treatment. $N = 10$/group for C-I. Data are presented as mean ± s.e.m. $^*P < 0.05$, $^{**}P < 0.01$, and $^{***}P < 0.001$. Representative muscle fibers are marked with stars in d and g.

with KYN compared to young and old controls (Figures 1(f) and 1(g)). PCR arrays for muscle atrophy genes did not show significant changes in ubiquitin ligase gene expression with KYN, but the expression of myosin heavy chain genes was significantly decreased with KYN treatment (Figure 1(h)). Functional, *in vivo* assessment of muscle contractile force showed that young KYN-treated mice lost significant peak muscle strength after 4 weeks of treatment (Figure 1(i)).

3.3. 1-MT Treatment Resulted in Attenuated Muscle Atrophy and Enhanced Muscle Strength in Old Female Mice. To test the effect of IDO inhibition on skeletal muscle *in vivo*, aged female C57/BL6 mice were given intraperitoneal injections of 1-MT at a low dose (10 mg/kg) and high dose (100 mg/kg) or VEH (1× PBS) daily for 4 weeks. Quadriceps weight relative to body weight was significantly increased in mice treated with a high dose of 1-MT compared to vehicle-treated mice (Figure 2(a)). Muscle fiber size in both treatment groups was significantly increased compared to that in vehicle-treated mice (Figures 2(b) and 2(c)). H_2O_2 levels were significantly lower in aged mice treated with a high dose of 1-MT compared to VEH (Figure 2(d)). Muscle peak contractile force was significantly higher in mice treated with the high dose of 1-MT compared to VEH controls (Figure 2(e)).

3.4. Proteomic Analysis of KYN-Treated and 1-MT-Treated Skeletal Muscle Reveals Differential Expression of Very-Long Chain Acyl-CoA Dehydrogenase. Quadriceps tissue from female young mice treated with KYN and aged mice treated with 1-MT were used for proteomic analysis. Both groups were compared to age-matched VEH-treated controls. Proteins that were decreased with KYN and increased with 1-MT or increased with KYN and decreased with 1-MT were selected. The top protein candidate that was differentially expressed with KYN and 1-MT compared to age-matched

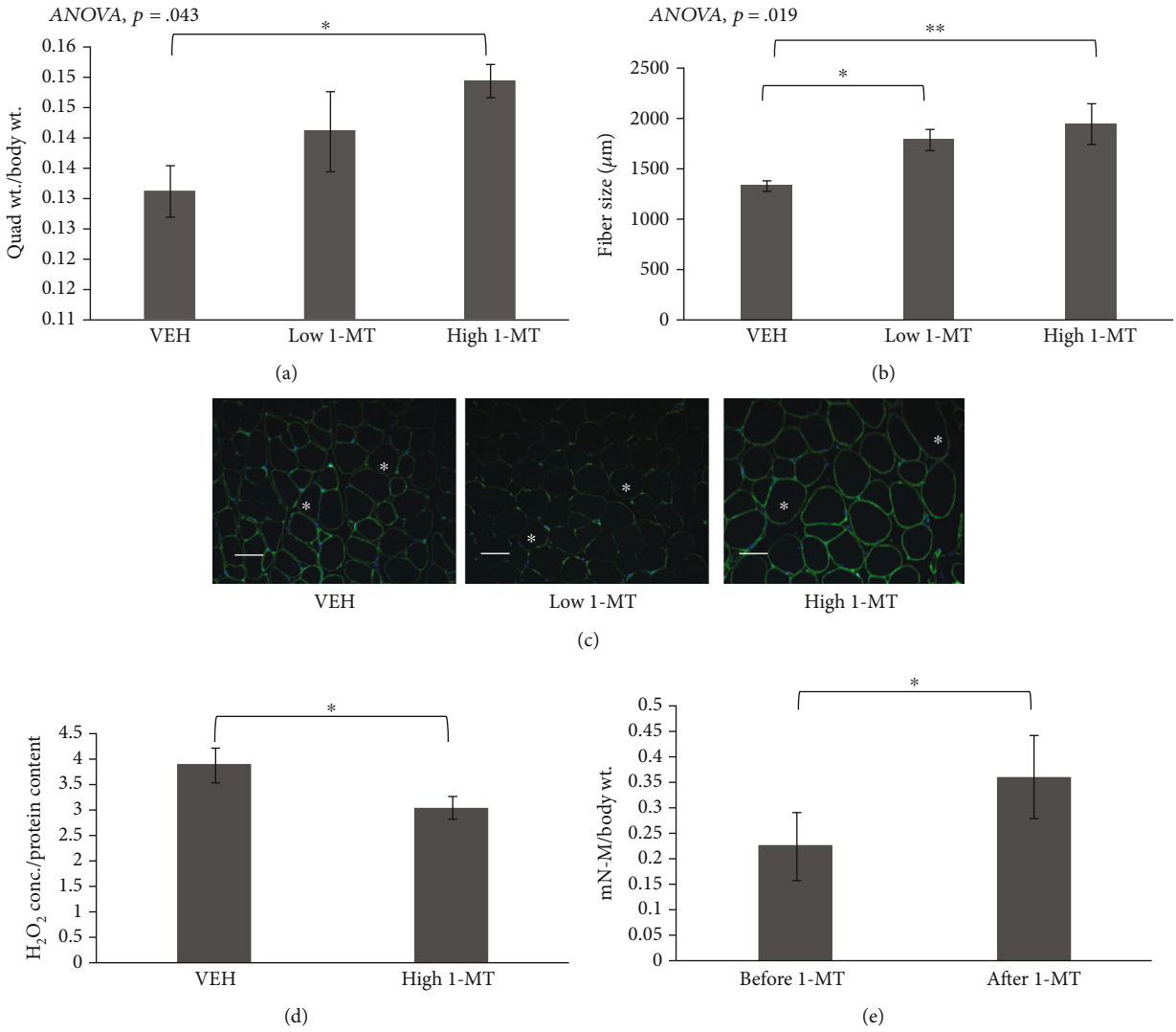

Figure 2: Oxidative stress and muscle morphology changes after 1-MT treatment in aged female mice. (a) Quadriceps muscle mass was significantly increased in mice treated with high-dose 1-MT compared to VEH. (b, c) Muscle fiber size was significantly increased in mice treated with low- and high-dose 1-MT compared to VEH, visualized with laminin staining. Representative muscle fibers are marked with stars. Scale bar: 100 μm. (d) H_2O_2 levels were significantly decreased in mouse quadriceps muscles with 1-MT treatment. (e) Aged mice gained significant peak muscle strength after 4 weeks of 1-MT treatment. $N = 20$/group. Data are presented as mean ± s.e.m. $^*P < 0.05$, $^{**}P < 0.01$, and $^{***}P < 0.001$.

VEH controls was VLCADm (Figure 3(a)). VLCADm was significantly increased at 1 μM and 10 μM KYN treatment of primary human myoblasts compared to VEH controls (Figures 3(b) and 3(c)).

3.5. AHR Inhibition In Vitro and AHR Deficiency In Vivo Do Not Inhibit KYN-Induced ROS Accumulation. To test if a KYN-induced increase in ROS is mediated through the activation of Ahr, C2C12 mouse myoblasts were treated with CH-223191, a specific small-molecule antagonist of Ahr in the presence and absence of 1 μM and 10 μM of KYN. All KYN-treated groups had significantly higher H_2O_2 than the VEH group, regardless of whether the Ahr inhibitor was present. The groups treated with 10 μm KYN and CH-223191 had significantly higher H_2O_2 levels than the group treated with KYN alone (Figure 4(a)). To further explore the relationship between Ahr and KYN in skeletal muscle, male and female global Ahr-KO mice (6-8 months old) were treated with KYN (10 mg/kg) or VEH (1× PBS) by intraperitoneal injections daily for 4 weeks. There was a not significant difference in H_2O_2 in Ahr-KO mice compared to VEH. Quadriceps muscle weight was significantly lower in Ahr-KO mice with KYN treatment compared to VEH treatment (Figure 4(c)). Muscle fiber size was not significantly different in Ahr-KO mice with KYN treatment compared to VEH. 4HNE staining was not significantly different in Ahr-KO mice with KYN treatment compared to VEH. No sex differences were observed; data shown in Figure 4 are pooled. A two-factor ANOVA was run with genotype (WT, Ahr KO) and treatment (VEH, KYN) as the two factors to determine whether the absence of the Ahr receptor would significantly impact lipid peroxidation assessed by 4HNE staining. We

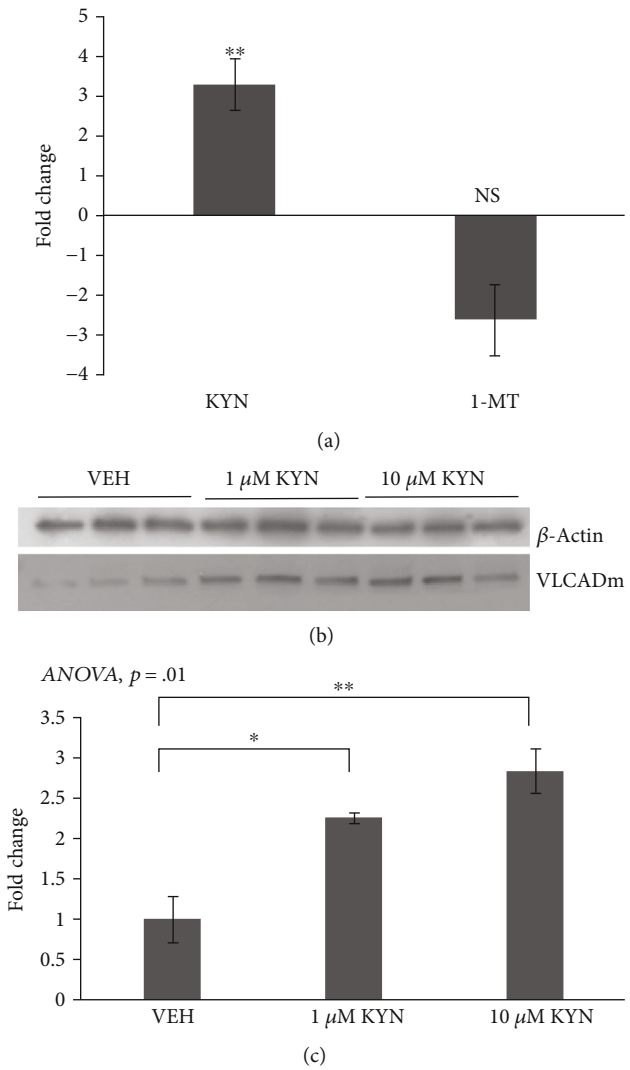

Figure 3: Mitochondrial very long-chain acyl-CoA dehydrogenase protein is differentially expressed with KYN or 1-MT treatment of female mice *in vivo* and human myoblasts *in vitro*. (a) Proteomics run on quadriceps muscle homogenates from young mice treated with KYN or aged mice treated with 1-MT showed that VLCADm was significantly increased with KYN treatment in young mice. (b) Representative western blots from primary human cells that showed a significant increase in VLCADm with KYN treatment. (c) VLCADm western blot results were normalized to β-actin controls and quantified. Data are presented as mean ± s.e.m. $^{*}P < 0.05$, $^{**}P < 0.01$, and $^{***}P < 0.001$.

found no significant genotype∗treatment interaction for either muscle fiber size ($F = 0.10$, $P = 0.75$) or 4HNE staining intensity ($F = 0.54$, $P = 0.47$), indicating that the loss of the Ahr receptor did not significantly alter the response of muscle to KYN treatment.

4. Discussion

The cellular and molecular processes leading to sarcopenia are incompletely understood. A number of factors may contribute to loss of muscle mass and strength with age including lack of physical activity, dietary protein deficiency, circulating inflammatory cytokines, and oxidative stress. Skeletal muscle has the ability to activate antioxidant proteins to quickly repair exercise-induced oxidative damage; however, these mechanisms are attenuated with age, causing an imbalance in ROS [22]. Accumulation of ROS has in particular been suggested to induce age-related declines in muscle [23, 24]. We addressed this knowledge gap by examining the cellular and molecular mechanisms underlying the age-associated accumulation of reactive oxygen species. KYN is a circulating tryptophan metabolite that increases with age and is correlated with frailty [11] and increased mortality in older adults [10]. Elevated circulating levels of KYN are also found to be associated with osteoporosis and Alzheimer's disease [7, 25, 26]. In the presence of IFNγ, IDO converts tryptophan to KYN [8] and IFNγ and IDO activity have both been shown to increase with age [9, 18].

As IDO activity is increased, the essential amino acid tryptophan is depleted from the tissue microenvironment and its metabolism is directed away from serotonin synthesis and toward the KYN pathway [8, 9]. Our study addressed the hypothesis that KYN contributes to the progression of sarcopenia. We found that KYN did not decrease quadriceps weight in young mice, but did decrease muscle fiber size. This discrepancy is most likely due to an increase in noncontractile tissue (fat or fibrotic tissue) within the muscles of KYN-treated mice (source). PCR array data identified several structural muscle proteins that were downregulated with KYN treatment. The PCR data suggest that reduction in fiber size with KYN treatment may be due to a loss of protein anabolism rather than an increase in protein catabolism. These results are consistent with those of several groups that have shown that protein anabolism is impaired with aging [27–30]. We observed an increase in the oxidative stress markers H_2O_2 and 4HNE in young mice treated with KYN. We noted that the levels of these oxidative stress markers were similar to those of aged mice and did not continue to increase with further KYN treatment in old mice. We speculate that the effects of KYN reach a threshold, such that additional exogenous KYN in animals that already have high KYN levels may yield no effects (kynurenine resistance), but further work to test this hypothesis is needed. We also demonstrated that inhibition of IDO helped to preserve muscle mass and function in aged mice, further suggesting that the kynurenine pathway plays an important role in muscle health.

KYN is a ligand of the aryl hydrocarbon receptor (Ahr) and is involved in immunosuppression [13]. Previous work on skin and vascular aging have suggested a potential for Ahr activation in the aging of various tissue types [15, 16]. Ahr is a xenobiotic drug response element that acts as a transcription factor and once it is activated stimulates the expression of Cyp1A1, which can further increase oxidative stress [13, 14]. We found that Ahr inhibition did not protect muscle cells from the detrimental effects of KYN treatment. Surprisingly, when myoblasts were treated with KYN and the Ahr small-molecule

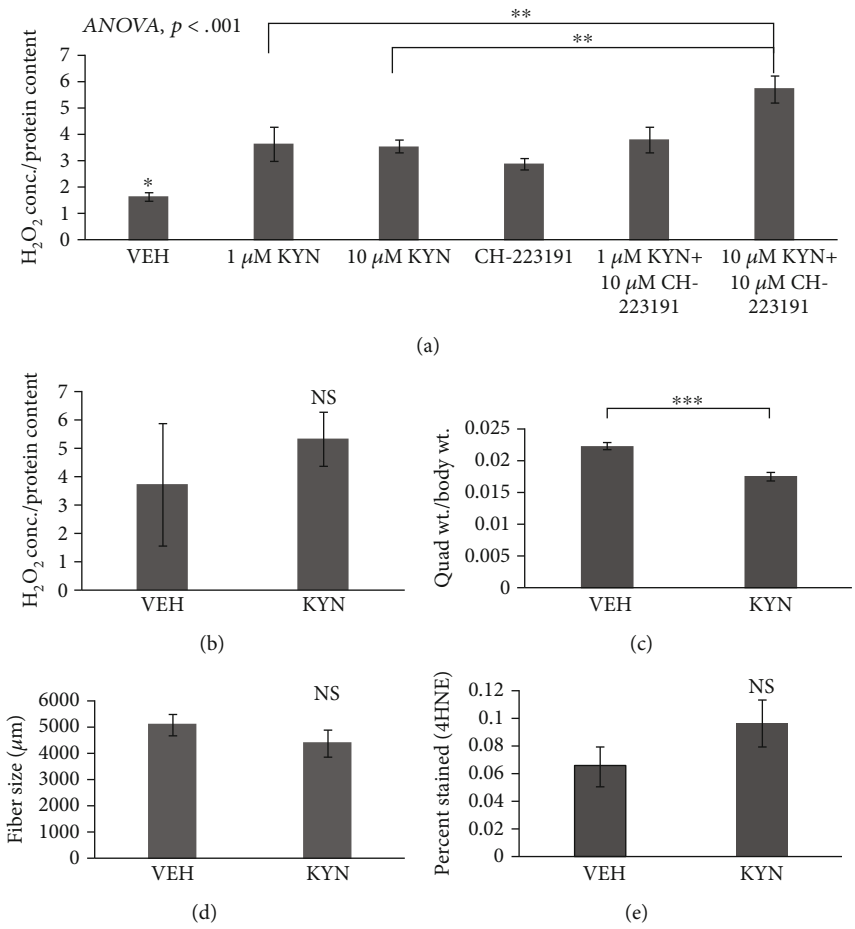

Figure 4: Effects of KYN with inhibition of Ahr *in vitro* and global knockout of Ahr *in vivo*. (a) Treatment of myoblasts with KYN and the small-molecule Ahr inhibitor CH-223191 simultaneously increased H_2O_2 significantly compared to KYN alone ($N = 6$/group). (b) H_2O_2 from quadriceps of Ahr-knockout mice treated with KYN was increased slightly but not significantly compared to that from VEH. (c) KYN treatment of Ahr-knockout mice significantly decreased quadriceps mass. (d) Fiber size of quadriceps muscles from Ahr-knockout mice decreased slightly but not significantly with KYN treatment. (e) 4HNE staining of quadriceps muscles increased slightly but not significantly with KYN treatment. Data are presented as mean ± s.e.m. $^{*}P < 0.05$, $^{**}P < 0.01$, and $^{***}P < 0.001$. (b–d) Pooled male and female: $N = (5\,\text{M} + 4\text{F per group})$.

inhibitor CH-223191, there were significantly higher levels of H_2O_2 than with KYN alone. CH-223191 is a highly specific inhibitor capable of blocking KYN's interactions with Ahr in cells such as bone marrow-derived murine dendritic cells (BMDCs) [18]; however, until now, the effects of KYN's interaction with Ahr has not been explored in skeletal muscle. Ahr-knockout mice treated with KYN had significantly lower quadriceps weight compared to VEH-treated controls, but there were no significant differences between VEH- and KYN-treated mice in muscle fiber size, H_2O_2, or 4HNE staining in Ahr-knockout mice. This could again be due to a threshold effect, or possibly a protective effect of Ahr in skeletal muscle. Overall, these results suggest that KYN-induced skeletal muscle loss with age may occur through a different pathway than the one mediated by Ahr.

Maintenance of skeletal muscle throughout life is dependent upon a balance of protein synthesis and protein catabolism [27–30]. We examined proteomics from young mice treated with KYN, and old mice treated with 1-MT, and found that lipid peroxidation products were differentially expressed with manipulation of the KYN pathway. We identified an increase in a mitochondrial lipid peroxidation enzyme, VLCADm, as a potential downstream target mechanism for KYN's contribution to sarcopenia. VLCADm has been shown to produce H_2O_2 [31] (Figure 5). Furthermore, Montes et al. demonstrated that lipid peroxidation markers can serve as indicators of sarcopenia [32], and Bellanti et al. found that lipid peroxidation products form aldehyde-protein hybrids that are increased in sarcopenic adults [33]. Exercise has been previously reported to increase skeletal muscle ROS as well as VLCADm [34], suggesting that in the setting of acute inflammation transient, elevated ROS and VLCADm levels may have beneficial effects on skeletal muscle; however, it is likely that chronically elevated ROS and VLCADm resulting from prolonged KYN exposure may ultimately have detrimental effects on muscle, which would explain the previous associations among aging, inflammation, circulating KYN, VLCADm, ROS, and sarcopenia noted above (Figure 5).

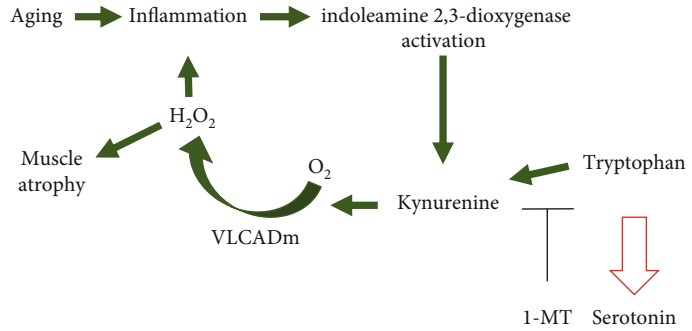

Figure 5: Proposed model for KYN's effects on lipid peroxidation, ROS generation, and age-related muscle atrophy. Aging causes an increase in systemic oxidative stress, and skeletal muscle antioxidant pathways are unable to meet the increased demand. Inflammatory cytokines like IFNγ activate IDO to convert tryptophan to KYN. KYN then induces the upregulation of mitochondrial VLCADm which degrades lipid and produces H_2O_2. The overexpression of ROS leads to further inflammation and muscle atrophy. 1-MT is an antagonist of IDO that can inhibit tryptophan's conversion into KYN, thereby attenuating KYN-induced tissue dysfunction with aging.

5. Conclusion

Our work provides evidence that an increase in KYN with age may contribute to sarcopenia by causing an increase in oxidative stress. Our working model is that the lipid peroxidation resulting from chronic KYN exposure contributes to sarcopenia (Figure 5). These results provide new insights into the mechanisms underlying sarcopenia and shed new light on potential therapeutic targets for the aging population.

Data Availability

All data used to support the findings of this study are available from the corresponding author upon request.

Disclosure

Data from certain experiments described in this paper were presented at the 2018 Experimental Biology meeting in San Diego, CA, USA.

Conflicts of Interest

Carlos M. Isales and Mark W. Hamrick are founders of Gerologix Inc. which seeks to target the KYN pathway for the treatment of age-related diseases. Helen Kaiser and Mark Hamrick hold intellectual property related to KYN inhibition in sarcopenia. These conflicts are managed in accordance with the university policy.

Authors' Contributions

Chirayu Pandya performed western blots, Kanglun Yu performed 4HNE staining, and Sadanand Fulzele assisted with cell culture. Bharati Mendhe performed MTT assays. All other experiments were performed by Helen Kaiser. Maribeth Johnson and Mark Hamrick assisted with statistical analysis, and Carlos M. Isales, Meghan McGee-Lawrence, and Mark Hamrick assisted in writing and preparing the manuscript.

Acknowledgments

This work was supported by the National Institute of Aging (AG036675). Technical assistance for tissue sectioning was provided by the Augusta University electron microscopy and histology core facility and for proteomics by the Augusta University proteomics and informatics core facilities. We are grateful to Madison Carpenter and Andrew Khayrullin for their assistance in this work and to Dr. Gabor Csanyi for his assistance with the Amplex™ Red assay.

Supplementary Materials

Supplemental Figure 1: the effect of KYN on C2C12 myoblast viability. (A–D) There was no change in C2C12 myoblast viability with a seeding density of 2500 cells/cm^2 or 5000 cells/cm^2 and 24 or 48 hours of treatment. *(Supplementary Materials)*

References

[1] United Nations, Department of Economic and Social Affairs, and Population Division, "World population ageing," United Nations, New York, NY, USA, 2013.

[2] J. C. Brown, M. O. Harhay, and M. N. Harhay, "Sarcopenia and mortality among a population-based sample of community-dwelling older adults," *Journal of Cachexia, Sarcopenia and Muscle*, vol. 7, no. 3, pp. 290–298, 2016.

[3] J. G. Ryall, J. D. Schertzer, and G. S. Lynch, "Cellular and molecular mechanisms underlying age-related skeletal muscle wasting and weakness," *Biogerontology*, vol. 9, no. 4, pp. 213–228, 2008.

[4] F. Landi, R. Calvani, M. Cesari et al., "Sarcopenia: an overview on current definitions, diagnosis and treatment," *Current Protein and Peptide Science*, vol. 19, no. 7, pp. 633–638, 2018.

[5] I. M. Conboy and T. A. Rando, "Heterochronic parabiosis for the study of the effects of aging on stem cells and their niches," *Cell Cycle*, vol. 11, no. 12, pp. 2260–2267, 2012.

[6] J. De Bie, J. Guest, G. J. Guillemin, and R. Grant, "Central kynurenine pathway shift with age in women," *Journal of Neurochemistry*, vol. 136, no. 5, pp. 995–1003, 2016.

[7] N. Braidy, G. J. Guillemin, H. Mansour, T. Chan-Ling, and R. Grant, "Changes in kynurenine pathway metabolism in the brain, liver and kidney of aged female Wistar rats," *The FEBS Journal*, vol. 278, no. 22, pp. 4425–4434, 2011.

[8] X. Dai and B. T. Zhu, "Indoleamine 2, 3-dioxygenase tissue distribution and cellular localization in mice: implications for its biological functions," *Journal of Histochemistry & Cytochemistry*, vol. 58, no. 1, pp. 17–28, 2010.

[9] A. A.-B. Badawy, "Kynurenine pathway of tryptophan metabolism: regulatory and functional aspects," *International Journal of Tryptophan Research*, vol. 10, 2017.

[10] M. Pertovaara, A. Raitala, T. Lehtimäki et al., "Indoleamine 2, 3-dioxygenase activity in nonagenarians is markedly increased and predicts mortality," *Mechanisms of Ageing and Development*, vol. 127, no. 5, pp. 497–499, 2006.

[11] V. Valdiglesias, D. Marcos-Pérez, M. Lorenzi et al., "Immunological alterations in frail older adults: a cross sectional study," *Experimental Gerontology*, vol. 112, pp. 119–126, 2018.

[12] R. Metz, J. B. DuHadaway, U. Kamasani, L. Laury-Kleintop, A. J. Muller, and G. C. Prendergast, "Novel tryptophan catabolic enzyme IDO2 is the preferred biochemical target of the antitumor indoleamine 2, 3-dioxygenase inhibitory compound D-1-methyl-tryptophan," *Cancer Research*, vol. 67, no. 15, pp. 7082–7087, 2007.

[13] S. H. Seok, Z. X. Ma, J. B. Feltenberger et al., "Trace derivatives of kynurenine potently activate the aryl hydrocarbon receptor (AHR)," *Journal of Biological Chemistry*, vol. 293, no. 6, pp. 1994–2005, 2018.

[14] B. N. Fukunaga, M. R. Probst, S. Reisz-Porszasz, and O. Hankinson, "Identification of functional domains of the aryl hydrocarbon receptor," *Journal of Biological Chemistry*, vol. 270, no. 49, pp. 29270–29278, 1995.

[15] A. Eckers, S. Jakob, C. Heiss et al., "The aryl hydrocarbon receptor promotes aging phenotypes across species," *Scientific Reports*, vol. 6, no. 1, article 19618, 2016.

[16] Y. Qiao, Q. Li, H. Y. du, Q. W. Wang, Y. Huang, and W. Liu, "Airborne polycyclic aromatic hydrocarbons trigger human skin cells aging through aryl hydrocarbon receptor," *Biochemical and Biophysical Research Communications*, vol. 488, no. 3, pp. 445–452, 2017.

[17] K. J. Smith, I. A. Murray, R. Tanos et al., "Identification of a high-affinity ligand that exhibits complete aryl hydrocarbon receptor antagonism," *Journal of Pharmacology and Experimental Therapeutics*, vol. 338, no. 1, pp. 318–327, 2011.

[18] J. D. Mezrich, J. H. Fechner, X. Zhang, B. P. Johnson, W. J. Burlingham, and C. A. Bradfield, "An interaction between kynurenine and the aryl hydrocarbon receptor can generate regulatory T cells," *The Journal of Immunology*, vol. 185, no. 6, pp. 3190–3198, 2010.

[19] J. A. Batsis, T. A. Mackenzie, L. K. Barre, F. Lopez-Jimenez, and S. J. Bartels, "Sarcopenia, sarcopenic obesity and mortality in older adults: results from the National Health and Nutrition Examination Survey III," *European Journal of Clinical Nutrition*, vol. 68, no. 9, pp. 1001–1007, 2014.

[20] M. E. Refaey, M. E. McGee-Lawrence, S. Fulzele et al., "Kynurenine, a tryptophan metabolite that accumulates with age, induces bone loss," *Journal of Bone and Mineral Research*, vol. 32, no. 11, pp. 2182–2193, 2017.

[21] L. Jia, K. Schweikart, J. Tomaszewski et al., "Toxicology and pharmacokinetics of 1-methyl-d-tryptophan: absence of toxicity due to saturating absorption," *Food and Chemical Toxicology*, vol. 46, no. 1, pp. 203–211, 2008.

[22] A. Vasilaki, F. McArdle, L. M. Iwanejko, and A. McArdle, "Adaptive responses of mouse skeletal muscle to contractile activity: the effect of age," *Mechanisms of Ageing and Development*, vol. 127, no. 11, pp. 830–839, 2006.

[23] N. T. Smith, A. Soriano-Arroquia, K. Goljanek-Whysall, M. J. Jackson, and B. McDonagh, "Redox responses are preserved across muscle fibres with differential susceptibility to aging," *Journal of Proteomics*, vol. 177, pp. 112–123, 2018.

[24] F. L. Muller, M. S. Lustgarten, Y. Jang, A. Richardson, and H. van Remmen, "Trends in oxidative aging theories," *Free Radical Biology & Medicine*, vol. 43, no. 4, pp. 477–503, 2007.

[25] S. Srivastava, "Emerging therapeutic roles for NAD^+ metabolism in mitochondrial and age-related disorders," *Clinical and Translational Medicine*, vol. 5, no. 1, p. 25, 2016.

[26] E. Bandrés, J. Merino, B. Vázquez et al., "The increase of IFN-γ production through aging correlates with the expanded $CD8^{+high}CD28^-$ $CD57^+$ subpopulation," *Clinical Immunology*, vol. 96, no. 3, pp. 230–235, 2000.

[27] P. J. Atherton, P. L. Greenhaff, S. M. Phillips, S. C. Bodine, C. M. Adams, and C. H. Lang, "Control of skeletal muscle atrophy in response to disuse: clinical/preclinical contentions and fallacies of evidence," *American Journal of Physiology-Endocrinology and Metabolism*, vol. 311, no. 3, pp. E594–E604, 2016.

[28] B. T. Wall, S. H. Gorissen, B. Pennings et al., "Aging is accompanied by a blunted muscle protein synthetic response to protein ingestion," *PLoS One*, vol. 10, no. 11, article e0140903, 2015.

[29] D. R. Moore, T. A. Churchward-Venne, O. Witard et al., "Protein ingestion to stimulate myofibrillar protein synthesis requires greater relative protein intakes in healthy older versus younger men," *The Journals of Gerontology Series A: Biological Sciences and Medical Sciences*, vol. 70, no. 1, pp. 57–62, 2014.

[30] D. Cuthbertson, K. Smith, J. Babraj et al., "Anabolic signaling deficits underlie amino acid resistance of wasting, aging muscle," *The FASEB Journal*, vol. 19, no. 3, pp. 422–424, 2005.

[31] P. A. H. B. Kakimoto, F. K. Tamaki, A. R. Cardoso, S. R. Marana, and A. J. Kowaltowski, "H_2O_2 release from the very long chain acyl-CoA dehydrogenase," *Redox Biology*, vol. 4, pp. 375–380, 2015.

[32] A. Coto Montes, J. A. Boga, C. Bermejo Millo et al., "Potential early biomarkers of sarcopenia among independent older adults," *Maturitas*, vol. 104, pp. 117–122, 2017.

[33] F. Bellanti, A. D. Romano, A. Lo Buglio et al., "Oxidative stress is increased in sarcopenia and associated with cardiovascular disease risk in sarcopenic obesity," *Maturitas*, vol. 109, pp. 6–12, 2018.

[34] J. F. Horowitz, T. C. Leone, W. Feng, D. P. Kelly, and S. Klein, "Effect of endurance training on lipid metabolism in women: a potential role for PPARα in the metabolic response to training," *American Journal of Physiology-Endocrinology And Metabolism*, vol. 279, no. 2, pp. E348–E355, 2000.

Hindawi
Oxidative Medicine and Cellular Longevity
Volume 2019, Article ID 7318796, 15 pages
https://doi.org/10.1155/2019/7318796

Review Article

Ankrd2 in Mechanotransduction and Oxidative Stress Response in Skeletal Muscle: New Cues for the Pathogenesis of Muscular Laminopathies

Vittoria Cenni,[1,2] **Snezana Kojic**,[3] **Cristina Capanni**,[1,2] **Georgine Faulkner**,[4] **and Giovanna Lattanzi**[1,2]

[1]*CNR National Research Council of Italy, Institute of Molecular Genetics, Unit of Bologna, 40126 Bologna, Italy*
[2]*IRCCS Istituto Ortopedico Rizzoli, 40126 Bologna, Italy*
[3]*Institute of Molecular Genetics and Genetic Engineering University of Belgrade, 11010 Belgrade, Serbia*
[4]*Department of Biology, University of Padua, 35121 Padua, Italy*

Correspondence should be addressed to Vittoria Cenni; vittoria.cenni@cnr.it and Giovanna Lattanzi; giovanna.lattanzi@cnr.it

Received 4 March 2019; Revised 2 May 2019; Accepted 19 May 2019; Published 24 July 2019

Guest Editor: Andrey J. Serra

Ankrd2 (ankyrin repeats containing domain 2) or Arpp (ankyrin repeat, PEST sequence, and proline-rich region) is a member of the muscle ankyrin repeat protein family. Ankrd2 is mostly expressed in skeletal muscle, where it plays an intriguing role in the transcriptional response to stress induced by mechanical stimulation as well as by cellular reactive oxygen species. Our studies in myoblasts from Emery-Dreifuss muscular dystrophy 2, a *LMNA*-linked disease affecting skeletal and cardiac muscles, demonstrated that Ankrd2 is a lamin A-binding protein and that mutated lamins found in Emery-Dreifuss muscular dystrophy change the dynamics of Ankrd2 nuclear import, thus affecting oxidative stress response. In this review, besides describing the latest advances related to Ankrd2 studies, including novel discoveries on Ankrd2 isoform-specific functions, we report the main findings on the relationship of Ankrd2 with A-type lamins and discuss known and potential mechanisms involving defective Ankrd2-lamin A interplay in the pathogenesis of muscular laminopathies.

1. Introduction

Ankrd2 (ankyrin repeats containing domain 2) or Arpp (ankyrin repeat, PEST sequence, and proline-rich region) is a member of the MARP (muscle ankyrin repeat protein) family of proteins that also includes Ankrd1, or Carp (Cardiac Ankyrin Repeat Protein), and Ankrd23, or DARP (Diabetes-related Ankyrin Repeat Protein) [1]. As we will describe in detail in this review, Ankrd2 is principally expressed in skeletal muscle, where it plays an intriguing role in the transcriptional response to stress induced by mechanical stimulation, as well as by cellular ROS (reactive oxygen species). In particular, although the Ankrd2 knockout mouse model has revealed that Ankrd2 is not necessary for life nor the direct cause of any muscular disorder, multiple evidence obtained from muscular cell lines or primary cultures from patients affected by muscular diseases suggest that an anomalous expression level of Ankrd2, as well as defective nuclear recruitment of the protein, might contribute to a muscular phenotype. Very recently, we found that Ankrd2 is a novel interactor of A-type lamins, which are produced by the *LMNA* gene and are the major constituents of the nuclear lamina. Mutations of *LMNA* gene are the cause of a substantial number of pathologies, some of which affecting skeletal and cardiac muscles. Moreover, altered expression of Ankrd2 was detected in myopathies [2], cardiomyopathies [3], and some tumors [4]. In this review, apart from describing the latest advances related to Ankrd2, including an ever-growing interest for Ankrd2 isoform-specific functions, we will report the main findings on Ankrd2 and its relation to lamins and discuss known and potential mechanisms, through which defective Ankrd2-lamin A interplay might have a role in the pathogenesis of *LMNA*-related muscular disorders.

2. Ankrd2 in Striated Muscles

Ankrd2, together with other proteins of the MARP family, is considered as STRaND (shuttling transcriptional regulators and non-DNA-binding protein), having signature features: shuttling from the cytoplasm to the nucleus, absence of DNA binding, and regulation of transcription via interaction with transcription factors [5]. Recently, data from Wette et al., obtained on single muscle fibers, have shown that Ankrd2 is mostly found (>70% of total Ankrd2) in the cytosol [6]. The remaining amount is distributed between intracellular structures, including the sarcomere and the nucleus, with proportions that reflect the physiology, such as the type (slow/fast) or the condition (forming/mature/regenerating/injured), of the fiber considered. In healthy striated muscle, Ankrd2 is found at the sarcomeric I-band [7, 8] where it contributes to the formation and function of the I-band mechanosensory complex, probably via interaction with calpain 3 and the elastic portion of titin (N2A region) [7, 9]. As extensively described in the next sections, Ankrd2 also interacts with nuclear proteins with both structural and enzymatic roles [1] and is accumulated in nuclei of injured muscle [10]. An overview of the main structural and functional features of Ankrd2, including protein domains, posttranslational modifications, expression profile, proposed functions, interacting proteins, and pathways affected by *ANKRD2* silencing in human myoblasts, is given in Table 1. In the nucleus, Ankrd2 participates in the regulation of genes involved in the cell cycle, myogenesis, and inflammatory response [11–15]. Of note, in mature muscle cells, the evidence reporting that the majority of Ankrd2 is freely diffusible in the cytosol [6] has for the first time pointed to the open question if Ankrd2, besides being involved in sarcomeric activity, might also participate in cellular functions in other subcellular districts, thus suggesting a role as a downstream signal transducer in mechanosignaling pathways. It is important to note that despite accumulated findings from cell culture experiments, direct evidence of Ankrd2 function in mature healthy and diseased striated muscles is still missing.

2.1. Ankrd2 Expression in Skeletal Muscle. Ankrd2 was reported for the first time in a study performed in 2000 by Kemp and colleagues as a protein upregulated in murine muscle exposed to prolonged passive stretch (7 days) [16]. Preferential expression in skeletal muscle, more specifically in slow (type I) muscle fibers, and responsiveness to mechanical stress are signature features of this protein. Recently, Ankrd2 was confirmed to be the most abundant MARP protein in human skeletal muscle, being ~30-fold more expressed than DARP and ~150-fold more than Ankrd1 [6]. In this study, performed on a group of four subjects, the absolute amount of Ankrd2 was subject-specific, ranging from 1.6 to 4.3 μmol/kg net weight, and proportional to the content of myosin heavy chain I (MHCI) protein, which is a marker of slow (type I) muscle fibers [6]. Almost double the amount of Ankrd2 was measured in slow (type I) fibers compared to that of fast (type II) fibers microdissected from the *vastus lateralis* (presenting approximately 32% of slow muscle fibers [17]), corroborating Ankrd2 preferential expression in slow fibers [6].

Although the existence of Ankrd2 isoforms was reported in 2003 by Miller et al. [7], their specific expression and localization in human skeletal and cardiac muscles, as well as in primary human myoblasts and myotubes, have been recently determined by studies in which their discrimination was enabled by specific antibodies [6, 18].

The most important Ankrd2 isoforms, namely, S-Ankrd2 (333 aa) and M-Ankrd2 (360 aa), are identical, except for 27 aa extension at the N-terminus of M-Ankrd2. According to qPCR results, the expression of Ankrd2 isoforms is regulated at the transcriptional level [18]. S-Ankrd2 is expressed in both heart and skeletal muscles [18] where it is the predominant form [6, 18]. The well-known chessboard pattern of Ankrd2 expression observed in transversal sections of skeletal muscle may be attributed almost exclusively to S-Ankrd2 [6, 18], which has been therefore proposed as the canonical Ankrd2 isoform. Although still a matter of debate, in mature muscle fibers, the small amount of M-Ankrd2 has been identified in nuclei [18]. In human myoblasts, S-Ankrd2 is expressed mainly in nuclei at a low level, while in myotubes, it is upregulated and localized in the cytoplasm. M-Ankrd2 is also upregulated upon differentiation of myoblasts to myotubes; however, it maintains its nuclear localization. Striking differences in expression and localization of Ankrd2 isoforms may mirror their different functions which however need to be further explored [18]. For example, M-Ankrd2 might have a more regulatory role, being predominantly nuclear, while sarcomeric and cytosolic S-Ankrd2 may have a structural and downstream signaling role, respectively. Domain organization, alignment, and updated database entries for all five Ankrd2 isoforms are shown in Figures 1(a)–1(c), respectively.

2.2. Ankrd2 Expression in Cardiac Muscle. Ankrd2 is expressed in the human heart, including ventricles, the interventricular septum, and the apex of the heart [4, 19], at a lower level compared to skeletal muscle. Ankrd2 expression in the heart is potentially regulated by cardiac-specific transcription factors Nkx2.5, Hand2, and Ankrd1 as demonstrated by their interaction with the *ANKRD2* promoter or by dual luciferase assay [20, 21]. Transcriptome profiling confirmed a lower level of Ankrd2 in the ventricles of human adult heart, compared to Ankrd1 [22]. Both S- and M-Ankrd2 isoforms are expressed in cardiac muscle; they have sarcomeric localization and are almost absent from nuclei [18]. The latter finding and the known interaction between Ankrd2 and the gap junction protein ZO-1 [20], enriched in ICDs, suggest a role for Ankrd2 in intercellular communication, which merits further investigation. In neonatal rat cardiomyocytes (NRCM), both sarcomeric and nuclear localizations of Ankrd2 were investigated during cellular differentiation and not shown to be affected by the maturation stage [22]. Moreover, doxorubicin had no effect on Ankrd2 expression, as opposed to Ankrd1, suggesting that Ankrd2 is not involved in cellular response to this cardiotoxic antineoplastic drug.

Table 1: Overview of the main structural and functional features of Ankrd2 (extensively reported in [122]).

Feature	Ref.
Structural domains	
Ankyrin repeats	[123]
Coiled coil	
Protein destabilization motif (PEST)	
Nuclear localization signal (NLS)	
Posttranslational modifications	
Phosphorylation by Akt2 kinase	[15]
Proteolytic cleavage by μ-calpain	[9]
Expression profile	
Skeletal muscle > heart > kidney	[4, 19, 123, 124]
Type I (slow) skeletal muscle fibers	[8, 123]
Localized in nuclei of myoblasts and cytoplasm of myotubes	[123]
Migrate from myofibrils to nucleus after muscle injury	[10]
Proposed functions	
Stress response in muscle (stretch, denervation, eccentric contractions, fatiguing jumping and other types of exercise, and injury)	[8, 10, 16, 46, 47, 49, 50, 55]
Muscle adaptation	[7, 10, 16, 20, 46, 47, 49, 50, 125, 126]
Transcriptional regulation	[1, 10]
Communication between the sarcoplasm and the nucleus	[1]
Myogenesis and myogenic differentiation	[11, 13, 14]
Inflammatory response	[12]
Interacting proteins	
Titin	[7]
Telethonin	[1]
ZASP	[30]
Calpain 3	[9]
Akt2	[15]
A-type lamins (lamin A, prelamin A, and lamin C)	[98]
Proteins with PDZ and SH3 domains, including ZO-1 and β1-syntrophin	[20]
Transcription factors, including YB1, p53, PML, PAX6, NFIL3, and MECP2	[20]
Pathways affected by Ankrd2 silencing in human myoblasts	
Intercellular communication	[20]
Cytokine-cytokine receptor interaction	
Focal adhesion	
Tight junction	
Gap junction	
Regulation of actin cytoskeleton	
Signaling involved in intracellular communication	
Calcium	
Insulin	
MAPK	
p53	
TGF-β	
Wnt	

It is interesting that, in addition to mild phenotype in skeletal muscle, morphology, basal cardiac function, and cardiac development were not impaired in triple knockout mice for three members of the MARP family (Ankrd1, Ankrd2, and DARP) up to 17 months of age [23]. Hypertrophic response to acute pressure overload induced by transverse aortic constriction was also unaffected. It is possible that Ankrd2 is involved in the response to other types of cardiac stress, still to be determined. On the other hand, as demonstrated for Ankrd1, overexpression of Ankrd2 may have more striking consequences. Overexpressed mouse Ankrd1 is indeed involved in inhibition of cardiac hypertrophy and development of fibrosis in response to pressure overload- and isoproterenol-induced cardiac hypertrophy [24].

Apart from altered expression in skeletal muscle disorders, Ankrd2 was found upregulated in dilated cardiomyopathy patients [3]. Together with several titin ligands associated with sarcomeric mechanosensory complexes, the expression pattern of Ankrd2 was determined in endomyocardial biopsies of patients with advanced idiopathic dilated cardiomyopathy (IDCM) characterized by extensive remodeling of the left ventricle [25]. Expression of Ankrd2, as well as Ankrd1 and TRIM63, was induced and in correlation with the disease stage. Ankrd2 expression was significantly higher in patients with severe symptoms, compared to patients with moderate symptoms. Although this finding has no clinical significance, experimental evidence strongly supports the involvement of Ankrd2 in pathological cardiac remodeling [25].

2.3. Ankrd2 and Mechanotransduction in Skeletal Muscle. Mechanotransduction is the ability of cells to sense external mechanical forces, create biochemical intracellular signals, and trigger the expression of specific genes that drive the adaptation to mechanical changes. An incorrect mechanotransduction may affect muscle differentiation, myofiber turnover, and stem cell renewal [26].

Ankrd2 plays an important role in sensing mechanical changes in skeletal myofibers. It is found at the elastic I-band segment of the sarcomere, where a well-defined signalosome, composed by several structural and regulatory proteins, resides [10]. In vitro studies suggest that Ankrd2 might be assembled on the N2A spring element of the giant protein titin [7]. Titin is the largest of mammalian proteins, spanning over half of a sarcomere, with its N-terminus located in the Z-disc and its C-terminus located in the M-line. In striated muscle, one of titin's classical roles is to provide elasticity to sarcomeres [27]. Titin is characterized

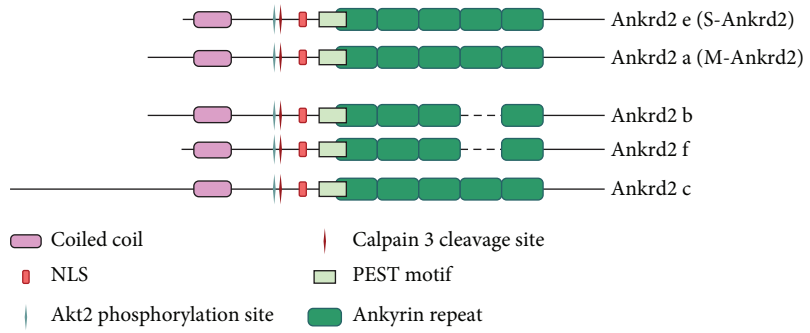

(a)

```
c  MQPAVPFCNSVALAKAQPVPSAQDRGWTGSFLHPCSWDTVPSGSNRPGVGGATGSAPWPWLPLLPGAARGEGDRWGRQVE
a  ------------------------------------------------------------------------------
e  ------------------------------------------------------------------------------
b  ------------------------------------------------------------------------------
f  ------------------------------------------------------------------------------

c  NWASELMAKAPSWAGVGALAYKAPEALWPAEAVMDGTMEDSEAVQRATALIEQRLAQEEENEKLRGDARQKLPMDLLVLE
a  ------MAKAPSWAGVGALAYKAPEALWPAEAVMDGTMEDSEAVQRATALIEQRLAQEEENEKLRGDARQKLPMDLLVLE
e  ---------------------------------MDGTMEDSEAVQRATALIEQRLAQEEENEKLRGDARQKLPMDLLVLE
b  ------MAKAPSWAGVGALAYKAPEALWPAEAVMDGTMEDSEAVQRATALIEQRLAQEEESEAVQRATALIEQRLAQEEE
f  ---------------------------------MDGTMEDSEAVQRATALIEQRLAQEEENEKLRGDARQKLPMDLLVLE
                                     *********************************************

c  DEKHHGAQSAALQKVKGQERVRKTSLDLRREIIDVGGIQNLIELRKKRKQKKRDALAASHEPPPEPEEITGPVDEETFLK
a  DEKHHGAQSAALQKVKGQERVRKTSLDLRREIIDVGGIQNLIELRKKRKQKKRDALAASHEPPPEPEEITGPVDEETFLK
e  DEKHHGAQSAALQKVKGQERVRKTSLDLRREIIDVGGIQNLIELRKKRKQKKRDALAASHEPPPEPEEITGPVDEETFLK
b  DEKHHGAQSAALQKVKGQERVRKTSLDLRREIIDVGGIQNLIELRKKRKQKKRDALAASHEPPPEPEEITGPVDEETFLK
f  DEKHHGAQSAALQKVKGQERVRKTSLDLRREIIDVGGIQNLIELRKKRKQKKRDALAASHEPPPEPEEITGPVDEETFLK
   ********************************************************************************

c  AAVEGKMKVIEKFLADGGSADTCDQFRRTALHRASLEGHMEILEKLLDNGATVDFQDRLDCTAMHWACRGGHLEVVKLLQ
a  AAVEGKMKVIEKFLADGGSADTCDQFRRTALHRASLEGHMEILEKLLDNGATVDFQDRLDCTAMHWACRGGHLEVVKLLQ
e  AAVEGKMKVIEKFLADGGSADTCDQFRRTALHRASLEGHMEILEKLLDNGATVDFQDRLDCTAMHWACRGGHLEVVKLLQ
b  AAVEGKMKVIEKFLADGGSADTCDQFRRTALHRASLEGHMEILEKLLDNGATVDFQDRLDCTAMHWACRGGHLEVVKLLQ
f  AAVEGKMKVIEKFLADGGSADTCDQFRRTALHRASLEGHMEILEKLLDNGATVDFQDRLDCTAMHWACRGGHLEVVKLLQ
   ********************************************************************************

c  SHGADTNVRDKLLSTPLHVAVRTGQVEIVEHFLSLGLEINARDREGDTALHDAVRLNRYKIIKLLLLHGADMMTKNLAGK
a  SHGADTNVRDKLLSTPLHVAVRTGQVEIVEHFLSLGLEINARDREGDTALHDAVRLNRYKIIKLLLLHGADMMTKNLAGK
e  SHGADTNVRDKLLSTPLHVAVRTGQVEIVEHFLSLGLEINARDREGDTALHDAVRLNRYKIIKLLLLHGADMMTKNLAGK
b  SHGADTNVR---------------------------------DREGDTALHDAVRLNRYKIIKLLLLHGADMMTKNLAGK
f  SHGADTNVR---------------------------------DREGDTALHDAVRLNRYKIIKLLLLHGADMMTKNLAGK
   *********                                  *:**********************************

c  TPTDLVQLWQADTRHALEHPEPGAEHNGLEGPNDSGRETPQPVPAQ 446
a  TPTDLVQLWQADTRHALEHPEPGAEHNGLEGPNDSGRETPQPVPAQ 360
e  TPTDLVQLWQADTRHALEHPEPGAEHNGLEGPNDSGRETPQPVPAQ 333
b  TPTDLVQLWQADTRHALEHPEPGAEHNGLEGPNDSGRETPQPVPAQ 327
f  TPTDLVQLWQADTRHALEHPEPGAEHNGLEGPNDSGRETPQPVPAQ 300
   *********************************************
```

(b)

NCBI isoform name	NCBI reference sequence*	Ensembl transcript	Protein length (aa)
Ankrd2 e (S-Ankrd2)	NP_001333722.1	ANKRD2-203	333
Ankrd2 a (M-Ankrd2)	NP_065082.2	ANKRD2-202	360
Ankrd2 b	NP_001123453.1	ANKRD2-201	327
Ankrd2 f	NP_001278148.2	ANKRD2-203	300
Ankrd2 c	NP_001278147.1	/	446

(c)

Figure 1: Overview of Ankrd2 isoforms. (a) Schematic presentation of the Ankrd2 domain structure. (b) Alignment of protein sequences of Ankrd2 isoforms. Numbers correspond to amino acids. (c) Entries for five Ankrd2 isoforms reported in NCBI and Ensembl databases. *NCBI entries were updated in 2018.

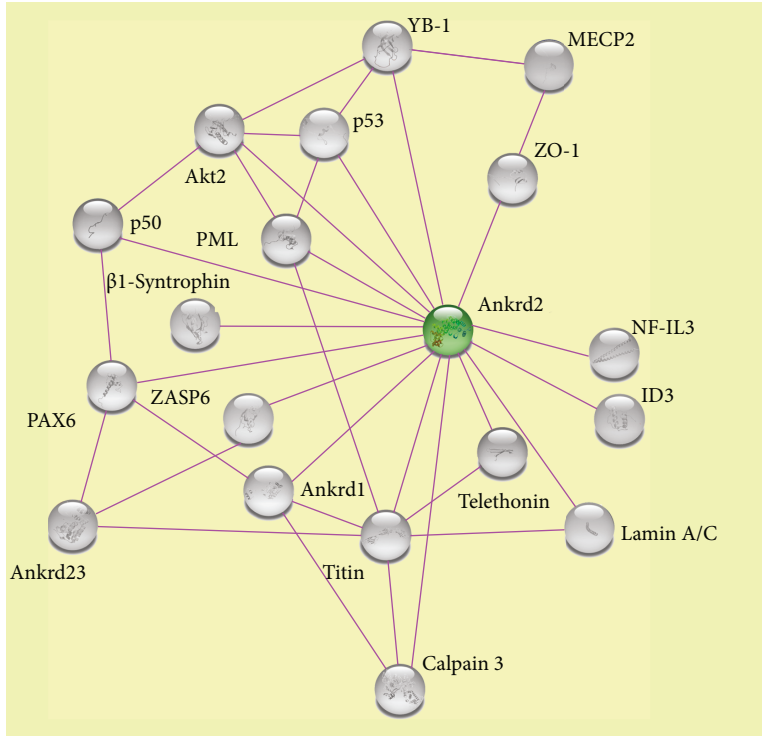

Figure 2: Interaction network for Ankrd2. Interactors listed in Table 1 were loaded into the STRING database: https://string-db.org/. The majority of Ankrd2 interactors, including titin, telethonin, Ankrd1, Ankrd23, ZASP6, and calpain 3, are involved in mechanosignaling. Other Ankrd2 interacting proteins are involved in DNA binding and regulation of transcription and include p53, MECP2, ID3, YB-1, PAX6, PML, and NF-IL3. A-type lamins, including lamin A, its precursor prelamin A, and lamin C, are Ankrd2 interactors and are involved in multiple cellular functions, including modulation of the nuclear stiffness in response to mechanical and oxidative stress and of epigenetic factor activity. Ankrd2 also interacts with protein kinases, as Akt2, and with proteins with PDZ or SH3 domains able to mediate protein-protein interactions (including ZO-1 and β1-syntrophin, respectively). Note that the majority of Ankrd2 interactors were identified from in vitro studies or in nonmuscular cellular systems (see text and Table 1 for references).

by multiple domains that interact with several sarcomeric proteins and also with enzymes regulating its own properties and resulting in the modulation of its stiffness. In humans, mutations or partial deletion of titin might cause muscular dystrophies, such as Tibial Muscular Dystrophy (TMD) [28] or limb-girdle muscular dystrophy 2J (LGMD-2J) [29]. In vitro evidence demonstrates that besides titin [7], Ankrd2 might also interact with calpain 3 [9] and Z-disc proteins telethonin/TCAP [1] and ZASP6 [30]. The interaction network of Ankrd2 is presented in Figure 2. In particular, calpain 3, a Ca^{2+}-dependent protease, coordinates signal transduction from other sarcomeric regions, including Z-disc and M-line where other signaling complexes are found. Interestingly, in the HEK293 cell line, calpain 3 binds and cuts murine Ankrd2 at the Arg104 of its PEST sequence [31] suggesting that calpain 3-mediated proteolysis of Ankrd2 might have a role in Ankrd2 sarcomeric sequestration. However, since these findings have been obtained on recombinant proteins or by using nonmuscular cellular models [9, 31] and since in skeletal muscle, the access of calpain 3 to substrates is restricted, being the majority of the enzyme sequestered by titin [32], results on Ankrd2 proteolysis by calpain 3 in muscular cells still need a proper validation.

Insufficient Ankrd2 recruitment at the I-band has been observed in exercised mice affected by a progressive muscular dystrophy due to an inactivation of calpain 3 (CAPN3-KI mice) [33]. Although this study does not provide sufficient proofs of Ankrd2 proteolysis by calpain 3, for example, loss of Ankrd2 or cleavage to a lower band, the altered Ankrd2 localization in CAPN3-KI muscle suggests that calpain 3 protease activity might be involved (directly or indirectly) in Ankrd2 recruitment at the sarcomere. The importance of a functional signalosome composed of Ankrd2 (as well as other MARPs), calpain 3, and the N2A region of titin is also observed in mdm (muscular dystrophy with myositis) mice, a model for human TMD, caused by the deletion of a large portion of the N2A region, bound by calpain 3. Homozygous mdm mice show a severe and progressive muscular degeneration. Interestingly, Ankrd2 and other MARPs are more abundantly expressed in the skeletal muscles of mdm when compared to wild-type mice [34]. In vitro, Ankrd2 also interacts with Z-disc proteins, including telethonin/TCAP [1] and ZASP6 [30]. Z-disc is involved in conveying mechanical signals and acts as a signaling hub for communication with the nucleus. On the other hand, telethonin links titin to the Z-disc [35]. Mutation of telethonin encoding gene (*TCAP*) may cause intense biomechanical

stress, maladaptation, apoptosis, and global heart failure, as well as LGMD-2G [36]. ZASP has several isoforms containing PDZ and LIM domains [30]. Interestingly, in vitro studies have demonstrated that point mutations in the *ZASP6* gene causative for a muscular disease called ZASPopathy prevented ZASP6 interaction with Ankrd2, opening the question of Ankrd2 involvement in the pathophysiology of this myofibrilar myopathy [30]. Myopalladin is a Z-disc protein involved in sarcomere assembly and regulation of gene expression and similarly to Ankrd2 is involved in bringing sarcomeric signals to the nucleus of muscle cells [37]. It is intriguing that, despite interacting with both Ankrd1 and Ankrd23 [7], myopalladin was not shown to bind Ankrd2, neither in vivo nor in vitro. Sarcomeric signalosomes have to be considered as highly dynamic complexes. Their protein components are subjected to a multitude of posttranslational modifications (PTMs) which might affect peculiar properties including their availability and stability, accessibility to interactors, turnover, and intracellular localization. This is the case, for example, of the binding between members of Z-disc FATZ (calsarcin/myozenin), myotilin, and Enigma families, which are modulated by phosphorylation [38]. As a matter of fact, in addition to structural proteins, sarcomeric signalosomes also contain protein-modifying enzymes, including protein kinases (PKC alpha, CaMKII δ, Erk1/2, and PKA [39]), E3 ubiquitin ligases (Mdm2 [40], TRIM63/MURF1 [41]), and autophagic protein carriers (p62/SQSTM1 [42]). Therefore, genetic mutations of both structural and enzymatic proteins of the sarcomere, causing a gain or a loss of function, may result in an impaired sensing of the mechanical stress and might be responsible for an inadequate transcriptional response, with harmful consequences for cell physiology.

Accordingly, also defects in Ankrd2 PTMs, including phosphorylation or proteolysis, by altering Ankrd2 binding to specific interactors or intracellular localization, might elicit pathogenetic effects.

Combining the aforementioned information together, we can hypothesize a scenario in which in muscle cells, Ankrd2 might cover multiple roles: a sensor one at the I-band of the sarcomere, where an Ankrd2 fraction might sense the stress, and a transducer one distributed between the cytoplasm, where the more abundant pool of Ankrd2 resides [7], and the nucleus of muscle cells [37] where a fraction of Ankrd2 is detected following stress condition. By mechanisms involving phosphorylation or other PTMs, Ankrd2 might dynamically translocate from the sarcomere, to the cytoplasm and to the nucleus and *vice versa*, participating in the integration of signals derived from mechanosensors or activated by oxidative stress, resulting in the modulation of transcriptional response to stress.

However, since the majority of the interactions between Ankrd2 and sarcomeric and nonsarcomeric proteins have been identified using recombinant proteins and in nonmuscular cellular systems, until their validation on skeletal muscle, the functional relevance of Ankrd2 association with these proteins remains to be demonstrated, and the role and the involvement of Ankrd2 in the physiology of muscle cells might at the moment be only speculated.

3. Ankrd2 in the Interplay between Oxidative and Mechanical Stresses

Physical exercise, including moderate and intense muscular activity, results in an increase of ROS. During or after aerobic exercise, as well as anaerobic exercise, the general increase of substrate utilization combined with the increase of oxygen uptake results in the activation of specific metabolic pathways, triggering the generation of ROS [43]. Although the exact redox mechanisms underlying the formation of exercise-induced ROS remain elusive to date, mitochondria, glutathione peroxidase, superoxide dismutase, catalase, NADPH oxidases, and xanthine oxidases have all been identified as potential contributors to ROS production. ROS themselves play a controversial role, since at high concentration they are detrimental for muscle biology [44]. However, low doses of ROS are fundamental to drive exercise adaptations, triggering molecular pathways that culminate with angiogenesis, mitochondria biogenesis, and muscle hypertrophy [43]. We hypothesize that upregulation of Ankrd2 in muscle exposed to mechanical stress is at least partly regulated by altered levels of ROS, as a consequence of increased muscle damage and regeneration [45].

3.1. Ankrd2 Upregulation in Response to Mechanical and Oxidative Stresses

3.1.1. Mechanical Stress. Although considered as a multitasking protein, the most striking signature of Ankrd2 is its stress-responsive function. Ankrd2 involvement in the physiology of stressed healthy and diseased muscles has been extensively studied. Ankrd2 expression increases in stress conditions caused by the application of mechanical forces. This was reported for the first time in murine *tibialis anterior* muscles exposed to passive stretch [16]. Subsequent studies further suggested that the increase of Ankrd2 upon passive stretch could be involved in the phenotypic adaptation of fast to slow fibers, which is generally related to long-endurance activities [46]. Increase of Ankrd2 expression in both murine and human muscles has also been reported following jumping exercise [47, 48] and eccentric contraction [49, 50] as well as denervation which reproduces muscle morphogenesis [8]. Of note, Ankrd2 expression in murine muscle is not stimulated by isometric contraction [50], while it is downregulated in inactive muscles [51, 52]. Increased expression of Ankrd2 in skeletal muscle in response to mechanical stress seems to be evolutionarily conserved. Recently, we have demonstrated mild upregulation of zebrafish Ankrd2 in skeletal muscle subjected to endurance exercise training by forced swimming [53].

Ankrd2 increase upon stress stimuli probably strengthens its structural and regulatory functions within the sarcomere. Accordingly, upregulation of Ankrd2 by ROS might contribute to initial events in the adaptative remodeling of exposed fibers, possibly by promoting sarcomerogenesis, the switch from fast to slow fibers [46], and the increase of the mechanotransducing activity.

3.1.2. Oxidative Stress. During oxidative stress caused by exposure of myoblasts to H_2O_2, Ankrd2 expression is slightly upregulated [15]. From a molecular point of view, Ankrd2 gene activation by ROS might be regulated by the well-known ROS-dependent activation of the transcription factor NF-κB [54]. As a matter of fact, although direct demonstration is missing, it is possible that upon oxidative stress, ROS-dependent increase of Ankrd2 expression occurs through two putative NF-κB-binding sites within the Ankrd2 gene promoter [12, 55]. However, the contribution of muscle-specific transcription factors and the possibility that ROS controls the Ankrd2 level by affecting its protein stability cannot be ruled out. Ankrd2 upregulation in some human dilated cardiomyopathies [3] and congenital myopathies [2] might be also related to an altered response to mechanical strain, as well as to altered levels of ROS reported in these disorders, as a consequence of increased muscle damage and regeneration [45].

3.2. Nuclear Translocation of Ankrd2 under Stress Conditions. Apart from increasing the Ankrd2 expression level, oxidative stress also induces Ankrd2 to partly relocate to the nucleus of muscle cells. For example, in differentiated C2C12 muscle cells, Ankrd2 is shuttled in the nucleus upon cellular exposure to ROS [15], following phosphorylation of Ankrd2 at Serine 99 [15].

In mature muscle injured by cardiotoxin injection, Ankrd2 translocates to the nuclei of myofibers located adjacent to severely damaged myofibers [10]. Similarly, Ankrd2 was shown to translocate to the nucleus also in healthy and CAPN3-KI muscles from mice subjected to exercise [33]. Opposite to findings reported for C2C12 muscle cells exposed to ROS, mechanisms ruling Ankrd2 nuclear localization in mature muscle cells remain hitherto to be determined. Further studies are needed to assess if Ankrd2 localization occurs in a fashion similar to that reported for ROS-treated C2C12 [15], involving Ankrd2 PTMs, or by the expression and/or activation of a specific nuclear Ankrd2 form, still to be determined.

Importantly, both nuclear translocation and increased expression of Ankrd2 induced by ROS or myogenic differentiation are related to retardation of myogenic differentiation, allowing cells to properly overcome stress before completing the differentiation program [11, 15]. In human myoblasts, this function is executed via its interaction with DNA-binding proteins, including transcription factors, such as the Y-box transcription factor 1 (YB1), the promyelocytic leukemia protein (PML), and p53 [1], whereas in primary myoblasts from mdm mice, Ankrd2 was shown to physically interact with the inhibitor of DNA-binding protein 3, ID3 [13]. Moreover, upon muscle stress stimulation, Ankrd2 was also shown to colocalize with acetylated histones, which generally mark active chromatin, in the nucleus of myocytes [10].

Nuclear Ankrd2 overexpression induced by ROS has a different outcome in regard to the phase of the cell cycle [11]. In cycling myoblasts, Ankrd2 overexpression induces apoptosis, and this effect is probably mediated by Ankrd2 and p53-dependent upregulation of p21 [1, 11]. On the other hand, Ankrd2 overexpression impairs myogenic differentiation through downregulation of MyoD and myogenin as well as their target Myh1, a terminal differentiation marker [11]. Supporting the altered myogenic program, Ankrd2 overexpressing myotubes also express Myf-5, which is normally expressed in cycling myoblasts [11]. An intriguing, albeit unexplored evidence of the transcriptional role of Ankrd2 came from the studies of triple knockout mice lacking all three MARPs [56]. They expressed a longer titin isoform, hinting at an unexpected link between titin gene expression and MARPs [56].

Studies from our laboratories have demonstrated that Ankrd2 also modulates the activity of NF-κB, through direct interaction with the NF-κB repressor p50 [12]. NF-κB is a transcription factor composed of homo- and heterodimers, affecting the expression of genes related to inflammatory and cell survival responses [57]. The interaction between Ankrd2 and p50 abrogates NF-κB activation, resulting in a negative regulation of its downstream genes. Moreover, p50/p50 homodimer negatively regulates the expression of Ankrd2 by binding its promoter, in a classic feedback inhibition manner [12]. In this condition, we have shown a significant reduction of proinflammatory cytokines, including IL-1β and IL-6 [12] that, at high concentrations, may cause proteolysis in muscle and participate in muscle wasting [45, 58].

4. Lamin A/C and Muscular Laminopathies

4.1. Role of Lamin A/C in Muscular Cellular Physiology. A-type lamins, including lamin A and lamin C, are the main products of the *LMNA* gene and are the major constituents of the nuclear lamina, a filamentous meshwork underneath the nuclear envelope that can be found in all vertebrate cells [59]. Lamin A is transcribed and translated as a precursor protein, prelamin A, which undergoes complex posttranslational processing [59]. Final cleavage by the protease ZMPSTE24 (zinc metallopeptidase STE24) eliminates the last 15 amino acids of prelamin A, releasing a short peptide and mature lamin A [60]. Notably, prelamin A and its processing pathway have been implicated in both physiological and pathogenic mechanisms [59].

Prelamin A increase occurs during the first steps of myoblast differentiation [61], and prelamin A-mediated recruitment of the nuclear envelope proteins SUN1, SUN2 [62], and Samp1 [63] is required for proper myonuclear positioning during myogenic differentiation. In cultured fibroblasts, prelamin A modulation during stress response is a physiological mechanism related to import of DNA repair factors [64] or activation of chromatin remodeling enzymes [65]. However, anomalous prelamin A accumulation, due to specific mutations in the *LMNA* or *ZMPSTE24* genes [59], causes toxicity leading to cellular senescence [66] and represents the molecular basis of progeroid laminopathies [59].

Via interaction with structural and enzymatic molecules, A-type lamins enable several cellular functions, including mechanotransduction [67], shuttling of proteins from the cytoplasm to the nucleus [68], and epigenetic modification

of chromatin, affecting the expression of proteins involved in the cell cycle and/or differentiation [69]. The pleiotropic involvement of A-type lamins in all these cellular events explains why mutations in the *LMNA* gene are the cause of a wide number of disorders, collectively known as "laminopathies," which may affect one or more specific tissues, including skeletal and cardiac muscles, tendons, adipose tissue, and peripheral neurons, or be systemic causing accelerated ageing [70].

One of the most important cellular activities affected by *LMNA* mutations is mechanotransduction [71], a function particularly relevant in striated muscle [26]. From a molecular point of view, mechanical changes propagate from the cytoskeleton to the nuclear membrane and chromatin through direct interaction between A-type lamins and the LINC (linker of nucleoskeleton and cytoskeleton) complex [72], which is formed by SUN1 and SUN2 at the inner nuclear membrane and nesprins, which also span the outer nuclear membrane. Nesprins interact with cytoskeletal actin and, by binding to plectin, with microtubules and intermediate filaments [73]. However, nesprins also interact with lamin A/C [74]. Mutation of each of the components of the LINC complex negatively affects the functions of this intricate mechanism, resulting in an interruption or an alteration of the modulation of mechanoresponse and mechanotransduction of muscle cells [75, 76]. Not surprisingly, LINC protein mutations cause muscular dystrophies including Emery-Dreifuss muscular dystrophy (EDMD) [77–80].

4.2. Muscular Laminopathies. Mutations in *LMNA* gene cause a variety of muscular diseases including EDMD, limb-girdle muscular dystrophy 1B (LGMD1B), dilated cardiomyopathy with conduction defects (DCM1A), and *LMNA*-related congenital muscular dystrophy (L-CMD) [60, 81, 82]. Moreover, muscle functionality may be impaired in cases of progeroid laminopathies or lipodystrophies [59, 83]. The inheritance pattern of *LMNA*-related muscle diseases is autosomal dominant and very rarely autosomal recessive. All these disorders are characterized by joint contractures, muscle weakness and wasting, and dilated cardiomyopathy. The L-CMD onset is at birth, whereas EDMD2 and EDMD3 (respectively, with dominant and recessive inheritance) have an onset in childhood or young adulthood, as most cases of LGMD1B. DCM1A, which is usually diagnosed in the second decade, is often associated with conduction disorders and cardiac arrhythmias with life-threatening outcome requiring defibrillator implantation and, in severe cases, heart transplantation [81]. Extracardiac features including skeletal muscle weakness and contractures may occur later in DCM1A, causing a phenotype overlapping with EDMD2 [84].

4.3. Pathogenetic Mechanisms in Muscular Laminopathies. *LMNA* gene mutations negatively modulate mechanoresponse and mechanotransduction in muscle cells essentially by two different ways. The first mechanism is related to the structural role played by A-type lamins in the assembly of a molecular platform able to connect and coordinate multiple mechanical and chemical stimuli. The second modality implies alteration of lamin A/C epigenetic activity that results in an abnormal regulation of responsive genes [65]. Cells lacking A-type lamins or expressing myopathic lamin A mutants show reduced nuclear stiffness and altered nuclear morphology and are unable to transmit forces to the nucleus [67]. In addition, the localization of various components of the LINC complex is severely disturbed in those cells [67]. For instance, in EDMD2 myotubes, the mislocalization of SUN1 and SUN2 due to reduced prelamin A interaction was responsible for an altered positioning of myonuclei [62]. The pathogenetic mechanism also involved mislocalization of the nuclear envelope protein Samp1 and defective interplay with the centrosomal protein pericentrin [63]. All these findings highlight the prominent role of A-type lamins in nucleocytoskeleton crosstalk. Importantly, it has been demonstrated that upon mechanical stress, the Ig fold domain of lamin A is able to partially unfold, leading to stretching of the entire molecule [85]. Interestingly, when the extracellular matrix (ECM) increases its stiffness, lamin A undergoes dephosphorylation at Serine 22, a condition enabling increased nuclear stiffness [86]. It is likely that phosphorylation of other residues of lamin A/C contributes to modulation of nuclear stiffness in response to ECM stimuli [87–89]. We found that the pathogenicity of an EDMD2-causative lamin A/C mutation, Arg401Cys, is related to impaired phosphorylation of Serine 404 by Akt1 [90]. It is conceivable that, since phosphorylation of Serine 404 is required for prelamin A and lamin A turnover, impaired phosphorylation might alter nuclear lamina composition and stiffness in response to mechanical stimuli [90, 91].

Altered chromatin organization is considered as a main pathogenic condition in muscular laminopathies [60]. Both high-order chromatin structure [92] and promoter-specific epigenetic defects lead to altered gene expression, consequently affecting muscle-specific gene expression [93, 94].

Another well-documented effect of *LMNA* mutations causing EDMD is altered PI3-kinase-Akt-Erk2 signaling, which has been demonstrated both in patient cells and in mouse models of the disease (reviewed by Brull et al. [95]). A dramatic effect of this altered signaling has been reported on the cardiac function, and the efficacy of therapies based on inhibition of hyperactivated MAP kinase-Erk1/2 signaling has been experimentally proven [96]. Of note, TGF-β 2 and its downstream effectors are increased in EDMD2 mouse models [97] as well as in serum and cells from laminopathic patients eliciting upregulation of fibrogenic molecules [82], a pathogenetic effect relevant to muscle and tendon fibrosis [82].

5. Ankrd2 and Lamin in Normal and Laminopathic Muscles

In C2C12 differentiated muscle cells, oxidative stress generated by exposure to H_2O_2 induces Akt2 kinase to phosphorylate Ankrd2 at Serine 99 [15]. By using a phosphorylation-defective mutant form of Ankrd2 (Ankrd2 Ser99Ala), we demonstrated that opposite to its wild-type counterpart, phosphorylation-defective Ankrd2 is unable to translocate into the nucleus upon cellular exposure to

oxidative stress [98]. Importantly, C2C12 myoblasts expressing Ankrd2 Ser99Ala mutant presented a faster differentiation kinetics [15]. We therefore reasoned that after sensing oxidative stress, Ankrd2 phosphorylation could be required to allow Ankrd2 translocation to the nucleus, where it could participate in the transcriptional modulation of the terminal steps of muscle differentiation. Supporting this hypothesis, we found that Serine 99 is proximal to Ankrd2 NLS (from Lysine 120 to Lysine 123 in the human protein) [15]. Therefore, although the molecular mechanism underlying Ankrd2 nuclear transport is still unclear, upon ROS stimulation, phosphorylation of Serine 99 might unmask the NLS, allowing Ankrd2 to translocate in the nucleus.

We have demonstrated that during ROS-induced nuclear relocation, Ankrd2 was complexed to A-type lamins, albeit with different affinities for diverse lamin A isoforms [98]. During muscle differentiation, prelamin A levels are increased [61–63], and Ankrd2 interacts with prelamin A with a higher affinity than that established with mature lamin A [98]. Upon the exposure to ROS, Ankrd2 transiently interacted with lamin A and prelamin A, entered the nucleus, and soon after went back to the cytosol. However, EDMD2-linked lamin A mutants constitutively bound Ankrd2, even in the absence of any stimulus, causing Ankrd2 to be retained in the nucleus [98]. We therefore suggest that while under physiological conditions, including muscle differentiation or oxidative stress response, Ankrd2 is transiently retained in the nucleus also due to a reversible increase of prelamin A levels [61, 62, 64, 99], EDMD2-linked lamin A mutants entrap Ankrd2 into the nucleus, affecting its dynamics [98]. Further experiments performed using cells overexpressing Ankrd2 and EDMD2-lamin A mutants revealed that permanent location of Ankrd2 in the nucleus increased release of cellular ROS, as well as apoptotic cell death [98]. Similarly, in laminopathic muscle, the effects of permanent Ankrd2 recruitment in the nucleus might be involved in the reduction of the vitality of myofibers, as well as satellite cells, affecting stem cell renewal and muscle regeneration and resulting in poor adaptation to stress stimuli. A model for a proposed Ankrd2 involvement in the pathogenesis of laminopathies is depicted in Figure 3.

Although direct observations of Ankrd2 localization and functions in EDMD2 muscle (including nascent, mature, or regenerating fibers) are still missing, we can suppose that the catastrophic effects of mutated A-type lamins in muscular laminopathies might be also due to the altered Ankrd2-lamin A interaction affecting both mechanosensing and transcriptional activity of Ankrd2.

6. Perspectives for the Study of Lamin A-Ankrd2 Interplay

6.1. Mechanosignaling Regulation through Ankrd2. Albeit still unexplored, a consequence of an altered nuclear recruitment of Ankrd2 observed in laminopathies might also be related to a reduced availability of cytoplasmic Ankrd2 at the I-bands of the sarcomere and thus to a decreased mechanosensing activity. Therefore, it would be worth evaluating the change in the Ankrd2 amount at the sarcomere in laminopathic conditions. Moreover, given the involvement of lamin A in mechanosignaling through the LINC complex, it would be worth deepening the potential involvement of Ankrd2 in lamin A/LINC complex-dependent mechanisms of response to mechanical strain.

6.2. Muscle Fiber Type Disproportion (FTD). Muscle fiber type disproportion (FTD) is a pathological condition in which there is the selective reduction of the size of slow and not fast myofibers. FTD is observed in many cardiac and skeletal muscle disorders, with severe effects on the functionality of all the striated muscle. Interestingly, since Ankrd2 is principally expressed in slow fibers, pathological nuclear recruitment of Ankrd2 might also be involved in the damage and atrophy of slow fibers reported in muscular laminopathies [100, 101].

In fact, FTD has been observed in some cases of LGMD1B [100, 102] as well as EDMD2 [100]. Furthermore, in skeletal muscle from $Lmna^{H222P/H222P}$ mice, in addition to FTD, atrophy of fast fibers was detected [101].

6.3. PML-NB. Promyelocytic leukemia protein-nuclear bodies (PML-NBs) are nuclear matrix-associated domains recruiting a variety of seemingly unrelated proteins with the aim of regulating many cellular functions from transcriptional regulation to growth regulation, tumor suppression, apoptosis, and storage of nuclear proteins under stress conditions [103]. PML-NBs are presumed to mediate protein-protein interactions and function as a platform that promotes protein posttranslational modification, for example, SUMOylation, acetylation, ubiquitination, and phosphorylation [104]. This has been demonstrated for p53, which is activated in PML-NBs of C2C12 myoblasts, upon exposure to ROS [105]. Interestingly, both Ankrd2 and lamin A/C bind to PML, a core constituent of PML-NBs, and albeit not essential for PML-NB function, it regulates their development under stress condition [106]. Since it has been reported that progerin, the truncated and toxic prelamin A responsible for the progeroid disease HGPS, progressively accumulated in PML bodies, altering their shape and number [107], it is therefore possible that other lamin A/C mutants might participate in the formation of PML-NBs under stress conditions, perturbing their downstream pathways involved in transcription, apoptosis, senescence, response to DNA damage, etc. As already reported, Ankrd2 localizes at PML-NBs under stress conditions [1]. The possibility that mutant A-type lamins and Ankrd2 localization at the PML-NBs concur to aberrantly regulate PML-NB activity under stress conditions warrants further investigation.

6.4. Therapeutic Perspectives. Sequestration of proteins at the nuclear envelope or inside the nucleus by lamin mutants as well as by excess levels of wild-type lamins has been widely reported and involves DNA-binding proteins such as BAF and transcription factors such as Oct-1, c-FOS, and AP-1 [108–118]. An interesting condition has been described in a *Drosophila* model of EDMD2 as well as in patient muscle fibers, where nuclear accumulation of the stress-responsive protein Nrf2 (Nuclear factor erythroid 2-related factor 2)

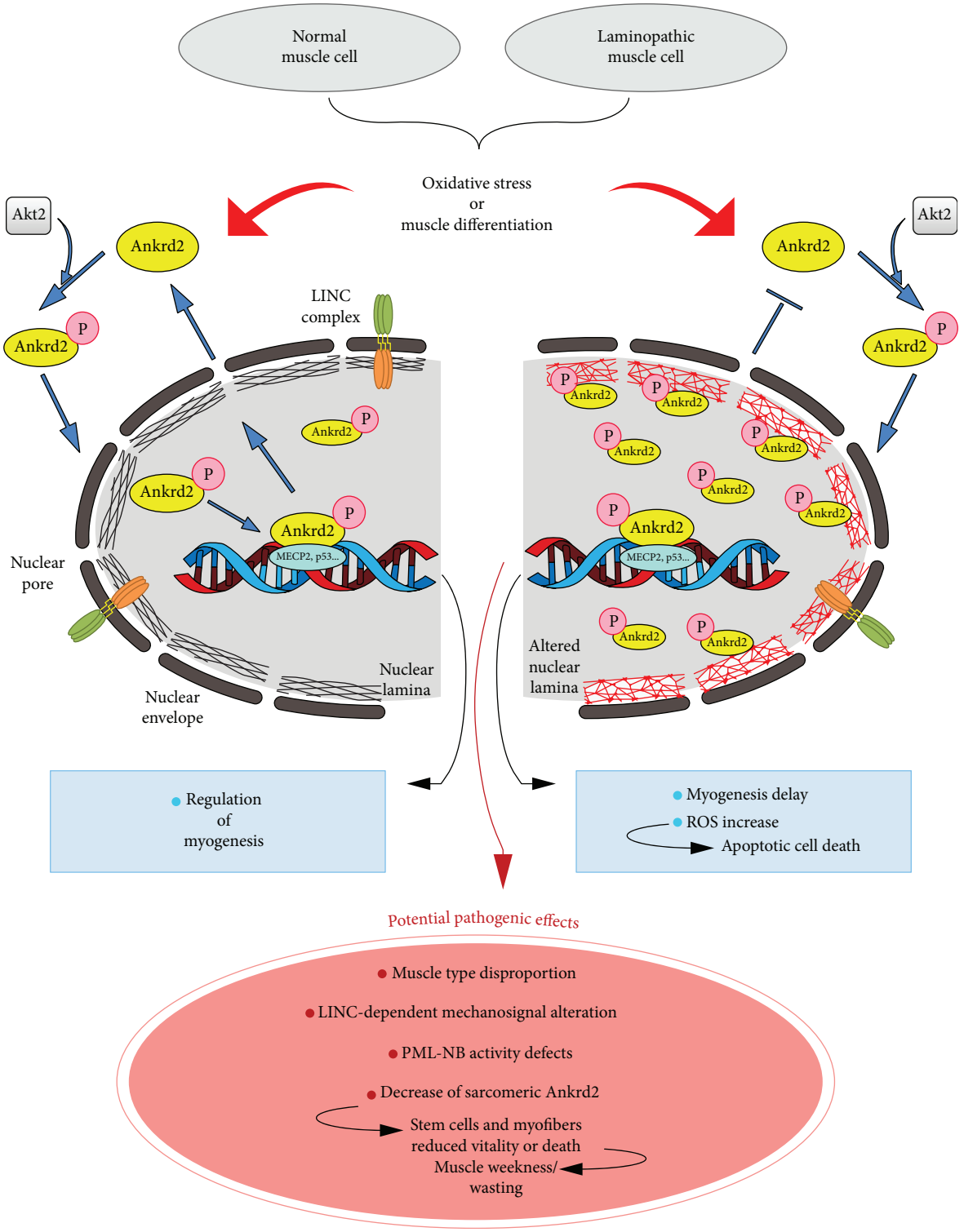

Figure 3: Proposed pathogenic mechanisms in which Ankrd2 might be involved. In healthy muscle cells, physiological amounts of ROS or muscle differentiation induce Ankrd2 phosphorylation by Akt2 [15] and translocation into the nucleus, by binding to A-type lamins (black mesh) [98]. In the nucleus, Ankrd2 modulates the activation of muscle-specific and stress-responsive genes, by interacting with transcription factors (see text and Table 1 for references). In laminopathic muscle cells, mutated A-type lamins (red mesh) even in the absence of external stimuli recruit Ankrd2 into the nucleus. In addition to the already reported consequences, including an anomalous increase of ROS release, myogenic delay, and apoptotic cell death [98], potential pathogenic mechanisms, through which the altered nuclear localization of Ankrd2 might contribute to the pathogenesis of *LMNA*-related muscular disorders, are proposed.

was observed [119]. It is conceivable that Nrf2 and Ankrd2 aberrant dynamics both contribute to altered stress response in EDMD2. The identification of molecules able to release aberrant interactions between mutated lamins and their binding partners, including Ankrd2, may provide innovative therapeutic tools for laminopathies.

7. Concluding Remarks

In conclusion, although direct evidence on Ankrd2 localization in forming, mature, and regenerating EDMD2 muscle fibers is still missing, we hypothesize that alterations in expression, PTMs, interactors, or nuclear localization of Ankrd2 might contribute to impair the response to mechanical and/or oxidative stress. Future studies exploiting different laminopathic animal models, including murine $Lmna^{H222P/H222P}$ KI, $Lmna^{\Delta K32}$ KI, or Lmna KO (respectively, reproducing conditions very close to human cardiomyopathy, L-CMD and EDMD [101, 120, 121]), would enable further novel insights into the role of Ankrd2 in the pathophysiology of muscular laminopathies.

Finally, a proteomic analysis of Ankrd2 interactome in mature muscle (healthy and EDMD2-affected), as well as the creation of animal models expressing unphosphorylatable Ankrd2 forms, will help to better define the role of Ankrd2 in muscular tissue, allowing the assignment of a specific role of oxidative stress-dependent phosphorylation to the pathology of other cardiac and skeletal muscle disorders.

Conflicts of Interest

The authors declare no conflict of interest.

Authors' Contributions

All of the authors contributed to the writing and editing of the article.

Acknowledgments

The authors thank the Italian Network for Laminopathies for discussion and support. The skilled technical assistance of Aurelio Valmori is gratefully acknowledged. V.C. and C.C. are funded by "Associazione Italiana Distrofia Muscolare di Emery-Dreifuss" (AIDMED) onlus and "Associazione Alessandra Proietti Onlus". G.L. is funded by MIUR PRIN 2015FBNB5Y. SK is supported by the Ministry of Education, Science and Technological Development of the Republic of Serbia, Project No. 173008.

References

[1] S. Kojic, E. Medeot, E. Guccione et al., "The Ankrd2 protein, a link between the sarcomere and the nucleus in skeletal muscle," *Journal of Molecular Biology*, vol. 339, no. 2, pp. 313–325, 2004.

[2] C. Nakada, Y. Tsukamoto, A. Oka et al., "Altered expression of ARPP protein in skeletal muscles of patients with muscular dystrophy, congenital myopathy and spinal muscular atrophy," *Pathobiology*, vol. 71, no. 1, pp. 43–51, 2004.

[3] S. F. Nagueh, G. Shah, Y. Wu et al., "Altered titin expression, myocardial stiffness, and left ventricular function in patients with dilated cardiomyopathy," *Circulation*, vol. 110, no. 2, pp. 155–162, 2004.

[4] N. Ishiguro, T. Baba, T. Ishida et al., "Carp, a cardiac ankyrin-repeated protein, and its new homologue, Arpp, are differentially expressed in heart, skeletal muscle, and rhabdomyosarcomas," *The American Journal of Pathology*, vol. 160, no. 5, pp. 1767–1778, 2002.

[5] M. Lu, M. R. Muers, and X. Lu, "Introducing STRaNDs: shuttling transcriptional regulators that are non-DNA binding," *Nature Reviews Molecular Cell Biology*, vol. 17, no. 8, pp. 523–532, 2016.

[6] S. G. Wette, H. K. Smith, G. D. Lamb, and R. M. Murphy, "Characterization of muscle ankyrin repeat proteins in human skeletal muscle," *American Journal of Physiology-Cell Physiology*, vol. 313, no. 3, pp. C327–C339, 2017.

[7] M. K. Miller, M.-L. Bang, C. C. Witt et al., "The muscle ankyrin repeat proteins: CARP, ankrd2/Arpp and DARP as a family of titin filament-based stress response molecules," *Journal of Molecular Biology*, vol. 333, no. 5, pp. 951–964, 2003.

[8] Y. Tsukamoto, T. Senda, T. Nakano et al., "Arpp, a new homolog of carp, is preferentially expressed in type 1 skeletal muscle fibers and is markedly induced by denervation," *Laboratory Investigation*, vol. 82, no. 5, pp. 645–655, 2002.

[9] C. Hayashi, Y. Ono, N. Doi et al., "Multiple molecular interactions implicate the connectin/titin N2A region as a modulating scaffold for p94/calpain 3 activity in skeletal muscle," *Journal of Biological Chemistry*, vol. 283, no. 21, pp. 14801–14814, 2008.

[10] Y. Tsukamoto, N. Hijiya, S. Yano et al., "Arpp/Ankrd2, a member of the muscle ankyrin repeat proteins (MARPs), translocates from the I-band to the nucleus after muscle injury," *Histochemistry and Cell Biology*, vol. 129, no. 1, pp. 55–64, 2008.

[11] C. Bean, N. Facchinello, G. Faulkner, and G. Lanfranchi, "The effects of Ankrd2 alteration indicate its involvement in cell cycle regulation during muscle differentiation," *Biochimica et Biophysica Acta*, vol. 1783, no. 6, pp. 1023–1035, 2008.

[12] C. Bean, N. K. Verma, D. L. Yamamoto et al., "Ankrd2 is a modulator of NF-κB-mediated inflammatory responses during muscle differentiation," *Cell Death & Disease*, vol. 5, no. 1, article e1002, 2014.

[13] J. S. Mohamed, M. A. Lopez, G. A. Cox, and A. M. Boriek, "Ankyrin repeat domain protein 2 and inhibitor of DNA binding 3 cooperatively inhibit myoblast differentiation by physical interaction," *Journal of Biological Chemistry*, vol. 288, no. 34, pp. 24560–24568, 2013.

[14] A. Blais, M. Tsikitis, D. Acosta-Alvear, R. Sharan, Y. Kluger, and B. D. Dynlacht, "An initial blueprint for myogenic differentiation," *Genes & Development*, vol. 19, no. 5, pp. 553–569, 2005.

[15] V. Cenni, A. Bavelloni, F. Beretti et al., "Ankrd2/ARPP is a novel Akt2 specific substrate and regulates myogenic differentiation upon cellular exposure to H(2)O(2)," *Molecular Biology of the Cell*, vol. 22, no. 16, pp. 2946–2956, 2011.

[16] T. J. Kemp, T. J. Sadusky, F. Saltisi et al., "Identification of Ankrd2, a novel skeletal muscle gene coding for a stretch-responsive ankyrin-repeat protein," *Genomics*, vol. 66, no. 3, pp. 229–241, 2000.

[17] V. R. Edgerton, J. L. Smith, and D. R. Simpson, "Muscle fibre type populations of human leg muscles," *The Histochemical Journal*, vol. 7, no. 3, pp. 259–266, 1975.

[18] J. Jasnic-Savovic, S. Krause, S. Savic et al., "Differential expression and localization of Ankrd2 isoforms in human skeletal and cardiac muscles," *Histochemistry and Cell Biology*, vol. 146, no. 5, pp. 569–584, 2016.

[19] M. Moriyama, Y. Tsukamoto, M. Fujiwara et al., "Identification of a novel human ankyrin-repeated protein homologous to CARP," *Biochemical and Biophysical Research Communications*, vol. 285, no. 3, pp. 715–723, 2001.

[20] A. Belgrano, L. Rakicevic, L. Mittempergher et al., "Multitasking role of the mechanosensing protein Ankrd2 in the signaling network of striated muscle," *PLoS One*, vol. 6, no. 10, article e25519, 2011.

[21] S. Kojic, A. Nestorovic, L. Rakicevic et al., "A novel role for cardiac ankyrin repeat protein Ankrd1/CARP as a co-activator of the p53 tumor suppressor protein," *Archives of Biochemistry and Biophysics*, vol. 502, no. 1, pp. 60–67, 2010.

[22] J. Jasnic-Savovic, A. Nestorovic, S. Savic et al., "Profiling of skeletal muscle Ankrd2 protein in human cardiac tissue and neonatal rat cardiomyocytes," *Histochemistry and Cell Biology*, vol. 143, no. 6, pp. 583–597, 2015.

[23] M. L. Bang, Y. Gu, N. D. Dalton, K. L. Peterson, K. R. Chien, and J. Chen, "The muscle ankyrin repeat proteins CARP, Ankrd2, and DARP are not essential for normal cardiac development and function at basal conditions and in response to pressure overload," *PLoS One*, vol. 9, no. 4, article e93638, 2014.

[24] Y. Song, J. Xu, Y. Li et al., "Cardiac Ankyrin Repeat Protein Attenuates Cardiac Hypertrophy by Inhibition of ERK1/2 and TGF-β Signaling Pathways," *PLoS One*, vol. 7, no. 12, article e50436, 2012.

[25] J. Bogomolovas, K. Brohm, J. Celutkiene et al., "Induction of Ankrd1 in dilated cardiomyopathy correlates with the heart failure progression," *BioMed Research International*, vol. 2015, Article ID 273936, 9 pages, 2015.

[26] K. N. Dahl, A. J. S. Ribeiro, and J. Lammerding, "Nuclear shape, mechanics, and mechanotransduction," *Circulation Research*, vol. 102, no. 11, pp. 1307–1318, 2008.

[27] L. Tskhovrebova and J. Trinick, "Titin: properties and family relationships," *Nature Reviews Molecular Cell Biology*, vol. 4, no. 9, pp. 679–689, 2003.

[28] P. Hackman, S. Marchand, J. Sarparanta et al., "Truncating mutations in C-terminal titin may cause more severe tibial muscular dystrophy (TMD)," *Neuromuscular Disorders*, vol. 18, no. 12, pp. 922–928, 2008.

[29] B. Udd, A. Vihola, J. Sarparanta, I. Richard, and P. Hackman, "Titinopathies and extension of the M-line mutation phenotype beyond distal myopathy and LGMD2J," *Neurology*, vol. 64, no. 4, pp. 636–642, 2005.

[30] V. C. Martinelli, W. B. Kyle, S. Kojic et al., "ZASP interacts with the mechanosensing protein Ankrd2 and p53 in the signalling network of striated muscle," *PLoS One*, vol. 9, no. 3, article e92259, 2014.

[31] K. I. Piatkov, J.-H. Oh, Y. Liu, and A. Varshavsky, "Calpain-generated natural protein fragments as short-lived substrates of the N-end rule pathway," *Proceedings of the National Academy of Sciences*, vol. 111, no. 9, pp. E817–E826, 2014.

[32] R. M. Murphy and G. D. Lamb, "Endogenous calpain-3 activation is primarily governed by small increases in resting cytoplasmic [Ca2+] and is not dependent on stretch," *Journal of Biological Chemistry*, vol. 284, no. 12, pp. 7811–7819, 2009.

[33] K. Ojima, Y. Kawabata, H. Nakao et al., "Dynamic distribution of muscle-specific calpain in mice has a key role in physical-stress adaptation and is impaired in muscular dystrophy," *Journal of Clinical Investigation*, vol. 120, no. 8, pp. 2672–2683, 2010.

[34] S. M. Garvey, C. Rajan, A. P. Lerner, W. N. Frankel, and G. A. Cox, "The muscular dystrophy with myositis (mdm) mouse mutation disrupts a skeletal muscle-specific domain of titin," *Genomics*, vol. 79, no. 2, pp. 146–149, 2002.

[35] A. Mues, P. F. M. van der Ven, P. Young, D. O. Fürst, and M. Gautel, "Two immunoglobulin-like domains of the Z-disc portion of titin interact in a conformation-dependent way with telethonin," *FEBS Letters*, vol. 428, no. 1-2, pp. 111–114, 1998.

[36] E. S. Moreira, T. J. Wiltshire, G. Faulkner et al., "Limb-girdle muscular dystrophy type 2G is caused by mutations in the gene encoding the sarcomeric protein telethonin," *Nature Genetics*, vol. 24, no. 2, pp. 163–166, 2000.

[37] M.-L. Bang, R. E. Mudry, A. S. McElhinny et al., "Myopalladin, a novel 145-kilodalton sarcomeric protein with multiple roles in Z-disc and I-band protein assemblies," *The Journal of Cell Biology*, vol. 153, no. 2, pp. 413–428, 2001.

[38] Y. Gontier, "The Z-disc proteins myotilin and FATZ-1 interact with each other and are connected to the sarcolemma via muscle-specific filamins," *Journal of Cell Science*, vol. 118, no. 16, pp. 3739–3749, 2005.

[39] M. Krüger and S. Kötter, "Titin, a central mediator for hypertrophic signaling, exercise-induced mechanosignaling and skeletal muscle remodeling," *Frontiers in Physiology*, vol. 7, p. 76, 2016.

[40] L.-F. Tian, H.-Y. Li, B.-F. Jin et al., "MDM2 interacts with and downregulates a sarcomeric protein, TCAP," *Biochemical and Biophysical Research Communications*, vol. 345, no. 1, pp. 355–361, 2006.

[41] A. S. McElhinny, K. Kakinuma, H. Sorimachi, S. Labeit, and C. C. Gregorio, "Muscle-specific RING finger-1 interacts with titin to regulate sarcomeric M-line and thick filament structure and may have nuclear functions via its interaction with glucocorticoid modulatory element binding protein-1," *The Journal of Cell Biology*, vol. 157, no. 1, pp. 125–136, 2002.

[42] S. Lange, "The kinase domain of titin controls muscle gene expression and protein turnover," *Science*, vol. 308, no. 5728, pp. 1599–1603, 2005.

[43] E. C. Gomes, A. N. Silva, and M. R. de Oliveira, "Oxidants, antioxidants, and the beneficial roles of exercise-induced production of reactive species," *Oxidative Medicine and Cellular Longevity*, vol. 2012, Article ID 756132, 12 pages, 2012.

[44] L. Zuo, T. Zhou, B. K. Pannell, A. C. Ziegler, and T. M. Best, "Biological and physiological role of reactive oxygen species – the good, the bad and the ugly," *Acta Physiologica*, vol. 214, no. 3, pp. 329–348, 2015.

[45] O. Zamir, P. O. Hasselgren, D. von Allmen, and J. E. Fischer, "In vivo administration of interleukin-1 alpha induces muscle proteolysis in normal and adrenalectomized rats," *Metabolism*, vol. 42, no. 2, pp. 204–208, 1993.

[46] G. Mckoy, Y. Hou, S. Y. Yang et al., "Expression of Ankrd2 in fast and slow muscles and its response to stretch are consistent with a role in slow muscle function," *Journal of Applied Physiology*, vol. 98, no. 6, pp. 2337–2343, 2005.

[47] M. Lehti, R. Kivelä, P. Komi, J. Komulainen, H. Kainulainen, and H. Kyröläinen, "Effects of fatiguing jumping exercise on mRNA expression of titin-complex proteins and calpains," *Journal of Applied Physiology*, vol. 106, no. 4, pp. 1419–1424, 2009.

[48] S. O. A. Koskinen, H. Kyrolainen, R. Flink et al., "Human skeletal muscle type 1 fibre distribution and response of stress-sensing proteins along the titin molecule after submaximal exhaustive exercise," *Histochemistry and Cell Biology*, vol. 148, no. 5, pp. 545–555, 2017.

[49] I. A. Barash, L. Mathew, A. F. Ryan, J. Chen, and R. L. Lieber, "Rapid muscle-specific gene expression changes after a single bout of eccentric contractions in the mouse," *American Journal of Physiology-Cell Physiology*, vol. 286, no. 2, pp. C355–C364, 2004.

[50] E. R. Hentzen, M. Lahey, D. Peters et al., "Stress-dependent and -independent expression of the myogenic regulatory factors and the MARP genes after eccentric contractions in rats," *The Journal of Physiology*, vol. 570, no. 1, pp. 157–167, 2006.

[51] M. D. Roberts, T. E. Childs, J. D. Brown, J. W. Davis, and F. W. Booth, "Early depression of Ankrd2 and Csrp3 mRNAs in the polyribosomal and whole tissue fractions in skeletal muscle with decreased voluntary running," *Journal of Applied Physiology*, vol. 112, no. 8, pp. 1291–1299, 2012.

[52] J. S. Pattison, L. C. Folk, R. W. Madsen, T. E. Childs, E. E. Spangenburg, and F. W. Booth, "Expression profiling identifies dysregulation of myosin heavy chains IIb and IIx during limb immobilization in the soleus muscles of old rats," *The Journal of Physiology*, vol. 553, no. 2, pp. 357–368, 2003.

[53] S. Boskovic, R. Marin-Juez, J. Jasnic et al., "Characterization of zebrafish (Danio rerio) muscle ankyrin repeat proteins reveals their conserved response to endurance exercise," *PLoS One*, vol. 13, no. 9, article e0204312, 2018.

[54] Y. Wei, K. Chen, A. T. Whaley-Connell, C. S. Stump, J. A. Ibdah, and J. R. Sowers, "Skeletal muscle insulin resistance: role of inflammatory cytokines and reactive oxygen species," *American Journal of Physiology-Regulatory, Integrative and Comparative Physiology*, vol. 294, no. 3, pp. R673–R680, 2008.

[55] J. S. Mohamed, M. A. Lopez, G. A. Cox, and A. M. Boriek, "Anisotropic regulation of Ankrd2 gene expression in skeletal muscle by mechanical stretch," *The FASEB Journal*, vol. 24, no. 9, pp. 3330–3340, 2010.

[56] I. A. Barash, M.-L. Bang, L. Mathew, M. L. Greaser, J. Chen, and R. L. Lieber, "Structural and regulatory roles of muscle ankyrin repeat protein family in skeletal muscle," *American Journal of Physiology-Cell Physiology*, vol. 293, no. 1, pp. C218–C227, 2007.

[57] J. M. Peterson, N. Bakkar, and D. C. Guttridge, "NF-κB signaling in skeletal muscle health and disease," *Current Topics in Developmental Biology*, vol. 96, pp. 85–119, 2011.

[58] J. E. Belizario, C. C. Fontes-Oliveira, J. P. Borges, J. A. Kashiabara, and E. Vannier, "Skeletal muscle wasting and renewal: a pivotal role of myokine IL-6," *SpringerPlus*, vol. 5, no. 1, p. 619, 2016.

[59] V. Cenni, M. R. D'Apice, P. Garagnani et al., "Mandibuloacral dysplasia: a premature ageing disease with aspects of physiological ageing," *Ageing Research Reviews*, vol. 42, pp. 1–13, 2018.

[60] D. Camozzi, C. Capanni, V. Cenni et al., "Diverse lamin-dependent mechanisms interact to control chromatin dynamics," *Nucleus*, vol. 5, no. 5, pp. 427–440, 2014.

[61] C. Capanni, R. Del Coco, S. Squarzoni et al., "Prelamin A is involved in early steps of muscle differentiation," *Experimental Cell Research*, vol. 314, no. 20, pp. 3628–3637, 2008.

[62] E. Mattioli, M. Columbaro, C. Capanni et al., "Prelamin A-mediated recruitment of SUN1 to the nuclear envelope directs nuclear positioning in human muscle," *Cell Death & Differentiation*, vol. 18, no. 8, pp. 1305–1315, 2011.

[63] E. Mattioli, M. Columbaro, M. H. Jafferali, E. Schena, E. Hallberg, and G. Lattanzi, "Samp1 mislocalization in Emery-Dreifuss muscular dystrophy," *Cells*, vol. 7, no. 10, p. 170, 2018.

[64] G. Lattanzi, M. Ortolani, M. Columbaro et al., "Lamins are rapamycin targets that impact human longevity: a study in centenarians," *Journal of Cell Science*, vol. 127, no. 1, pp. 147–157, 2014.

[65] E. Mattioli, D. Andrenacci, C. Garofalo et al., "Altered modulation of lamin A/C-HDAC2 interaction and p21 expression during oxidative stress response in HGPS," *Aging Cell*, vol. 17, no. 5, article e12824, 2018.

[66] Y. Liu, I. Drozdov, R. Shroff, L. E. Beltran, and C. M. Shanahan, "Prelamin A accelerates vascular calcification via activation of the DNA damage response and senescence-associated secretory phenotype in vascular smooth muscle cells," *Circulation Research*, vol. 112, no. 10, pp. e99–109, 2013.

[67] M. Zwerger, D. E. Jaalouk, M. L. Lombardi et al., "Myopathic lamin mutations impair nuclear stability in cells and tissue and disrupt nucleo-cytoskeletal coupling," *Human Molecular Genetics*, vol. 22, no. 12, pp. 2335–2349, 2013.

[68] A. Busch, T. Kiel, W. M. Heupel, M. Wehnert, and S. Hubner, "Nuclear protein import is reduced in cells expressing nuclear envelopathy-causing lamin A mutants," *Experimental Cell Research*, vol. 315, no. 14, pp. 2373–2385, 2009.

[69] D. K. Shumaker, T. Dechat, A. Kohlmaier et al., "Mutant nuclear lamin A leads to progressive alterations of epigenetic control in premature aging," *Proceedings of the National Academy of Sciences of U S A.*, vol. 103, no. 23, pp. 8703–8708, 2006.

[70] N. M. Maraldi, C. Capanni, V. Cenni, M. Fini, and G. Lattanzi, "Laminopathies and lamin-associated signaling pathways," *Journal of Cellular Biochemistry*, vol. 112, no. 4, pp. 979–992, 2011.

[71] S. Osmanagic-Myers, T. Dechat, and R. Foisner, "Lamins at the crossroads of mechanosignaling," *Genes and Development*, vol. 29, no. 3, pp. 225–237, 2015.

[72] E. C. Tapley and D. A. Starr, "Connecting the nucleus to the cytoskeleton by SUN-KASH bridges across the nuclear envelope," *Current Opinion in Cell Biology*, vol. 25, no. 1, pp. 57–62, 2013.

[73] A. Mejat and T. Misteli, "LINC complexes in health and disease," *Nucleus*, vol. 1, no. 1, pp. 40–52, 2010.

[74] L. Yang, M. Munck, K. Swaminathan, L. E. Kapinos, A. A. Noegel, and S. Neumann, "Mutations in LMNA modulate the lamin A–nesprin-2 interaction and cause LINC complex alterations," *PLoS One*, vol. 8, no. 8, article e71850, 2013.

[75] F. Haque, D. Mazzeo, J. T. Patel et al., "Mammalian SUN protein interaction networks at the inner nuclear membrane and their role in laminopathy disease processes," *Journal of Biological Chemistry*, vol. 285, no. 5, pp. 3487–3498, 2010.

[76] P. J. Stewart-Hutchinson, C. M. Hale, D. Wirtz, and D. Hodzic, "Structural requirements for the assembly of

LINC complexes and their function in cellular mechanical stiffness," *Experimental Cell Research*, vol. 314, no. 8, pp. 1892–1905, 2008.

[77] P. Meinke, E. Mattioli, F. Haque et al., "Muscular dystrophy-associated SUN1 and SUN2 variants disrupt nuclear-cytoskeletal connections and myonuclear organization," *PLOS Genetics*, vol. 10, no. 9, article e1004605, 2014.

[78] C. Zhou, C. Li, B. Zhou et al., "Novel nesprin-1 mutations associated with dilated cardiomyopathy cause nuclear envelope disruption and defects in myogenesis," *Human Molecular Genetics*, vol. 26, no. 12, pp. 2258–2276, 2017.

[79] C. Zhou, L. Rao, C. M. Shanahan, and Q. Zhang, "Nesprin-1/2: roles in nuclear envelope organisation, myogenesis and muscle disease," *Biochemical Society Transactions*, vol. 46, no. 2, pp. 311–320, 2018.

[80] F. Chiarini, C. Evangelisti, V. Cenni et al., "The cutting edge: the role of mTOR signaling in laminopathies," *International Journal of Molecular Sciences*, vol. 20, no. 4, p. 847, 2019.

[81] G. Boriani, E. Biagini, M. Ziacchi et al., "Cardiolaminopathies from bench to bedside: challenges in clinical decision-making with focus on arrhythmia-related outcomes," *Nucleus*, vol. 9, no. 1, pp. 442–459, 2018.

[82] P. Bernasconi, N. Carboni, G. Ricci et al., "Elevated TGF β2 serum levels in Emery-Dreifuss muscular dystrophy: implications for myocyte and tenocyte differentiation and fibrogenic processes," *Nucleus*, vol. 9, no. 1, pp. 337–349, 2018.

[83] F. Lombardi, F. Gullotta, M. Columbaro et al., "Compound heterozygosity for mutations in LMNA in a patient with a myopathic and lipodystrophic mandibuloacral dysplasia type A phenotype," *The Journal of Clinical Endocrinology & Metabolism*, vol. 92, no. 11, pp. 4467–4471, 2007.

[84] L. Maggi, N. Carboni, and P. Bernasconi, "Skeletal muscle laminopathies: a review of clinical and molecular features," *Cells*, vol. 5, no. 3, p. 33, 2016.

[85] M. Bera, H. C. Kotamarthi, S. Dutta et al., "Characterization of unfolding mechanism of human lamin A Ig fold by single-molecule force spectroscopy-implications in EDMD," *Biochemistry*, vol. 53, no. 46, pp. 7247–7258, 2014.

[86] A. Buxboim, J. Swift, J. Irianto et al., "Matrix elasticity regulates lamin-A,C phosphorylation and turnover with feedback to actomyosin," *Current Biology*, vol. 24, no. 16, pp. 1909–1917, 2014.

[87] E. Torvaldson, V. Kochin, and J. E. Eriksson, "Phosphorylation of lamins determine their structural properties and signaling functions," *Nucleus*, vol. 6, no. 3, pp. 166–171, 2015.

[88] V. Kochin, T. Shimi, E. Torvaldson et al., "Interphase phosphorylation of lamin A," *Journal of Cell Science*, vol. 127, no. 12, pp. 2683–2696, 2014.

[89] V. Cenni, P. Sabatelli, E. Mattioli et al., "Lamin A N-terminal phosphorylation is associated with myoblast activation: impairment in Emery-Dreifuss muscular dystrophy," *Journal of Medical Genetics*, vol. 42, no. 3, pp. 214–220, 2005.

[90] V. Cenni, J. Bertacchini, F. Beretti et al., "Lamin A Ser404 is a nuclear target of Akt phosphorylation in C2C12 cells," *Journal of Proteome Research*, vol. 7, no. 11, pp. 4727–4735, 2008.

[91] J. Bertacchini, F. Beretti, V. Cenni et al., "The protein kinase Akt/PKB regulates both prelamin A degradation and Lmna gene expression," *The FASEB Journal*, vol. 27, no. 6, pp. 2145–2155, 2013.

[92] P. Sabatelli, P. Bonaldo, G. Lattanzi et al., "Collagen VI deficiency affects the organization of fibronectin in the extracellular matrix of cultured fibroblasts," *Matrix Biology*, vol. 20, no. 7, pp. 475–486, 2001.

[93] A. Mattout, B. . L. Pike, B. . D. Towbin et al., "An EDMD mutation in C. elegans lamin blocks muscle-specific gene relocation and compromises muscle integrity," *Current Biology*, vol. 21, no. 19, pp. 1603–1614, 2011.

[94] J. Perovanovic, S. Dell'Orso, V. F. Gnochi et al., "Laminopathies disrupt epigenomic developmental programs and cell fate," *Science Translational Medicine*, vol. 8, no. 335, p. 335ra58, 2016.

[95] A. Brull, B. Morales Rodriguez, G. Bonne, A. Muchir, and A. T. Bertrand, "The pathogenesis and therapies of striated muscle laminopathies," *Frontiers in Physiology*, vol. 9, article 1533, 2018.

[96] H. J. Worman, "Cell signaling abnormalities in cardiomyopathy caused by lamin A/C gene mutations," *Biochemical Society Transactions*, vol. 46, no. 1, pp. 37–42, 2018.

[97] M. Chatzifrangkeskou, C. Le Dour, W. Wu et al., "ERK1/2 directly acts on CTGF/CCN2 expression to mediate myocardial fibrosis in cardiomyopathy caused by mutations in the lamin A/C gene," *Human Molecular Genetics*, vol. 25, no. 11, pp. 2220–2233, 2016.

[98] S. Angori, C. Capanni, G. Faulkner et al., "Emery-Dreifuss muscular dystrophy-associated mutant forms of lamin A recruit the stress responsive protein Ankrd2 into the nucleus, affecting the cellular response to oxidative stress," *Cellular Physiology and Biochemistry*, vol. 42, no. 1, pp. 169–184, 2017.

[99] E. Mattioli, D. Andrenacci, A. Mai et al., "Statins and histone deacetylase inhibitors affect lamin A/C - histone deacetylase 2 interaction in human cells," *Frontiers in Cell and Developmental Biology*, vol. 7, p. 6, 2019.

[100] M. Mittelbronn, F. Hanisch, M. Gleichmann et al., "Myofiber degeneration in autosomal dominant Emery–Dreifuss muscular dystrophy (AD-EDMD) (LGMD1B)," *Brain Pathology*, vol. 16, no. 4, pp. 266–272, 2006.

[101] T. Arimura, A. Helbling-Leclerc, C. Massart et al., "Mouse model carrying H222P- Lmna mutation develops muscular dystrophy and dilated cardiomyopathy similar to human striated muscle laminopathies," *Human Molecular Genetics*, vol. 14, no. 1, pp. 155–169, 2005.

[102] L. Ruggiero, C. Fiorillo, A. Tessa et al., "Muscle fiber type disproportion (FTD) in a family with mutations in the LMNA gene," *Muscle & Nerve*, vol. 51, no. 4, pp. 604–608, 2015.

[103] V. Lallemand-Breitenbach and H. de Thé, "PML nuclear bodies: from architecture to function," *Current Opinion in Cell Biology*, vol. 52, pp. 154–161, 2018.

[104] D. Guan and H.-Y. Kao, "The function, regulation and therapeutic implications of the tumor suppressor protein,PML," *Cell & Bioscience*, vol. 5, no. 1, p. 60, 2015.

[105] M. Niwa-Kawakita, O. Ferhi, H. Soilihi, M. Le Bras, V. Lallemand-Breitenbach, and H. de Thé, "PML is a ROS sensor activating p53 upon oxidative stress," *The Journal of Experimental Medicine*, vol. 214, no. 11, pp. 3197–3206, 2017.

[106] D. T. Warren, T. Tajsic, L. J. Porter et al., "Nesprin-2-dependent ERK1/2 compartmentalisation regulates the DNA damage response in vascular smooth muscle cell ageing," *Cell Death & Differentiation*, vol. 22, no. 9, pp. 1540–1550, 2015.

[107] K. Harhouri, C. Navarro, D. Depetris et al., "MG132-induced progerin clearance is mediated by autophagy activation and splicing regulation," *EMBO Molecular Medicine*, vol. 9, no. 9, pp. 1294–1313, 2017.

[108] C. Capanni, E. Mattioli, M. Columbaro et al., "Altered pre-lamin A processing is a common mechanism leading to lipodystrophy," *Human Molecular Genetics*, vol. 14, no. 11, pp. 1489–1502, 2005.

[109] C. Ivorra, M. Kubicek, J. M. Gonzalez et al., "A mechanism of AP-1 suppression through interaction of c-Fos with lamin A/C," *Genes & Development*, vol. 20, no. 3, pp. 307–320, 2006.

[110] K. Tilgner, K. Wojciechowicz, C. Jahoda, C. Hutchison, and E. Markiewicz, "Dynamic complexes of A-type lamins and emerin influence adipogenic capacity of the cell via nucleocytoplasmic distribution of beta-catenin," *Journal of Cell Science*, vol. 122, no. 3, pp. 401–413, 2009.

[111] C. Capanni, V. Cenni, T. Haraguchi et al., "Lamin A precursor induces barrier-to-autointegration factor nuclear localization," *Cell Cycle*, vol. 9, no. 13, pp. 2600–2610, 2010.

[112] C. Capanni, S. Squarzoni, V. Cenni et al., "Familial partial lipodystrophy, mandibuloacral dysplasia and restrictive dermopathy feature barrier-to-autointegration factor (BAF) nuclear redistribution," *Cell Cycle*, vol. 11, no. 19, pp. 3568–3577, 2012.

[113] G. Ruiz de Eguino, A. Infante, K. Schlangen et al., "Sp1 transcription factor interaction with accumulated prelamin a impairs adipose lineage differentiation in human mesenchymal stem cells: essential role of sp1 in the integrity of lipid vesicles," *Stem Cells Translational Medicine*, vol. 1, no. 4, pp. 309–321, 2012.

[114] V. Cenni, C. Capanni, E. Mattioli et al., "Rapamycin treatment of Mandibuloacral dysplasia cells rescues localization of chromatin-associated proteins and cell cycle dynamics," *Aging*, vol. 6, no. 9, pp. 755–769, 2014.

[115] A. Infante, A. Gago, G. R. de Eguino et al., "Prelamin A accumulation and stress conditions induce impaired Oct-1 activity and autophagy in prematurely aged human mesenchymal stem cell," *Aging*, vol. 6, no. 4, pp. 264–280, 2014.

[116] A. Infante and C. I. Rodriguez, "Pathologically relevant prelamin A interactions with transcription factors," *Methods in Enzymology*, vol. 569, pp. 485–501, 2016.

[117] M. Loi, V. Cenni, S. Duchi et al., "Barrier-to-autointegration factor (BAF) involvement in prelamin A-related chromatin organization changes," *Oncotarget*, vol. 7, no. 13, pp. 15662–15677, 2016.

[118] I. I. Boubriak, A. N. Malhas, M. M. Drozdz, L. Pytowski, and D. J. Vaux, "Stress-induced release of Oct-1 from the nuclear envelope is mediated by JNK phosphorylation of lamin B1," *PLoS One*, vol. 12, no. 5, article e0177990, 2017.

[119] G. Dialynas, O. K. Shrestha, J. M. Ponce et al., "Myopathic lamin mutations cause reductive stress and activate the nrf2/keap-1 pathway," *Plos Genetics*, vol. 11, no. 5, article e1005231, 2015.

[120] A. T. Bertrand, L. Renou, A. Papadopoulos et al., "DelK32-lamin A/C has abnormal location and induces incomplete tissue maturation and severe metabolic defects leading to premature death," *Human Molecular Genetics*, vol. 21, no. 5, pp. 1037–1048, 2012.

[121] T. Sullivan, D. Escalante-Alcalde, H. Bhatt et al., "Loss of A-type lamin expression compromises nuclear envelope integrity leading to muscular dystrophy," *Journal of Cell Biology*, vol. 147, no. 5, pp. 913–920, 1999.

[122] S. Kojic, D. Radojkovic, and G. Faulkner, "Muscle ankyrin repeat proteins: their role in striated muscle function in health and disease," *Critical Reviews in Clinical Laboratory Sciences*, vol. 48, no. 5-6, pp. 269–294, 2011.

[123] A. Pallavicini, S. Kojic, C. Bean et al., "Characterization of human skeletal muscle Ankrd2," *Biochemical and Biophysical Research Communications*, vol. 285, no. 2, pp. 378–386, 2001.

[124] C. Bean, M. Salamon, A. Raffaello, S. Campanaro, A. Pallavicini, and G. Lanfranchi, "The Ankrd2, Cdkn1c and calcyclin genes are under the control of MyoD during myogenic differentiation," *Journal of Molecular Biology*, vol. 349, no. 2, pp. 349–366, 2005.

[125] J. A. Carson, D. Nettleton, and J. M. Reecy, "Differential gene expression in the rat soleus muscle during early work overload-induced hypertrophy," *The FASEB Journal*, vol. 16, no. 2, pp. 207–209, 2002.

[126] Y. W. Chen, G. A. Nader, K. R. Baar, M. J. Fedele, E. P. Hoffman, and K. A. Esser, "Response of rat muscle to acute resistance exercise defined by transcriptional and translational profiling," *The Journal of Physiology*, vol. 545, no. 1, pp. 27–41, 2002.

Hindawi
Oxidative Medicine and Cellular Longevity
Volume 2019, Article ID 1302985, 13 pages
https://doi.org/10.1155/2019/1302985

Research Article

Effect of Telmisartan in the Oxidative Stress Components Induced by Ischemia Reperfusion in Rats

Simón Quetzalcoatl Rodríguez-Lara,[1] **Walter Angel Trujillo-Rangel**,[2] **Araceli Castillo-Romero**,[3] **Sylvia Elena Totsuka-Sutto**,[2] **Teresa Arcelia Garcia-Cobián**,[2] **Ernesto German Cardona-Muñoz**,[2] **Alejandra Guillermina Miranda-Díaz**,[2] **Ernesto Javier Ramírez-Lizardo**,[2] **and Leonel García-Benavides**[2,4]

[1]*International Program, Instituto de Ciencias Biomédicas, Universidad Autónoma de Guadalajara, A.C. Av. Montevideo, esq. Av. Acueducto, Col. Prados Providencia, Guadalajara, Jalisco, C.P. 44670, Mexico*
[2]*Instituto de Terapéutica Experimental y Clínica, Departamento de Fisiología, CUCS, Universidad de Guadalajara, Calle Sierra Mojada 950, Colonia Independencia, CP 44340 Guadalajara, Jalisco, Mexico*
[3]*Departamento de Microbiología y Patología, CUCS, Universidad de Guadalajara, Calle Sierra Mojada 950, Colonia Independencia, CP 44340 Guadalajara, Jalisco, Mexico*
[4]*Departamento de Ciencias Biomédicas, CUTonala, Universidad de Guadalajara, Avenida Nuevo Periférico No. 555, Ejido San José Tateposco, CP 45425 Tonalá, Jalisco, Mexico*

Correspondence should be addressed to Leonel García-Benavides; drleonelgb@hotmail.com

Received 9 February 2019; Revised 15 April 2019; Accepted 15 May 2019; Published 2 July 2019

Guest Editor: José R. Pinto

The therapeutic effects of telmisartan, an angiotensin II receptor antagonist and a peroxisome proliferator-activated receptor-γ (PPAR-γ) agonist, have been demonstrated in several disorders. It has antioxidant and immune response modulator properties and has shown promising results in the treatment of an ischemia/reperfusion (I/R) lesion. In this study, a skeletal muscle (right gastrocnemius muscle) I/R lesion was induced in rats and different reperfusion times (1 h, 24 h, 72 h, 7-day, and 14-day subgroups) were assessed. Furthermore, levels of oxidative markers such as enzymatic scavengers (catalase (CAT) and superoxide dismutase (SOD)) and metabolites (nitrates and 8-oxo-deoxyguanosine) were determined. The degree of tissue injury (total lesioned fibers and inflammatory cell count) was also evaluated. We observed an increase in CAT and SOD expression levels under telmisartan treatment, with a decrease in injury and oxidative biomarker levels in the 72 h, 7-day, and 14-day subgroups. Telmisartan reduced oxidative stress and decreased the damage of the I/R lesion.

1. Introduction

Ischemia reperfusion (I/R) is a phenomenon that occurs after the occlusion of arterial blood flow to a specific organ or tissue. The ischemia causes an imbalance in metabolic substrate levels on the exposed cells; depending on the hypoxia duration, several mechanisms, which can help cell survival or induce further damage, are activated [1–3]. Reperfusion is the restoration of the blood flow and reoxygenation of the affected tissues. It is related to an exacerbation of the initial lesion and followed by several physiopathological mechanisms in the affected cells, such as increments of cations in cytosol, formation of reactive oxygen species and nitrogen species, disruption of the signaling redox (oxidative stress (OS)), mitochondrial lesion, transcriptional reprograming, endothelial lesion, no-reflow phenomenon, immunity-mediated lesion, apoptosis, autophagy, and necrosis. From all these processes, the pathological changes in the affected tissue can be divided into acute (first 72 h) and chronic (15–90 days) at onset, which are determined by factors, such as the time of ischemia and the response to inflammation and oxidative stress [3, 4]. These two processes produce tissue

damage, leading to the malfunction or dysfunction of the affected tissues by many mechanisms [3, 4]. The I/R phenomenon impact is most pronounced in patients with myocardial infarction or cerebral ischemia. Its repercussions can produce deleterious effects in the patients, and their prevalence affects the health care system [5–8]. Despite the impact of this phenomenon, no specific pharmacological approach has been established to decrease lesion development [9].

In the OS component of the I/R lesions, the role of enzymatic scavengers such as superoxide dismutase (SOD) and catalase (CAT) is crucial for cell survival [1–3], not only because they are the first line of defense against reactive oxygen radicals (ROS) and nitrogen (RNS) but also because their absence or malfunction leads to signaling redox disruption in the cell, inducing or increasing the I/R lesion. The I/R lesion formation process may be complex because of all the pathophysiological components, but the increase in enzymatic scavengers' expression, function, or activity may partially improve the affected tissue survival [10, 11]. Several authors have described that telmisartan, an angiotensin type 1 receptor antagonist and peroxisome proliferator-activated receptor-γ (PPAR-γ) receptor partial agonist, produces a beneficial effect on OS-induced damage in different pathological process (diabetes, dyslipidemia, hypertension, cancer, etc.) and has shown encouraging results even in the animal models of I/R lesions [12–22]. Telmisartan has been shown to affect the concentration and activity of some enzymatic scavengers (SOD, CAT, NADPH, etc.), but its mechanism of action and the impact on the extent of I/R lesion progression have not been well elucidated [12–22]. The effects of the PPAR-γ receptor activation have shown expression in many tissues, but its maximal expression has been shown in the adipocyte and immune cells. The pathways involved in the signaling effects are related to the activation of the extracellular signal-regulated kinase–mitogen-activated protein kinase (ERK-MAPK) cascade, which can induce activation and differentiation of macrophages, increasing the expression of CD36, stimulating recruitment activity, and inducing the survival of the cells under OS [23, 24].

We aimed to determine the effect of telmisartan on the expression of SOD and CAT and on the production of oxidative metabolites like nitrates (products of protein nitrosylation) and 8-oxo-deoxyguanosine (products of DNA oxidation). Furthermore, we evaluated the histological impact of telmisartan on I/R lesion-induced muscle tissue damage in the limbs of Wistar rats.

2. Material and Methods

2.1. Animals. Male Wistar rats, weighing 250–350 g, were housed in colony rooms with a 12/12 h light/dark cycle at 21–25°C and had free access to food and water. All animal experiments were performed in accordance with the Centro Universitario de Ciencias de la Salud of the Universidad de Guadalajara ethical committee regulations (register number: CEI/19/2015). All guidelines for laboratory animal care of the Mexican legislation were followed (NOM-062-ZOO-1999).

2.2. Pharmacological Intervention. Telmisartan was obtained in the form of tablets (from Boehringer Ingelheim) that were powdered and titled according to each rat's weight, using a sterile technique, diluted with injectable water, vortexed, and administered using an orogastric cannula. The drug was administered at single doses of 20 mg/kg/day, which was selected taking under consideration other studies [22], in the morning in the therapeutic intervention group, whereas injectable water was used as vehicle for the no therapeutic intervention group. The rats received telmisartan or injectable water daily for 7 days prior to the induction of an I/R lesion and following the induction of the lesion until the sacrifice of the animals at the specified time points.

2.3. Experimental Procedure to Induce Ischemia Reperfusion. All rats were anesthetized with an intraperitoneal injection of Zoletil 50 (tiletamine 125 mg/zolazepam 125 mg) at a dose of 40 mg/kg and ketamine at a dose of 80 mg/kg [25]. No additional anesthesia administration was necessary during the procedure.

The skin in the area of the procedure in the right inguinal fold was disinfected and shaved; a 1 cm incision was made and dissection was performed using a dulled technique until the vascular-nerve plexus. A tourniquet was placed on the entire plexus using prolene 3-0 to induce ischemia in the gastrocnemius muscle, and the incision was closed using silk 3-0. Ischemia was maintained for 6 h. Following this, the animals were anesthetized again; the incision was reopened; and for reperfusion, the tourniquet was removed, avoiding damage to the plexus, using a fine blade under a magnifying glass and direct visualization. After reperfusion, the animals were sacrificed under anesthesia; blood and gastrocnemius muscle samples were obtained for RNA extraction and histological analysis, as well as for SOD, CAT, and 8-oxo-deoxgyuanosine quantification using enzyme-linked immunosorbent assay (ELISA) and nitrite/nitrate quantification using colorimetric analysis.

2.4. Experimental Protocol. Overall, 50 rats were included in the experiment and were divided into two groups of 25 rats each. Group 1 received a therapeutic intervention (telmisartan), whereas group 2 received only injectable water.

Both groups were subdivided into five subgroups (each comprising 5 rats) based on 1 h, 24 h, 72 h, 7 days, and 14 days of reperfusion (Figure 1).

2.5. Gene Expression. The muscle samples were stabilized using RNAlater from Thermo Fisher Scientific (Cat. AM7020) and frozen at −80°C until RNA extraction was performed. RNA extraction was performed from the muscle samples within 24 h following the sacrifice. The samples were cut in 50 to 100 mg pieces, using a sterile technique, and homogenized with TRIzol from Invitrogen (Cat. 15596026) and TissueRuptor from QIAGEN. RNA concentration and integrity were evaluated using the Eppendorf NanoDrop spectrophotometer. RNAs isolated from different samples had similar gel electrophoresis profiles. Total RNA yield from each tissue sample (50–100 mg) equaled at least 150 μg and was sufficient for endpoint QRT-PCR analysis. cDNA synthesis was performed using Verso cDNA synthesis from the

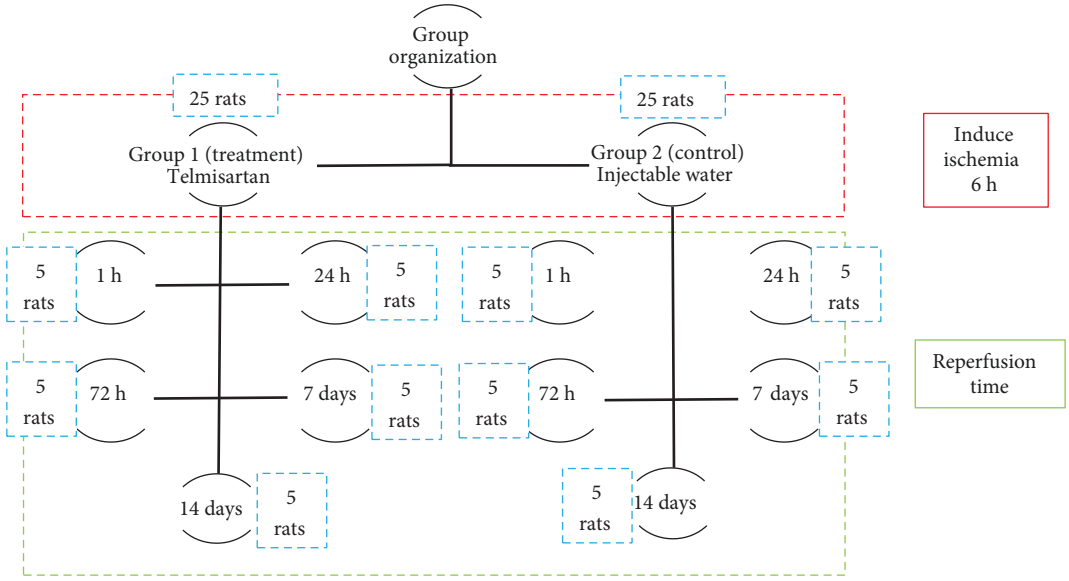

Figure 1: Group organization. Ischemia was induced for 6 h in all groups.

Thermo Fisher Scientific kit (Cat. AB1453A) in a volume of 20 μL: cDNA synthesis 4 μL, dNTP mix 2 μL, RNA primer 1 μL, RT enhancer 1 μL, Verso enzyme mix 1 μL, template RNA 5 μg, and DEPC water up to 20 μL.

The primer was designed using the sequences from the GenBank of the PubMed database and the program FastPCR 6.5 version. The primers had the following sequences: (1) for SOD-2, FW TTC AGG GAA GCC ATT CAG CAC CAT and RW ACT GTT ACC TTG TCA GGG A; (2) for CAT, FW TTG GCA GAG CCT GAA GTC ACC ACT and RW TGG TCA GGA CAT CGG GTT TCT G; and (3) for β-actin (constitutive), FW AGT ACA ACC TTC TTG CAG CTC and RW AGT CCT TCT GAC CCA TAC CC.

The gene expression levels were assessed using endpoint QRT-PCR. The amplification reactions were performed in a volume of 10 μL using the Thermo Fisher Scientific DreamTaq Green PCR Master Mix (Cat. K1089BID). The procedure was performed using the DreamTaq Green PCR Master Mix 5 μL, FW primer 0.5 μL, RW primer 0.5 μL, template 1 μL, and injectable water 3 μL. Tm-normalized hybridization conditions were as follows: initial denaturalization for 1 min at 95°C, 40 amplification cycles (30 s/95°C, 30 s/57°C, and 1 min/72°C), and extinction for 7 min at 72°C. Hybridization was performed in triplicates in a Thermo Scientific thermal cycler. Samples were run on a 1% agarose gel at 70 mV, 400 amp for 45 min in a Bio-Rad electrophoresis chamber and visualized in a 360 nm transilluminator; the obtained images were evaluated using the program "ImageJ" for all sample quantifications [26].

2.6. Biochemical Assay. SOD-2, CAT, and 8-oxo-dG residue protein levels were measured using sandwich ELISA kits (R&D Cat. DYC3419-5, MBS Cat. 701908, and Trevigen Cat. 4380-096-k, respectively). Nitrite concentration was determined using a colorimetric assay kit (Sigma cat. 23479-1KT-F). All experimental procedures were performed following the manufacturers' specifications. The Sinergy HT spectrophotometer was utilized for processing and the program GEN5 11 version for curve plots and calculations.

2.7. Histological Tissue Evaluation. The tissue samples were immersed in 4% paraformaldehyde and processed into 5 μm sections from the proximal, medial, and distal areas of the right gastrocnemius muscle. They were subsequently processed in a paraffin bath and stained with hematoxylin and eosin. Microscopic evaluation was performed under an Axiostar plus microscope. Images were captured using the Carl Zeiss Axiocam, and measurements were performed using the AxioVision 8.1 program.

Cell and tissue damage was evaluated independently by three different pathologists, using full-frame counting, fourfold, and stratified techniques [27]. The lesioned muscle fibers were assessed individually, and inflammatory cells were accounted for.

3. Statistical Analysis

Data are expressed as mean ± standard error of the mean. Normality of the data was assessed using the Shapiro–Wilk test. For between-group comparisons, the Kruskal–Wallis test, followed by the Mann–Whitney U test, was used. p values < 0.05 were considered significant.

4. Results

4.1. Effect of Telmisartan on Gene Expression. Data quantification was performed using the ImageJ program by measuring optical densities (ODs) [28]. OD normalization for each sample was performed using a constitutive gene (β-actin). For gene expression comparisons, OD from the no treatment group was divided by that from the treatment group. The normalization procedure was performed by measuring the gel image of each gene in triplicates, averaging the values, and dividing the constitutive gene value by the

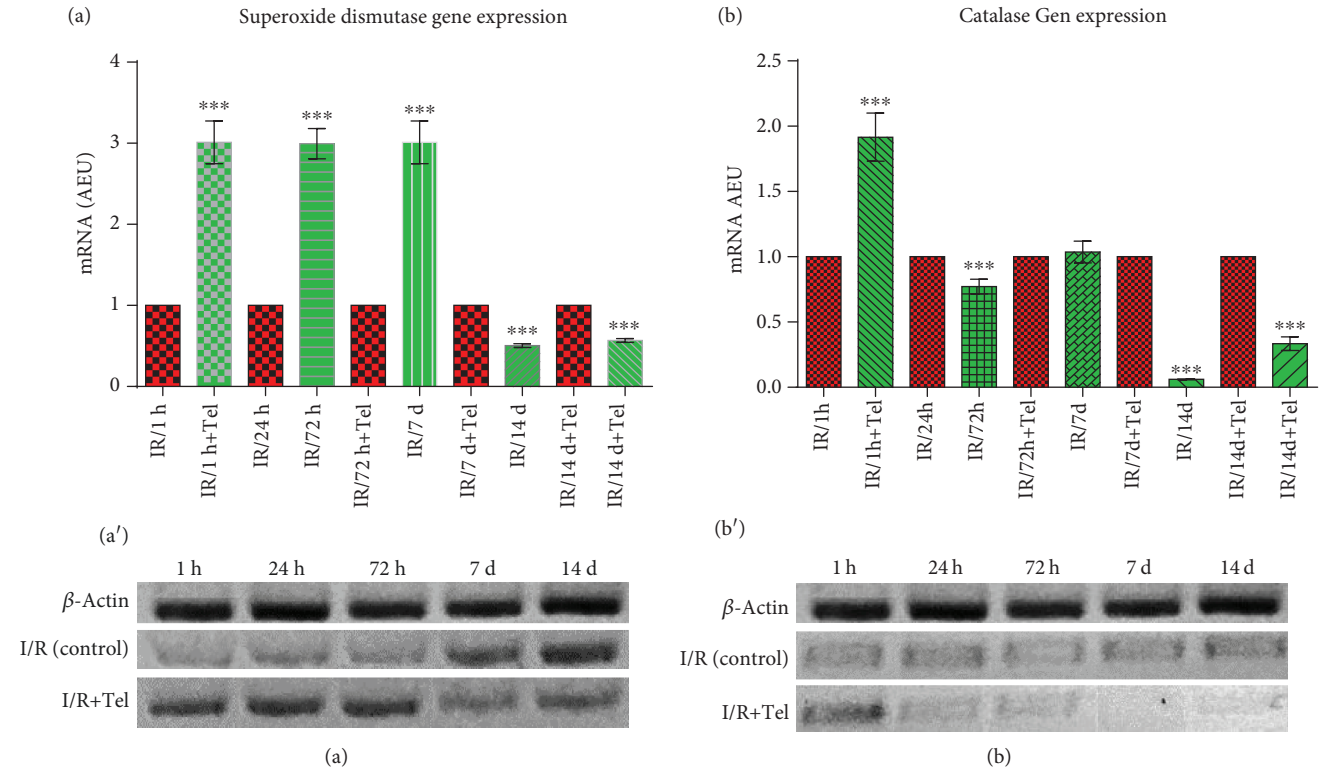

Figure 2: Gene expression of superoxide dismutase and catalase. (a) Comparison catalase gene expression between group 1 and group 2. (a′) Comparison of the agarose 1% gel gene expression of catalase. (b) Comparison SOD-2 gene expression between group 1 and group 2. (b′) Comparison of the agarose 1% gel gene expression of SOD-2. All control values were normalized to 1. ***p values < 0.001; AEU: arbitrary expression units.

corresponding gene sample value. For the comparison of samples, the normalized values of the expected gene were divided by the values of the gene of interest ((I/R)/(IR + Telm)). Data were normalized to 1 and plotted in arbitrary expression units (AEUs) for analysis using GraphPad Prism 6.1 [29].

SOD-2 gene expression demonstrated upregulation in the 1 h (3.012 AEU), 24 h (2.994 AEU), and 72 h (3.010 AEU) telmisartan treatment subgroups compared with the control subgroups ($p < 0.0006$) and demonstrated a decrease in the 7-day (0.5049 AEU) and 14-day (0.5669 AEU) telmisartan subgroups ($p < 0.0006$) (Figure 2(a)).

CAT gene expression demonstrated significant upregulation in the 1 h telmisartan subgroup (1.916 AEU) compared with the control subgroups ($p < 0.001$). No differences were detected in the 72 h subgroup; however, a significant decrease in gene expression was detected in the 24 h (0.771 AEU), 7-day (0.060 AEU), and 14-day (0.334 AEU) telmisartan subgroups compared with the control subgroups ($p < 0.0006$) (Figure 2(b)).

4.2. Effect of Telmisartan on Catalase and Superoxide Dismutase Protein Levels. CAT protein levels were significantly increased in the 1 h (844.3 mIU/mL), 72 h (905.5 mIU/mL), 7-day (1218 mIU/mL), and 14-day (2239 mIU/mL) telmisartan subgroups compared with the control subgroups ($p < 0.05$); however, these levels were decreased in the 24 h telmisartan subgroup (410.6 mIU/mL) compared with the control subgroups ($p < 0.05$) (Figure 3(a)). In the intragroup comparison of the telmisartan subgroups, a significant decrease in the CAT protein levels was found between the 1 h and 24 h subgroups, although the remaining subgroups showed a significant progressive increase from the 24 h to the 14-day subgroup ($p < 0.0001$) (Table 1).

SOD protein levels showed a significant increase in the 1 h (689.8 pg/mL) and 72 h (540.9 pg/mL) telmisartan subgroups compared with the control subgroups ($p < 0.05$). Furthermore, these levels demonstrated a significant decrease in the 14-day (425.2 pg/mL) telmisartan subgroup compared with the control subgroups ($p < 0.05$); however, no differences were observed between the 24 h and 7-day subgroups (Figure 3(b)). In the intragroup comparison of the telmisartan subgroups, a significant decrease in the levels was found between the 1 h and other subgroups ($p < 0.001$), but no differences were found among the 24 h, 72 h, 7 day, and 14 day subgroups (Table 1).

4.3. Effect of Telmisartan on Oxidative Metabolites. 8-Oxo-dG concentration was significantly decreased in the 72 h (5,347 pg/mL), 7-day (6,296 pg/mL), and 14-day (8,926 pg/mL) telmisartan subgroups compared with the control subgroups ($p < 0.001$); however, the 24 h subgroup did not show any significant difference. Furthermore, 8-oxo-dG levels were significantly increased in the 1 h telmisartan subgroup (17,271 pg/mL) compared with the control subgroups

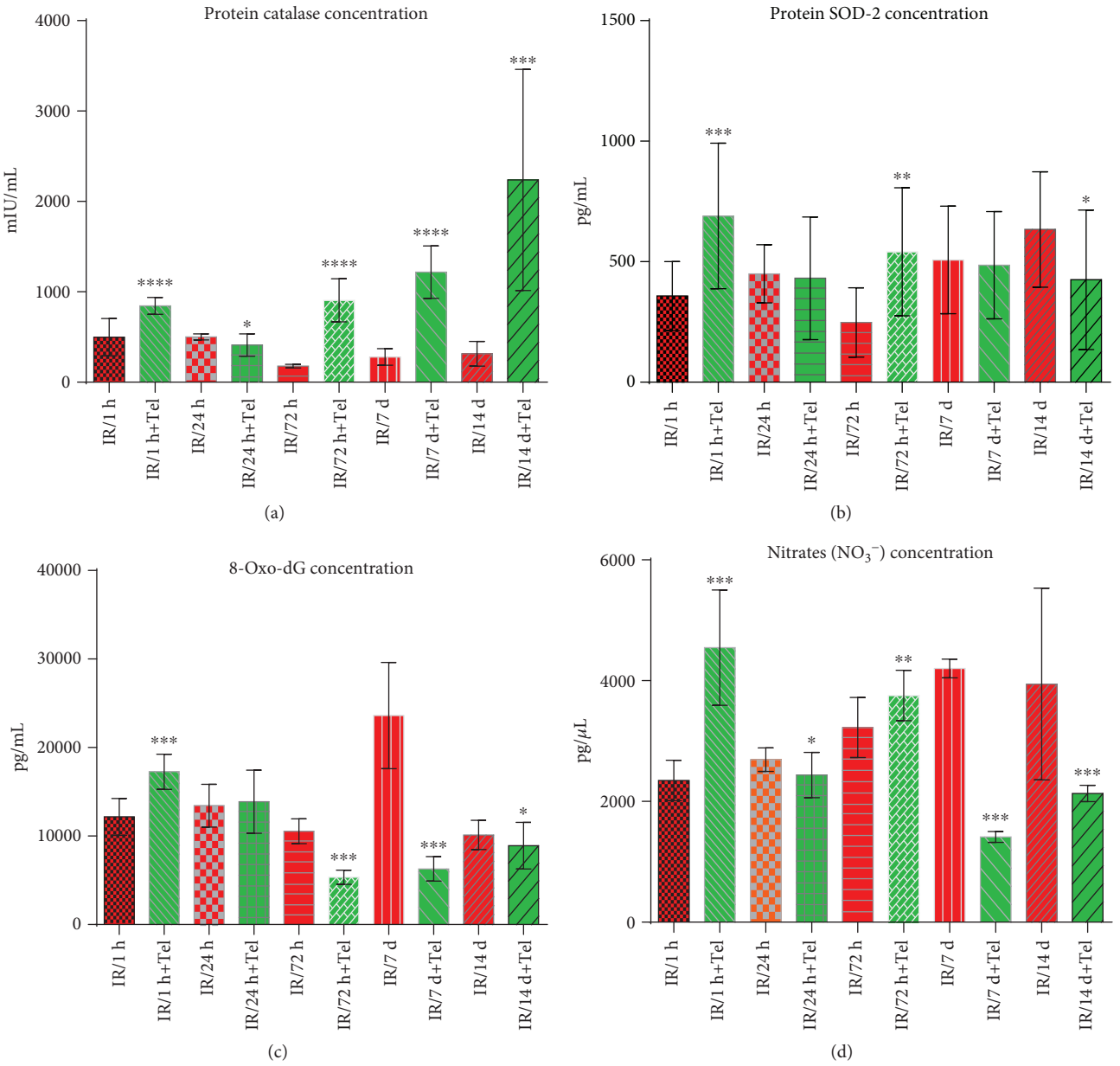

Figure 3: Concentration of enzyme scavengers and oxidative metabolites. Comparison between therapeutic intervention (telmisartan) and control groups: (a) catalase protein concentration; (b) SOD-2 protein concentration; (c) 8-oxo-dG concentration; (d) nitrate concentration. $^{*}p \leq 0.05$, $^{**}p \leq 0.005$, $^{***}p \leq 0.0005$, and $^{****}p \leq 0.00005$. mIU/mL: milli-international units per milliliter; pg/mL: picograms per milliliter; pg/μL: picograms per microliter.

($p < 0.001$) (Figure 3(c)). In the intragroup comparison of the telmisartan subgroups, a significant and progressive decrease was observed in 8-oxo-dG levels from the 1 h to the 72 h subgroups ($p < 0.001$); nevertheless, a progressive increase was detected in the 7-day and 14-day subgroups compared with the other subgroups ($p < 0.0001$) (Table 1).

Nitrate concentration was significantly decreased in the 24 h (2,438 pg/μL), 7-day (1,412 pg/μL), and 14-day (2,131 pg/μL) telmisartan subgroups compared with the control subgroups ($p < 0.005$). A significant nitrate concentration increase was detected in the 1 h (4,549 pg/μL) and 72 h (3,754 pg/μL) telmisartan subgroups compared with the control subgroups ($p < 0.0001$ and $p < 0.0005$, respectively) (Figure 3(d)). In the intragroup comparisons of the telmisartan subgroups, three significant peaks of nitrate concentration increase in the 1 h, 72 h, and 14-day ($p < 0.0001$) telmisartan subgroups as well as two significant peaks of decrease in the 24 h and 7-day telmisartan subgroups were observed ($p < 0.001$) (Table 1).

4.4. Effect of Telmisartan on Tissue Lesions. The lesion assessment (Figure 4) was performed using full-frame counting, fourfold, and stratified techniques. The comparison was done using three variables: lesioned muscle fibers, inflammatory cell infiltrates, and nonlesioned fibers [27]. Tissue damage was defined as a fiber injury characterized by broken or

Table 1: Correlation of all results.

Groups	1 hour		24 hours		72 hours		7 days		14 days	
Biomarker	C	T	C	T	C	T	C	T	C	T
SOD-2 gen (AEU)	1	3.012 (SD 0.264)	1	2.994 (SD 0.187)	1	3.01 (SD 0.263)	1	0.50 (SD 0.023)	1	0.566 (SD 0.023)
SOD-2 protein (pg/mL)	357.6 (SD 142.9)	689.8 (SD 301.4)	449.9 (SD 120.3)	431.4 (SD 254.8)	248.2 (SD 143.2)	540.9 (SD 265.7)	507.4 (SD 22.8)	486.1 (SD 22.6)	634.2 (SD 239.3)	425.2 (SD 289)
CAT gen (AEU)	1	1.916 (SD 0.184)	1	0.771 (SD 0.056)	1	1.036 (SD 0.083)	1	0.060 (SD 0.002)	1	0.334 (SD 0.052)
CAT protein (mIU/mL)	498.4 (SD 205.9)	844.3 (SD 92.43)	501.6 (SD 34.35)	410.6 (SD 123.1)	177.5 (SD 20.15)	905.5 (SD 238.4)	279.9 (SD 92.5)	1,218 (SD 290.1)	315 (SD 135.7)	2239 (SD 1,223)
8-Oxo-dG (pg/mL)	12,168 (SD 2,091)	17,271 (SD 1,981)	13,442 (SD 2,411)	13,877 (SD 3,559)	10,552 (SD 1396)	5,347 (SD 807.2)	23,609 (SD 6,002)	6,296 (SD 1,394)	10,125 (SD 1,653)	8,926 (SD 2,630)
NO_3^- (pg/μL)	2,346 (SD 334.3)	4,549 (SD 954.8)	2,694 (SD 194.7)	2,438 (SD 376.2)	3,224 (SD 497)	3,754 (SD 418.6)	4,202 (SD 154.1)	1,412 (SD 90.72)	3,943 (SD 1,587)	2,133 (SD 133.9)
Inflammatory cells (full count)	344.8 (SD 158.1)	427.8 (SD 24.63)	383.5 (SD 58.09)	193.3 (SD 13.44)	393.4 (SD 140.4)	305.3 (SD 19.67)	497.2 (SD 66.7)	383.8 (SD 16.54)	618 (SD 158.4)	923.4 (SD 22.58)
Injured cells (full count)	127.5 (SD 52.45)	98.85 (SD 9.17)	49.75 (SD 13.89)	52.50 (SD 5.73)	242 (SD 56.78)	15.50 (SD 4.5)	227.4 (SD 61.3)	7.4 (SD 1.93)	23.25 (SD 17.42)	0

All values are in mean and with confidence interval of 95%. C: control groups; T: telmisartan groups; SD: standard deviation; AEU: arbitrary expression units; pg/mL: picograms per milliliter; pg/μL: picograms per microliter; mIU/mL: milli-international units per milliliter.

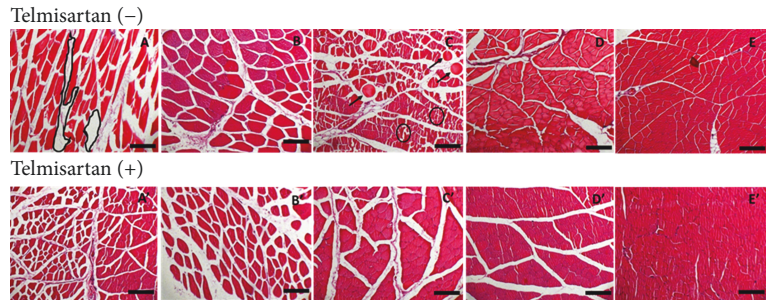

Figure 4: Histological hematoxylin and eosin stain evaluation. (A) I/R 1 h control group: in the delineated black mark, the increase of the interstitial space is observed. (A′) I/R+Telm 1 h group. (B) I/R 24 h control group. (B′) I/R+Telm 24 h group. (C) I/R 72 h control group: the black arrows pinpoint the absence of muscular cells with the delimitation of the stain; the black circles show fragile places at the moment of the cut. (C′) I/R+Telm 72 h group. (D) I/R 7-day control group. (D′) I/R+Telm 7-day group. (E) I/R 14-day control group: its observed reorganization and compaction of the tissue. (E′) I/R+Telm 14-day group: its observed reorganization and compaction of the tissue; inflammatory cells are increasing in comparison with the control group. The black scale bar represents 200 μm. 100x in all pictures.

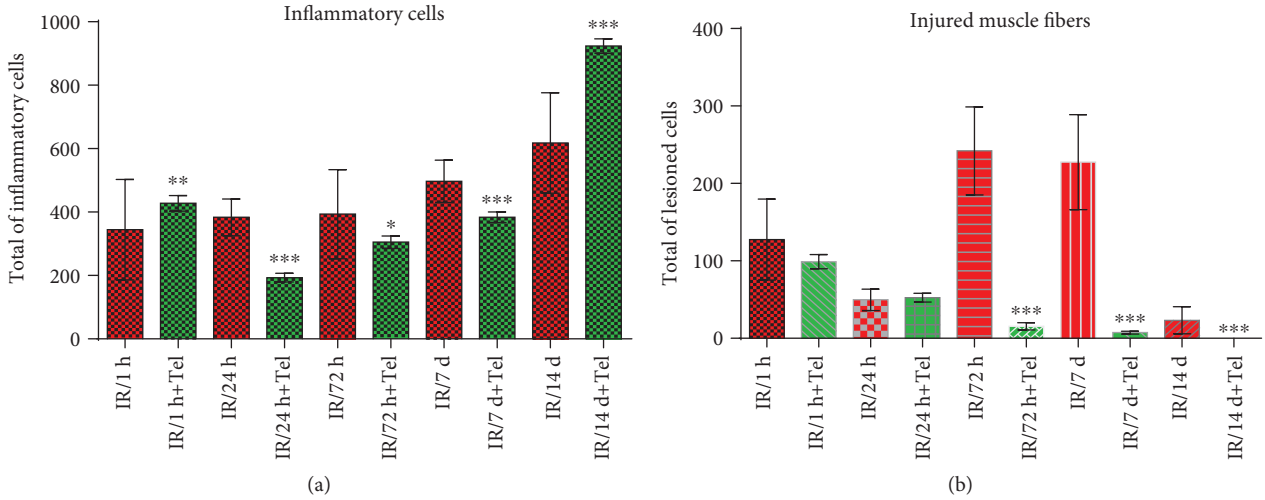

Figure 5: Inflammatory and injured cells. Comparison between therapeutic intervention (telmisartan) and control groups: (a) full count of inflammatory cells; (b) full count of injured cells. $^{*}p \leq 0.05$, $^{**}p \leq 0.005$, and $^{***}p \leq 0.0005$.

ragged borders, inconsistent texture and color throughout the myocyte, presence of holes, and/or detached nuclei. Uninjured muscular fibers were characterized by well-defined borders, uniform texture and color throughout the myocyte, and absence of holes or ruptures in membranes. Pericellular nuclei or satellite cells could be observed adjacent to uninjured myocytes. Because of the hematoxylin and eosin (H&E) stain, it is not possible to precisely differentiate the type of inflammatory cells, so all the inflammatory cells were counted one by one and evaluated as a whole, using the same technique for each picture, and independently by three different pathologists.

The inflammatory cell infiltrate was significantly decreased in the 24 h (193.3 cells), 72 h (305.3 cells), and 7-day (383.8 cells) telmisartan subgroups compared with the control subgroups ($p < 0.007$, $p < 0.003$, and $p < 0.01$, respectively) (Figure 5(a)). Furthermore, the inflammatory cell infiltrate was increased in the 1 h (427.8 cells) and 14-day (923.4 cells) telmisartan subgroups compared with the control subgroups ($p < 0.0001$ and $p < 0.007$, respectively) (Figure 5(a)). In the intragroup comparison of the telmisartan subgroups, a significant decrease was detected in the 24 h subgroup ($p < 0.001$); nevertheless, a significant progressive increase from the 24 h subgroup to the 14-day subgroup was detected ($p < 0.0001$) (Table 1).

The number of injured fibers was decreased in the 72 h (15.5 cells), 7-day (7.4 cells), and 14-day (0 cells) telmisartan subgroups compared with the control subgroups ($p < 0.0008$, $p < 0.01$, and $p < 0.0001$, respectively). No significant differences were detected in the 1 h and 24 h telmisartan subgroups (Figure 5(b)). In the intragroup comparisons of the telmisartan subgroups, a progressive decrease until the 14-day subgroup was detected ($p < 0.0001$) (Table 1).

5. Discussion

OS has been shown to play an important role in the development and propagation of permanent injury in I/R lesions [1–3]. Under physiological conditions, scavenger systems, including the enzymes such as SOD and CAT, control OS [10, 30–32]. The enzymes are initially responsible for the reduction of excess OS, and their role in signaling

redox modulation is crucial. However, during reperfusion, these systems are overwhelmed, and the overproduction of free radicals (ROS and RNS) results in the oxidation of multiple cellular molecules through such proteins (NO_3^-) and DNA (8-oxo-dG) (Figure 6). Telmisartan has been described as a modulator of some oxidative and antioxidant biomarkers, but its mechanism of action is not well understood [15, 18, 20, 21, 33–39]. In the present study, we found that telmisartan produced changes in the SOD-2 and CAT gene expression but to a different degree and time-course regarding reperfusion.

CAT expression modulation has been described as an adaptive response for cell survival after OS injury; furthermore, telmisartan treatment after OS injury has been shown to increase CAT activity and concentration [39–41]. We observed an increase in CAT gene expression and protein concentration only in the 1 h subgroup without any changes in the concentration of oxidative biomarkers and extent of tissue injury. Nevertheless, CAT protein levels decreased in the 24 h subgroup and subsequently persistently increased in the 72 h, 7-day, and 14-day subgroups; this was associated with a decrease in the extent of injured tissues and expression of oxidative markers.

CAT gene expression is a complex process; this is positively regulated by the presence of PPAR-γ through a response element at −12 kb from the transcription initiation site of the human catalase gene. Excess reactive oxygen and nitrogen species can induce a negative CAT and PPAR-γ gene expression [40, 42–46], reducing CAT and PPAR-γ protein levels in the affected tissues. In addition, during the reparation process, the signaling pathways mediated by TGF-β and TNF-α were activated throughout the inflammatory processes, consequently downregulating the CAT gene expression [40, 42–46]. Telmisartan directly increases PPAR-γ gene and protein expression, consecutively increasing the CAT gene expression [39, 41].

The behavior of the CAT gene expression during the first hour reflected a preconditioning effect, which produces an overexpression of CAT, increases the protein levels, and prepares the cells to tolerate oxidative stress. However, at 24 h of reperfusion, we can see a significant decrease in the CAT gene expression due to the overproduction of ROS and RNS, which surpasses the preconditioning effect caused by telmisartan. This negative feedback in the CAT gene expression is observed in all body cells due to the fact that ROS and RNS are released in the body; however, telmisartan could have an effect in the nonaffected cells, which are overexpressing CAT; thus, we can see a normalization on the levels of CAT gene expression and an increase in the levels of CAT protein in serum at 72 h. As a consequence to I/R in locally affected tissues, we see a decrease of the CAT gene expression at 7 and 14 days accompanied with an increase of CAT protein in serum. To explain this behavior, we could take into account the downregulation induced by the activation of the inflammatory and reparation mechanisms (TGF-β and TNF-α) in the affected tissues at 72 h, which decrease gene expression. The increase of the CAT protein is related to the continuous effect of telmisartan on the nonaffected cells. These changes correlate with the tissue reparation, which starts at 72 h and is completely established at 14 days (histological images). The direct and indirect effects of telmisartan in the immune system were beneficial to the early recovery of the damaged cells. The histological stains with a higher immune cell count demonstrated a better recruitment of inflammatory cells in the tissue affected by I/R and displayed a faster recovery of the tissue compared with those not treated with telmisartan.

SOD-2 is the first enzymatic scavenger after an OS perturbation, and its expression is upregulated when an inflammatory process is coactivated [47–52]. In our study, SOD-2 gene expression (in the 1 h, 24 h, and 72 h subgroups) and protein levels (in the 1 h and 72 h subgroups) were increased; however, this high gene and protein expression apparently had no impact on the extent of tissue injury in the 1 h subgroup (Figure 5(b)). Nevertheless, among the telmisartan subgroups, we observed a decrease in gene expression in the 7- and 14-day subgroups, but not in the protein levels in the 24 h and 14-day subgroups. We did not measure enzyme activity; however, we propose that telmisartan may increase CAT and SOD bioavailability because we detected an increase in protein levels without gene expression increase after treatment with it.

The variability in NO synthase explains the behavior of the levels of nitrates during the experiment, due to the fact that it is modulated by multiple mechanisms, local and systemic [53–55]. There are differences in these regulation mechanisms for the different isoforms of this enzyme (endothelial, neuronal, mitochondrial, and inducible) [53–58].

Telmisartan and other ARB increase the expression and the activity of eNOS in endothelial cells, giving protection in circumstances of stress [53, 55, 59]. However, in the presence of severe hypoxia with an excessive production of ROS and RNS, eNOS will induce a rearrangement of these enzymes in the cellular membrane and a malfunctioning that will affect the production of NO [35, 53, 54, 56, 57, 60].

Great quantities of ROS cause a systemic effect that decreases the expression and activity of SOD, which coincides with the decrease of nitrates we observed during the first 24 hours and is related with the inactivity of eNOS. We consider that once the activity of endothelial eNOS and ROS is regulated through other modulation mechanisms such as those mediated by the immune system, there is a decrease in the concentration of systemic nitrates, which is what we would observe at 72 hours and 14 days.

Telmisartan may decrease oxidative biomarker levels and improve injury recovery through OS and inflammatory response modulation in the local tissue. In our study, telmisartan's effect on injury attenuation and OS product reduction was present between 24 h and 14 days. Analyzing the lesion extent and progress in nontreated rats from the start (1 h) to the time when recovery of the lesion (14 days) is observed, we conclude that the progress of the I/R lesion is divided into two periods. The first is damage limitation that can occur until 7 days after the start of the reperfusion. The second is the start of the reparation process that can be underhanded since the first 72 h after the start of the reperfusion. The repair mechanism activation

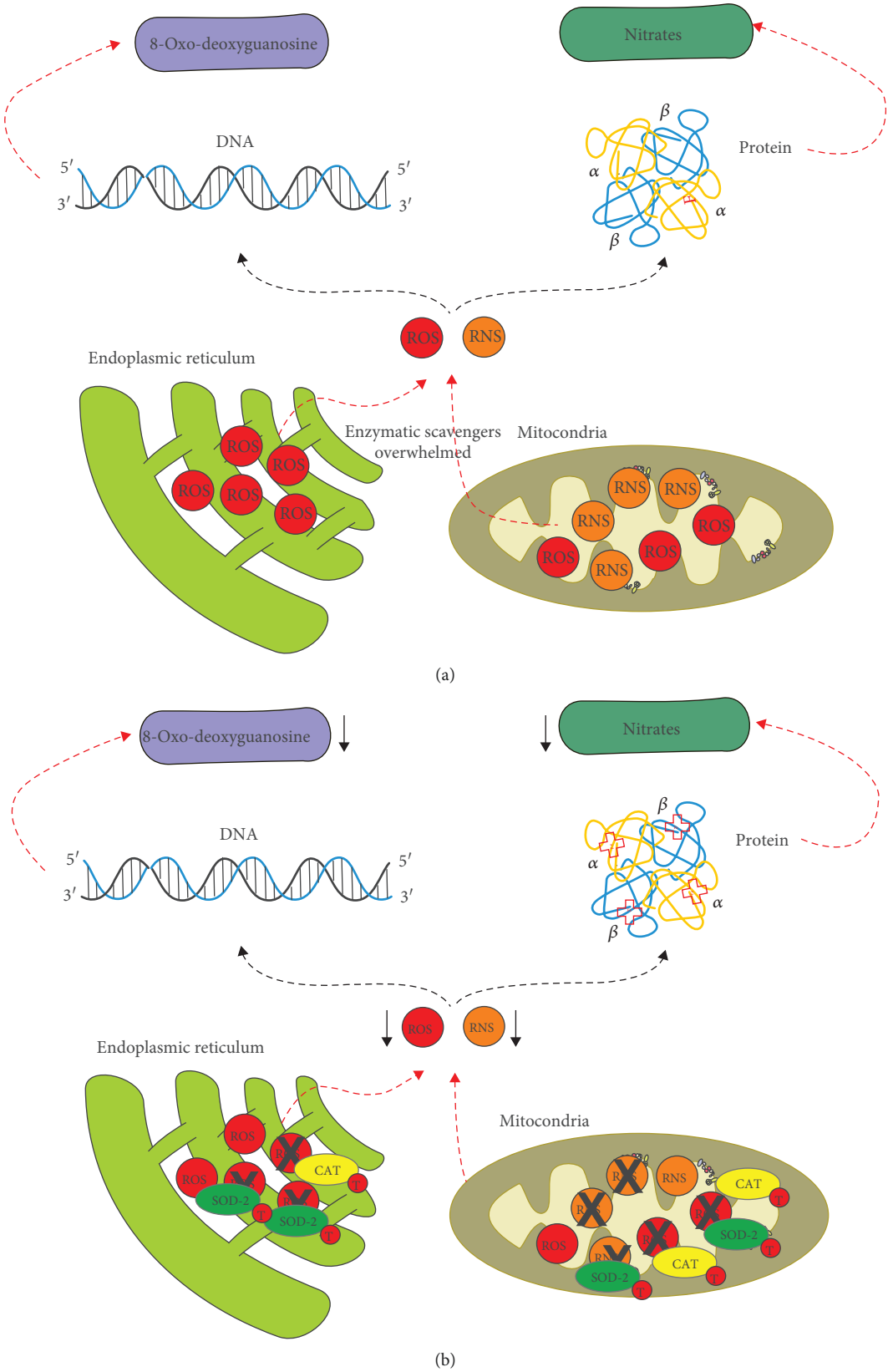

Figure 6: Modulation of oxidative stress during the I/R lesion. (a) Production of OS during the I/R lesion without telmisartan; overproduction of ROS and RNS overpasses the enzymatic scavenger systems, increasing the damage of the components of the cell such as DNA and proteins. (b) Modulation of OS by telmisartan; producing the increase of SOD and CAT that induces reduction of ROS and RNS.

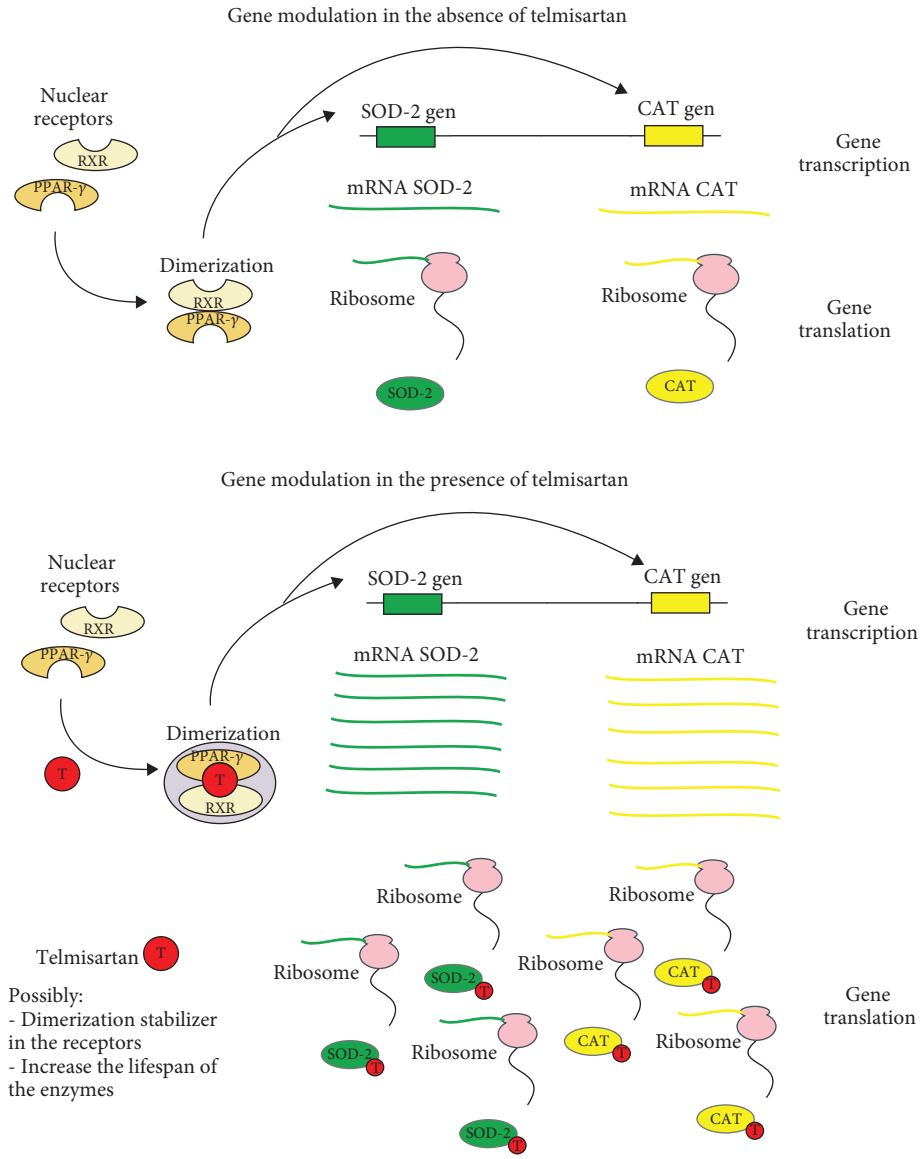

Figure 7: Telmisartan's possible mechanisms of action.

involves many regulatory steps that are influenced by local and systemic responses that exceed the scope of this study. Nevertheless, these two processes are probably coactivated by several gene regulation and signaling mechanisms. One of the most important check points should be OS modulation because we demonstrated that enzyme system modulation improves the damage limitation and the recovery process. We also evaluated the presence of immune modulation by telmisartan [19, 20, 33, 37, 61, 62], apparently increasing the recovery effect on the muscle skeletal cells. Telmisartan affected the inflammatory response by causing a continuous increase in inflammatory cell infiltration, but at the same time, tissue damage improvement in the muscle skeletal cells was demonstrated for the first time. Apparently, the influence of telmisartan on gene expression within the first 72 h and the increase in the bioavailability of enzyme systems that modulate OS help in the upregulation of the reparatory immune cells, besides overactivation of the damage limitation of the immune system. However, because no specific biomarkers of inflammatory response and histological markers exist, no definitive conclusions can be drawn.

6. Conclusions

Telmisartan treatment results in the upregulation of the enzyme scavengers SOD and CAT during an I/R lesion formation, possibly not only through gene expression induction but also through prolongation of the lifespan of the enzymes (Figure 7). Modulation of gene expression of SOD and CAT levels contributes to the recovery as well as to a decrease in the damage during the late phase of the I/R lesion.

Data Availability

We guarantee the veracity of the data shown here, and if you require us, we can provide the databases of each one of the experiments and the authorization document of the ethics and research committee.

Conflicts of Interest

The authors declare that they have no conflicts of interest.

References

[1] T. Kalogeris, C. P. Baines, M. Krenz, and R. J. Korthuis, "Ischemia/reperfusion," *Comprehensive Physiology*, vol. 7, no. 1, pp. 113–170, 2016.

[2] S. Q. Rodríguez-Lara, L. García-Benavides, and A. G. Miranda-Díaz, "The renin-angiotensin-aldosterone system as a therapeutic target in late injury caused by ischemia-reperfusion," *International Journal of Endocrinology*, vol. 2018, Article ID 3614303, 18 pages, 2018.

[3] S. Q. Rodríguez-Lara, E. G. Cardona-Muñoz, E. J. Ramírez-Lizardo et al., "Alternative interventions to prevent oxidative damage following ischemia/reperfusion," *Oxidative Medicine and Cellular Longevity*, vol. 2016, Article ID 7190943, 16 pages, 2016.

[4] T. Kalogeris, C. P. Baines, M. Krenz, and R. J. Korthuis, "Cell biology of ischemia/reperfusion injury," *International Review of Cell and Molecular Biology*, vol. 298, pp. 229–317, 2012.

[5] F. Sanchis-Gomar, C. Perez-Quilis, R. Leischik, and A. Lucia, "Epidemiology of coronary heart disease and acute coronary syndrome," *Annals of Translational Medicine*, vol. 4, no. 13, p. 256, 2016.

[6] B. Ziaeian and G. C. Fonarow, "Epidemiology and aetiology of heart failure," *Nature Reviews Cardiology*, vol. 13, no. 6, pp. 368–378, 2016.

[7] D. Smajlović, "Strokes in young adults: epidemiology and prevention," *Vascular Health and Risk Management*, vol. 11, pp. 157–164, 2015.

[8] W. J. Powers, A. A. Rabinstein, T. Ackerson et al., "2018 guidelines for the early management of patients with acute ischemic stroke: a guideline for healthcare professionals from the American Heart Association/American Stroke Association," *Stroke*, vol. 49, no. 3, pp. e46–e99, 2018.

[9] D. J. Hausenloy and D. M. Yellon, "Myocardial ischemia-reperfusion injury: a neglected therapeutic target," *The Journal of Clinical Investigation*, vol. 123, no. 1, pp. 92–100, 2013.

[10] E. Birben, U. M. Sahiner, C. Sackesen, S. Erzurum, and O. Kalayci, "Oxidative stress and antioxidant defense," *World Allergy Organization Journal*, vol. 5, no. 1, pp. 9–19, 2012.

[11] C. Penna, D. Mancardi, S. Raimondo, S. Geuna, and P. Pagliaro, "The paradigm of postconditioning to protect the heart," *Journal of Cellular and Molecular Medicine*, vol. 12, no. 2, pp. 435–458, 2008.

[12] S. Y. Lee, K. N. Kang, J. H. Kang et al., "Pharmacokinetics of a telmisartan, amlodipine and hydrochlorothiazide fixed-dose combination: a replicate crossover study in healthy Korean male subjects," *Tropical Journal of Pharmaceutical Research*, vol. 16, no. 9, pp. 2245–2253, 2017.

[13] P. Patel, "Telmisartan: clinical evidence across the cardiovascular and renal disease continuum," *Drugs & Therapy Perspectives*, vol. 33, no. 2, pp. 77–87, 2017.

[14] Y. Fan, D. Zhang, and D. Xiang, "Delayed protective effect of telmisartan on lung ischemia/reperfusion injury in valve replacement operations," *Experimental and Therapeutic Medicine*, vol. 12, no. 4, pp. 2577–2581, 2016.

[15] H. Eslami, A. M. Sharifi, H. Rahimi, and M. Rahati, "Protective effect of telmisartan against oxidative damage induced by high glucose in neuronal PC12 cell," *Neuroscience Letters*, vol. 558, pp. 31–36, 2014.

[16] K. Ozeki, S. Tanida, C. Morimoto et al., "Telmisartan inhibits cell proliferation by blocking nuclear translocation of ProHB-EGF C-terminal fragment in colon cancer cells," *PLoS One*, vol. 8, no. 2, article e56770, 2013.

[17] K. Takeuchi, K. Yamamoto, M. Ohishi et al., "Telmisartan modulates mitochondrial function in vascular smooth muscle cells," *Hypertension Research*, vol. 36, no. 5, pp. 433–439, 2013.

[18] H. Fujita, H. Fujishima, T. Morii et al., "Modulation of renal superoxide dismutase by telmisartan therapy in C57BL/6-*Ins2*^{Akita} diabetic mice," *Hypertension Research*, vol. 35, no. 2, pp. 213–220, 2012.

[19] T. Pang, J. Benicky, J. Wang, M. Orecna, E. Sanchez-Lemus, and J. M. Saavedra, "Telmisartan ameliorates lipopolysaccharide-induced innate immune response through *peroxisome proliferator-activated receptor-γ* activation in human monocytes," *Journal of Hypertension*, vol. 30, no. 1, pp. 87–96, 2012.

[20] T. Pang, J. Wang, J. Benicky, E. Sanchez-Lemus, and J. M. Saavedra, "Telmisartan directly ameliorates the neuronal inflammatory response to IL-1β partly through the JNK/c-Jun and NADPH oxidase pathways," *Journal of Neuroinflammation*, vol. 9, no. 1, p. 102, 2012.

[21] H. Fujita, T. Sakamoto, K. Komatsu et al., "Reduction of circulating superoxide dismutase activity in type 2 diabetic patients with microalbuminuria and its modulation by telmisartan therapy," *Hypertension Research*, vol. 34, no. 12, pp. 1302–1308, 2011.

[22] Y. Kumtepe, F. Odabasoglu, M. Karaca et al., "Protective effects of telmisartan on ischemia/reperfusion injury of rat ovary: biochemical and histopathologic evaluation," *Fertility and Sterility*, vol. 93, no. 4, pp. 1299–1307, 2010.

[23] M. Lehrke and M. A. Lazar, "The many faces of PPARγ," *Cell*, vol. 123, no. 6, pp. 993–999, 2005.

[24] J. Camps, A. García-Heredia, A. Rull et al., "PPARs in regulation of paraoxonases: control of oxidative stress and inflammation pathways," *PPAR Research*, vol. 2012, Article ID 616371, 10 pages, 2012.

[25] UU E National Research Council, *Guide for the Care and Use of Laboratory Animals*, National Academy Press, Washington DC, USA, 2001.

[26] W. M. Freeman, S. J. Walker, and K. E. Vrana, "Quantitative RT-PCR: pitfalls and potential," *BioTechniques*, vol. 26, no. 1, pp. 112–125, 1999.

[27] M. C. McCormack, E. Kwon, K. R. Eberlin et al., "Development of reproducible histologic injury severity scores: skeletal muscle reperfusion injury," *Surgery*, vol. 143, no. 1, pp. 126–133, 2008.

[28] C. Hu, F. E. Muller-Karger, and R. G. Zepp, "Absorbance, absorption coefficient, and apparent quantum yield: a

comment on common ambiguity in the use of these optical concepts," *Limnology and Oceanography*, vol. 47, no. 4, pp. 1261–1267, 2002.

[29] H. D. VanGuilder, K. E. Vrana, and W. M. Freeman, "Twenty-five years of quantitative PCR for gene expression analysis," *BioTechniques*, vol. 44, no. 5, pp. 619–626, 2008.

[30] V. Demidchik, "Mechanisms of oxidative stress in plants: from classical chemistry to cell biology," *Environmental and Experimental Botany*, vol. 109, pp. 212–228, 2015.

[31] A. Daiber, M. Mader, P. Stamm et al., "Oxidative stress and vascular function," *Cell Membranes and Free Radical Research*, vol. 5, no. 1, pp. 221–231, 2013.

[32] D. P. Jones, "Redefining oxidative stress," *Antioxidants & Redox Signaling*, vol. 8, no. 9-10, pp. 1865–1879, 2006.

[33] M. T. Kelleni, S. A. Ibrahim, and A. M. Abdelrahman, "Effect of captopril and telmisartan on methotrexate-induced hepatotoxicity in rats: impact of oxidative stress, inflammation and apoptosis," *Toxicology Mechanisms and Methods*, vol. 26, no. 5, pp. 371–377, 2016.

[34] M. Dessì, A. Piras, C. Madeddu et al., "Long-term protective effects of the angiotensin receptor blocker telmisartan on epirubicin-induced inflammation, oxidative stress and myocardial dysfunction," *Experimental and Therapeutic Medicine*, vol. 2, no. 5, pp. 1003–1009, 2011.

[35] M. Knorr, M. Hausding, S. Kröller-Schuhmacher et al., "Nitroglycerin-induced endothelial dysfunction and tolerance involve adverse phosphorylation and S-glutathionylation of endothelial nitric oxide synthase: beneficial effects of therapy with the AT1 receptor blocker telmisartan," *Arteriosclerosis, Thrombosis, and Vascular Biology*, vol. 31, no. 10, pp. 2223–2231, 2011.

[36] K. Washida, M. Ihara, K. Nishio et al., "Nonhypotensive dose of telmisartan attenuates cognitive impairment partially due to peroxisome proliferator-activated Receptor-γ activation in mice with chronic cerebral hypoperfusion," *Stroke*, vol. 41, no. 8, pp. 1798–1806, 2010.

[37] S. Cianchetti, A. Del Fiorentino, R. Colognato, R. Di Stefano, F. Franzoni, and R. Pedrinelli, "Anti-inflammatory and antioxidant properties of telmisartan in cultured human umbilical vein endothelial cells," *Atherosclerosis*, vol. 198, no. 1, pp. 22–28, 2008.

[38] T. Matsui, S. Yamagishi, S. Ueda et al., "Telmisartan, an angiotensin II type 1 receptor blocker, inhibits advanced glycation end-product (AGE)-induced monocyte chemoattractant protein-1 expression in mesangial cells through downregulation of receptor for AGEs via peroxisome proliferator-activated receptor-γ activation," *Journal of International Medical Research*, vol. 35, no. 4, pp. 482–489, 2007.

[39] H. Sugiyama, M. Kobayashi, D.-H. Wang et al., "Telmisartan inhibits both oxidative stress and renal fibrosis after unilateral ureteral obstruction in acatalasemic mice," *Nephrology Dialysis Transplantation*, vol. 20, no. 12, pp. 2670–2680, 2005.

[40] M. M. Goyal and A. Basak, "Human catalase: looking for complete identity," *Protein & Cell*, vol. 1, no. 10, pp. 888–897, 2010.

[41] M. Iqbal, K. Dubey, T. Anwer, A. Ashish, and K. K. Pillai, "Protective effects of telmisartan against acute doxorubicin-induced cardiotoxicity in rats," *Pharmacological Reports*, vol. 60, no. 3, pp. 382–390, 2008.

[42] C. Glorieux, M. Zamocky, J. M. Sandoval, J. Verrax, and P. B. Calderon, "Regulation of catalase expression in healthy and cancerous cells," *Free Radical Biology & Medicine*, vol. 87, pp. 84–97, 2015.

[43] J. Kodydková, L. Vávrová, M. Kocík, and A. Zak, "Human catalase, its polymorphisms, regulation and changes of its activity in different diseases," *Folia Biologica*, vol. 60, no. 4, p. 153, 2014.

[44] Y. Okuno, M. Matsuda, Y. Miyata et al., "Human catalase gene is regulated by peroxisome proliferator activated receptor-gamma through a response element distinct from that of mouse," *Endocrine Journal*, vol. 57, no. 4, pp. 303–309, 2010.

[45] Y. Okuno, M. Matsuda, H. Kobayashi et al., "Adipose expression of catalase is regulated via a novel remote PPARγ-responsive region," *Biochemical and Biophysical Research Communications*, vol. 366, no. 3, pp. 698–704, 2008.

[46] G. D. Girnun, F. E. Domann, S. A. Moore, and M. E. C. Robbins, "Identification of a functional peroxisome proliferator-activated receptor response element in the rat catalase promoter," *Molecular Endocrinology*, vol. 16, no. 12, pp. 2793–2801, 2002.

[47] M. B. Nolly, C. I. Caldiz, A. M. Yeves et al., "The signaling pathway for aldosterone-induced mitochondrial production of superoxide anion in the myocardium," *Journal of Molecular and Cellular Cardiology*, vol. 67, pp. 60–68, 2014.

[48] T. P. Tran, H. Tu, I. I. Pipinos, R. L. Muelleman, H. Albadawi, and Y. L. Li, "Tourniquet-induced acute ischemia–reperfusion injury in mouse skeletal muscles: involvement of superoxide," *European Journal of Pharmacology*, vol. 650, no. 1, pp. 328–334, 2011.

[49] V. G. Grivennikova and A. D. Vinogradov, "Generation of superoxide by the mitochondrial complex I," *Biochimica et Biophysica Acta (BBA) - Bioenergetics*, vol. 1757, no. 5-6, pp. 553–561, 2006.

[50] A. G. Estevez and J. Jordan, "Nitric oxide and superoxide, a deadly cocktail," *Annals of the New York Academy of Sciences*, vol. 962, no. 1, pp. 207–211, 2002.

[51] K. R. Messner and J. A. Imlay, "Mechanism of superoxide and hydrogen peroxide formation by fumarate reductase, succinate dehydrogenase, and aspartate oxidase," *Journal of Biological Chemistry*, vol. 277, no. 45, pp. 42563–42571, 2002.

[52] S. Bhakdi and E. Martin, "Superoxide generation by human neutrophils induced by low doses of Escherichia coli hemolysin," *Infection and Immunity*, vol. 59, no. 9, pp. 2955–2962, 1991.

[53] U. Förstermann and W. C. Sessa, "Nitric oxide synthases: regulation and function," *European Heart Journal*, vol. 33, no. 7, pp. 829–837, 2012.

[54] U. Förstermann and H. Li, "Therapeutic effect of enhancing endothelial nitric oxide synthase (eNOS) expression and preventing eNOS uncoupling," *British Journal of Pharmacology*, vol. 164, no. 2, pp. 213–223, 2011.

[55] H. Kleinert, J. Art, and A. Pautz, "Regulation of the expression of inducible nitric oxide synthase," in *Nitric Oxide*, pp. 211–267, Elsevier, 2010.

[56] U. Förstermann, N. Xia, and H. Li, "Roles of vascular oxidative stress and nitric oxide in the pathogenesis of atherosclerosis," *Circulation Research*, vol. 120, no. 4, pp. 713–735, 2017.

[57] S. M. Davidson and M. R. Duchen, "Endothelial mitochondria: contributing to vascular function and disease," *Circulation Research*, vol. 100, no. 8, pp. 1128–1141, 2007.

[58] P. Ghafourifar and E. Cadenas, "Mitochondrial nitric oxide synthase," *Trends in Pharmacological Sciences*, vol. 26, no. 4, pp. 190–195, 2005.

[59] W. O. Sampaio, R. A. Souza dos Santos, R. Faria-Silva, L. T. da Mata Machado, E. L. Schiffrin, and R. M. Touyz, "Angiotensin-(1-7) through receptor Mas mediates endothelial nitric oxide synthase activation via Akt-dependent pathways," *Hypertension*, vol. 49, no. 1, pp. 185–192, 2007.

[60] D. D. Thomas, X. Liu, S. P. Kantrow, and J. R. Lancaster, "The biological lifetime of nitric oxide: implications for the perivascular dynamics of NO and O_2," *Proceedings of the National Academy of Sciences of the United States of America*, vol. 98, no. 1, pp. 355–360, 2001.

[61] A. Nakano, Y. Hattori, C. Aoki, T. Jojima, and K. Kasai, "Telmisartan inhibits cytokine-induced nuclear factor-κB activation independently of the peroxisome proliferator-activated receptor-γ," *Hypertension Research*, vol. 32, no. 9, pp. 765–769, 2009.

[62] Q. Tian, R. Miyazaki, T. Ichiki et al., "Inhibition of tumor necrosis factor-α–induced interleukin-6 expression by telmisartan through cross-talk of peroxisome proliferator-activated receptor-γ with nuclear factor κB and CCAAT/enhancer-binding protein-β," *Hypertension*, vol. 53, no. 5, pp. 798–804, 2009.

Hindawi
Oxidative Medicine and Cellular Longevity
Volume 2019, Article ID 3520789, 16 pages
https://doi.org/10.1155/2019/3520789

Research Article

Chlorella vulgaris Improves the Regenerative Capacity of Young and Senescent Myoblasts and Promotes Muscle Regeneration

Nurhazirah Zainul Azlan,[1,2] **Yasmin Anum Mohd Yusof**,[1] **Ekram Alias**,[1] **and Suzana Makpol**[1]

[1]*Department of Biochemistry, Faculty of Medicine, Level 17, Preclinical Building, Universiti Kebangsaan Malaysia Medical Centre, Jalan Yaacob Latif, Bandar Tun Razak, Cheras, 56000 Kuala Lumpur, Malaysia*
[2]*Department of Basic Medical Sciences for Nursing, Kulliyyah of Nursing, International Islamic University Malaysia, P. O. Box 141, 25710 Kuantan, Pahang, Malaysia*

Correspondence should be addressed to Suzana Makpol; suzanamakpol@ppukm.ukm.edu.my

Received 8 February 2019; Revised 18 April 2019; Accepted 7 May 2019; Published 4 June 2019

Guest Editor: Andrea Vasconsuelo

Sarcopenia is characterized by the loss of muscle mass, strength, and function with ageing. With increasing life expectancy, greater attention has been given to counteracting the effects of sarcopenia on the growing elderly population. *Chlorella vulgaris*, a microscopic, unicellular, green alga with the potential for various pharmaceutical uses, has been widely studied in this context. This study is aimed at determining the effects of *C. vulgaris* on promoting muscle regeneration by evaluating myoblast regenerative capacity *in vitro*. Human skeletal myoblast cells were cultured and underwent serial passaging into young and senescent phases and were then treated with *C. vulgaris*, followed by the induction of differentiation. The ability of *C. vulgaris* to promote myoblast differentiation was analysed through cellular morphology, real-time monitoring, cell proliferation, senescence-associated β-galactosidase (SA-β-gal) expression, myogenic differentiation, myogenin expression, and cell cycle profiling. The results obtained showed that senescent myoblasts exhibited an enlarged and flattened morphology, with increased SA-β-gal expression, reduced myogenic differentiation, decreased expression of myogenin, and an increased percentage of cells in the G_0/G_1 phase. Treatment with *C. vulgaris* resulted in decreased SA-β-gal expression and promotion of myogenic differentiation, as observed via an increased fusion index, maturation index, myotube size, and surface area and an increased percentage of cells that stained positive for myogenin. In conclusion, *C. vulgaris* improves the regenerative capacity of young and senescent myoblasts and promotes myoblast differentiation, indicating its potential to promote muscle regeneration.

1. Introduction

A decrease in performance of bodily functions is observed with the progression of ageing. Various organs and systems, such as the nervous system, digestive system, and cardiovascular system, are affected by ageing. In the muscular skeletal system, a sequential loss of skeletal muscle mass, strength, and function is observed with increasing age. This condition is known as sarcopenia [1, 2]. Sarcopenia has been described as an age-related decline of muscle mass, function, and strength, with high prevalence after ageing [3]. A longitudinal study revealed muscle mass loss at a rate of 0.64% to 0.70% per year in women and 0.80% to 0.98% per year in men, along with muscle strength loss at a rate of 2.5% to 3% per year in women and 3% to 4% per year in men, in people aged 75 years and older [4].

Although sarcopenia manifests in older people, the causes of this condition are multifactorial and involve changes in the body, such as chronic disease, inflammation, and insulin resistance, in addition to environmental factors like nutritional deficiencies, bed rest, and physical inactivity [1]. An average of 36% and 42% of the female body and male body, respectively, consists of skeletal muscle mass that has the ability to contract or stretch to produce skeletal movement. Skeletal muscle generates heat for the maintenance of body temperature, stores protein reserves, and maintains body posture, while also supporting and protecting soft tissues [2, 5, 6].

The negative effects of sarcopenia include a decrease in the number of motor units and muscle fibre size and an increase in muscle fibre atrophy. However, other factors such as nutrition, hormones, metabolism, immunological conditions, and a sedentary lifestyle can also lead to a decrease in muscle mass and strength. These cause increased abnormal gait, impaired oxidative metabolism, poor glucose regulation, weakness, loss of independence, decreased mobility, falls and fractures, and eventually, morbidity, and mortality [2, 5, 7]. Findings from a previous body composition study demonstrated a marked decrease in skeletal muscle mass, changes in muscle composition, and a greater infiltration of fat into muscles in individuals with sarcopenia, which is associated with ageing [8].

Currently, sarcopenia is an alarming problem in the elderly due to longer life expectancies. Several strategies have been used to fight sarcopenia, such as physical exercise, nutritional supplements, and hormone therapy, e.g., testosterone and oestrogen, which have been shown to improve muscle mass and strength [7, 9, 10]. Greater attention has been given to dealing with the outcomes of sarcopenia, with the aim of reducing the effects of this age-associated disability. In this study, *Chlorella vulgaris* was used to treat myoblast cells in culture in an attempt to determine its effect on the promotion of myoblast differentiation.

C. vulgaris was discovered in 1890 by a Dutch researcher named Martinus Willem Beijerinck, who described it as coccoid green algal "balls" with well-defined nuclei [11, 12]. *C. vulgaris* is a microscopic, unicellular freshwater green alga that contains highly nutritious substances such as proteins, nucleic acids, carbohydrates, chlorophylls, vitamins, and minerals and has been widely studied thanks to its potential applications in the pharmaceutical industry [13]. It also contains β-carotene, lutein, chlorophyll-a and chlorophyll-b, ascorbic acid, tocopherol, riboflavin, and retinol [14, 15].

Various studies have reported on the beneficial effects of *C. vulgaris*, such as its hypolipidemic action [16, 17] and its effects against diabetes [18, 19] and cancer [20–22]. A previous study reported that glucose and insulin resistance were increased and triglyceride, cholesterol, and free fatty acid levels were decreased in high-fat diet-induced insulin-resistant obese mice treated with *C. vulgaris* [17]. In a liver cancer rat model, treatment with *C. vulgaris* decreased hepatocyte proliferation by decreasing Bcl-2 expression and promoted apoptosis by increasing caspase-8 expression [21]. These potential protective effects of *C. vulgaris* might be due to the presence of bioactive compounds. This study is aimed at determining the effects of *C. vulgaris* on the differentiation of myoblast cells during the formation of mature myotubes in culture and thus investigated its potential for the promotion of muscle regeneration to combat sarcopenia.

2. Materials and Methods

2.1. Experimental Design. Human skeletal muscle myoblast (HSMM) cells (Lonza, Walkersville, MD, USA) were chosen as a model of replicative senescence in this study. The myoblast cells underwent serial passaging to reach the desired population doubling (PD), and a lifespan curve was determined. The morphology of myoblast cells was observed throughout the serial passaging. A senescence biomarker, SA-β-gal, was measured in young and senescent myoblast cells, in addition to myogenic purity, to allow for dependable statistical analysis of different PDs. The viability of control and *C. vulgaris*-treated cells was determined by the CellTiter 96® Aqueous Non-Radioactive Cell Proliferation Assay (MTS; Promega, Madison, WI, USA) and monitored by real-time monitoring using the iCELLigence system (ACEA Biosciences Inc., San Diego, CA, USA). After the optimum dosage of *C. vulgaris* was administered, myoblast cells were induced to differentiate. The differentiation of myoblast cells into mature myotubes was further characterized on days 1, 3, 5, and 7 of differentiation induction by determining the fusion index, maturation index, and myotube size and surface area. The number of cells expressing the differentiation marker myogenin was also determined. This was followed by determination of the cell cycle profile using a fluorescence-activated cell sorter (FACS), the BD FACSVerse™ flow cytometer (Becton Dickinson, USA).

2.2. Cell Culture. Human skeletal muscle myoblasts (HSMM) were purchased from Lonza (Walkersville, MD, USA) from two different donors, a 20-year-old Caucasian female and a 17-year-old Caucasian female. The skeletal muscle myoblasts were cultured in skeletal muscle basal medium (SkBM) with supplementation of 50 ml foetal bovine serum (FBS), 10 ml L-glutamine, 0.5 ml human epidermal growth factor (hEGF), 0.5 ml dexamethasone, and 0.5 ml gentamicin/amphotericin-B (Lonza, Walkersville, MD, USA). Cells were cultured at 37°C in a humid atmosphere containing 5% CO_2. The skeletal muscle myoblast cells then underwent serial passaging to reach senescence. The population doubling (PD) of the cells was calculated for each passage according to the formula $\ln(N/n)/\ln 2$, where N is the number of cells at the harvesting stage and n is the number of cells at the seeding stage [23]. The starting PD for this study was PD 8. The skeletal muscle myoblast cells reached replicative senescence when the cells could no longer proliferate, as indicated by a very slow proliferation rate even with consecutive replenishment. Morphological changes in the myoblast cells were observed throughout passaging, and the myoblast cell lifespan curve was developed based on the PD and number of days.

2.3. Real-Time Monitoring. The iCELLigence system (ACEA Biosciences Inc., San Diego, CA, USA) was utilized to monitor cellular events in real time by recording the electrical impedance signal, followed by converting the impedance value into a cell index (CI) value. The CI is an arbitrary unit that reflects the cell number, morphology, and viability in a given culture well. 1×10^4 myoblast cells were plated in each well of an E-plate L8 and further cultivated at 37°C in a humid atmosphere containing 5% CO_2. Seeding was allowed for 24 h followed by treatment with *C. vulgaris* and incubation for up to seven days. The CI value was recorded every 10 minutes, and the graph of myoblast cell proliferation was plotted using RTCA Data Analysis Software version 1 (ACEA Biosciences Inc., San Diego, CA, USA). Two E-plate

L8 plates were run simultaneously for all dosages of *C. vulgaris* treatment, with two replicates ($n = 2$) for all treatment groups.

2.4. Determination of Myogenic Purity. Immunocytochemistry was used to determine myoblast cell purity. Skeletal muscle myoblast cells were seeded at a density of 5×10^3 cells per well in a 96-well plate. After cells were washed with phosphate buffer saline (PBS), the cells were fixed in cold 100% ethanol for 10 minutes followed by incubation with 1% FBS for 30 minutes, with 3x PBS washes in between these procedures. Then, the cells were incubated sequentially with an anti-desmin monoclonal antibody in a dark environment for 1 h (D33, Dako, Glostrup, Denmark) and Alexa Flour 488 goat anti-mouse in a dark environment for 1 h 45 min (Life Technologies, Carlsbad, CA, USA), with 3x PBS washes in between incubations. Hoechst 33342 (Life Technologies, Carlsbad, CA, USA) was then used to visualize the cell nuclei. The cells were viewed under an EVOS FL Digital Inverted Fluorescence Microscope (Life Technologies, Carlsbad, CA, USA). The percentage of desmin-positive cells was determined by examining a minimum of 50 cells from three independent cultures [24].

2.5. Determination of Senescence Biomarkers. Identification of senescent skeletal muscle myoblast cells was carried out using the Senescent Cell Histochemical Staining Kit (Sigma-Aldrich, St. Louis, Missouri, USA) according to the manufacturer's instructions. This assay detects the activity of β-galactosidase, which is normally present in senescent cells. Briefly, cells at a density of 8×10^4 were cultured in a 6-well plate, washed twice with PBS, and fixed using fixation buffer for 7 minutes. Then, cells were washed with PBS three times before overnight incubation in the staining mixture solution at 37°C in the absence of CO_2. Blue-stained cells were observed under a light microscope using 40x magnification. The percentage of blue-stained cells versus the total number of counted cells was calculated, with a minimum of 100 cells being observed.

2.6. Preparation of Chlorella vulgaris. A stock of *C. vulgaris* Beijerinck (strain 072) was obtained from the University of Malaya Algae Culture Collection (UMACC, Malaysia). The stock was grown in Bold's Basal Medium (BBM) with a 12 h dark and 12 h light cycle. The alga was then harvested by centrifugation at 1000 rpm and dried using a freeze dryer. Later, the alga was dissolved in distilled water at a concentration of 10% (w/v) and boiled at 100°C for 20 minutes using the reflux method. The alga was centrifuged and lyophilised using a freeze dryer to obtain *C. vulgaris* in a powdered form.

2.7. Cell Viability Assay. Cell viability was determined using the CellTiter 96® Aqueous Non-Radioactive Cell Proliferation Assay (MTS; Promega, Madison, WI, USA) according to the manufacturer's instructions. A total of 5×10^3 cells was cultured in a 96-well plate and incubated in a CO_2 incubator at 37°C for 24 h. Then, the media were replaced with media containing *C. vulgaris* at various concentrations—0, 10, 50, 100, 200, 300, 400, and 500 μg/ml—and left in the CO_2 incubator at 37°C for 24 h. Next, 20 μl of 3-(4,5-dimethylthiazol-2-yl)-5-(3-carboxymethoxyphenyl)-2-(4-sulfophenyl)-2H-tetrazolium/phenazine methosulfate (MTS/PMS) solution was added into each well in a dark environment and cells were further incubated in the CO_2 incubator at 37°C for 2 h. The absorbance of MTS formazan was measured at 490 nm with a multimode plate reader (PerkinElmer, Waltham, MA, USA). The average reading of control myoblast cells was used to represent 100% cell viability, and the averages of triplicate readings of different concentrations of *C. vulgaris* were converted to a percentage value. The optimum dose of treatment was identified and used for subsequent experiments.

2.8. Induction of Myogenic Differentiation. For induction of muscle cell differentiation, the proliferation medium SkBM was replaced with a differentiation medium, DMEM:F12 (Lonza, Walkersville, MD, USA) with supplementation of 2% horse serum (ATCC, Baltimore, USA). The differentiation medium was changed every two days until the desired day of differentiation for parameter measurement.

2.9. Determination of Myogenic Differentiation. The differentiation of myoblast cells into mature myotubes was represented using the fusion index, maturation index, and myotube size and surface area, which revealed the efficiency of myogenic differentiation. Myoblast cells were cultured in a 96-well plate, and immunocytochemistry was used to stain the differentiated cells on days 1, 3, 5, and 7 of differentiation as described earlier in the myogenic purity methodology. The myotube surface area was measured using ImageJ software version 1.50i (National Institutes of Health, USA). The myotube size was determined by the number of nuclei per myotube in a minimum of 11 multinucleated cells in 3 different randomly chosen optical fields [24]. The formulas for calculating the fusion index [25] and maturation index [26] are shown below, and a minimum of 50 nuclei was counted in 3 different randomly chosen optical fields.

$$\text{Fusion index} = \frac{\text{the number of nuclei in myotubes}(\geq 2 \text{ nuclei})}{\text{the total number of desmin-positive nuclei}} \times 100\%,$$
$$\text{Maturation index} = \frac{\text{the number of nuclei in myotubes}(\geq 5 \text{ nuclei})}{\text{the total number of desmin-positive nuclei}} \times 100\%. \quad (1)$$

2.10. Determination of Myogenin Expression. The number of cells expressing myogenin was determined on day 1 and day 3 of differentiation using immunocytochemistry as described earlier in the myogenic purity methodology, but with a different primary antibody: a mouse monoclonal anti-myogenin antibody (F5D, Dako, Produktionsvej, Denmark) at a 1 : 20 dilution at 4°C overnight. This was followed by incubation with the secondary antibody Alexa Fluor 488 at a 1 : 1000 dilution at room temperature for 1 h 45 min. Cells were incubated with Hoechst 33342 at room temperature for 10 minutes to visualize the nuclei. The cells were viewed under an EVOS FL Digital Inverted Fluorescence Microscope (Life Technologies, Carlsbad, CA, USA). Myogenin expression

was calculated as the percentage of cells with myogenin-positive nuclei compared to the total number of nuclei.

2.11. Analysis of Cell Cycle by Flow Cytometry. DNA content was determined using the BD Cycletest^{TM} Plus DNA kit (Becton Dickinson, San Jose, CA, USA) according to the manufacturer's instructions. A total of 5×10^5 myoblast cells were washed with buffer solution before staining. The cells were first resuspended in Solution A and incubated at room temperature for 10 minutes. Next, Solution B was added and cells were incubated at room temperature for 10 minutes. Finally, Solution C was added and cells were incubated in the dark at 4°C for 10 minutes. Cells were then filtered with a 35 μm cell strainer cap. The cell cycle phase distribution of nuclear DNA was determined using a flow cytometer fluorescence-activated cell sorter (FACS), the BD FACS-Verse^{TM} flow cytometer (Becton Dickinson, USA). A total of 10,000 events were acquired, and the data obtained was analysed using MODFIT software (FACSCalibur BD, USA). The DNA content (x-axis, PI fluorescence) versus counts (y-axis) was plotted as a histogram.

2.12. Statistical Analysis. Data obtained were expressed as means ± SD, and statistical analysis was carried out using SPSS software version 23. Data were analysed using one-way ANOVA followed by Tukey's post hoc test for comparison between treatment and days and between dosages of treatments on a desired day. A p value < 0.05 was considered statistically significant.

3. Results

3.1. Myoblast Cells as an In Vitro Model of Cellular Senescence. The morphology of myoblast cells at PD 14 (young) and PD 21 (senescent) exhibited different characteristics: cells at PD 14 were spindle shaped with round nuclei, more branching, and multinucleation (Figure 1(a)), while cells at PD 21 were larger and flatter with few nuclei and less branching. Intermediate filaments became more prominent at PD 21, and the presence of vacuoles was observed (Figure 1(b)). Desmin staining was also performed to further elucidate the morphology of myoblast cells at PD 14 (Figure 1(c)) and PD 21 (Figure 1(d)). Myoblast cells at PD 14 were multinucleated, and myoblast cells at PD 21 showed formation of intermediate filaments. Cells at PD 21 also possessed a slower proliferation rate even with consecutive renewal of growth media. Serial passaging was carried out on myoblasts from both donors to achieve replicative senescence. A lifespan curve of myoblasts from the 20-year-old donor was plotted showing cumulative population doublings (PD) versus the number of days (Figure 1(e)). The lifespan curve showed a progressive increase in the proliferation of myoblast cells as the number of days increased. However, the lifespan curve began to plateau at higher PDs, indicating a slower proliferation rate as cells moved towards replicative senescence. The increase in PD resulted in an increased percentage of cells that stained positive for SA-β-gal, as seen through the significantly higher SA-β-gal expression observed in PD 21 cells compared to both PD 14 and PD 18 cells (Figure 1(f)). Thus, myoblast cells at PD 14 were considered young, while cells above PD 20 were considered senescent cells. The presence of more than 92% desmin-positive cells in each PD of the myoblasts confirmed no loss of myogenicity, allowing for dependable statistical comparison among PDs throughout the study (Table 1).

3.2. Effects of C. vulgaris on Cell Viability and Proliferation. Real-time recording by iCELLigence was applied to determine the cell indexes of myoblasts from both donors at PD 14 (young cells) and PD 21 (senescent cells). The cell index graph of both PDs showed an increase in the cell indexes throughout the seven days of incubation for myoblasts from both the 17-year-old (Figures 2(a) and 2(b)) and 20-year-old (Figures 2(c) and 2(d)) donors. Treatment with *C. vulgaris* at various concentrations did not affect the proliferation of myoblast cells at both PDs for both the 17-year-old (Figures 3(a) and 3(b)) and 20-year-old (Figures 3(c) and 3(d)) donors which was increased with increasing number of days. No significant difference was observed in the cell proliferation and viability of myoblasts from both donors when treated with *C. vulgaris* at different PDs. However, myoblast cells from the 20-year-old donor exerted a greater index of proliferation throughout the study when treated with *C. vulgaris* as compared to myoblasts from the 17-year-old donor (Figures 3(c) and 3(d)). Therefore, for subsequent experiments, myoblasts from the 20-year-old donor were used.

The cell viability test demonstrated that incubation with *C. vulgaris* at various concentrations maintained the viability of young (PD 14) myoblast cells. However, a significant decrease in the viability of senescent (PD 21) myoblasts was observed when cells were treated with *C. vulgaris* at concentrations of 400 and 500 μg/ml (Figure 4). Myoblast cells treated with *C. vulgaris* at concentrations of 10 and 100 μg/ml demonstrated the highest percentage of viable cells in both young and senescent myoblasts. Therefore, *C. vulgaris* at concentrations of 10 and 100 μg/ml were chosen for subsequent experiments.

3.3. Effects of C. vulgaris on the Replicative Senescence of Human Myoblasts. Young (PD 14) and senescent (PD 21) myoblasts undergoing various treatments were stained for SA-β-gal as shown in Figures 5(a)–5(f). The percentage of cells that stained positive for SA-β-gal was significantly higher in senescent myoblasts compared to young cells (Figure 5(g)). However, treatment of senescent cells with *C. vulgaris* at 10 and 100 μg/ml decreased the percentage of cells that stained positive for SA-β-gal compared to untreated controls ($p < 0.05$).

3.4. Effect of C.vulgaris on the Promotion of Myoblast Differentiation. Young (PD 14) and senescent (PD 21) myoblast cells were differentiated for 7 days to form myotubes. Photomicrographs of desmin staining for young control myoblasts and *C. vulgaris*-treated young myoblasts are shown in Figures 6(a)–6(c), and those for senescent control myoblasts and *C. vulgaris*-treated senescent myoblasts are shown in Figures 6(d)–6(f). Myoblast differentiation was

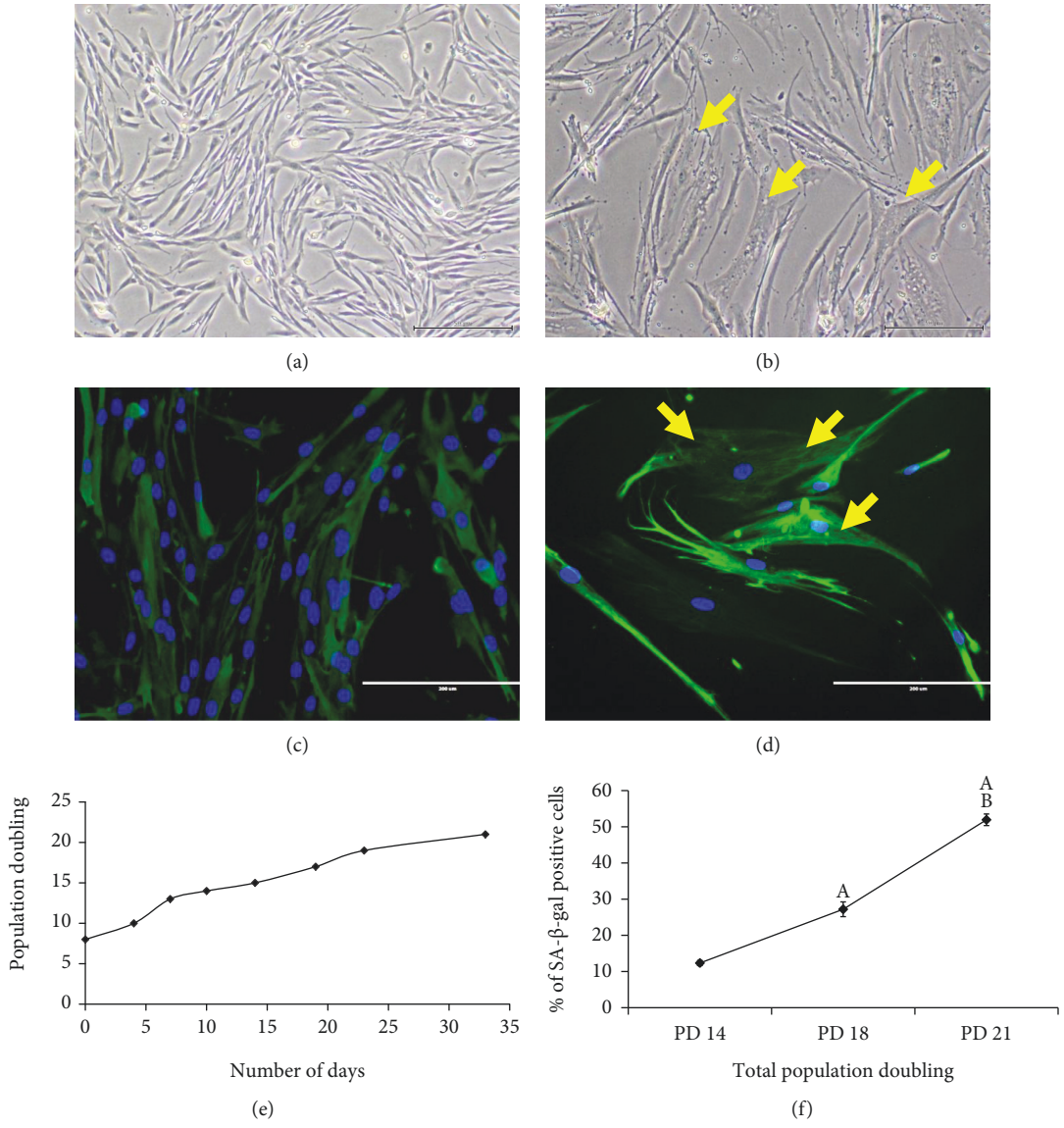

Figure 1: Morphological changes and serial passaging of myoblast cells in culture. Myoblast cells exhibited different morphological characteristics, as seen in the photomicrographs of young (a) and senescent (b) myoblast cells (magnification: 50x), and the photomicrographs of desmin staining of young (c) and senescent (d) cells (magnification: 200x). Myoblasts were stained for desmin (green) and nuclei (blue). Arrows indicate the intermediate filaments and vacuoles observed in senescent myoblast cells. Myoblast cells also lost their proliferative capacity with serial passaging as observed in the proliferation-lifespan curve of myoblast cells (e) and in the increased percentage of cells that stained positive for SA-β-gal at higher PDs (f). The data are presented as the means ± SD, $n = 3$. $^{A}p < 0.05$: significantly different compared to myoblasts at PD 14 (young); $^{B}p < 0.05$: significantly different compared to myoblasts at PD 18 (presenescent), with a post hoc Tukey HSD test.

Table 1: The percentage of desmin-positive cells in various population doublings that demonstrated no loss of myogenicity in myoblast cells. The data are presented as the means ± SD, $n = 3$.

Myoblast	PD 14	PD 16	PD 18	PD 20
Desmin positive (%)	97.89 ± 2.12	92.92 ± 1.08	95.55 ± 2.80	94.49 ± 2.54

determined by the ability of myoblasts to differentiate, fuse, and form mature multinucleated myotubes. Young control myoblast cells were able to fuse together, forming large, branched, multinucleated myotubes (Figure 6(a)). With *C. vulgaris* treatment, more multinucleated myotubes formed, as shown in Figures 6(b) and 6(c). In senescent control myoblasts, the myotubes formed were smaller with fewer branches compared to those in young myoblasts (Figure 6(d)). However, the formation of myotubes in senescent myoblasts improved with *C. vulgaris* treatment

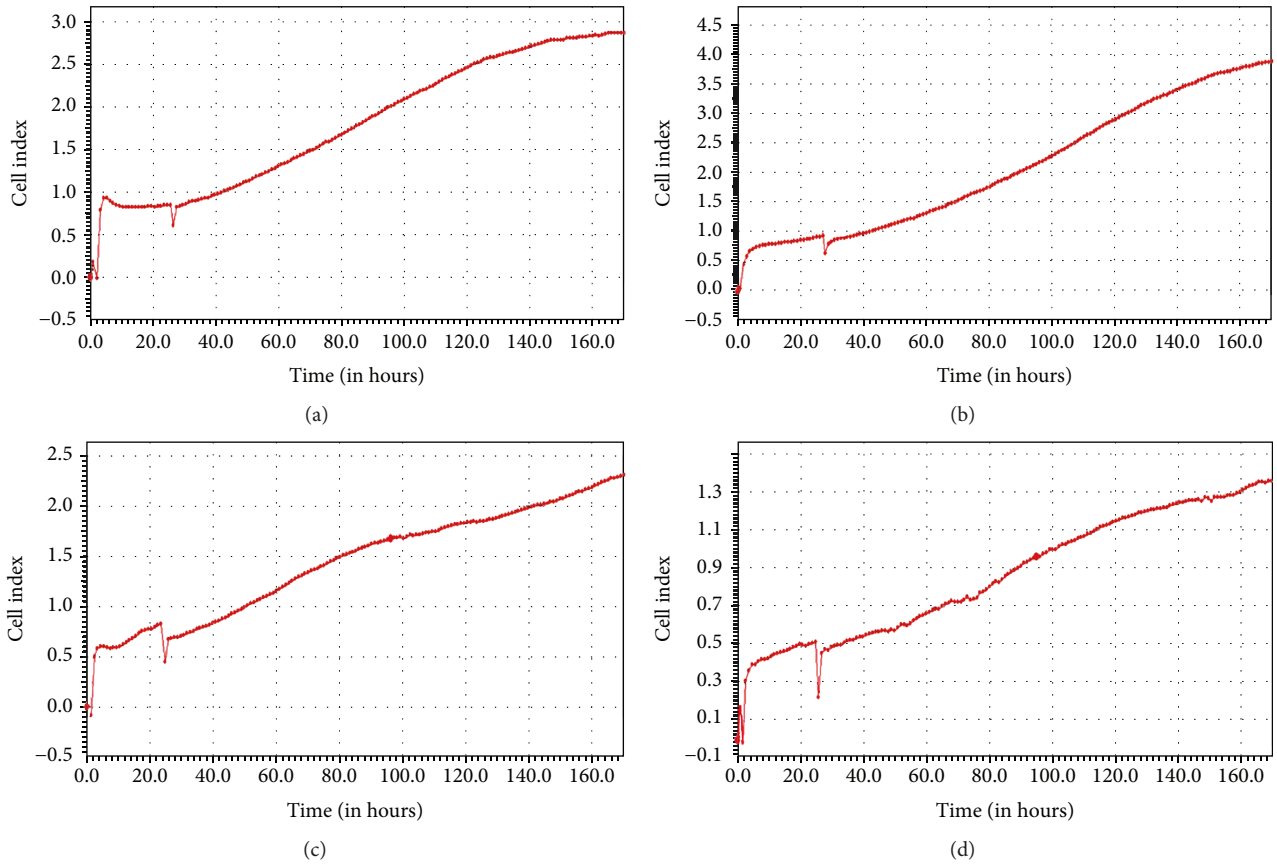

Figure 2: The proliferation rates of myoblast cells from two different donors were represented using cell indexes (CI) for (a) young myoblasts from the 17-year-old donor, (b) senescent myoblasts from the 17-year-old donor, (c) young myoblasts from the 20-year-old donor, and (d) senescent myoblasts from the 20-year-old donor. Data are presented as means, $n = 2$.

and more branched, multinucleated myotubes were observed (Figures 6(e)–6(f)).

The fusion index of young control myoblasts was significantly higher on days 3, 5, and 7 of differentiation compared to day 1 ($p < 0.05$) (Figure 7(a)). Treatment with *C. vulgaris* at 10 and 100 μg/ml significantly increased the fusion index of young myoblasts compared to young control myoblasts on day 5 of differentiation ($p < 0.05$).

The maturation index of young control myoblasts was significantly higher on days 5 and 7 of differentiation compared to day 1 ($p < 0.05$) (Figure 7(b)). Treatment with *C. vulgaris* at 100 μg/ml significantly increased the fusion index of young myoblasts compared to young control myoblasts on day 5 of differentiation ($p < 0.05$).

The number of nuclei per myotube in young control myoblasts was significantly higher on day 7 of differentiation compared to day 1 ($p < 0.05$) (Figure 7(c)), while the surface area of myotubes of young control myoblasts was significantly higher on days 5 and 7 of differentiation compared to day 1 ($p < 0.05$) (Figure 7(d)). Treatment with *C. vulgaris* at 100 μg/ml significantly increased the surface area of myotubes of young myoblasts compared to young control myoblasts on day 3 of differentiation ($p < 0.05$).

For senescent myoblast cells, the fusion index and myotube surface area of senescent control myoblasts were significantly increased on days 5 and 7 of differentiation ($p < 0.05$) (Figures 8(a) and 8(d)) while the maturation index and the number of nuclei per myotube were significantly increased on day 7 of differentiation ($p < 0.05$) (Figures 8(b) and 8(c)). No significant differences were observed in the fusion indexes, maturation indexes, number of nuclei per myotube, and myotube surface areas of senescent myoblasts treated with *C. vulgaris* compared to the controls on a given day.

Photomicrographs of myogenin staining are shown in Figures 9(a)–9(c) for young myoblast cells and in Figures 9(d)–9(f) for senescent myoblast cells. Quantitative data for myogenin expression showed that there was a significant increase in myogenin expression on day 3 of differentiation in young myoblasts treated with 10 and 100 μg/ml of *C. vulgaris* compared to young control myoblasts (0 μg/ml *C. vulgaris*) ($p < 0.05$) (Figure 9(g)). The expression of myogenin in myoblasts treated with *C. vulgaris* at 10 and 100 μg/ml was also significantly higher on day 3 of differentiation compared to day 1 ($p < 0.05$).

For senescent myoblasts, treatment with 10 and 100 μg/ml of *C. vulgaris* increased the expression of myogenin significantly on days 1 and 3 of differentiation compared to senescent control myoblasts (0 μg/ml *C. vulgaris*) ($p < 0.05$) (Figure 9(h)). On day 3 of differentiation, the expression of myogenin was significantly increased in both control and *C. vulgaris*-treated myoblasts compared to day 1 ($p < 0.05$).

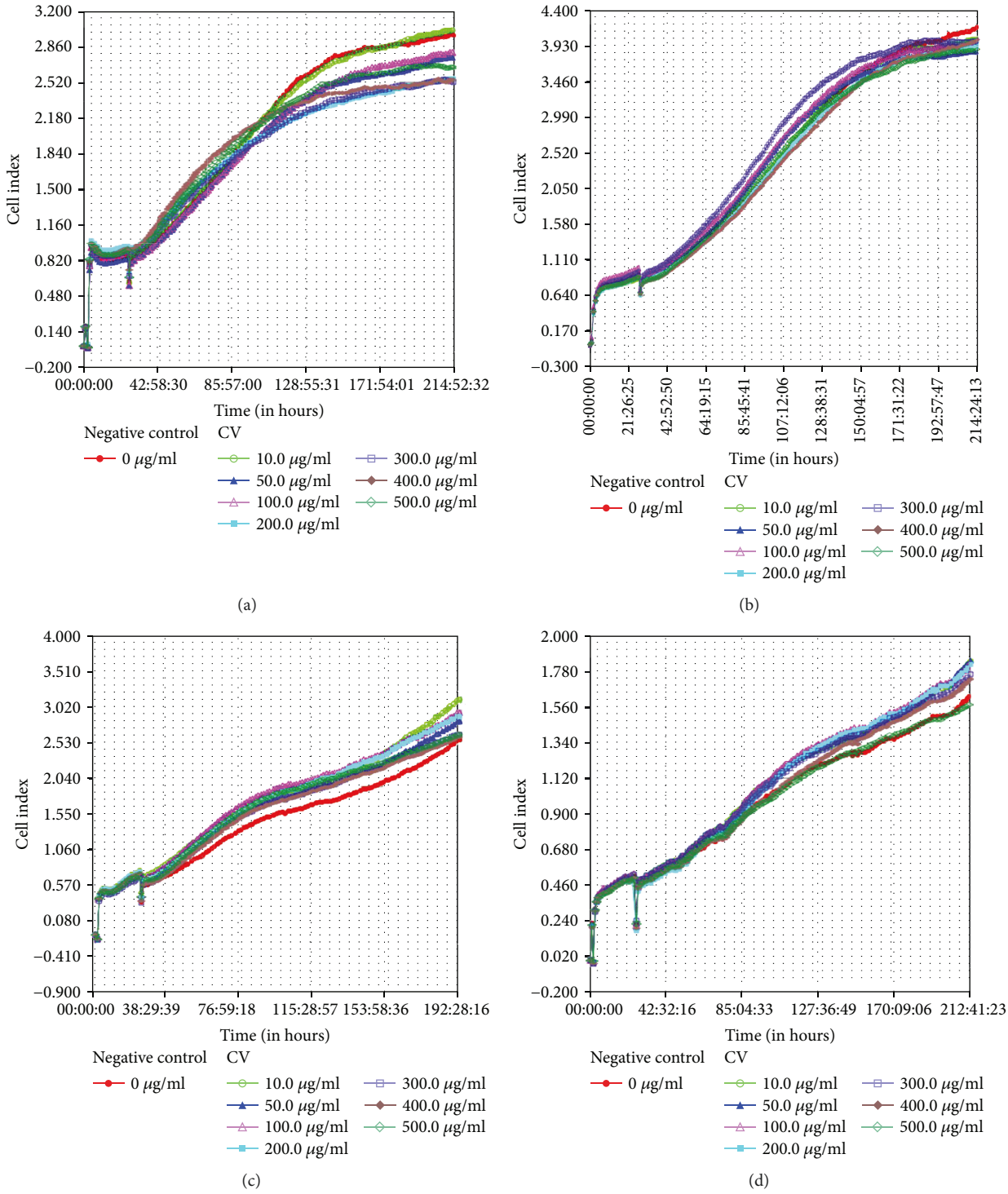

Figure 3: The proliferation rates of myoblast cells from two different donors treated with different concentrations of *C. vulgaris* were calculated using the cell indexes (CI) for (a) young myoblasts from the 17-year-old donor, (b) senescent myoblasts from the 17-year-old donor, (c) young myoblasts from the 20-year-old donor, and (d) senescent myoblasts from the 20-year-old donor. Myoblast cells without *C. vulgaris* treatment is considered as negative control. Data are presented as means, $n = 2$.

3.5. Effects of C. vulgaris on Cell Cycle Profiles. The percentage of senescent control cells in the G_0/G_1 phase was significantly increased on day 0 of differentiation to 92.45% ± 0.51% compared to that of young control myoblasts at 91.04% ± 0.62%, while the percentage of senescent control cells in the G_2/M phase was significantly decreased compared to that of young control cells (Figure 10(a)) ($p < 0.05$). On day 1 of differentiation, young myoblasts treated with 10 μg/ml *C. vulgaris*

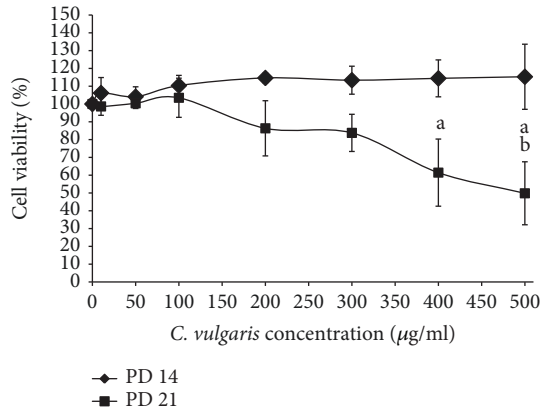

FIGURE 4: *C. vulgaris* treatment helped to maintain the cell viability of young myoblasts and decrease the viability of senescent myoblasts at high concentrations (400 and 500 μg/ml), as shown in the dose-response curve for *C. vulgaris* treatment in young and senescent myoblast cells. The data are presented as the means ± SD, $n = 3$. [a]$p < 0.05$: significantly different compared to 0, 10, 50, and 100 μg/ml; [b]$p < 0.05$: significantly different compared to 200 μg/ml, with a post hoc Tukey HSD test.

showed a significant increase in the percentage of G_0/G_1 phase cells and decreased *S* phase cells compared to young control myoblasts ($p < 0.05$) (Figure 10(b)). A similar increase in the percentage of senescent myoblast cells in the G_0/G_1 phase, and decreased *S* phase and G_2/M phase cells were observed with *C. vulgaris* treatment on day 1 of differentiation compared to young control myoblasts ($p < 0.05$) (Figure 10(b)).

4. Discussion

Although sarcopenia is most common in the elderly, it also affects entire communities due to the economic burden imposed by the disease. Current approaches and interventions for the prevention and management of sarcopenia, such as physical exercise, nutritional supplements, and hormone therapy, show promising results. Higher life expectancies have contributed to an increase in health problems amongst the elderly. Consequently, the introduction of natural remedies such as supplements or dietary interventions has been widely studied. A previous study, which evaluated the effect of *Chlorella* on muscle atrophy in a muscle-specific mitochondrial aldehyde dehydrogenase 2 activity-deficient mouse model, showed that supplementation with *Chlorella* for 6 months resulted in the prevention of age-related muscle atrophy [27].

The current study demonstrated the potential effects of *C. vulgaris* on skeletal myoblast cell regeneration *in vitro*, wherein human skeletal myoblast cells were chosen as a model for replicative senescence. Replicative senescence has been described as an irreversible growth arrest that occurs in cells that have exhausted their proliferative capacity. The results of our study showed that cells undergoing serial passaging *in vitro* achieved a certain number of population doublings (PDs), shown in a constructed lifespan curve. The human skeletal myoblast cells used in this study have the ability to proliferate up to a certain number of proliferation doublings and then lose their capacity to proliferate upon reaching replicative or cellular senescence. Cells were considered young during the first one-third of their lifespan and senescent at the end of their lifespan, after which cells failed to proliferate even with repeated feeding [25].

In the present study, the morphology of myoblast cells at PD 14 exhibited the characteristics of young cells, with more spindle-shaped cells being present. At PD 21, these cells became flatter and larger with the presence of intermediate filaments and vacuoles, indicating senescence, which was also reported by other studies [24, 28]. A previous study reported that the morphology of myoblast cells that reached a senescent state resembled a flattened cell with enlarged cytoplasm and extended cytosolic processes [25]. This could be due to the exhaustion of satellite cells as a large number of degeneration/regeneration cycles occurred [29]. Senescent cells were further verified using SA-β-gal staining that stained for β-galactosidase activity, which is detectable in senescent cells and undetectable in quiescent cells. Our findings showed that the percentage of cells that stained positive for SA-β-gal was significantly higher in PD 20 cells compared to PD 14 and PD 18 myoblasts. Therefore, in this study, myoblasts at PD 14 were used to represent young cells and myoblasts at PD 21 represented senescent cells, which was in line with our previous study [24].

Myogenic purity analysis was carried out to ensure no contamination from myogenic cells, such as fibroblasts, that could obstruct the proliferation of myoblasts. Myogenic purity was maintained in this study, as indicated by the presence of >92% desmin-positive cells in each population doubling. These findings confirmed that there was no loss of myogenicity throughout the replication of experiments and thus that reliable statistical analysis could be carried out between PDs. Real-time recording was performed for seven days on myoblasts from two different donors, showing a similar pattern in the lifespans of myoblasts at both PD 14 and PD 21, as shown by an increase in proliferation along with the increasing number of days.

Various concentrations of *C. vulgaris* were used to treat myoblasts from two different donors, and real-time recording was used to monitor the progression of cells for seven days. An increase in proliferation with the increasing number of days was observed up to a dosage of 500 μg/ml *C. vulgaris*. Previous studies showed that there was no observed difference in myogenic behaviour between myoblasts from young and myoblasts from elderly donors [25, 30]. The dose-response curve of myoblast cells treated with *C. vulgaris* showed increased cell proliferation in young myoblasts treated with up to 500 μg/ml *C. vulgaris* and in senescent myoblasts treated with up to 100 μg/ml *C. vulgaris*. To further elucidate the effects of *C. vulgaris* on replicative senescence, the senescence biomarker SA-β-gal was used to identify the presence of senescent cells. The number of cells that stained positive for SA-β-gal grew significantly higher

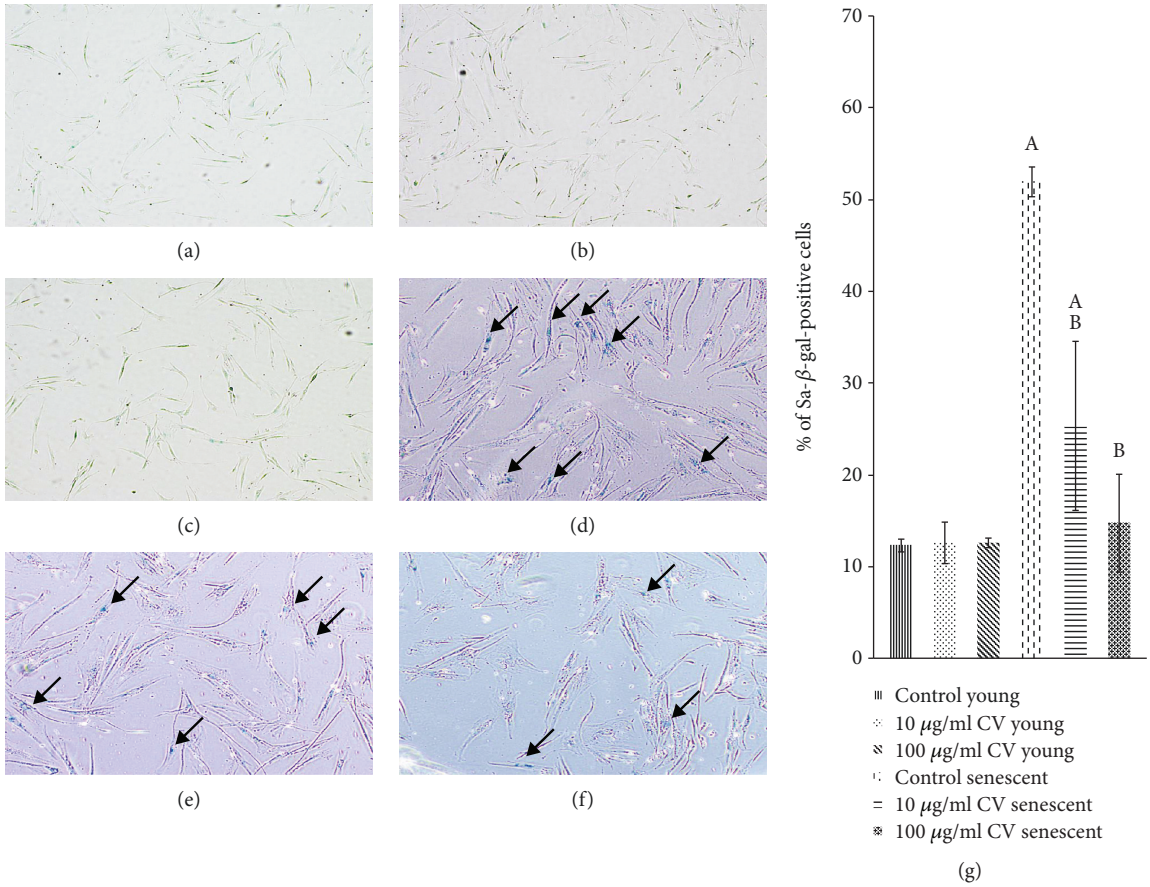

Figure 5: *C. vulgaris* treatment decreased the percentage of SA-β-gal-positive senescent cells. SA-β-gal staining was used as a senescence biomarker, shown in photomicrographs of young control cells (a), young cells treated with 10 μg/ml *C. vulgaris* (b), young cells treated with 100 μg/ml *C. vulgaris* (c), senescent control cells (d), senescent cells treated with 10 μg/ml *C. vulgaris* (e), and senescent cells treated with 100 μg/ml *C. vulgaris* (f) (magnification: 40x). This data was quantified by the percentage of cells that stained positive for SA-β-gal (g). The data are presented as the means ± SD, $n = 3$. $^{A}p < 0.05$: significantly different compared to young controls; $^{B}p < 0.05$: significantly different compared to senescent controls, with a post hoc Tukey HSD test.

with the increase in PD. However, treatment with *C. vulgaris* significantly decreased the activity of SA-β-gal in senescent cells, therefore demonstrating the reversal of ageing caused by *C. vulgaris*.

Fusion indexes and maturation indexes were measured to confirm the ability of myoblast cells to differentiate and form mature myotubes, which are multinucleated cells. The findings of this study showed that both young and senescent myoblasts underwent differentiation in culture. However, young myoblasts differentiated more efficiently compared to senescent myoblasts, as indicated by increased fusion indexes, maturation indexes, number of nuclei per myotube, and myotube surface areas on as early as day 3 of differentiation. Treatment with *C. vulgaris* was found to improve the differentiation process in young myoblasts, as shown by increases in the fusion index, the maturation index, and the myotube surface area. However, a similar increase was not observed in senescent myoblasts treated with *C. vulgaris*. These results reveal the ability of *C. vulgaris* to promote cell differentiation and thus myoblast cell regeneration, in young myoblasts.

The differentiation of myoblasts involves the activation of quiescent muscle satellite cells to promote the formation of myotubes through the upregulation of myogenin. Subsequently, immature myotubes are promoted to mature myotubes. Myogenin belongs to a group of muscle-specific regulatory factors (MRFs), proteins that regulate the differentiation of myoblasts [31]. Our results showed that treatment with *C. vulgaris* resulted in a significant increase in myogenin expression on day 3 of differentiation in young myoblasts. In senescent myoblasts, however, myogenin expression was increased on both day 1 and day 3 of differentiation after *C. vulgaris* treatment, indicating the role of *C. vulgaris* in upregulating the expression of myogenin for the promotion of muscle differentiation.

Cell cycle profiles indicate the status of cellular proliferation and the effect of *C. vulgaris* on myoblast differentiation. Our results showed that the percentage of senescent control myoblast cells in the G_0/G_1 phase was significantly increased on day 0 of differentiation, indicating replicative senescence. Cell cycle arrest occurs as a result of the inability of the senescent myoblasts to replicate. On day 1 of differentiation,

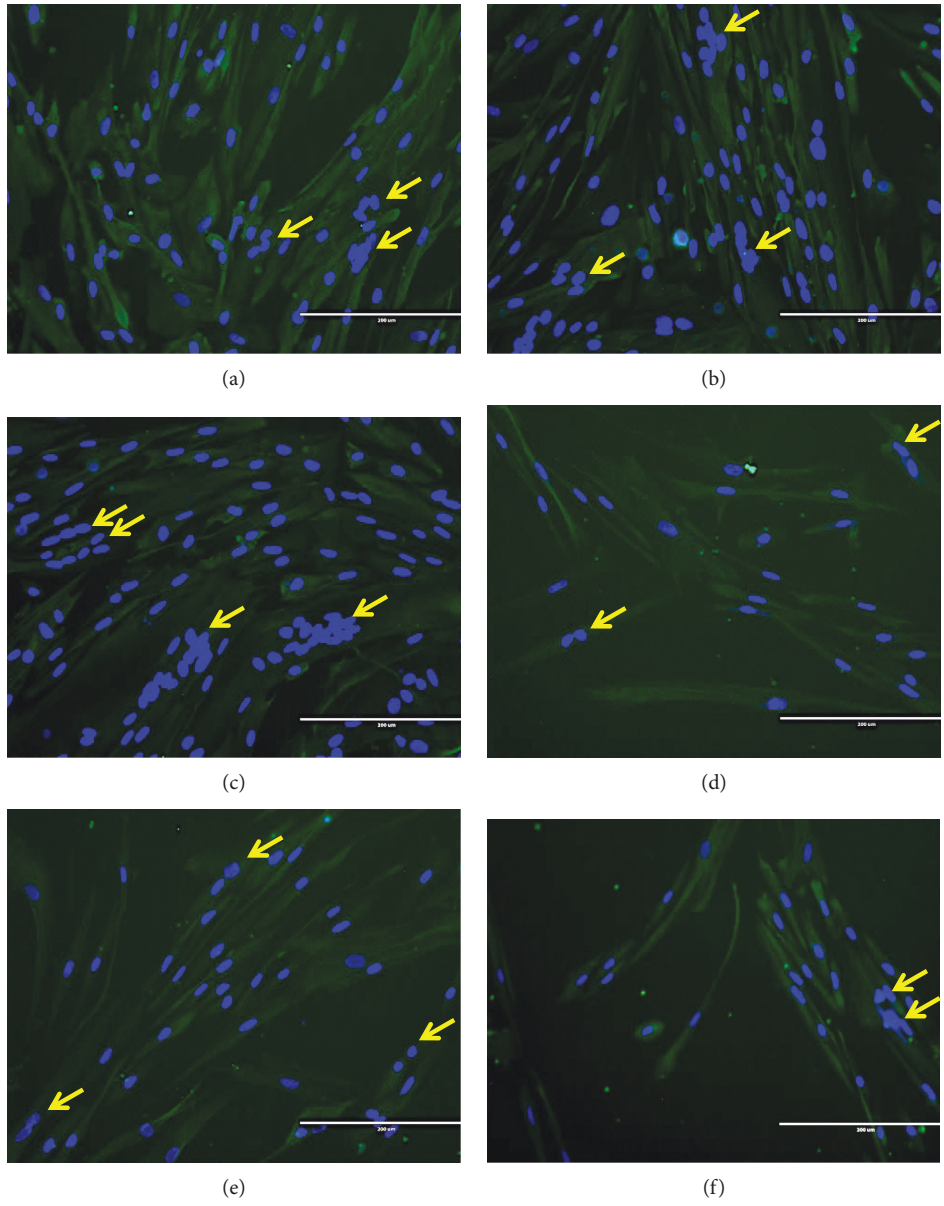

Figure 6: Desmin staining of differentiated myoblasts, indicating the presence of multinucleated cells in mature myotubes. Photomicrographs of desmin staining on day 3 for young control myoblasts (a), young myoblasts treated with 10 μg/ml *C. vulgaris* (b), young myoblasts treated with 100 μg/ml *C. vulgaris* (c), senescent control myoblasts (d), senescent myoblasts treated with 10 μg/ml *C. vulgaris* (e), and senescent myoblasts treated with 100 μg/ml *C. vulgaris* (f) (magnification: 200x). Myoblasts were stained for desmin (green) and nuclei (blue). Arrows indicate the multinucleated cells formed during the differentiation and fusion process.

young myoblast cells treated with 10 μg/ml *C. vulgaris* showed a significant increase in the percentage of G_0/G_1 phase cells and a significant decrease in *S* phase cells, indicating inhibition of cell proliferation and promotion of cell differentiation. A previous study reported that during differentiation, there is inhibition of myoblast proliferation, and thus, more cells are present in the G_0/G_1 phase in order to allow differentiation to take place [32]. However, a similar pattern of cell cycle phases was not observed in senescent myoblasts treated with *C. vulgaris*. The increased percentage of G_0/G_1 phase cells and decreased *S* phase and G_2/M phase of senescent cells with *C. vulgaris* treatment were not significant when compared to control senescent myoblasts indicating that these changes were due to the age of senescent myoblasts in culture and not due to *C. vulgaris* treatment. These findings may explain why a more prominent differentiation effect of *C. vulgaris* treatment on young myoblasts was observed in this study.

C. vulgaris has been reported on previously due to its potential activity as an antiageing agent by decreasing the expression of aging biomarkers in senescent human diploid fibroblasts (HDFs) [33]. It contains numerous active compounds that contribute to its antiageing properties [34, 35]. However, it may not be possible to identify the specific

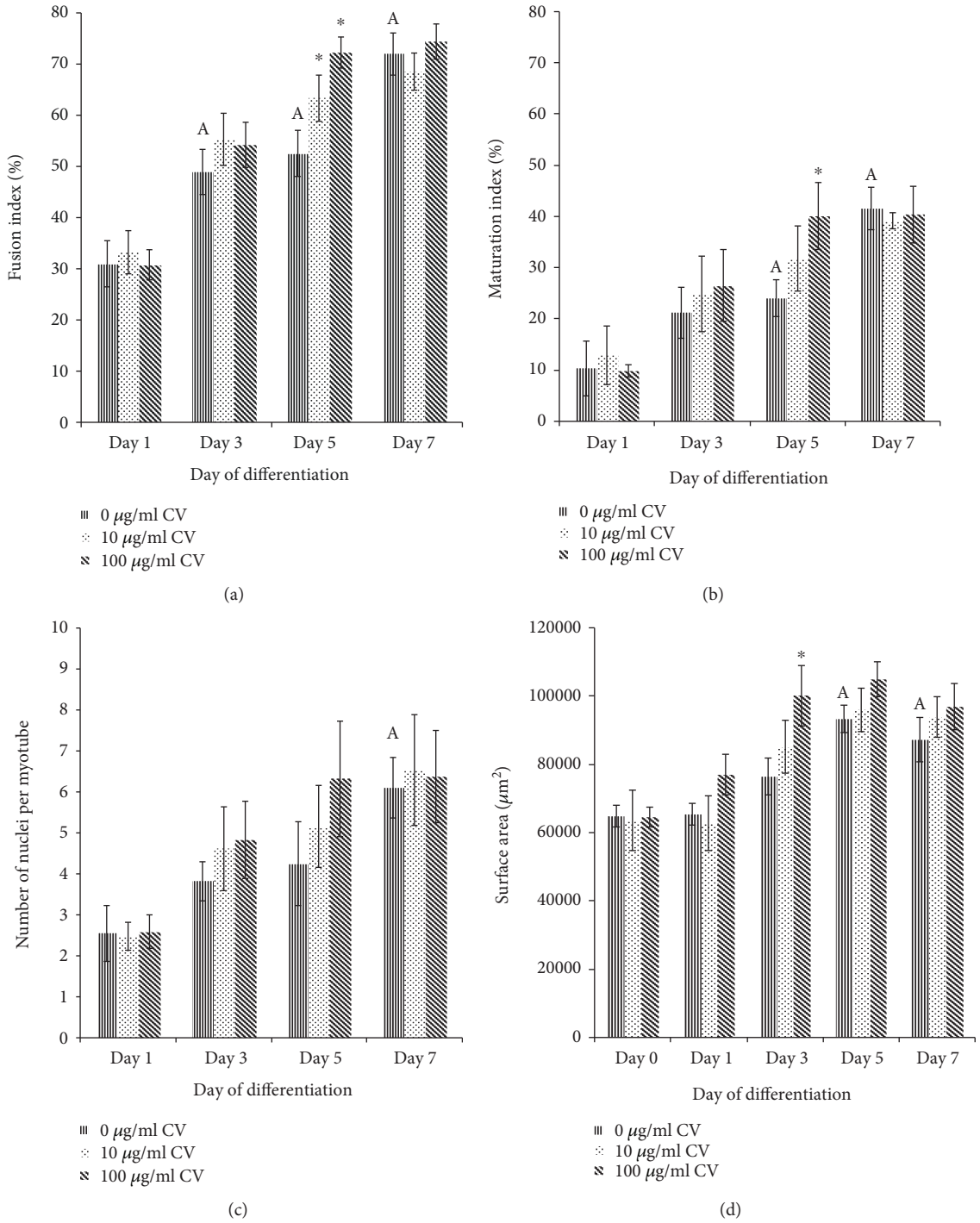

Figure 7: Index of differentiation for young myoblasts. The fusion indexes (a), maturation indexes (b), myotube sizes (c), and myotube surface areas (d) of young myoblasts. Data are presented as means ± SD, $n = 3$. $^{*}p < 0.05$: significantly different compared to young control myoblasts on a given day; $^{A}p < 0.05$: significantly different compared to young control myoblasts on day 1, with a post hoc Tukey HSD test.

compound that contributes to this effect. In addition, *C. vulgaris* may produce its beneficial effects through a synergistic response generated by multiple compounds found in these algae [27]. *C. vulgaris* is considered a good source of antioxidants because it contains nutritious substances such as β-carotene, lutein, chlorophyll-a, chlorophyll-b, vitamin A (retinol), vitamin B2 (riboflavin), vitamin C (ascorbic acid), vitamin E (tocopherol), and minerals [14, 36, 37].

C. vulgaris has also been reported to contain various essential amino acids, including branched-chain amino acids (BCAA) such as valine, leucine, and isoleucine [37–39], which are the vital components of actin- and myosin-composed muscle. Leucine has been reported to be the most potent BCAA for the stimulation of muscle protein synthesis [40–42]. These findings indicate that *C. vulgaris* could be a remedy for the prevention and treatment of sarcopenia. A

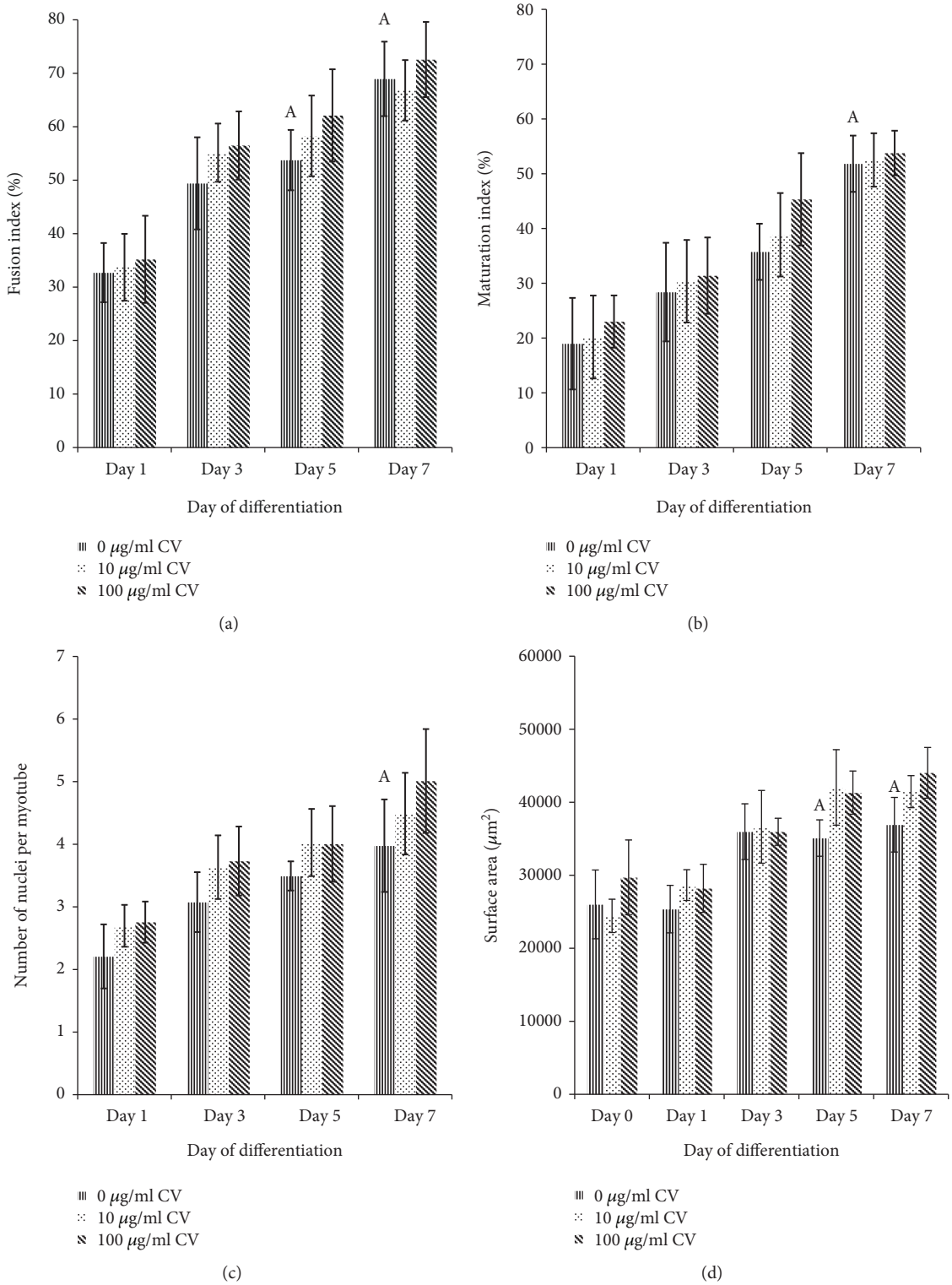

Figure 8: Index of differentiation for senescent myoblasts. The fusion indexes (a), maturation indexes (b), myotube sizes (c), and myotube surface areas (d) of senescent myoblasts. The data are presented as the means ± SD, $n = 3$. $^{A}p < 0.05$: significantly different compared to senescent control myoblasts on day 1, with a post hoc Tukey HSD test.

previous study also reported that the proteins extracted from these microalgae are comparable to or higher than commercial proteins, such as soybean proteins and sodium caseinate [39].

C. vulgaris is a good source of n-3 polyunsaturated fatty acids (n-3 PUFAs) due to its high content compared to other microalgae, such as *Spirulina platensis* and *Isochrysis galbana* [15, 43]. A previous study reported that the negative effects of

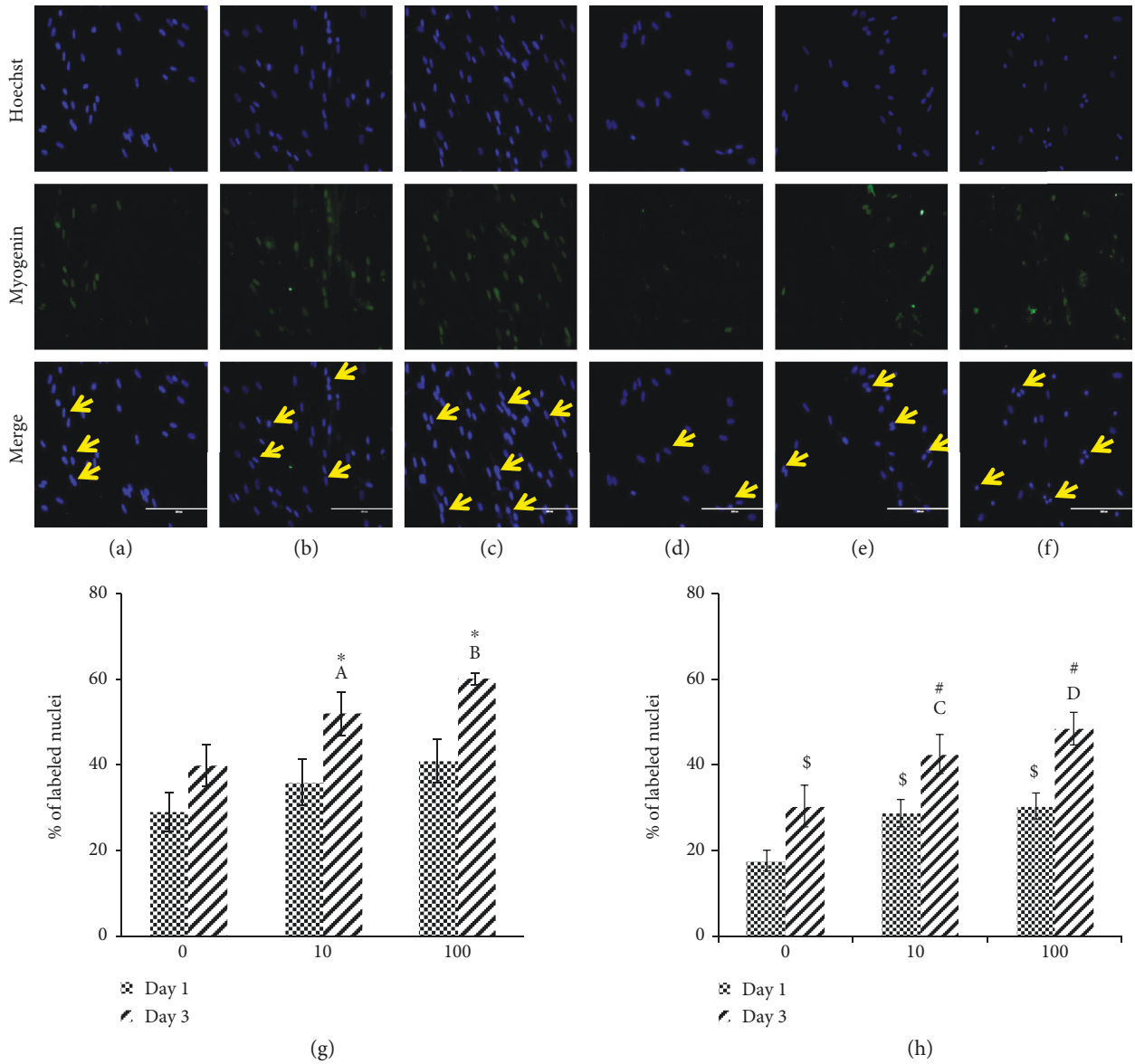

FIGURE 9: Myogenin expression in young and senescent myoblasts during differentiation induction. Photomicrographs of myogenin staining on day 3 for young control myoblasts (a), young myoblasts treated with 10 μg/ml *C. vulgaris* (b), young myoblasts treated with 100 μg/ml *C. vulgaris* (c), senescent control myoblasts (d), senescent myoblasts treated with 10 μg/ml *C. vulgaris* (e), and senescent myoblasts treated with 100 μg/ml *C. vulgaris* (f) (magnification: 200x), with the presence of nuclei (blue) and myogenin (green) shown using arrows. Quantification of myogenin expression on days 1 and 3 of differentiation for young myoblasts (g) and senescent myoblasts (h). The data are presented as the means ± SD, $n = 3$. $^{*}p < 0.05$: significantly different compared to young control myoblasts on day 3; $^{A}p < 0.05$: significantly different compared to young myoblasts treated with 10 μg/ml *C. vulgaris* on day 1; $^{B}p < 0.05$: significantly different compared to young myoblasts treated with 100 μg/ml *C. vulgaris* on day 1; $^{\$}p < 0.05$: significantly different compared to senescent control myoblasts on day 1; $^{\#}p < 0.05$: significantly different compared to senescent control myoblasts on day 3; $^{C}p < 0.05$: significantly different compared to senescent myoblasts treated with 10 μg/ml *C. vulgaris* on day 1; $^{D}p < 0.05$: significantly different compared to senescent myoblasts treated with 100 μg/ml *C. vulgaris* on day 1, with a post hoc Tukey HSD test.

palmitate and tumour necrosis factor-alpha (TNF-α) were inhibited by n-3 PUFAs. They also promote differentiation by activating anti-inflammatory pathways within satellite cells [42, 44]. Tocopherol, which is also present in *C. vulgaris*, was shown to help senescent myoblasts to reclaim the morphology of young cells, increasing cell viability and decreasing the expression of SA-β-gal [24]. These antioxidant properties of *C. vulgaris* may be responsible for the promotion of myoblast cell differentiation in both young and senescent cells and, thus, the promotion of muscle regeneration, which consequently leads to the reversal of muscle ageing.

5. Conclusions

C. vulgaris improves the regenerative capacity of young and senescent myoblasts and promotes myoblast differentiation,

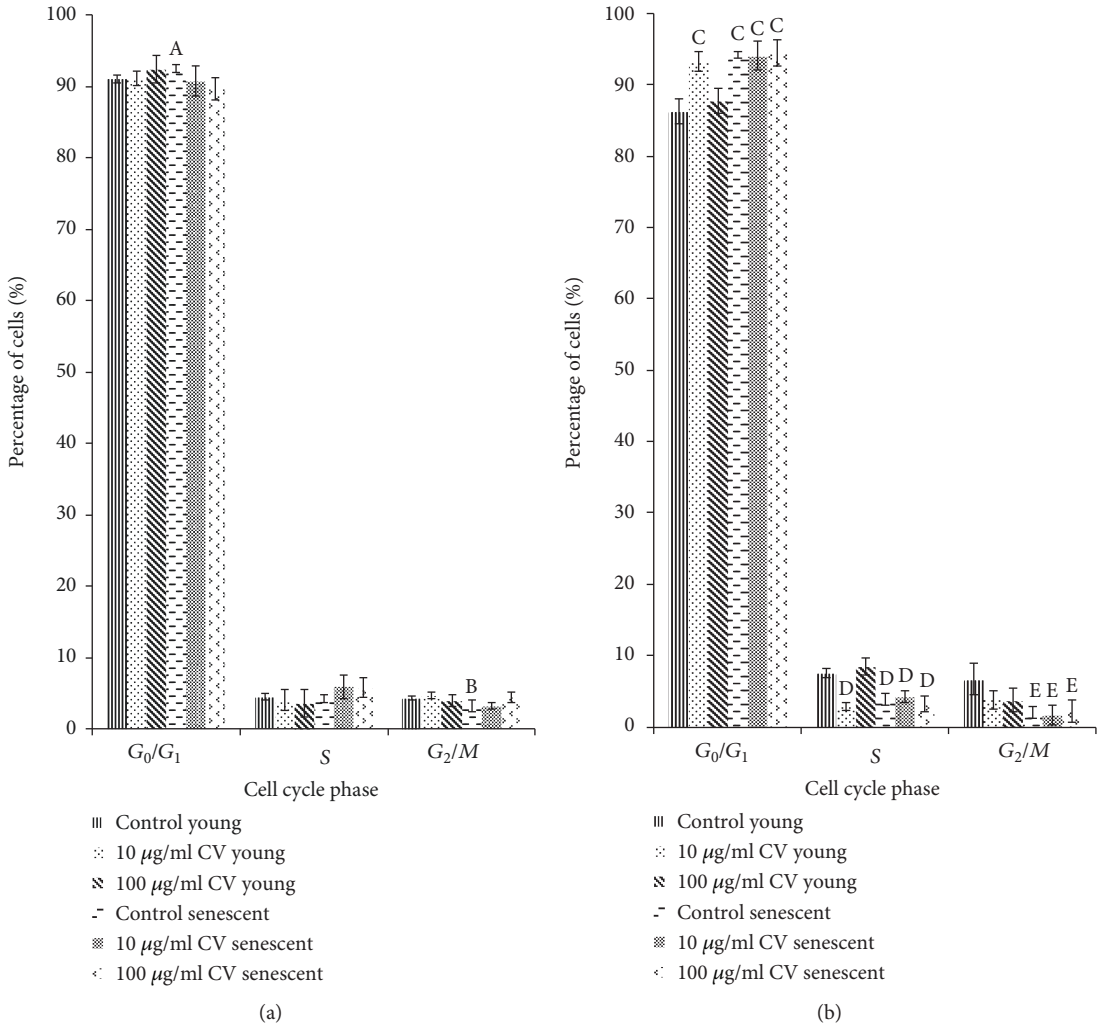

Figure 10: Cell cycle tests were performed on days 0 and 1 of differentiation to determine the myoblast cell population after the induction of differentiation and the effects of treatment with *C. vulgaris*. Cell populations of young and senescent myoblasts both untreated and treated with *C. vulgaris* on (a) day 0 and (b) day 1. The data are presented as means ± SD, $n = 3$. $^{A}p < 0.05$: significantly different compared to young control myoblasts in the G_0/G_1 phase on day 0; $^{B}p < 0.05$: significantly different compared to young control myoblasts in the G_2/M phase on day 0; $^{C}p < 0.05$: significantly different compared to young control myoblasts in the G_0/G_1 phase on day 1; $^{D}p < 0.05$: significantly different compared to young control myoblasts in the S phase on day 1; $^{E}p < 0.05$: significantly different compared to young control myoblasts in the G_2/M phase on day 1, with a post hoc Tukey HSD test.

indicating its potential in promoting muscle regeneration. It may also act as an antiageing agent, as shown by its effects on delaying replicative senescence in myoblast cells.

Data Availability

The raw data used to support the findings of the study are available from the corresponding author upon request.

Conflicts of Interest

The authors declare that there is no conflict of interest regarding the publication of this paper.

Acknowledgments

This work was supported by the Ministry of Education (MOE), Malaysia (grant number: FRGS/2/2014/SKK01/UKM/01/1), and the Universiti Kebangsaan Malaysia (grant number: UKM-FF-2016-318).

References

[1] W. J. Evans, "Skeletal muscle loss: cachexia, sarcopenia, and inactivity," *The American Journal of Clinical Nutrition*, vol. 91, no. 4, pp. 1123S–1127S, 2010.

[2] L. A. Burton and D. Sumukadas, "Optimal management of sarcopenia," *Clinical interventions in aging*, vol. 5, pp. 217–228, 2010.

[3] M. M. Ziaaldini, E. Marzetti, A. Picca, and Z. Murlasits, "Biochemical pathways of sarcopenia and their modulation by physical exercise: a narrative review," *Frontiers in Medicine*, vol. 4, no. 167, pp. 1–8, 2017.

[4] W. K. Mitchell, P. J. Atherton, J. Williams, M. Larvin, J. N. Lund, and M. Narici, "Sarcopenia, dynapenia, and the impact of advancing age on human skeletal muscle size and strength; a quantitative review," *Frontiers in Physiology*, vol. 3, no. 260, pp. 1–18, 2012.

[5] I. Janssen, "Evolution of sarcopenia research," *Applied Physiology, Nutrition, and Metabolism*, vol. 35, no. 5, pp. 707–712, 2010.

[6] M. Horak, J. Novak, and J. Bienertova-Vasku, "Muscle-specific microRNAs in skeletal muscle development," *Developmental Biology*, vol. 410, no. 1, pp. 1–13, 2016.

[7] N. N. Hairi, A. Bulgiba, T. G. Hiong, and I. Mudla, "Sarcopenia in older people," in *Geriatrics*, C. S. Atwood, Ed., pp. 29–40, IntechOpen, 2012.

[8] M. Visser, "Epidemiology of muscle mass loss with age," in *Sarcopenia*, pp. 1–7, John Wiley & Sons, Ltd., 2012.

[9] C. D. McMahon, R. Chai, H. G. Radley-Crabb et al., "Lifelong exercise and locally produced insulin-like growth factor-1 (IGF-1) have a modest influence on reducing age-related muscle wasting in mice," *Scandinavian Journal of Medicine & Science in Sports*, vol. 24, no. 6, pp. e423–e435, 2014.

[10] C. Vigorito and F. Giallauria, "Effects of exercise on cardiovascular performance in the elderly," *Frontiers in physiology*, vol. 5, p. 51, 2014.

[11] C. Safi, B. Zebib, O. Merah, P.-Y. Pontalier, and C. Vaca-Garcia, "Morphology, composition, production, processing and applications of Chlorella vulgaris: a review," *Renewable and Sustainable Energy Reviews*, vol. 35, pp. 265–278, 2014.

[12] L. Krienitz, V. A. R. Huss, and C. Bock, "Chlorella: 125 years of the green survivalist," *Trends in Plant Science*, vol. 20, no. 2, pp. 67–69, 2015.

[13] S. M. Saad, Y. A. M. Yusof, and W. Z. W. Ngah, "Comparison between locally produced Chlorella vulgaris and Chlorella vulgaris from Japan on proliferation and apoptosis of liver cancer cell line, HepG2," *Malaysian Journal of Biochemistry and Molecular Biology*, vol. 13, no. 1, pp. 32–36, 2006.

[14] K. Kitada, S. Machmudah, M. Sasaki et al., "Supercritical CO_2 extraction of pigment components with pharmaceutical importance from *Chlorella vulgaris*," *Journal of Chemical Technology and Biotechnology*, vol. 84, no. 5, pp. 657–661, 2009.

[15] Y. Panahi, B. Pishgoo, H. R. Jalalian et al., "Investigation of the effects of *Chlorella vulgaris* as an adjunctive therapy for dyslipidemia: results of a randomised open-label clinical trial," *Nutrition & Dietetics*, vol. 69, no. 1, pp. 13–19, 2012.

[16] H. S. Lee, H. J. Park, and M. K. Kim, "Effect of Chlorella vulgaris on lipid metabolism in Wistar rats fed high fat diet," *Nutrition Research and Practice*, vol. 2, no. 4, pp. 204–210, 2008.

[17] J. F. Vecina, A. G. Oliveira, T. G. Araujo et al., "Chlorella modulates insulin signaling pathway and prevents high-fat diet-induced insulin resistance in mice," *Life Sciences*, vol. 95, no. 1, pp. 45–52, 2014.

[18] H. Jeong, H. J. Kwon, and M. K. Kim, "Hypoglycemic effect of Chlorella vulgaris intake in type 2 diabetic Goto-Kakizaki and normal Wistar rats," *Nutrition Research and Practice*, vol. 3, no. 1, pp. 23–30, 2009.

[19] O. Aizzat, S. Yap, H. Sopiah et al., "Modulation of oxidative stress by *Chlorella vulgaris* in streptozotocin (STZ) induced diabetic Sprague-Dawley rats," *Advances in Medical Sciences*, vol. 55, no. 2, pp. 281–288, 2010.

[20] S. Sulaiman, N. A. Shamaan, W. Z. W. Ngah, and Y. A. M. Yusof, "Chemopreventive effect of *Chlorella vulgaris* in choline deficient diet and ethionine induced liver carcinogenesis in rats," *International Journal of Cancer Research*, vol. 2, no. 3, pp. 234–241, 2006.

[21] E. S. M. Azamai, S. Sulaiman, S. H. M. Habib et al., "Chlorella vulgaris triggers apoptosis in hepatocarcinogenesis-induced rats," *Journal of Zhejiang University Science B*, vol. 10, no. 1, pp. 14–21, 2009.

[22] N. A. Mukti, S. Sulaiman, S. M. Saad, and H. Basari, "*Chlorella vulgaris* menunjukkan kesan antioksidan dan antitumor terhadap kanser hepar dalam kajian *in vivo* dan *in vitro*," *Sains Malaysiana*, vol. 38, no. 5, pp. 773–784, 2009.

[23] P. Lorenzon, E. Bandi, F. de Guarrini et al., "Ageing affects the differentiation potential of human myoblasts," *Experimental gerontology*, vol. 39, no. 10, pp. 1545–1554, 2004.

[24] S. C. Khor, A. M. Razak, W. Z. Wan Ngah, Y. A. Mohd Yusof, N. Abdul Karim, and S. Makpol, "The tocotrienol-rich fraction is superior to tocopherol in promoting myogenic differentiation in the prevention of replicative senescence of myoblasts," *PLoS One*, vol. 11, no. 2, article e0149265, 2016.

[25] A. Bigot, V. Jacquemin, F. Debacq-Chainiaux et al., "Replicative aging down-regulates the myogenic regulatory factors in human myoblasts," *Biology of the Cell*, vol. 100, no. 3, pp. 189–199, 2008.

[26] Y. Sun, Y. Ge, J. Drnevich, Y. Zhao, M. Band, and J. Chen, "Mammalian target of rapamycin regulates mirna-1 and follistatin in skeletal myogenesis," *The Journal of Cell Biology*, vol. 189, no. 7, pp. 1157–1169, 2010.

[27] Y. Nakashima, I. Ohsawa, K. Nishimaki et al., "Preventive effects of Chlorella on skeletal muscle atrophy in muscle-specific mitochondrial aldehyde dehydrogenase 2 activity-deficient mice," *BMC Complementary and Alternative Medicine*, vol. 14, no. 1, pp. 1–9, 2014.

[28] J. J. Lim, W. Z. Wan Ngah, V. Mouly, and N. Abdul Karim, "Reversal of myoblast aging by tocotrienol rich fraction post-treatment," *Oxidative Medicine and Cellular Longevity*, vol. 2013, Article ID 978101, 11 pages, 2013.

[29] E. Kudryashova, I. Kramerova, and M. J. Spencer, "Satellite cell senescence underlies myopathy in a mouse model of limb-girdle muscular dystrophy 2H," *The Journal of Clinical Investigation*, vol. 122, no. 5, pp. 1764–1776, 2012.

[30] M. Alsharidah, N. R. Lazarus, T. E. George, C. C. Agley, C. P. Velloso, and S. D. R. Harridge, "Primary human muscle precursor cells obtained from young and old donors produce similar proliferative, differentiation and senescent profiles in culture," *Aging Cell*, vol. 12, no. 3, pp. 333–344, 2013.

[31] D. Salvatore, W. S. Simonides, M. Dentice, A. M. Zavacki, and P. R. Larsen, "Thyroid hormones and skeletal muscle—new insights and potential implications," *Nature Reviews Endocrinology*, vol. 10, no. 4, pp. 206–214, 2014.

[32] X. Yu, L. Zhang, G. Wen et al., "Upregulated sirtuin 1 by miRNA-34a is required for smooth muscle cell differentiation from pluripotent stem cells," *Cell Death and Differentiation*, vol. 22, no. 7, pp. 1170–1180, 2015.

[33] T. Saberbaghi, F. Abbasian, M. Yusof, Y. Anum, and S. Makpol, "Modulation of cell cycle profile by *Chlorella*

vulgaris prevents replicative senescence of human diploid fibroblasts," *Evidence-Based Complementary and Alternative Medicine*, vol. 2013, Article ID 780504, 12 pages, 2013.

[34] N. S. Aliahmat, M. R. M. Noor, W. J. W. Yusof, S. Makpol, W. Z. W. Ngah, and Y. A. M. Yusof, "Antioxidant enzyme activity and malondialdehyde levels can be modulated by Piper betle, tocotrienol rich fraction and *Chlorella vulgaris* in aging C57BL/6 mice," *Clinics*, vol. 67, no. 12, pp. 1447–1454, 2012.

[35] S. Makpol, T. W. Yeoh, F. A. C. Ruslam, K. T. Arifin, and Y. A. M. Yusof, "Comparative effect of Piper betle, *Chlorella vulgaris* and tocotrienol-rich fraction on antioxidant enzymes activity in cellular ageing of human diploid fibroblasts," *BMC complementary and alternative medicine*, vol. 13, no. 1, pp. 210–220, 2013.

[36] I. Maruyama, T. Nakao, I. Shigeno, Y. Ando, and K. Hirayama, "Application of unicellular algae *Chlorella vulgaris* for the mass-culture of marine rotifer *Brachionus*," *Hydrobiologia*, vol. 358, no. 1/3, pp. 133–138, 1997.

[37] S. Radhakrishnan, P. S. Bhavan, C. Seenivasan, and T. Muralisankar, "Nutritional profile of *Spirulina platensis*, *Chlorella vulgaris* and *Azolla pinnata* to novel protein source for aquaculture feed formulation," *Austin Journal of Aquaculture and Marine Biology*, vol. 2, no. 1, pp. 1–8, 2017.

[38] C. Safi, M. Charton, O. Pignolet, F. Silvestre, C. Vaca-Garcia, and P.-Y. Pontalier, "Influence of microalgae cell wall characteristics on protein extractability and determination of nitrogen-to-protein conversion factors," *Journal of Applied Phycology*, vol. 25, no. 2, pp. 523–529, 2013.

[39] A.-V. Ursu, A. Marcati, T. Sayd, V. Sante-Lhoutellier, G. Djelveh, and P. Michaud, "Extraction, fractionation and functional properties of proteins from the microalgae *Chlorella vulgaris*," *Bioresource Technology*, vol. 157, pp. 134–139, 2014.

[40] H. C. Dreyer and E. Volpi, "Role of protein and amino acids in the pathophysiology and treatment of sarcopenia," *Journal of the American College of Nutrition*, vol. 24, no. 2, pp. 140S–145S, 2005.

[41] S. Fujita and E. Volpi, "Amino acids and muscle loss with aging," *The Journal of nutrition*, vol. 136, no. 1, pp. 277S–280S, 2006.

[42] I. Bosaeus and E. Rothenberg, "Nutrition and physical activity for the prevention and treatment of age-related sarcopenia," *Proceedings of the Nutrition Society*, vol. 75, no. 2, pp. 174–180, 2016.

[43] Ö. Tokuşoglu and M. K. Üunal, "Biomass nutrient profiles of three microalgae: *Spirulina platensis*, *Chlorella vulgaris*, and *Isochrisis galbana*," *Journal of food science*, vol. 68, no. 4, pp. 1144–1148, 2003.

[44] B. Tachtsis, D. Camera, and O. Lacham-Kaplan, "Potential roles of n-3 PUFAs during skeletal muscle growth and regeneration," *Nutrients*, vol. 10, no. 3, p. 309, 2018.

Hindawi
Oxidative Medicine and Cellular Longevity
Volume 2019, Article ID 6835341, 11 pages
https://doi.org/10.1155/2019/6835341

Research Article

Vitamin D Deficiency Is Associated with Muscle Atrophy and Reduced Mitochondrial Function in Patients with Chronic Low Back Pain

Katarzyna Patrycja Dzik,[1] Wojciech Skrobot,[2] Katarzyna Barbara Kaczor,[3] Damian Jozef Flis,[4] Mateusz Jakub Karnia,[1] Witold Libionka,[1,5] Jedrzej Antosiewicz,[3,6] Wojciech Kloc,[5,7] and Jan Jacek Kaczor[1]

[1]*Department of Neurobiology of Muscle, Gdansk University of Physical Education and Sport, K. Gorskiego 1, 80-336 Gdansk, Poland*
[2]*Department of Kinesiology, Gdansk University of Physical Education and Sport, K. Gorskiego 1, 80-336 Gdansk, Poland*
[3]*Department of Bioenergetics and Physiology of Exercise, Medical University of Gdansk, 80-211 Gdansk, Poland*
[4]*Department of Bioenergetics and Nutrition, Gdansk University of Physical Education and Sport, K. Gorskiego 1, 80-336 Gdansk, Poland*
[5]*Department of Neurosurgery, Copernicus Hospital, Gdansk, Poland*
[6]*Department of Biochemistry, Gdansk University of Physical Education and Sport, K. Gorskiego 1, 80-336 Gdansk, Poland*
[7]*Department of Neurology and Neurosurgery, University of Warmia and Mazury in Olsztyn, Poland*

Correspondence should be addressed to Jan Jacek Kaczor; jacek.kaczor@awf.gda.pl

Received 31 January 2019; Accepted 7 April 2019; Published 2 June 2019

Guest Editor: Marko D. Prokić

Recent studies show that vitamin D deficiency may be responsible for muscle atrophy. The purpose of this study was to investigate markers of muscle atrophy, signalling proteins, and mitochondrial capacity in patients with chronic low back pain with a focus on gender and serum vitamin D level. The study involved patients with chronic low back pain (LBP) qualified for posterior lumbar interbody fusion (PLIF). Patients were divided into three groups: supplemented (SUPL) with vitamin D (3200 IU/day for 5 weeks), placebo with normal levels of vitamin D (SUF), and the placebo group with vitamin D deficiency (DEF). The marker of muscle atrophy including atrogin-1 and protein content for IGF-1, Akt, FOXO3a, PGC-1α, and citrate synthase (CS) activity were determined in collected multifidus muscle. In the paraspinal muscle, IGF-1 levels were higher in the SUF group as compared to both the SUPL and DEF groups ($p < 0.05$). In the SUPL group, we found significantly increased protein content for pAkt ($p < 0.05$) and decreased level of FOXO3a ($p < 0.05$). Atrogin-1 content was significantly different between men and women ($p < 0.05$). The protein content of PGC-1α was significantly higher in the SUF group as compared to the DEF group ($p < 0.05$). CS activity in the paraspinal muscle was higher in the SUPL group than in the DEF group ($p < 0.05$). Our results suggest that vitamin D deficiency is associated with elevated oxidative stress, muscle atrophy, and reduced mitochondrial function in the multifidus muscle. Therefore, vitamin D-deficient LBP patients might have reduced possibilities on early and effective rehabilitation after PLIF surgery.

1. Introduction

Skeletal muscle atrophy occurs when the normal balance between synthesis and degradation of muscle structural proteins is disturbed. Chronic low back pain (LBP), one of the most prevalent musculoskeletal disorders in modern society [1], leads to the atrophy of paraspinal muscles [2]. Muscle atrophy Fbox (MAFbx/atrogin-1), was identified as a gene of muscle specific ubiquitin ligase (E3). This ligase, along with muscle RING finger 1 (MuRF1), is responsible for the degradation of the muscle structural proteins in atrophied skeletal muscles that are caused by immobilization

[3], disuse, dietary restriction, aging, cancer, etc. [4–6]. In particular, these genes have been known to be significantly responsible for muscle atrophy since their inhibition reduces muscle atrophy caused by denervation. Additionally, they have been shown to play a key role in the induction of muscle atrophy in multiple animal disuse models [4, 5, 7]. Notwithstanding this data, the exact mechanism underlying muscle atrophy has not been fully elucidated.

LBP may be caused by different factors including the loss of lumbar spinal stability through nonsufficient activation of the deep lumbar stabilizing muscles such as the multifidus muscle [8]. Hence, reduced activation of the multifidus muscle is a major cause of its progressive muscle atrophy and upregulation of atrogin-1 gene expression. The serine/threonine-specific protein kinase (Akt)/forkhead box O3 (FOXO3) axis controls the expression of atrogin-1 gene [9]. FOXO transcription factors are thought to control half of the genes identified in the molecular "common atrophy blueprint" present in different atrophy types [10, 11]. Akt is a protein kinase, which is important in signalling pathways involved in protein synthesis and skeletal muscle growth [12]. Also, overproduction of reactive oxygen species (ROS), disturbed redox status, and a weakened antioxidant defense system are known as the major contributing factors toward atrophy [13]. Recently, we demonstrated that vitamin D deficiency is associated with higher oxidative stress and elevated activity of antioxidant enzymes in the paraspinal muscle of patients with LBP [14].

Vitamin D seems to act as a multifunctional regulator in skeletal muscle [15]. Vitamin D contributes to maintain musculoskeletal health in healthy subjects as well as in patients who display the combination of paraspinal muscle wasting and weakness such as LBP patients [16]. Cross-sectional studies found a positive association between vitamin D status and total or appendicular muscle mass in men and women [17–19]. The actions of the vitamin D hormone are mediated by the vitamin D receptor (VDR), a ligand-activated transcription factor that controls gene expression [20, 21]. An increasing number of studies in both nonhuman and human skeletal muscle cells report that the actions of vitamin D are also mediated by the VDR located within skeletal muscle cells [22–24]. Interestingly, the recent study shows that pharmacologically induced muscle loss in $VDR^{-/-}$ mice is greater in slow muscles, such as the multifidus muscle, than in fast muscles [25]. The exact mechanism of action of vitamin D in the muscle remains unknown. Insulin-like growth factor 1 (IGF-1), an anabolic hormone, has been shown to positively correlate with 25-hydroxy vitamin D serum level [26]. Therefore, we assume that vitamin D deficiency might be associated with downregulated IGF-1 in the atrophied skeletal muscle. Recently, we have reported that long term of vitamin D deficiency leads to VDR ablation, oxidative stress, and consequence mitochondrial dysfunction, which induces muscle atrophy [27].

The purpose of this study was to estimate and compare the levels of selected markers of muscle atrophy, signalling proteins, and mitochondrial capacity in the skeletal muscles of patients deficient in and with normal vitamin D level, and patients supplemented with vitamin D or placebo. Moreover, based on the recent data [14], we assumed that the possible mechanism of vitamin D in the prevention of muscle atrophy may be mediated through oxidative stress and the IGF-1/Akt/FOXO3 pathway. Specifically, we propose that muscle atrophy linked with serum vitamin D deficiency is associated with a reduction of IGF-1 and deactivation and activation of Akt and FOXO3. Furthermore, normalized levels of serum vitamin D would ameliorate relative muscle atrophy and maintain physiological mitochondrial function.

2. Materials and Methods

2.1. LBP Patients. The study population was previously described by Dzik and coworkers [14]. Briefly, nineteen women and nineteen men participated in the study. All patients were Caucasian. Pregnant or lactating women were not included. All patients had experienced chronic LBP secondary to the degenerative disease and general instability and were qualified for lumbar spine surgery utilizing static or dynamic implants (posterior lumbar interbody fusion (PLIF)). There were no significant differences in pain duration and intensity between genders. In all cases, the LBP causes were nonspecific and mechanical. All subjects gave their informed consent for inclusion before they participated in the study. The study was conducted in accordance with the Declaration of Helsinki, and the protocol was approved by the local institutional Bioethical Committee in Gdansk (No. NKBBN/120/2012).

2.2. Study Design. The study design was previously described by Dzik and coworkers [14]. Briefly, patients were randomly assigned to the group supplemented with 3200 IU of $25(OH)D_3$/day for 5 weeks (SUPL, $n = 14$) or the placebo group supplemented with vegetable oil. Blood samples were taken at baseline and after 5 weeks of supplementation for the determination of serum vitamin D concentration. Based on serum vitamin D concentration, patients from the placebo group were divided into two groups: the placebo group with normal concentration of vitamin D (SUF, $n = 10$) with $25(OH)D_3$ level above 50 nmol/L and the placebo group with vitamin D deficiency (DEF, $n = 14$) with $25(OH)D_3$ serum level between 30 and 49 nmol/L [28]. After 5 weeks of supplementation, multifidus muscle samples were obtained from all the patients during PLIF surgery. Patients' characteristics are summarized in Table 1.

2.3. Blood Analysis and Collection. Blood samples were taken at baseline and after 5 weeks of supplementation. The samples were centrifuged at 2000 g for 10 min at 4°C. The separated serum samples were frozen and kept at -80°C until later analysis. The tubes containing the serum samples were number-coded in order to blind the laboratory personnel regarding the treatment group and the sequence of sample collection. IGF-1 in serum was measured with an immunoassay kit (DG100, R&D Systems, USA) according to the manufacturer's instructions.

2.4. Human Muscle Sample. After 5 weeks of supplementation, multifidus muscle samples were obtained from all patients during PLIF surgery. All muscle samples were

Table 1: Characteristics of LBP patients.

	Age	BMI	25(OH)D_3 (nmol/L) Before	25(OH)D_3 (nmol/L) After	p
DEF ($n = 14$)	49.7 ± 2.6	30.3 ± 0.9	39.8 ± 2.4	38.2 ± 2.1	n.s
F ($n = 6$)	51.2 ± 5.2	28.0 ± 0.8	37.6 ± 4.2	36.9 ± 3.9	n.s
M ($n = 8$)	48.8 ± 2.5	32.3 ± 1.1	41.5 ± 3.0	39.1 ± 2.4	n.s
SUF ($n = 10$)	45.8 ± 3.1	27.9 ± 0.9	73.3 ± 2.9*	72.5 ± 6.8#	n.s
F ($n = 5$)	45.8 ± 2.6	27.3 ± 1.4	71.5 ± 5.2*	72.1 ± 7.1#	n.s
M ($n = 5$)	45.8 ± 6.0	28.5 ± 1.2	75.1 ± 3.1*	72.9 ± 12.5#	n.s
SUPL ($n = 14$)	48.2 ± 2.8	28.5 ± 1.4	52.8 ± 3.0	86.6 ± 3.2	<0.005
F ($n = 8$)	50.5 ± 3.4	28.1 ± 1.9	50.8 ± 3.8	85.1 ± 4.0	<0.005
M ($n = 6$)	45.2 ± 4.9	29.4 ± 0.4	55.4 ± 4.9	88.7 ± 5.3	<0.005

Values are the means (±SEM). F: female; M: male. * $p < 0.001$—difference between the indicated result/mean and DEF and SUPL groups at the same time point. # $p < 0.001$—difference between the indicated result/mean and DEF group at the same time point.

taken between the tenth thoracic and fifth lumbar vertebrae. 40-150 mg multifidus muscle specimens were collected and immediately frozen at -80°C.

2.5. Muscle Homogenization. The tissue samples were reconstituted in ice-cold lysis buffer containing 50 mM Tris-HCl, 1 mM EDTA, 1.15% KCl, 0.5 mM DTT, 0.2% protease inhibitor cocktail (Sigma-Aldrich, P834), and phosphatase inhibitor tablets PhosSTOP (Roche, Italy). The final homogenate concentration was 8%. The samples were centrifuged at 750 g for 10 min at 4°C, and the supernatant was divided into serial aliquots for enzyme activity, enzyme-linked immunosorbent assay (ELISA), and western blot (WB) measurements. Samples for WB were centrifuged at 16000 g and for ELISA at 5000 g. Protein concentration was determined using the Bradford protein assay (Sigma-Aldrich, B6916) according to the manufacturer's instructions.

2.6. Assays: Muscle Analysis. Insulin-like growth factor 1 (IGF-1) and atrogin-1 in muscle homogenates were determined using immunoassay kits (IGF-1-SEA050Hu. Cloud Clone Corporation; atrogin-1- EH4228, Fine Test), according to the manufacturer's instructions.

2.7. Mitochondrial Citrate Synthase Activity. Citrate synthase (CS) activity was measured at 37°C according to De Lisio et al. [29]. Briefly, 30 μl of supernatant (diluted to 4% final concentration; 750 g) was added to 850 μl of buffer (0.1 M Tris-HCl, 5 mM EDTA, 0.05% Triton-X100, pH 8.1), plus 100 μl of freshly made DTNB (1 mM), 10 μl acetyl-CoA (10 μM), and 10 μl of freshly made oxaloacetic acid (10 mM) to initiate the reaction. The reactions were conducted in duplicate, and absorbance was read at 412 nm in a spectrophotometer (CE9200, Cecil Instruments Limited, Cambridge, UK). CS activity was expressed as nmol/min/mg of protein.

2.8. Western Blotting. Equal amounts of total tissue lysates were separated on either 4-20%, 30 μl Mini-PROTEAN TGX™ gels (Bio-Rad Laboratories, USA) or 10% SDS-polyacrylamide gel electrophoresis (SDS-PAGE) and transferred onto a polyvinylidene difluoride (PVDF) membrane. The membranes were then blocked with a solution containing 10 mM Tris-buffered saline, 0.05% Tween 20, and 5% nonfat dry milk or 5% bovine serum albumin (BSA) (Sigma-Aldrich) and then incubated with primary antibodies including PGC-1α (Santa Cruz, sc-13067, dilution 1 : 500), Akt 1/2/3, (Santa Cruz, sc-8312, dilution 1 : 500), P-Akt 1/2/3 (Ser^{473}) (Santa Cruz, sc-7985-R, dilution 1 : 500), FoxO3a (Cell Signaling, 2497, dilution 1 : 500), P-FoxO3a (Abcam, ab154786, dilution 1 : 500), Fbx32 (Abcam, ab168372, dilution 1 : 1000), and β-tubulin (Cell Signaling, 2146, dilution 1 : 500) over night at 4°C. The membranes were treated with secondary anti-rabbit and anti-mouse antibody (dilution 1 : 20000) for 1 h at room temperature. Following treatment with the appropriate secondary antibody, the bands were visualized using Image-Quant LAS 500 (GE Healthcare). The changes in the protein level were quantified by a densitometric method using the LASImage software. β-Tubulin was used as a lane loading control. The immunoblotting was performed at least two times.

2.9. Statistical Analysis. Statistical analyses were performed using a software package (Statistica v. 13.1, StatSoft Inc., Tulsa, OK, USA). The results are expressed as the mean ± SEM. The differences between men and women in the same group were tested by Student's t-test. To identify significant differences between groups, results were analyzed by ANOVA followed by the Least Significant Difference (LSD) test. Differences with a p value of at least $p \leq 0.05$ were considered statistically significant.

3. Results

Data with patients' serum 25(OH)D_3 level before and after the supplementation were previously published [14] and are summarized in Table 1. Briefly, serum 25(OH)D_3 level was significantly different between the placebo groups, the DEF and SUF groups, both before and after the supplementation period. Five weeks of supplementation with a daily

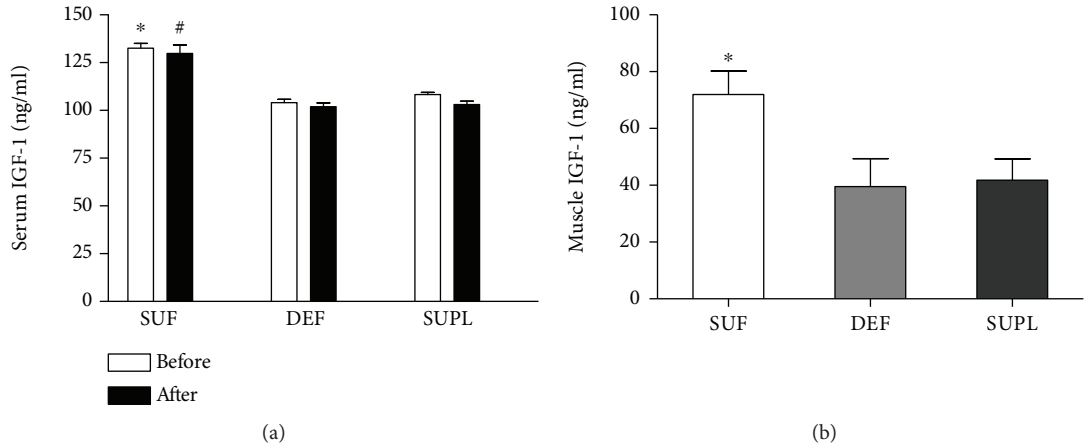

Figure 1: The level of IGF-1 in (a) serum and (b) skeletal muscle of LBP patients. Results were expressed as the mean ± SEM. (a) DEF ($n = 13$), SUF ($n = 9$), and SUPL ($n = 14$). (b) SUF ($n = 4$), DEF ($n = 6$), and SUPL ($n = 8$). $^{*}p < 0.05$—difference between the indicated result/mean and DEF and SUPL groups at the same time point. $^{\#}p < 0.005$—difference between the indicated result/mean and DEF and SUPL groups at the same time point.

dose of 3200 IU vitamin D_3 raised serum vitamin D level by an average of 53 nmol/L in the SUPL group and placed the level of serum 25(OH)D_3 above 87 nmol/L, which is 12 nmol/L higher than the level indicated as a threshold for optimal vitamin D level for adults [28, 30].

Circulating IGF-1 content was significantly higher in the SUF group as compared to both the DEF and SUPL groups before and after the supplementation. Before the supplementation, serum IGF-1 content was 108.3 ± 4.2, 104.1 ± 6.3, and 132.6 ± 7.4 ng/mL in the SUPL, DEF, and SUF groups, respectively (Figure 1(a), $p < 0.05$). After the supplementation, serum IGF-1 level was as 103.1 ± 6.5 ng/mL in the SUPL group, 101.9 ± 7.3 ng/mL in the DEF group, and 129.7 ± 13.3 ng/mL in the SUF group (Figure 1(a), $p < 0.05$). We did not observe any difference neither before and after the supplementation nor between men and women in particular groups. Muscle IGF-1 concentration was the highest in the SUF group, 71.9 ± 8.2 ng/mL. It was significantly lower in the DEF and SUPL groups (Figure 1(b), $p < 0.05$). The level of IGF-1 in the DEF group was 39.5 ± 9.8 and 41.8 ± 7.5 ng/mL in the SUPL group. We did not find any difference between men and women in muscle IGF-1 levels.

Western blotting analysis of the muscle atrophy marker Fbx32 (atrogin-1) showed that in the DEF atrogin-1 content was 38.7% higher than in the SUP group and 22% higher than in the SUF group (Figure 2(a)). The muscular concentration of atrogin-1, measured with ELISA, was the highest in the DEF group (35.7 ± 8.5 ng/mg protein). In the SUF and SUPL groups, the content of atrogin-1 was 23.1 ± 2.6 and 24.8 ± 4.1 ng/mg, respectively (Figure 2(b)). There was a significant difference in atrogin-1 muscle content between men and women overall. Muscle atrogin-1 level was 50% higher in women as compared to men (36.9 ± 5.4 ng/mg and 17.9 ± 1.9 ng/mg, respectively). There was no difference among men in atrogin-1 content in the muscle (15.9 ± 1.8, 23.4 ± 4.2, and 15.2 ± 3.4 ng/mg protein in the DEF, SUF, and SUPL groups, respectively). However, there was a difference observed among women between the three groups. Women in the DEF group had significantly higher atrogin-1 level as compared to those in the SUF group (Figure 2(b), $p < 0.05$). Vitamin D-deficient women had an average of 55.4 ± 12.7 ng/mg, and women sufficient in vitamin D had an average of 22.7 ± 3.6 ng/mg. Among women supplemented with vitamin D, the protein content of atrogin-1 was 32.0 ± 5.6 ng/mg. Furthermore, women in the DEF and SUPL groups had significantly higher atrogin-1 content as compared to the corresponding groups of men (Figure 2(b), $p < 0.05$). There was no difference between men and women in the SUF group.

The activity of citrate synthase (CS) in the muscle, which is commonly used as a marker of mitochondrial function [31], was significantly higher in the SUPL group when compared with the DEF group. In the SUF group, CS activity tended to be higher than in the DEF group, but the difference was not significant. The activity of CS in all patients was 67.7 ± 7.4, 61.5 ± 12.3, and 41.6 ± 4.5 nmol/min/mg of protein in the SUPL, SUF, and DEF groups, respectively (Figure 3, $p < 0.05$). Among women, we did not observe any differences between the groups, whereas in men there was significantly higher CS activity in the SUPL group when compared with the DEF group (Figure 3, $p < 0.05$).

The protein content of the mitochondrial biogenesis transcription factor—PGC-1α—was significantly higher in the SUF group as compared to the DEF group (Figure 4, $p < 0.05$). In the SUPL group, the PGC-1α content was also higher than in the DEF group, but the difference did not reach the significance.

To determine the possible mechanism of vitamin D on muscle atrophy, we investigated the phosphorylation states of Akt and FOXO3a. The protein content of phosphorylated Akt (pAkt) and phosphorylated FOXO3a (pFOXO3a) was similar in the DEF and SUF groups. In the SUPL group, we observed significantly higher levels of pAkt (Figure 5, $p < 0.05$) and decreased level of FOXO3a (Figure 6, $p < 0.05$).

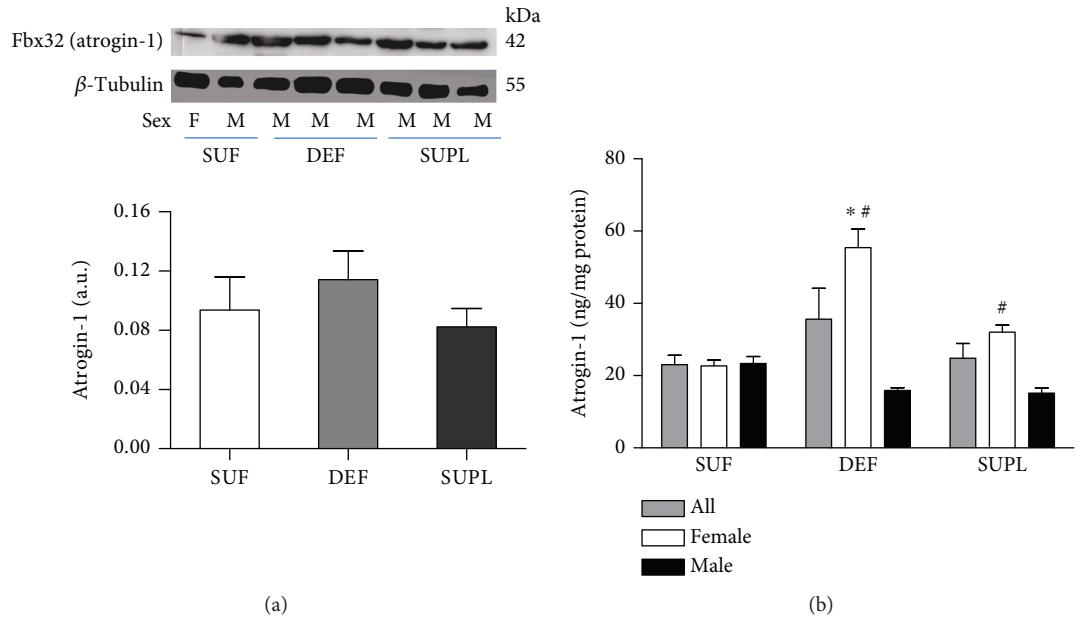

Figure 2: The level of atrogin-1 (Fbx32) visualized by representative western blotting (a) and measured with ELISA (b) in all LBP patients, female and male in skeletal muscle. Changes in WB protein densitometry levels were normalized against β-tubulin. a.u.: arbitrary units; F: female; M: male. Results were expressed as the mean ± SEM. (a) SUF ($n = 6$), DEF ($n = 7$), and SUPL ($n = 6$). (b) SUF ($n = 10$), DEF ($n = 12$), SUPL ($n = 14$), SUF F ($n = 5$), SUF M ($n = 5$), DEF F ($n = 6$), DEF M ($n = 6$), SUPL F ($n = 8$), and SUPL M ($n = 6$). $^{*}p < 0.05$—difference between the indicated result/mean and female SUF group. $^{\#}p < 0.05$—difference between the indicated result/mean and men in the same group.

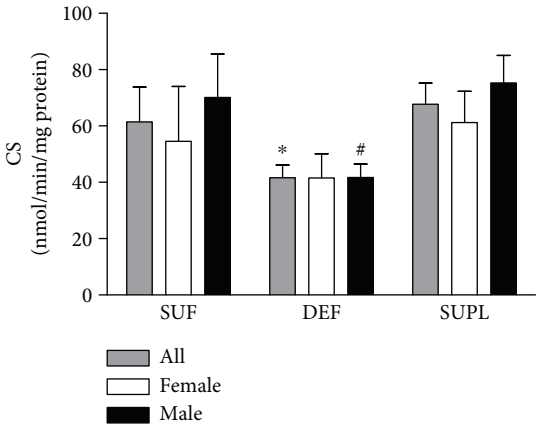

Figure 3: The CS enzyme activity in the skeletal muscle of all LBP patients. Results were expressed as the mean ± SEM. SUF ($n = 9$), DEF ($n = 13$), SUPL ($n = 13$), SUF F ($n = 5$), SUF M ($n = 4$), DEF F ($n = 6$), DEF M ($n = 7$), SUPL F ($n = 7$), and SUPL M ($n = 6$). $^{*}p < 0.05$—difference between the indicated result/mean and SUPL in all patients. $^{\#}p < 0.05$—difference between the indicated result/mean and men in the SUPL group.

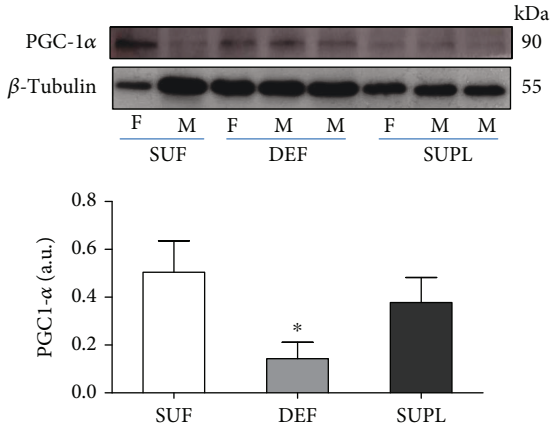

Figure 4: The content of PGC1-α in the muscles of LBP patients, visualized by representative western blotting. Changes in all presented protein densitometry levels were normalized against β-tubulin. a.u.: arbitrary units; F: female; M: male. Results were expressed as the mean ± SEM. SUF ($n = 5$), DEF ($n = 4$), and SUPL ($n = 6$). $^{*}p < 0.05$—difference between the indicated result/mean and SUF.

4. Discussion

The main findings of our study are that LBP patients with serum vitamin D deficiency show attenuated CS activity, increased content of atrogin-1, and decreased PGC-1α protein content in the multifidus muscle. In addition, we noticed higher IGF-1 content, in both serum and muscle, in patients with sufficient vitamin D level. Moreover, we observed significantly increased level of pAkt and decreased level of FOXO3a in patients supplemented with vitamin D. Together, our results suggest that the action of vitamin D in the muscle may be triggered through either the Akt/FOXO3a pathway or PGC-1α as a result of ROS generation.

Hitherto, the interplay between vitamin D and IGF-1, a hormone which displays an anabolic effect on skeletal

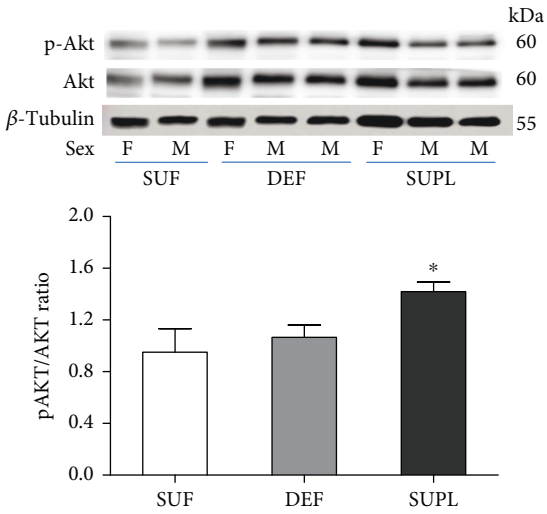

Figure 5: The ratio of pAkt/Akt content in the muscles of LBP patients, visualized by representative western blotting. Changes in all presented protein densitometry levels were normalized against β-tubulin. F: female; M: male. Results were expressed as the mean ± SEM. SUF ($n = 4$), DEF ($n = 6$), and SUPL ($n = 6$). $^*p < 0.05$—difference between the indicated result/mean and other groups.

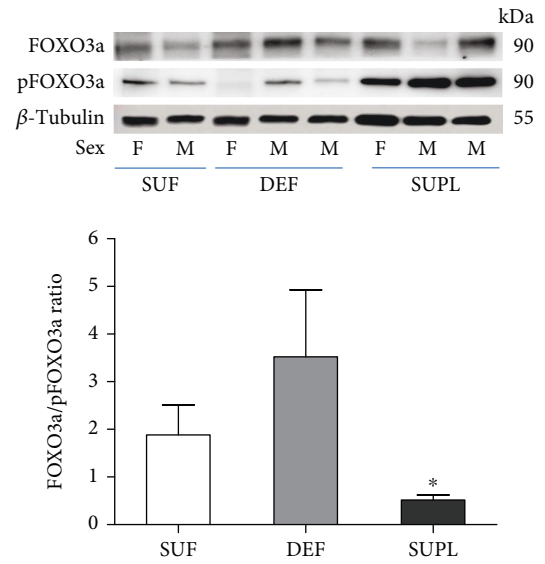

Figure 6: The ratio of FOXO3a/pFOXO3a content in the muscles of LBP patients, visualized by representative western blotting. Changes in all presented protein densitometry levels were normalized against β-tubulin. F: female; M: male. Results were expressed as the mean ± SEM. SUF ($n = 4$), DEF ($n = 6$), and SUPL ($n = 6$). $^*p < 0.05$—difference between the indicated result/mean and DEF.

muscle, has been well described in reference to their circulation level. Wei and coworkers showed that IGF-1 caused an increase in the blood levels of $1,25(OH)_2D_3$, the hormonally active vitamin D metabolite, by stimulating the expression and activity of the hydroxylase-1α that produces $1,25(OH)_2D_3$ in the kidney [32]. Moreover, when vitamin D was administered to humans, IGF-1 levels in the blood increased [33]. On the other hand, another study showed that one year of high-dose vitamin D supplementation did not significantly alter serum IGF-1 among women at a high risk of breast cancer [34] nor in prediabetes subjects [35]. Our results revealed that patients in the SUF group had higher serum IGF-1 level than patients in the DEF and SUPL groups, both before and after the supplementation period. Patients with normal vitamin D levels presented with approximately a 20% higher IGF-1 serum concentration than those deficient in vitamin D or those supplemented with it. However, we did not observe any changes regarding supplementation itself within particular groups. Muscle IGF-1 content was higher in patients with sufficient serum vitamin D level as compared to the other groups, and this was consistent with circulating IGF-1 level. Surprisingly, we did not find any difference between patients supplemented with vitamin D and patients deficient in it. Recently, Hayakawa and coworkers showed that IGF-1 is not directly affected by $1,25(OH)_2D_3$ in the skeletal muscle. They suggested that vitamin D stimulated IGF-1 production in tissues other than the skeletal muscle and that the induced IGF-1 could enter systemic circulation and exert hypertrophic effects on the muscle tissue or supportive effects on muscle function [15]. In this study, we showed elevated serum and muscle IGF-1 content in LBP patients sufficient in vitamin D. The lack of an increase in IGF-1 in the SUPL group suggests that either IGF-1 is not directly influenced by vitamin D or its induction is time dependent. This raises an interesting point that should be addressed in future studies. Notably, how long sufficient vitamin D level must be present in circulation in order to increase IGF-1 muscle content in humans who were previously deficient in vitamin D? It is important to note that we do not find any correlation between IGF-1 and atrogin-1, which suggests that the mechanism of action of vitamin D on skeletal muscle atrophy might involve other factors.

In the present study, we analyzed the muscle content of atrogin-1 and showed that atrogin-1 was the highest in patients deficient in vitamin D and lowest in patients sufficient in it. Vitamin D supplementation seems to repel atrophic changes since we observed almost as low a content of atrogin-1 in the SUPL group as in the SUF group. Notwithstanding, these results are not significant when we consider men and women together. The present study shows that women and men respond differently to vitamin D deficiency and supplementation. Men seem to be less responsive to vitamin D in regard to paraspinal muscle atrophy. Notably, among women, there was an elevated level of atrogin-1 in the group deficient in vitamin D as compared to those sufficient in it. It seems that vitamin D deficiency escalates muscle atrophy among women. Our findings are consistent with the latest study on the effect of long-term vitamin D supplementation on the global transcriptomic profile which showed that vitamin D regulates 3.2-fold more genes in women than in men [36]. Hereby, we could detect a stronger effect of vitamin D supplementation on gene expression in women when compared to men. Moreover, we observed almost the same level of atrogin-1 among women sufficient in vitamin D as in women supplemented with vitamin D

who were deficient in vitamin D at baseline and whose serum vitamin D level increased to normal levels. This observation may suggest a need for vitamin D supplementation for women in order to delay the onset muscle atrophy.

Mitochondrial dysfunction in vitamin D-deficient individuals was attributed to intramitochondrial calcium deficiency [37] or deficient enzyme function of the oxidative pathway [38]. In the present study, we report that mitochondrial function was improved in patients supplemented with vitamin D and those with normal levels of vitamin D as compared with patients deficient in it. The activity of CS was 32% lower in the DEF group than in the SUF group and 38% lower compared to the SUPL group. Our data are consistent with the studies undertaken in symptomatic, vitamin D-deficient individuals, which showed that vitamin D therapy augmented muscle mitochondrial maximal oxidative phosphorylation after exercise [39] and increased skeletal muscle CS activity and exercise-mediated cardiorespiratory fitness [40]. Also, recent studies of Ryan and coworkers demonstrated an increased oxygen consumption rate of skeletal muscle cells after treatment with vitamin D, indicating vitamin D action in the regulation of mitochondrial oxygen consumption and dynamics [41]. In addition, our study shows that CS activity was the highest in the SUPL group among men and women as well, when compared with other groups of the same sex. Both women and men in the DEF group had the lowest CS activity among other groups within the same sex. We also found lower protein content of PGC-1α, a transcriptional coactivator involved in the formation of slow-twitch fibers and mitochondria biogenesis [42]. This suggests that vitamin D induces PGC-1α synthesis and thus may be involved in mitigating muscle atrophy through enhanced mitochondrial function. Although it is well established that the decrease in protein synthesis contributes to disuse atrophy, to date, there has been no data suggesting that PGC-1α signalling directly mediates protein synthesis pathways [43]. However, PGC-1α transcriptional activity was shown to prevent muscle protein degradation. This was firstly demonstrated by Sandri and coworkers, who showed that overexpression of PGC-1α in mice prevented denervation-induced muscle atrophy by preventing the expression of key genes in the ubiquitin proteasome pathway and autophagy [44]. Also, a study on human skeletal muscle showed that PGC-1α mRNA is significantly downregulated during both the early and late phases of immobilization-induced muscle atrophy [45]. What is more, the expression of PGC-1α in skeletal muscle protects from age-related and denervation-induced muscle atrophy, as well as delays the onset of mitochondrial myopathies [46]. Recently, we demonstrated that vitamin D deficiency caused oxidative stress and higher activity of antioxidant enzymes: manganese superoxide dismutase (MnSOD) and glutathione peroxidase (GPx) in the muscle [14]. Taken together, the lower activity of CS and decreased PGC-1α protein content and a higher activity of MnSOD in the muscle indicate impaired mitochondrial function in vitamin D-deficient LBP patients.

As mentioned above, vitamin D acts through the VDR. VDR gene expression is known to be regulated by a variety of hormones including parathyroid hormone, retinoic acid [47], and glucocorticoids [48]. Also, a recent study on HuLM cells showed that estrogen inhibits VDR and that vitamin D has the potential to suppress the expression of estrogen receptor-α [49]. Another study reported that 16 weeks of vitamin D intervention induced a 20% increase in human skeletal muscle VDR gene expression in older, mobility-limited, vitamin D-insufficient women [50]. Previously, we presented that VDR muscle content was higher in patients sufficient and supplemented with vitamin D. Furthermore, we showed that lower content of VDR in patients with vitamin D deficiency evokes ROS generation with higher markers of lipid and protein peroxidation as well as increased muscle antioxidant enzyme activity [14]. In order to investigate the possible link between vitamin D and muscle atrophy, we examined PGC-1α, FOXO3a, and Akt muscle protein content. FOXO proteins are an important factor in muscle atrophy, which induce the expression of proteasomal genes, MuRF1 and atrogin-1. It is important to note that elevated PGC-1α content, besides its function in mitochondrial biogenesis, prevents transcriptional activity of FOXO3a [44], and therefore, the mitochondria might be involved in the progression of skeletal muscle atrophy.

Akt blocks the function of FOXO3 by phosphorylation of conserved residues, leading to their sequestration in the cytoplasm away from target genes [51]. Phosphorylated FOXO3a does not translocate to the nucleus, and consequently, the expression of atrogin-1 and MuRF, both target genes of FOXO, is inhibited. It was shown that FOXO3 might also be regulated by the action of peroxisome proliferator-activated receptor gamma coactivator 1-alpha (PGC-1α) [44], which is widely accepted to be the master controller of mitochondrial biogenesis as well as a regulator of many genes involved in energy metabolism [52]. In the present study, we found increased levels of Akt and decreased protein content of FOXO3a in the group supplemented with vitamin D as compared to the DEF and SUF groups. Moreover, we observed higher protein content of PGC-1α in the muscle of LBP patients with normal vitamin D level and after supplementation with vitamin D. This observation suggests that both vitamin D sufficiency and vitamin D supplementation may contribute to the reversion of atrophic changes. The possible mechanism of action of vitamin D in the skeletal muscle still needs to be addressed in future studies. According to one proposed model, in cases of muscle atrophy associated with disuse, decreases in IGF-1 cause the inhibition of Akt and dephosphorylation of FOXO3a. Dephosphorylated FOXO3a translocates to the nucleus and promotes the expression of atrogin-1 and MuRF1 and subsequently accelerates the degradation of muscle proteins [10]. Our data confirms that the possible action of vitamin D in the prevention of muscle atrophy may be mediated through the IGF-1/Akt/FOXO3a pathway. Nevertheless, with no changes in serum IGF-1 in the supplemented patients, our observations indicate that PGC-1α and mitochondria may play a crucial role in muscle atrophy through regulating mitochondrial function. Also, as mentioned above, PGC-1α might inactivate FOXO3a and therefore contribute to resisting muscle atrophy and restore the physiological functions of

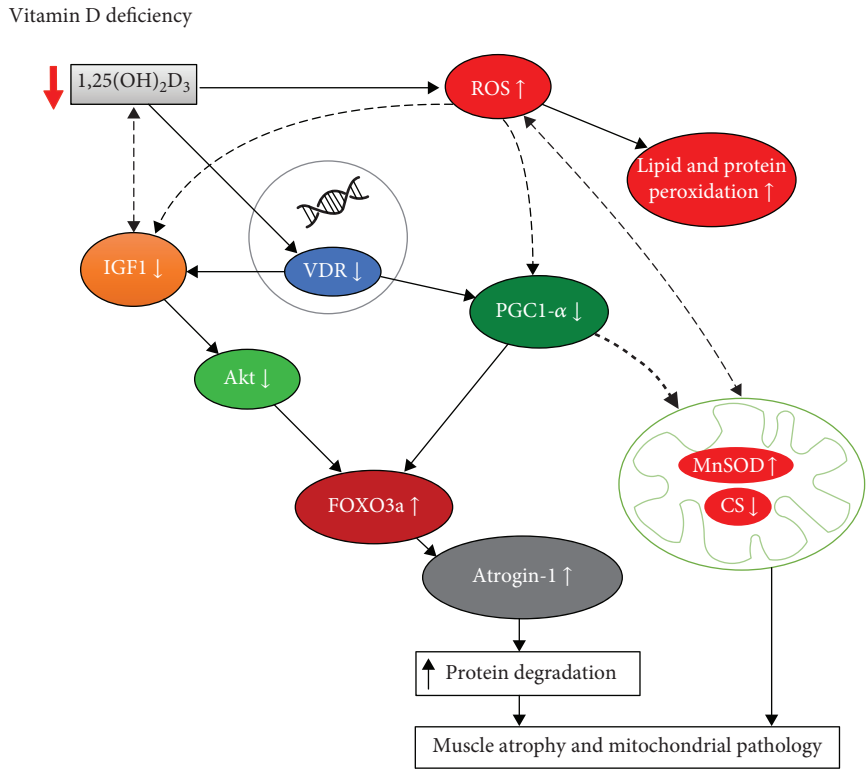

Figure 7: The vitamin D action in the skeletal muscle under the vitamin D deficiency conditions. Bold lines represent established pathways confirmed with our results while thin lines represent possible interactions as a result of vitamin D deficiency. Vitamin D deficiency decreases IGF-1 and PGC-1α via VDR—the nuclear receptor. IGF-1/Akt/FOXO3a signalling cascade triggers the muscle atrophy through atrogin-1. ROS generation causes the inhibition of PGC-1α and potentially activates FOXO3a thus inducing the muscle atrophy through atrogin-1. The lower protein content of PGC-1α directly aggravates mitochondrial biogenesis and function and may cause the oxidative stress. Furthermore, mitochondria are both the source and target of ROS generation. We assume that vitamin D deficiency induces oxidative stress, which is involved and played an important role in muscle atrophy and leads to mitochondrial dysfunction.

the mitochondria. Moreover, it was shown that FOXO3a activation caused the upregulation of MnSOD gene expression and downregulation of mitochondrial gene expression [53]. Our previously published data confirms this observation. We reported increased MnSOD activity in vitamin D-deficient patients. Taken together, our findings show that the action of vitamin D may be mediated through the IGF-1/Akt/FOXO3 pathway or through PGC-1α and FOXO3a independently (Figure 7).

In summary, we show that vitamin D deficiency is associated with attenuated CS activity, decreased protein content of PGC-1α, and previously published oxidative stress in the multifidus muscle of LBP patients [14]. We detected increased protein content of atrogin-1, in the muscle of women with lower vitamin D level. These results suggest that vitamin D deficiency induces muscle atrophy and reduces mitochondrial function in the paraspinal muscle. In addition, we observed higher IGF-1 content in both serum and muscle in patients with sufficient vitamin D level. Our results suggest that the action of vitamin D in the muscle may be triggered through either the Akt/FOXO3a pathway or PGC-1α and mitochondria. Supplementation with vitamin D to sufficient serum vitamin D level in LBP patients increased mitochondrial function and inhibited muscle atrophy in the multifidus muscle, and it may have a beneficial impact on an effective early rehabilitation in LBP patients. However, future studies on muscular function should also consider the supplementation of patients sufficient in vitamin D and patients with different BMI and age for better understanding of the mechanism of vitamin D function. There should be patients' stratification according to BMI and different hormonal and physiological gender responses.

Abbreviations

Akt:	Serine/threonine-specific protein kinase
Cu/ZnSOD:	Copper/zinc-dependent dismutase
CS:	Citrate synthase
FOXO3:	Forkhead box O3
GPx:	Glutathione peroxidase
IGF-1:	Insulin-like growth factor 1
LBP:	Low back pain
MnSOD:	Manganese-dependent superoxide dismutase
PGC-1α:	Peroxisome proliferator-activated receptor gamma coactivator 1-alpha
PLIF:	Posterior lumbar interbody fusion
ROS:	Reactive oxygen species
VDR:	Vitamin D receptor.

Data Availability

The data used to support the findings of this study are included within the supplementary information file.

Conflicts of Interest

The authors declared that there is no conflict of interest regarding the publication of this article.

Acknowledgments

This study was funded by the National Science Centre, Poland (UMO-2012/05/B/NZ7/02493). We would like to thank Dr. Gianni Parise for the revision and dedicated comments that helped improve our manuscript.

Supplementary Materials

GR: groups; DEF: deficient; SUF: sufficient; SUPL: an adequate level of vitamin D in serum; Serum IGF-1 before: serum insulin-like growth factor before supplementation with vitamin D; Serum IGF-1 after: serum insulin-like growth factor after supplementation with vitamin D; IGF-1: the muscle insulin-like growth factor after supplementation with vitamin D and placebo; CS: citrate synthase activity in the muscle after supplementation with vitamin D and placebo; atrogin-1; the muscular concentration of atrogin-1, measured with ELISA; Akt: the ratio of phosphorylated and dephosphorylated serine/threonine-specific protein kinase versus loading control, β-tubulin, measured in the muscle after supplementation with vitamin D and placebo; FOXO3: the ratio of phosphorylated and dephosphorylated forkhead box O3 versus loading control, β-tubulin, measured in the muscle after supplementation with vitamin D and placebo; PGC-1α: the muscular peroxisome proliferator-activated receptor gamma coactivator 1-alpha versus loading control, β-tubulin, measured in the muscle after supplementation with vitamin D and placebo; Fbx32 (atrogin-1): the muscular protein content of atrogin-1 versus loading control, β-tubulin, measured in the muscle after supplementation with vitamin D and placebo. *(Supplementary Materials)*

References

[1] C. J. Murray, C. Atkinson, K. Bhalla et al., "The state of US health, 1990-2010: burden of diseases, injuries, and risk factors," *JAMA*, vol. 310, no. 6, pp. 591–608, 2013.

[2] L. A. Danneels, G. G. Vanderstraeten, D. C. Cambier, E. E. Witvrouw, H. J. de Cuyper, and L. Danneels, "CT imaging of trunk muscles in chronic low back pain patients and healthy control subjects," *European Spine Journal*, vol. 9, no. 4, pp. 266–272, 2000.

[3] M. L. Dirks, B. T. Wall, T. Snijders, C. L. P. Ottenbros, L. B. Verdijk, and L. J. C. van Loon, "Neuromuscular electrical stimulation prevents muscle disuse atrophy during leg immobilization in humans," *Acta Physiologica*, vol. 210, no. 3, pp. 628–641, 2014.

[4] S. C. Bodine, E. Latres, S. Baumhueter et al., "Identification of ubiquitin ligases required for skeletal muscle atrophy," *Science*, vol. 294, no. 5547, pp. 1704–1708, 2001.

[5] M. D. Gomes, S. H. Lecker, R. T. Jagoe, A. Navon, and A. L. Goldberg, "Atrogin-1, a muscle-specific F-box protein highly expressed during muscle atrophy," *Proceedings of the National Academy of Sciences of the United States of America*, vol. 98, no. 25, pp. 14440–14445, 2001.

[6] A. Safdar, M. J. Hamadeh, J. J. Kaczor, S. Raha, J. deBeer, and M. A. Tarnopolsky, "Aberrant mitochondrial homeostasis in the skeletal muscle of sedentary older adults," *PLoS One*, vol. 5, no. 5, article e10778, 2010.

[7] J. M. Sacheck, J.-P. K. Hyatt, A. Raffaello et al., "Rapid disuse and denervation atrophy involve transcriptional changes similar to those of muscle wasting during systemic diseases," *The FASEB Journal*, vol. 21, no. 1, pp. 140–155, 2007.

[8] L. Danneels, P. Coorevits, A. Cools et al., "Differences in electromyographic activity in the multifidus muscle and the iliocostalis lumborum between healthy subjects and patients with sub-acute and chronic low back pain," *European Spine Journal*, vol. 11, no. 1, pp. 13–19, 2002.

[9] A. Mele, G. M. Camerino, S. Calzolaro, M. Cannone, D. Conte, and D. Tricarico, "Dual response of the KATP channels to staurosporine: a novel role of SUR2B, SUR1 and Kir6.2 subunits in the regulation of the atrophy in different skeletal muscle phenotypes," *Biochemical Pharmacology*, vol. 91, no. 2, pp. 266–275, 2014.

[10] M. Sandri, C. Sandri, A. Gilbert et al., "Foxo transcription factors induce the atrophy-related ubiquitin ligase atrogin-1 and cause skeletal muscle atrophy," *Cell*, vol. 117, no. 3, pp. 399–412, 2004.

[11] G. Milan, V. Romanello, F. Pescatore et al., "Regulation of autophagy and the ubiquitin-proteasome system by the FoxO transcriptional network during muscle atrophy," *Nature Communications*, vol. 6, no. 1, 2015.

[12] S. Schiaffino and C. Mammucari, "Regulation of skeletal muscle growth by the IGF1-Akt/PKB pathway: insights from genetic models," *Skeletal Muscle*, vol. 1, no. 1, p. 4, 2011.

[13] N. Kaur, P. Gupta, V. Saini et al., "Cinnamaldehyde regulates H_2O_2-induced skeletal muscle atrophy by ameliorating the proteolytic and antioxidant defense systems," *Journal of Cellular Physiology*, vol. 234, no. 5, pp. 6194–6208, 2019.

[14] K. Dzik, W. Skrobot, D. J. Flis et al., "Vitamin D supplementation attenuates oxidative stress in paraspinal skeletal muscles in patients with low back pain," *European Journal of Applied Physiology*, vol. 118, no. 1, pp. 143–151, 2018.

[15] N. Hayakawa, J. Fukumura, H. Yasuno, K. Fujimoto-Ouchi, and H. Kitamura, "1α,25(OH)2D3 downregulates gene expression levels of muscle ubiquitin ligases MAFbx and MuRF1 in human myotubes," *Biomedical Research*, vol. 36, no. 2, pp. 71–80, 2015.

[16] J. Zadro, D. Shirley, M. Ferreira et al., "Mapping the association between vitamin D and low back pain: a systematic review and meta-analysis of observational studies," *Pain Physician*, vol. 20, no. 7, pp. 611–640, 2017.

[17] M. Visser, D. J. Deeg, P. Lips, and Longitudinal Aging Study Amsterdam, "Low vitamin D and high parathyroid hormone levels as determinants of loss of muscle strength and muscle mass (sarcopenia): the Longitudinal Aging Study Amsterdam," *The Journal of Clinical Endocrinology & Metabolism*, vol. 88, no. 12, pp. 5766–5772, 2003.

[18] I. Marantes, S. J. Achenbach, E. J. Atkinson, S. Khosla, L. J. Melton III, and S. Amin, "Is vitamin D a determinant of muscle mass and strength?," *Journal of Bone and Mineral Research*, vol. 26, no. 12, pp. 2860–2871, 2011.

[19] D. Scott, L. Blizzard, J. Fell, C. Ding, T. Winzenberg, and G. Jones, "A prospective study of the associations between 25-hydroxy-vitamin D, sarcopenia progression and physical activity in older adults," *Clinical Endocrinology*, vol. 73, no. 5, pp. 581–587, 2010.

[20] J. W. Pike and M. B. Meyer, "The vitamin D receptor: new paradigms for the regulation of gene expression by 1,25-dihydroxyvitamin D(3)," *Endocrinology and Metabolism Clinics of North America*, vol. 39, no. 2, pp. 255–269, 2010, table of contents.

[21] P. Molina, J. J. Carrero, J. Bover et al., "Vitamin D, a modulator of musculoskeletal health in chronic kidney disease," *Journal of Cachexia, Sarcopenia and Muscle*, vol. 8, no. 5, pp. 686–701, 2017.

[22] H. A. Bischoff, H. B. Stähelin, W. Dick et al., "Effects of vitamin D and calcium supplementation on falls: a randomized controlled trial," *Journal of Bone and Mineral Research*, vol. 18, no. 2, pp. 343–351, 2003.

[23] A. S. Dusso, A. J. Brown, and E. Slatopolsky, "Vitamin D," *American Journal of Physiology-Renal Physiology*, vol. 289, no. 1, pp. F8–28, 2005.

[24] C. Annweiler, A. M. Schott, M. Montero-Odasso et al., "Cross-sectional association between serum vitamin D concentration and walking speed measured at usual and fast pace among older women: the EPIDOS study," *Journal of Bone and Mineral Research*, vol. 25, no. 8, pp. 1858–1866, 2010.

[25] S. D. Gopinath, A. E. Webb, A. Brunet, and T. A. Rando, "FOXO3 promotes quiescence in adult muscle stem cells during the process of self-renewal," *Stem Cell Reports*, vol. 2, no. 4, pp. 414–426, 2014.

[26] E. Hypponen, B. J. Boucher, D. J. Berry, and C. Power, "25-Hydroxyvitamin D, IGF-1, and metabolic syndrome at 45 years of age: a cross-sectional study in the 1958 British Birth Cohort," *Diabetes*, vol. 57, no. 2, pp. 298–305, 2008.

[27] K. P. Dzik and J. J. Kaczor, "Mechanisms of vitamin D on skeletal muscle function: oxidative stress, energy metabolism and anabolic state," *European Journal of Applied Physiology*, vol. 119, no. 4, pp. 825–839, 2019.

[28] M. F. Holick, N. C. Binkley, H. A. Bischoff-Ferrari et al., "Evaluation, treatment, and prevention of vitamin D deficiency: an Endocrine Society clinical practice guideline," *The Journal of Clinical Endocrinology & Metabolism*, vol. 96, no. 7, pp. 1911–1930, 2011.

[29] M. De Lisio, J. J. Kaczor, N. Phan, M. A. Tarnopolsky, D. R. Boreham, and G. Parise, "Exercise training enhances the skeletal muscle response to radiation-induced oxidative stress," *Muscle & Nerve*, vol. 43, no. 1, pp. 58–64, 2011.

[30] P. Pludowski, M. F. Holick, W. B. Grant et al., "Vitamin D supplementation guidelines," *The Journal of Steroid Biochemistry and Molecular Biology*, vol. 175, pp. 125–135, 2018.

[31] M. Mogensen, M. Bagger, P. K. Pedersen, M. Fernstrom, and K. Sahlin, "Cycling efficiency in humans is related to low UCP3 content and to type I fibres but not to mitochondrial efficiency," *The Journal of Physiology*, vol. 571, no. 3, Part 3, pp. 669–681, 2006.

[32] S. Wei, H. Tanaka, and Y. Seino, "Local action of exogenous growth hormone and insulin-like growth factor-I on dihydroxyvitamin D production in LLC-PK1 cells," *European Journal of Endocrinology*, vol. 139, no. 4, pp. 454–460, 1998.

[33] P. Ameri, A. Giusti, M. Boschetti et al., "Vitamin D increases circulating IGF1 in adults: potential implication for the treatment of GH deficiency," *European Journal of Endocrinology*, vol. 169, no. 6, pp. 767–772, 2013.

[34] K. D. Crew, T. Xiao, P. S. Thomas et al., "Safety, feasibility, and biomarker effects of high-dose vitamin D supplementation among women at high risk for breast cancer," *International Journal of Food Science, Nutrition and Dietetics*, vol. 2015, Supplement 1, pp. 1–9, 2015.

[35] I. Sinha-Hikim, P. Duran, R. Shen, M. Lee, T. C. Friedman, and M. B. Davidson, "Effect of long term vitamin D supplementation on biomarkers of inflammation in Latino and African-American subjects with pre-diabetes and hypovitaminosis D," *Hormone and Metabolic Research*, vol. 47, no. 4, pp. 280–283, 2015.

[36] Y. Pasing, C. G. Fenton, R. Jorde, and R. H. Paulssen, "Changes in the human transcriptome upon vitamin D supplementation," *The Journal of Steroid Biochemistry and Molecular Biology*, vol. 173, pp. 93–99, 2017.

[37] A. Mukherjee, J. E. Zerwekh, M. J. Nicar, K. McCoy, and L. M. Buja, "Effect of chronic vitamin D deficiency on chick heart mitochondrial oxidative phosphorylation," *Journal of Molecular and Cellular Cardiology*, vol. 13, no. 2, pp. 171–183, 1981.

[38] R. Bouillon and A. Verstuyf, "Vitamin D, mitochondria, and muscle," *The Journal of Clinical Endocrinology & Metabolism*, vol. 98, no. 3, pp. 961–963, 2013.

[39] A. Sinha, K. G. Hollingsworth, S. Ball, and T. Cheetham, "Improving the vitamin D status of vitamin D deficient adults is associated with improved mitochondrial oxidative function in skeletal muscle," *The Journal of Clinical Endocrinology & Metabolism*, vol. 98, no. 3, pp. E509–E513, 2013.

[40] M. Singla, A. Rastogi, A. N. Aggarwal, O. M. Bhat, D. Badal, and A. Bhansali, "Vitamin D supplementation improves simvastatin-mediated decline in exercise performance: a randomized double-blind placebo-controlled study," *Journal of Diabetes*, vol. 9, no. 12, pp. 1100–1106, 2017.

[41] Z. C. Ryan, T. A. Craig, C. D. Folmes et al., "1α,25-Dihydroxyvitamin D_3 regulates mitochondrial oxygen consumption and dynamics in human skeletal muscle cells," *The Journal of Biological Chemistry*, vol. 291, no. 3, pp. 1514–1528, 2016.

[42] M. Schuler, F. Ali, C. Chambon et al., "PGC1alpha expression is controlled in skeletal muscles by PPARbeta, whose ablation results in fiber-type switching, obesity, and type 2 diabetes," *Cell Metabolism*, vol. 4, no. 5, pp. 407–414, 2006.

[43] J. J. Brault, J. G. Jespersen, and A. L. Goldberg, "Peroxisome proliferator-activated receptor gamma coactivator 1alpha or 1beta overexpression inhibits muscle protein degradation, induction of ubiquitin ligases, and disuse atrophy," *The Journal of Biological Chemistry*, vol. 285, no. 25, pp. 19460–19471, 2010.

[44] M. Sandri, J. Lin, C. Handschin et al., "PGC-1α protects skeletal muscle from atrophy by suppressing FoxO3 action and atrophy-specific gene transcription," *Proceedings of the National Academy of Sciences of the United States of America*, vol. 103, no. 44, pp. 16260–16265, 2006.

[45] A. Abadi, E. I. Glover, R. J. Isfort et al., "Limb immobilization induces a coordinate down-regulation of mitochondrial and other metabolic pathways in men and women," *PLoS One*, vol. 4, no. 8, article e6518, 2009.

[46] T. Wenz, S. G. Rossi, R. L. Rotundo, B. M. Spiegelman, and C. T. Moraes, "Increased muscle PGC-1α expression protects from sarcopenia and metabolic disease during aging," *Proceedings of the National Academy of Sciences of the United States of America*, vol. 106, no. 48, pp. 20405–20410, 2009.

[47] A. Marchwicka, M. Cebrat, A. Łaszkiewicz, Ł. Śnieżewski, G. Brown, and E. Marcinkowska, "Regulation of vitamin D receptor expression by retinoic acid receptor alpha in acute myeloid leukemia cells," *The Journal of Steroid Biochemistry and Molecular Biology*, vol. 159, pp. 121–130, 2016.

[48] A. A. Hidalgo, D. L. Trump, and C. S. Johnson, "Glucocorticoid regulation of the vitamin D receptor," *The Journal of Steroid Biochemistry and Molecular Biology*, vol. 121, no. 1-2, pp. 372–375, 2010.

[49] A. Al-Hendy, M. P. Diamond, A. El-Sohemy, and S. K. Halder, "1,25-Dihydroxyvitamin D3 regulates expression of sex steroid receptors in human uterine fibroid cells," *The Journal of Clinical Endocrinology & Metabolism*, vol. 100, no. 4, pp. E572–E582, 2015.

[50] R. M. Pojednic, L. Ceglia, K. Olsson et al., "Effects of 1,25-dihydroxyvitamin D3 and vitamin D3 on the expression of the vitamin d receptor in human skeletal muscle cells," *Calcified Tissue International*, vol. 96, no. 3, pp. 256–263, 2015.

[51] A. Brunet, A. Bonni, M. J. Zigmond et al., "Akt promotes cell survival by phosphorylating and inhibiting a Forkhead transcription factor," *Cell*, vol. 96, no. 6, pp. 857–868, 1999.

[52] M. Nalbandian and M. Takeda, "Lactate as a signaling molecule that regulates exercise-induced adaptations," *Biology*, vol. 5, no. 4, p. 38, 2016.

[53] E. C. Ferber, B. Peck, O. Delpuech, G. P. Bell, P. East, and A. Schulze, "FOXO3a regulates reactive oxygen metabolism by inhibiting mitochondrial gene expression," *Cell Death and Differentiation*, vol. 19, no. 6, pp. 968–979, 2012.

Hindawi
Oxidative Medicine and Cellular Longevity
Volume 2019, Article ID 1704650, 9 pages
https://doi.org/10.1155/2019/1704650

Research Article

Age-Dependent Oxidative Stress Elevates Arginase 1 and Uncoupled Nitric Oxide Synthesis in Skeletal Muscle of Aged Mice

Chirayu D. Pandya,[1,2] Byung Lee,[1] Haroldo A. Toque,[3] Bharati Mendhe,[4] Robert T. Bragg,[1] Bhaumik Pandya,[5] Reem T. Atawia,[3] Carlos Isales,[6,7] Mark Hamrick,[4,7] R. William Caldwell,[3] and Sadanand Fulzele[1,7]

[1]*Department of Orthopaedic Surgery, Augusta University, Augusta, GA 30912, USA*
[2]*Department of Neurosurgery, University of Kentucky, Lexington, KY 40506, USA*
[3]*Department of Pharmacology and Toxicology, Augusta University, Augusta, GA 30912, USA*
[4]*Department of Cell Biology and Anatomy, Augusta University, Augusta, GA 30912, USA*
[5]*Georgia Cancer Center, Augusta University, Augusta, GA 30912, USA*
[6]*Department of Endocrinology, Augusta University, Augusta, GA 30912, USA*
[7]*Center for Healthy Aging, Augusta University, Augusta, GA 30912, USA*

Correspondence should be addressed to Sadanand Fulzele; sfulzele@augusta.edu

Received 7 December 2018; Accepted 4 March 2019; Published 8 May 2019

Guest Editor: Andrey J. Serra

Aging is associated with reduced muscle mass (sarcopenia) and poor bone quality (osteoporosis), which together increase the incidence of falls and bone fractures. It is widely appreciated that aging triggers systemic oxidative stress, which can impair myoblast cell survival and differentiation. We previously reported that arginase plays an important role in oxidative stress-dependent bone loss. We hypothesized that arginase activity is dysregulated with aging in muscles and may be involved in muscle pathophysiology. To investigate this, we analyzed arginase activity and its expression in skeletal muscles of young and aged mice. We found that arginase activity and arginase 1 expression were significantly elevated in aged muscles. We also demonstrated that SOD2, GPx1, and NOX2 increased with age in skeletal muscle. Most importantly, we also demonstrated elevated levels of peroxynitrite formation and uncoupling of eNOS in aged muscles. Our in vitro studies using C2C12 myoblasts showed that the oxidative stress treatment increased arginase activity, decreased cell survival, and increased apoptotic markers. These effects were reversed by treatment with an arginase inhibitor, 2(S)-amino-6-boronohexanoic acid (ABH). Our study provides strong evidence that L-arginine metabolism is altered in aged muscle and that arginase inhibition could be used as a novel therapeutic target for age-related muscle complications.

1. Introduction

Aging is associated with reduced muscle mass (sarcopenia) and strength (dynapenia), which can increase the incidence of falls and bone fractures [1]. As the number of older adults continues to increase, the problem of muscle loss becomes a significant public health concern [1–3]. Falls and fractures in turn lead to prolonged disability, poor quality of life, and significant financial burden [4]. It is widely appreciated that aging triggers systemic oxidative stress, which can impair myoblast differentiation and cell survival, which also leads to muscle loss [5, 6]. Recent studies have shown that elevated levels of reactive oxygen species (ROS) have deleterious effects on the musculoskeletal system and are critical in muscle-related pathophysiology [5–10]. At the molecular level, generation of ROS elicits a wide range of effects on cells such as autophagy, cell differentiation and proliferation arrest, DNA damage, and cell death by activation of

numerous cell signaling pathways [5, 6]. We previously reported that oxidative stress decreases cell attachment, proliferation, and migration of bone marrow stromal cells and antioxidant supplementation can reverse these effects [11].

We recently reported that bone marrow stromal cells express arginase 1 (ARG1) and its expression is regulated by high glucose [12]. Arginase is an enzyme which metabolizes L-arginine to form urea and L-ornithine in the urea cycle. There are two known arginase isoforms: arginase 1 (ARG1) and arginase 2 (ARG2). ARG1 is a cytosolic enzyme and is expressed most abundantly in the liver where it plays a vital role in the urea cycle, while ARG2 is located in mitochondria of various cell types [13]. Arginine is a semiessential amino acid which is the substrate for both nitric oxide synthase (NOS) and arginase enzyme. ARG1 is known to regulate oxidative stress in various degenerative diseases by modulating nitric oxides (NO) [14–16]. Recent studies indicated that NO is one of the important therapeutic targets for a number of cardiovascular and age-related diseases [17–19]. Our laboratory previously reported that ARG1 expression is elevated in diabetic bone and bone marrow [12]. Furthermore, diabetic bones were osteoporotic in nature. Interestingly, we found that treatment with the ARG1 inhibitor improved the quality of diabetic mice [12]. Based on our previous studies, we speculate that ARG1 becomes dysregulated in aged muscle. Until now, little is known about the role of oxidative stress in ARG1 regulation in aging muscle.

In the present study, we investigated the arginase activity and arginase 1 expression in aged muscles. We also analyzed the expression of important oxidative stress-related signaling molecules in muscles of aged mice. Furthermore, we performed in vitro studies on the myoblast cell line (C2C12) and arginase inhibitor (ABH) to investigate the role of arginase in myoblast pathophysiology. We found elevated levels of ROS accumulation and ARG1 expression/arginase activity and uncoupling of eNOS in aged muscles. Additionally, our in vitro studies showed that the arginase inhibitor prevented the formation of ROS accumulation and NOS uncoupling in myoblasts and improves the physiological health of myoblast cells.

2. Material and Methods

2.1. Animal Preparation and Experimental Design. All animal protocols were approved by the Institutional Animal Care and Use Committee at Augusta University. Male C57BL/6 mice from 3 months and 22 months of age (10 mice per age group) were obtained from the aged rodent colony at the National Institute on Aging. Animals were housed in a 12 h light/dark cycle and had free access to food and water throughout the study. Mice were sacrificed, and the quadriceps muscle was dissected free from the hindlimb and used for protein isolation for arginase activity, western blot, and RNA isolation.

2.2. Arginase Activity Assay. Muscle homogenate lysates were prepared in Tris buffer (50 mM Tris HCl, 0.1 mmol/L EDTA and EGTA (pH 7.5), containing protease inhibitors) and were used for the arginase activity assay as previously described [12]. Briefly, 25 μL of 10 mM MnCl2 was added to 25 μL of homogenates (cell or tissue) and heated at 57°C for 10 min to activate arginase. Next, 50 μL of 0.5 M L-arginine was then added to the reaction tube and incubated at 37°C for 1 h, and 400 μL of acid mixture ($H_2SO : H_3PO4 : H_2O$ in a ratio of 1 : 3 : 7) was added to stop the reaction. Then, 25 μL of 9% a-isonitrosopropiophenone (in ethanol) was added, and the mixture was heated for 45 min at 100°C and placed in the dark for 10 min to develop color. Arginase activity was measured by loading 200 μL of the reaction mixture in a 96-well plate, and absorbance was read at 540 nm.

2.3. Isolation of RNA, Synthesis of cDNA, and Real-Time PCR. Real-time PCR was performed as per our published method [11, 12]. Total RNA was isolated from the quadriceps muscles of mice. The muscle was homogenized and dissolved in TRIzol. RNA was isolated using the TRIzol method following the manufacturer's instructions, and the quality of the RNA preparations was monitored by absorbance at 260 and 280 nm (Helios Gamma, Thermo Spectronic, Rochester, NY). The RNA was reverse-transcribed into complementary deoxyribonucleic acid (cDNA) using iScript reagents from Bio-Rad on a programmable thermal cycler (PCR Sprint, Thermo Electron, Milford, MA). The cDNA (50 ng) was amplified by real-time PCR using a Bio-Rad iCycler and ABgene reagents (Fisher Scientific, Pittsburgh, PA) and ARG1 primers [12]. Glyceraldehyde-3-phosphate dehydrogenase (GAPDH) was used as the internal control for normalization.

2.4. Western Blot Analysis. Protein was extracted from quadriceps muscle and cell culture lysate, subjected to SDS-PAGE, and transferred to nitrocellulose membranes. Membranes were incubated with a polyclonal antibody against glutathione peroxidase (GPx1), superoxide dismutase (SOD2) (Santa Cruz Biotechnology, Santa Cruz, CA), NOX2, 3-NT, eNOS (Santa Cruz Biotechnology, Santa Cruz, CA), and GAPDH (Santa Cruz Biotechnology, Santa Cruz, CA) overnight at 4°C, followed by incubation with an appropriate secondary antibody. Proteins were visualized with an ECL western blot detection system (Thermo Scientific, Waltham, MA). For detection of eNOS dimers, we ran a low-temperature SDS-PAGE (LT-PAGE) gel using reported procedures [20] with slight modification. The protein lysates were prepared using 1× Laemmli buffer without 2-mercaptoethanol. The samples were then subjected to SDS-PAGE with 7.5% gel and run at a low temperature by keeping the buffer tank surrounded by ice. The gels were transferred, and the blots were probed as described above.

2.5. Arginase Inhibitor Prevents C2C12 Cells from Oxidative Stress Damage. C2C12 cells were cultured and pretreated with or without the arginase inhibitor ABH (100 μM) for 4 h followed by hydrogen peroxide (100 μM) treatment alone or in combination with ABH for 24 h. Arginase activity, RT-PCR, MTT assay, and staining were performed as described below. Superoxide and hydrogen peroxide levels

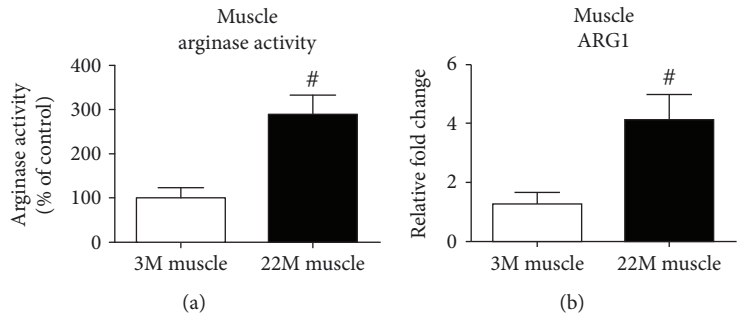

Figure 1: Aging increases arginase activity and mRNA expression in muscles. (a) Arginase activity was determined using an assay for urea formation in muscle lysates from young and old muscles, and (b) real-time PCR analysis of Arg1 mRNA in young and old mice. Data for each sample were normalized to GAPDH mRNA and represented as the fold change in expression compared to young mice. Results are means ± SD (n = 5-6 $^{\#}p < 0.01$); data were analyzed using an unpaired t-test.

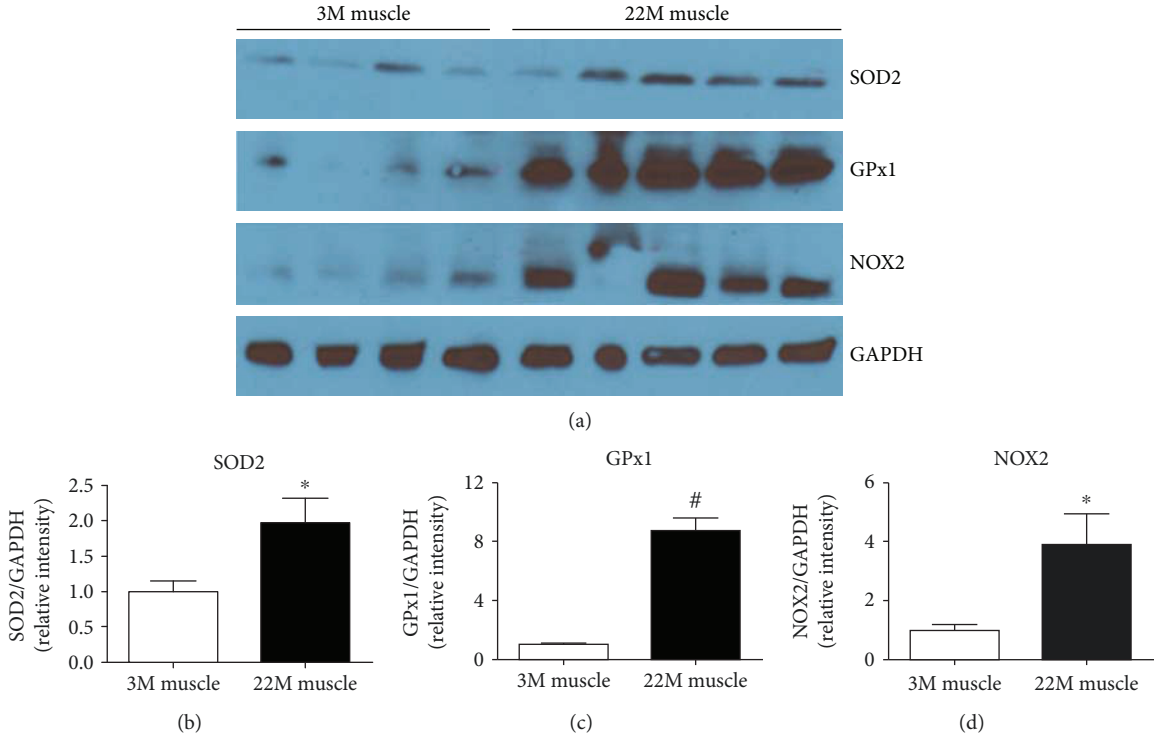

Figure 2: Elevated level of oxidative stress in young and old mouse muscles. (a) Representative western blots of protein extracted from young and old muscle samples. Densitometry quantification of (b) SOD2, (c) NOX2, and (d) GPx1. Values are normalized to the expression levels of the housekeeping gene GAPDH. Results are means ± SD (n = 5-6, $^{*}p < 0.05$, $^{\#}p < 0.01$); data were analyzed using an unpaired t-test.

were detected in culture cells with dihydroethidium (DHE) staining dye as previously described [21, 22]. C2C12 cells were incubated with the DHE dye mentioned above in PBS for 30 min at 37°C. Fluorescence was monitored using a fluorescence microscope at 20x magnification.

2.6. Cell Survival Assay. To investigate the effect of oxidative stress on C2C12 cell survival, the CellTiter 96® AQueous One MTS Cell Assay kit (Promega, G3580) was used as per the published method [23, 24]. After cell culture treatment (as described above), cells were washed twice with PBS and 150 μL of MTS (CellTiter 96® AQueous One Solution Reagent, Promega) assay buffer was added. Cells were then incubated for 2 h at 37°C in a humidified 5% CO_2 incubator. Optical density (OD) was read at 490 nm.

2.7. Statistical Analysis. GraphPad Prism 5 (La Jolla, CA) was utilized to perform one-way ANOVA with Bonferroni pairwise comparison or unpaired t-tests as appropriate. A p value of <0.05 was considered significant.

3. Results

3.1. Elevated Level of Arginase Activity and Expression in Aged Muscles. Our published data demonstrated that chronic oxidative stress increased arginase activity in various disease conditions [12, 21, 22]. We hypothesized that arginase

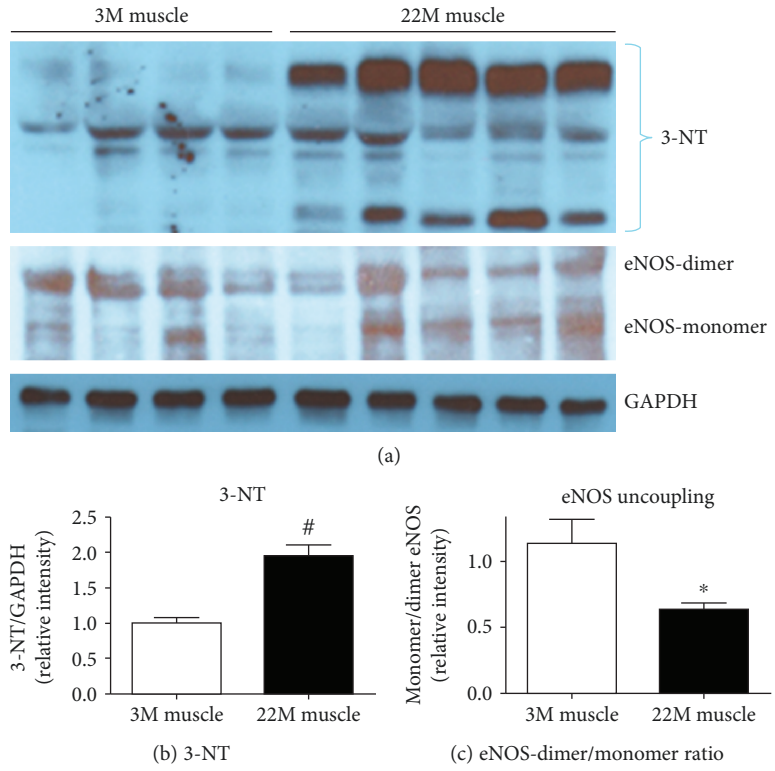

Figure 3: Elevated level of peroxynitrite ($ONOO^-$) formation and uncoupling of eNOS in aged muscle. (a) Representative western blots of protein extracted from young and old muscle samples for 3-NT and eNOS uncoupling. Densitometry quantification of (b) 3-NT and (c) eNOS uncoupling. Values are normalized to the expression levels of the housekeeping gene GAPDH. Results are means ± SD ($n = 5$-6, $^*p < 0.05$, $^\#p < 0.01$); data were analyzed using an unpaired t-test.

expression and activity became dysregulated in aged muscles. Our data showed that this is indeed the case that arginase activity (p value = 0.01) and arginase 1 expression (p value = 0.01) were significantly elevated in 22-month-old aged muscle (Figure 1). Previously, our group reported that muscle mass declined significantly between 18 and 24 months of age [25].

3.2. Elevated Level of Oxidative Stress in Aged Muscle. To evaluate the activities of the antioxidant defense system in aged muscles, we determined the level of superoxide dismutase 2 (SOD2) and glutathione peroxidase 1 (GPx1). SOD2 and GPx1 are antioxidant enzymes that play a vital role in the suppression or prevention of the formation of free radical or reactive species in cells and tissues [26, 27]. Our western blot data showed that SOD2 (p value = 0.05) and GPx1 (p value = 0.001) antioxidant enzymes significantly (p value = 0.04) increased in the muscle from 22-month-old mice compared to 3-month-old young animals [28, 29].

NADPH oxidase is one of the important enzymes known for generation of reactive oxygen species with age [28, 29]. We analyzed NOX2 (gp91-phox) levels in young (3 months) and old (22 months) mouse muscle samples. We found a significant (p value = 0.039) increase in NOX2 level in old muscles compared to young muscles (Figure 2).

3.3. Increased Peroxynitrite and ROS in Aging Muscles. Aging affects the ROS and reactive nitrogen species (RNS) homeostasis, which leads to musculoskeletal-related complications. ROS and RNS play important roles in various age-related diseases including sarcopenia [5, 6, 8–10]. We investigated the RNS status in aged muscle using 3-nitrotyrosine (3-NT), a specific marker for reactive nitrogen species [30]. Our data demonstrated that 22-month-old muscles have significantly (p value = 0.0041) higher levels of 3-NT compared to young muscles (Figures 3(a) and 3(b)). Elevated levels of 3-NT in aged muscles suggest activation of the nitrating pathway and production of increased reactive nitrogen intermediate products.

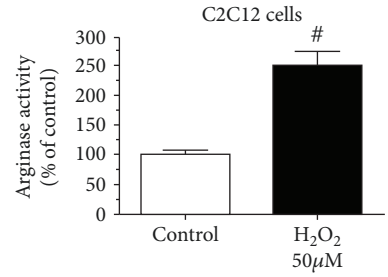

Figure 4: Effect of oxidative stress on arginase activity on myoblasts. C2C12 cells were incubated in DMEM (2% FBS, 50 mM L-arginine) with and without hydrogen peroxide (50 μM) for 48 h. Arginase activity in cell lysate was determined by the arginase activity assay ($^\#p < 0.01$, $n = 6$).

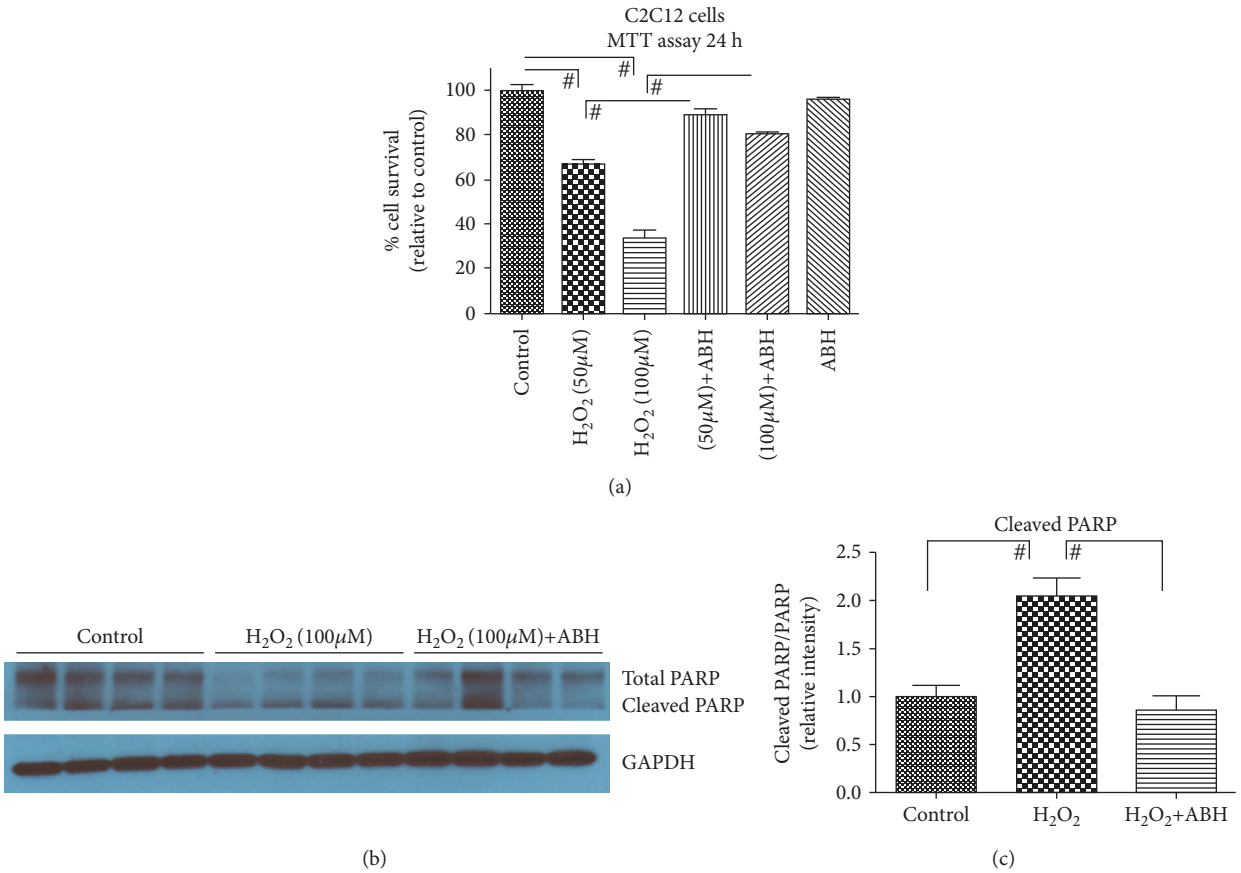

Figure 5: Arginase inhibitor prevents C2C12 cells from oxidative stress damage. (a) C2C12 cells were treated with H_2O_2 (50 and 100 μM) in the presence or absence of ABH (100 μM) for 24 h. MTS analysis was performed after 24 h following treatment. (b) Representative western blots for total PARP and cleaved PARP on C2C12 cells. (c) Densitometry ratio of total PARP and cleaved PARP. Values are normalized to the expression levels of the housekeeping gene GAPDH. Data were analyzed by one-way ANOVA followed by the Bonferroni post hoc test ($^{\#}p < 0.01$, $n = 8$).

3.4. Dysregulation of the Monomer-to-Dimer Ratio (Uncoupling) of eNOS in Aged Mouse Muscles. Previously, eNOS uncoupling is related to several age-related diseases [20, 31–33]. We hypothesized that eNOS might be uncoupled because of the elevated level of oxidative stress in aged muscles. We analyzed the eNOS monomer and dimer in young and old muscles using a low-temperature SDF-PAGE gel. We found significant (p value = 0.04) uncoupling of eNOS in aged muscles (Figures 3(a) and 3(c)). The ratio of eNOS monomer to dimer was significantly higher in aged muscles compared to young muscles (Figures 3(a) and 3(c)).

3.5. Oxidative Stress Regulates Arginase Activity in Myoblasts (C2C12 Cells). Our data (Figure 1) demonstrates that arginase activity and ARG1 expression are upregulated in muscles with aging. To further demonstrate the role of arginase in oxidative stress-dependent myoblast biology and cell survival, we treated C2C12 cells with hydrogen peroxide (oxidative stress) and estimated arginase activity. We found significantly (p value = 0.01) elevated levels of arginase activity in H_2O_2-treated cells (Figure 4). Based on this data, we hypothesized that an arginase inhibitor might prevent cells from the harmful effects of oxidative stress. We subjected cells to oxidative stress in the presence or absence of the arginase inhibitor (ABH), performed a cell survival assay, and investigated cell apoptotic markers. The cell survival assay was performed using the MTS assay, in which we found a dose-dependent significant (p value = 0.001) decrease in the C2C12 cell number in oxidative stress samples, and the arginase inhibitor prevents cell death (p value = 0.001) (Figure 5(a)). Western blot analysis of the apoptotic marker (cleaved PARP) showed a significant (p value = 0.01) increase in cleaved PARP in the presence of oxidative stress. Treatment with the arginase inhibitor prevented this effect (Figures 5(b) and 5(c)).

3.6. Arginase Inhibitor Prevents Superoxide Radical Formation in C2C12 Cells. To assess the involvement of arginase in myoblasts during oxidative stress, we performed *in vitro* studies using C2C12 cells. C2C12 cells were cultured and treated with H_2O_2 to induce oxidative stress in the presence or absence of the arginase inhibitor (ABH) and stained with DHE staining dye. Dihydroethidium (DHE) is a cell-permeable dye that reacts with a superoxide anion and forms a red fluorescent product [34]. Our data showed increased red fluorescence in oxidative stress-subjected samples. Increased fluorescence of DHE staining in the cells revealed increased superoxide radical formation.

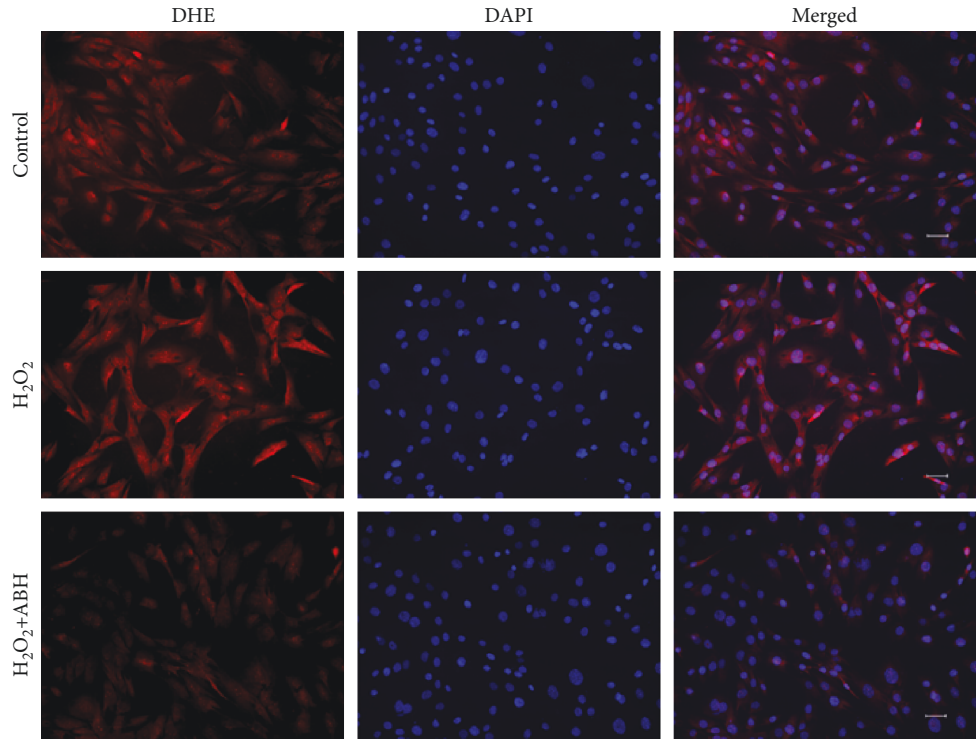

Figure 6: Fluorescence microscopy images show that the arginase inhibitor prevents the accumulation of ROS in C2C12 cells. C2C12 cells were treated with H_2O_2 (50 μM) in the presence or absence of ABH (100 μM) for 24 h. ROS production was detected by DHE staining. Representative fluorescent images show that the arginase inhibitor prevents the accumulation of ROS in C2C12 cells.

Furthermore, treatment with ABH (Figure 6) prevented the increase in DHE fluorescence indicating the prevention of superoxide production in cells.

4. Discussion

Aging affects the homeostasis of ROS, which is characterized by the increased accumulation of intracellular hydrogen peroxide/RNS and decreased antioxidant properties of cells/tissues. Imbalance (generation and elimination) in the homeostasis of ROS leads to musculoskeletal pathophysiology, such as muscle atrophy and fibrosis [6, 35]. When ROS levels are above the physiologic level, cells respond to stress through compensatory mechanisms by increasing antioxidant signaling to prevent the damaging effects of ROS. In chronic stress conditions, such as aging, ROS levels continue to increase while antioxidant systems become hampered, leading to muscle atrophy and fibrosis. Previously, our group and others have shown accumulation of reactive oxygen species and muscle loss with age [6, 25, 35–38]. We hypothesized that with aging, elevated levels of oxidative stress increase arginase activity and ARG1 expression in muscle.

In this study, we analyzed the expression of arginase 1 and its activity in young and aged muscles. Our study is the first to demonstrate both arginase activity and expression elevation with age in muscles. Recently, we demonstrated the elevated levels of oxidative stress and ARG1 expression in diabetic mouse bone and bone marrow [12]. Furthermore, our group also demonstrated ARG1 dysregulation in various tissues and organs of diabetic and hypertension disease models [12, 21, 22, 39–42].

Previously, our group reported that NADPH oxidase 2 (NOX2) activation led to elevated ROS and ARG1 expression and activity in diabetic retinal endothelial dysfunction [43]. NADPH oxidase plays an important role in the production of superoxide free radicals to protect cells from foreign microorganisms [44]. Controlled regulation of NADPH oxidase is important to maintain the health level of ROS. Chronic stress continuously elevates NADPH oxidase, which is harmful for cells and induces degenerative effect [43]. We speculate that NADPH oxidase 2 expression might be affected by aging. To investigate this, we assessed the expression of NADPH oxidase 2 (NOX2). As expected, we found elevated level of NOX2 expressed in aged muscles compared to young muscles. Whitehead and his group [45] previously reported elevated NADPH oxidase expression in tibialis anterior muscles from dystrophic (mdx) mice. Similar results were also reported by Heymes et al. [46] in the pathophysiology of human congestive heart failure. We hypothesized that aging-induced oxidative stress (e.g., NOX2) elevates arginase expression, thus limiting L-arginine bioavailability and reducing NO production in muscle. Elevated arginase activity can limit the bioavailability of L-arginine to NOS causing its uncoupling, which results in less NO formation and more superoxide ($O2^{\cdot-}$) production. The NO rapidly reacts with $O2^{\cdot-}$ to produce peroxynitrite ($ONOO^{-}$), another potent oxidant [47]. It has been well established that peroxynitrite

participates in oxidation reactions, which results in the modification of amino acid residue of proteins (protein tyrosine nitration) leading to degenerative changes [48, 49]. We speculate that in aged muscles, peroxynitrite level might be higher than that in young muscles. We analyzed the presence of 3-nitrotyrosine (3-NT) in young and old muscles, which indirectly measures the presence of peroxynitrite [50]. We found increased level of 3-NT in aged muscle compared to young muscle. Pearson et al. [51] also reported similar findings with ours showing elevated level of 3-NT in gastrocnemius muscles of old mice.

Formation of peroxynitrite and superoxide affects eNOS uncoupling in various age-related diseases [20, 31–33]. In this study, we demonstrated that the eNOS monomer-to-dimer ratio is disturbed in aged muscles. To the best of our knowledge, ours is the first study to directly demonstrate eNOS uncoupling in aged muscle. Low-temperature SDF-PAGE gel demonstrated a higher eNOS monomer-to-dimer ratio in aged muscles. For the effective function of eNOS, dimerization of eNOS is required, which catalyzes the L-arginine to generate NO [52]. Our *in vitro* data further confirm the above findings; we used mouse myoblast (C2C12) cell lines to perform these studies. Subjecting C2C12 cells to oxidative stress resulted in elevated level of ROS and arginase activity, and pretreatment with the arginase inhibitor reversed the effects suggesting the role of arginase in myoblast pathophysiology. We also found that oxidative stress decreases C2C12 cell survival and increases cell apoptosis, while the arginase inhibitor prevented this effect.

Overall, our study showed that aging elevates arginase activity, which contributes to less NO production due to competition for L-arginine and eNOS uncoupling. Further studies are needed to fully understand the mechanism of age-induced increases in arginase activity and its specific role in uncoupling of eNOS. Our study demonstrated that limiting arginase activity in muscle with aging can prevent or slow down the degenerative effect. Further studies are needed to investigate the therapeutic role of the arginase inhibitor in age-related muscle loss/complications. The aging population is at increased risk of falls and fractures due to low muscle mass and strength [1–3]. As the number of older adults continues to increase, the problem of muscle loss becomes a significant public health concern. Our study outcome has a significant translational impact because it suggested that the arginase inhibitor could be used as a novel therapeutic target for age-related muscle loss.

Data Availability

The quantitative data used to support the findings of this study will be available from the corresponding author upon request.

Conflicts of Interest

The authors also declare that there is no conflict of interest regarding the publication of this manuscript.

Acknowledgments

This publication is based upon the work supported in part by the National Institutes of Health (NIA-AG036675—SF, MH, and CS).

References

[1] E. Curtis, A. Litwic, C. Cooper, and E. Dennison, "Determinants of muscle and bone aging," *Journal of Cellular Physiology*, vol. 230, no. 11, pp. 2618–2625, 2015.

[2] L. Ferrucci, M. Baroni, A. Ranchelli et al., "Interaction between bone and muscle in older persons with mobility limitations," *Current Pharmaceutical Design*, vol. 20, no. 19, pp. 3178–3197, 2014.

[3] N. M. Peel, "Epidemiology of falls in older age," *Canadian Journal on Aging*, vol. 30, no. 1, pp. 7–19, 2011.

[4] K. Mazur, K. Wilczyński, and J. Szewieczek, "Geriatric falls in the context of a hospital fall prevention program: delirium, low body mass index, and other risk factors," *Clinical Interventions in Aging*, vol. 11, pp. 1253–1261, 2016.

[5] A. Espinosa, C. Henríquez-Olguín, and E. Jaimovich, "Reactive oxygen species and calcium signals in skeletal muscle: a crosstalk involved in both normal signaling and disease," *Cell Calcium*, vol. 60, no. 3, pp. 172–179, 2016.

[6] M. Kozakowska, K. Pietraszek-Gremplewicz, A. Jozkowicz, and J. Dulak, "The role of oxidative stress in skeletal muscle injury and regeneration: focus on antioxidant enzymes," *Journal of Muscle Research and Cell Motility*, vol. 36, no. 6, pp. 377–393, 2015.

[7] S. Dalle, L. Rossmeislova, and K. Koppo, "The role of inflammation in age-related sarcopenia," *Frontiers in Physiology*, vol. 8, article 1045, 2017.

[8] R. Nemes, E. Koltai, A. W. Taylor, K. Suzuki, F. Gyori, and Z. Radak, "Reactive oxygen and nitrogen species regulate key metabolic, anabolic, and catabolic pathways in skeletal muscle," *Antioxidants*, vol. 7, no. 7, p. 85, 2018.

[9] B. Fougere, G. A. van Kan, B. Vellas, and M. Cesari, "Redox systems, antioxidants and sarcopenia," *Current Protein & Peptide Science*, vol. 19, no. 7, pp. 643–648, 2018.

[10] P. Rossi, B. Marzani, S. Giardina, M. Negro, and F. Marzatico, "Human skeletal muscle aging and the oxidative system: cellular events," *Current Aging Science*, vol. 1, no. 3, pp. 182–191, 2008.

[11] R. Sangani, C. D. Pandya, M. H. Bhattacharyya et al., "Knockdown of SVCT2 impairs *in-vitro* cell attachment, migration and wound healing in bone marrow stromal cells," *Stem Cell Research*, vol. 12, no. 2, pp. 354–363, 2014.

[12] A. Bhatta, R. Sangani, R. Kolhe et al., "Deregulation of arginase induces bone complications in high-fat/high-sucrose diet diabetic mouse model," *Molecular and Cellular Endocrinology*, vol. 422, pp. 211–220, 2016.

[13] S. P. Narayanan, M. Rojas, J. Suwanpradid, H. A. Toque, R. W. Caldwell, and R. B. Caldwell, "Arginase in retinopathy," *Progress in Retinal and Eye Research*, vol. 36, pp. 260–280, 2013.

[14] M. Rath, I. Müller, P. Kropf, E. I. Closs, and M. Munder, "Metabolism via arginase or nitric oxide synthase: two competing arginine pathways in macrophages," *Frontiers in Immunology*, vol. 5, p. 532, 2014.

[15] A. G. Estévez, M. A. Sahawneh, P. S. Lange, N. Bae, M. Egea, and R. R. Ratan, "Arginase 1 regulation of nitric oxide

production is key to survival of trophic factor-deprived motor neurons," *The Journal of Neuroscience*, vol. 26, no. 33, pp. 8512–8516, 2006.

[16] J. B. Hunt, K. R. Nash, D. Placides et al., "Sustained arginase 1 expression modulates pathological tau deposits in a mouse model of tauopathy," *The Journal of Neuroscience*, vol. 35, no. 44, pp. 14842–14860, 2015.

[17] J. Pernow and C. Jung, "The emerging role of arginase in endothelial dysfunction in diabetes," *Current Vascular Pharmacology*, vol. 14, no. 2, pp. 155–162, 2016.

[18] Z. Yang and X. F. Ming, "Arginase: the emerging therapeutic target for vascular oxidative stress and inflammation," *Frontiers in Immunology*, vol. 4, p. 149, 2013.

[19] Z. Yang and X. F. Ming, "Endothelial arginase: a new target in atherosclerosis," *Current Hypertension Reports*, vol. 8, no. 1, pp. 54–59, 2006.

[20] Y. M. Yang, A. Huang, G. Kaley, and D. Sun, "eNOS uncoupling and endothelial dysfunction in aged vessels," *American Journal of Physiology-Heart and Circulatory Physiology*, vol. 297, no. 5, pp. H1829–H1836, 2009.

[21] L. Wang, A. Bhatta, H. A. Toque et al., "Arginase inhibition enhances angiogenesis in endothelial cells exposed to hypoxia," *Microvascular Research*, vol. 98, pp. 1–8, 2015.

[22] J. Suwanpradid, M. Rojas, M. A. Behzadian, R. W. Caldwell, and R. B. Caldwell, "Arginase 2 deficiency prevents oxidative stress and limits hyperoxia-induced retinal vascular degeneration," *PLoS One*, vol. 9, no. 11, article e110604, 2014.

[23] S. Fulzele, P. Arounleut, M. Cain et al., "Role of myostatin (GDF-8) signaling in the human anterior cruciate ligament," *Journal of Orthopaedic Research*, vol. 28, no. 8, pp. 1113–1118, 2010.

[24] R. Sangani, S. Periyasamy-Thandavan, R. Pathania et al., "The crucial role of vitamin C and its transporter (SVCT2) in bone marrow stromal cell autophagy and apoptosis," *Stem Cell Research*, vol. 15, no. 2, pp. 312–321, 2015.

[25] M. W. Hamrick, K. H. Ding, C. Pennington et al., "Age-related loss of muscle mass and bone strength in mice is associated with a decline in physical activity and serum leptin," *Bone*, vol. 39, no. 4, pp. 845–853, 2006.

[26] O. M. Ighodaro and O. A. Akinloye, "First line defence antioxidants-superoxide dismutase (SOD), catalase (CAT) and glutathione peroxidase (GPX): their fundamental role in the entire antioxidant defence grid," *Alexandria Journal of Medicine*, vol. 54, no. 4, pp. 287–293, 2018.

[27] L. A. Pham-Huy, H. He, and C. Pham-Huy, "Free radicals, antioxidants in disease and health," *International Journal of Biomedical Science*, vol. 4, no. 2, pp. 89–96, 2008.

[28] L. M. Fan, S. Cahill-Smith, L. Geng, J. Du, G. Brooks, and J. M. Li, "Aging-associated metabolic disorder induces Nox2 activation and oxidative damage of endothelial function," *Free Radical Biology & Medicine*, vol. 108, pp. 940–951, 2017.

[29] Z. Du, Q. Yang, L. Liu et al., "NADPH oxidase 2-dependent oxidative stress, mitochondrial damage and apoptosis in the ventral cochlear nucleus of D-galactose-induced aging rats," *Neuroscience*, vol. 286, pp. 281–292, 2015.

[30] L. Shu, A. Vivekanandan-Giri, S. Pennathur et al., "Establishing 3-nitrotyrosine as a biomarker for the vasculopathy of Fabry disease," *Kidney International*, vol. 86, no. 1, pp. 58–66, 2014.

[31] J. M. Johnson, T. J. Bivalacqua, G. A. Lagoda, A. L. Burnett, and B. Musicki, "eNOS-uncoupling in age-related erectile dysfunction," *International Journal of Impotence Research*, vol. 23, no. 2, pp. 43–48, 2011.

[32] T. Thum, D. Fraccarollo, M. Schultheiss et al., "Endothelial nitric oxide synthase uncoupling impairs endothelial progenitor cell mobilization and function in diabetes," *Diabetes*, vol. 56, no. 3, pp. 666–674, 2007.

[33] C. Zhu, Y. Yu, J. P. Montani, X. F. Ming, and Z. Yang, "Arginase-I enhances vascular endothelial inflammation and senescence through eNOS-uncoupling," *BMC Research Notes*, vol. 10, no. 1, p. 82, 2017.

[34] Q. Chen, Y. C. Chai, S. Mazumder et al., "The late increase in intracellular free radical oxygen species during apoptosis is associated with cytochrome c release, caspase activation, and mitochondrial dysfunction," *Cell Death and Differentiation*, vol. 10, no. 3, pp. 323–334, 2003.

[35] M. H. Choi, J. R. Ow, N. D. Yang, and R. Taneja, "Oxidative stress-mediated skeletal muscle degeneration: molecules, mechanisms, and therapies," *Oxidative Medicine and Cellular Longevity*, vol. 2016, Article ID 6842568, 13 pages, 2016.

[36] E. Rigamonti, T. Touvier, E. Clementi, A. A. Manfredi, S. Brunelli, and P. Rovere-Querini, "Requirement of inducible nitric oxide synthase for skeletal muscle regeneration after acute damage," *Journal of Immunology*, vol. 190, no. 4, pp. 1767–1777, 2013.

[37] T. Bettis, B. J. Kim, and M. W. Hamrick, "Impact of muscle atrophy on bone metabolism and bone strength: implications for muscle-bone crosstalk with aging and disuse," *Osteoporosis International*, vol. 29, no. 8, pp. 1713–1720, 2018.

[38] S. A. Novotny, G. L. Warren, and M. W. Hamrick, "Aging and the muscle-bone relationship," *Physiology*, vol. 30, no. 1, pp. 8–16, 2015.

[39] A. Y. Fouda, Z. Xu, E. Shosha et al., "Arginase 1 promotes retinal neurovascular protection from ischemia through suppression of macrophage inflammatory responses," *Cell Death & Disease*, vol. 9, no. 10, p. 1001, 2018.

[40] E. Shosha, Z. Xu, S. P. Narayanan et al., "Mechanisms of diabetes-induced endothelial cell senescence: role of arginase 1," *International Journal of Molecular Sciences*, vol. 19, no. 4, article 1215, 2018.

[41] H. A. Toque, K. P. Nunes, M. Rojas et al., "Arginase 1 mediates increased blood pressure and contributes to vascular endothelial dysfunction in deoxycorticosterone acetate-salt hypertension," *Frontiers in Immunology*, vol. 4, p. 219, 2013.

[42] L. Yao, A. Bhatta, Z. Xu et al., "Obesity-induced vascular inflammation involves elevated arginase activity," *American Journal of Physiology-Regulatory, Integrative and Comparative Physiology*, vol. 313, no. 5, pp. R560–R571, 2017.

[43] M. Rojas, T. Lemtalsi, H. A. Toque et al., "NOX2-induced activation of arginase and diabetes-induced retinal endothelial cell senescence," *Antioxidants*, vol. 6, no. 2, p. 43, 2017.

[44] P. Behe and A. W. Segal, "The function of the NADPH oxidase of phagocytes, and its relationship to other NOXs," *Biochemical Society Transactions*, vol. 35, no. 5, pp. 1100–1103, 2007.

[45] N. P. Whitehead, E. W. Yeung, S. C. Froehner, and D. G. Allen, "Skeletal muscle NADPH oxidase is increased and triggers stretch-induced damage in the *mdx* mouse," *PLoS One*, vol. 5, no. 12, article e15354, 2010.

[46] C. Heymes, J. K. Bendall, P. Ratajczak et al., "Increased myocardial NADPH oxidase activity in human heart failure," *Journal of the American College of Cardiology*, vol. 41, no. 12, pp. 2164–2171, 2003.

[47] D. Jourd'heuil, F. L. Jourd'heuil, P. S. Kutchukian, R. A. Musah, D. A. Wink, and M. B. Grisham, "Reaction of superoxide and nitric oxide with peroxynitrite. Implications for peroxynitrite-mediated oxidation reactions *in vivo*," *Journal of Biological Chemistry*, vol. 276, no. 31, pp. 28799–28805, 2001.

[48] R. Radi, "Protein tyrosine nitration: biochemical mechanisms and structural basis of functional effects," *Accounts of Chemical Research*, vol. 46, no. 2, pp. 550–559, 2013.

[49] M. B. Feeney and C. Schöneich, "Tyrosine modifications in aging," *Antioxidants & Redox Signaling*, vol. 17, no. 11, pp. 1571–1579, 2012.

[50] A. Ceriello, F. Mercuri, L. Quagliaro et al., "Detection of nitrotyrosine in the diabetic plasma: evidence of oxidative stress," *Diabetologia*, vol. 44, no. 7, pp. 834–838, 2001.

[51] T. Pearson, A. McArdle, and M. J. Jackson, "Nitric oxide availability is increased in contracting skeletal muscle from aged mice, but does not differentially decrease muscle superoxide," *Free Radical Biology & Medicine*, vol. 78, pp. 82–88, 2015.

[52] W. Chen, H. Xiao, A. N. Rizzo, W. Zhang, Y. Mai, and M. Ye, "Endothelial nitric oxide synthase dimerization is regulated by heat shock protein 90 rather than by phosphorylation," *PLoS One*, vol. 9, no. 8, article e105479, 2014.